AD-A009 515

FLUIDS, LUBRICATION, FUELS AND RELATED MATERIALS

E. Erwin Klaus, et al

Pennsylvania State University

Prepared for:

Air Force Materials Laboratory

June 1974

UNCLASSIFIED
Security Classification

DOCUMENT CONTROL DATA - R&D AD. A009515
(Security classification of title, body of abstract and indexing annotation must be entered when the overall report is classified)

1. ORIGINATING ACTIVITY (Corporate author)
Petroleum Refining Laboratory
Chemical Engineering Department
The Pennsylvania State University

2a. REPORT SECURITY CLASSIFICATION
UNCLASSIFIED

2b GROUP

3. REPORT TITLE
FLUIDS, LUBRICATION, FUELS AND RELATED MATERIALS

4. DESCRIPTIVE NOTES (Type of report and inclusive dates)
Annual 1 May 1973 through 30 April 1974

5. AUTHOR(S) (Last name, first name, initial)
Klaus, E. Erwin; Tewksbury, Elmer J., et al.

6. REPORT DATE	7a. TOTAL NO. OF PAGES	7b. NO. OF REFS
June 1974	251	57

8a. CONTRACT OR GRANT NO.	9a. ORIGINATOR'S REPORT NUMBER(S)
AF33615-73-C-5101	
b. PROJECT NO. 7343	
c. Task NR: 734303	9b. OTHER REPORT NO(S) (Any other numbers that may be assigned this report) AFML-TR-74-201, Part I
d.	

10. AVAILABILITY/LIMITATION NOTICES
"Approved for public release; distribution unlimited.

11. SUPPLEMENTARY NOTES	12. SPONSORING MILITARY ACTIVITY
	Air Force Materials Laboratory Air Force Systems Command Wright-Patterson AFB, Ohio 45433

13. ABSTRACT

Oxidation studies with a variety of fluids at high temperatures are presented. These studies emphasize the evaluation of oxygen tolerance of the fluids as opposed to conventional tests measuring the stable life or induction period of fluids. Oxygen assimilation rates are measured using gas chromatographic methods. Temperature-programmed gas chromatography using an internal standard is used for the quantitative evaluation of the oxidized product. Temperature measurements are being made for both the liquid and the vapor space in the reaction zone. The effect of the volatility of the fluid and of the volatile oxidation products on the rate of oxygen assimilation is determined. Test conditions necessary to optimize the relationship between temperature control of the vapor phase and the degree of oxidation in the liquid phase are suggested. Procedures for the recovery and analysis of the debris formed at the wear surfaces in a four-ball wear tester are presented. A lubrication model based on metal-fluid interaction in the concentrated contact is proposed. Environmental conditions in the concentrated contact are shown to be capable of providing fluid degradation products. A material balance used to quantify the lubrication debris recovered is discussed. Atomic absorption spectrophotometry is used to obtain the metal content of the various fractions of the wear debris. Some preliminary data on the effect of several materials on the wear behavior of steel-on-titanium and titanium-on-titanium are presented. Bulk modulus measurements for some Spec. MIL-H-83282 fluids are given.

DD FORM 1473

UNCLASSIFIED
Security Classification

14. KEY WORDS	LINK A		LINK B		LINK C	
	ROLE	WT	ROLE	WT	ROLE	WT
Fluids, Lubricants, Lubrication, Gas Chromatography, Oxidation						

INSTRUCTIONS

1. ORIGINATING ACTIVITY: Enter the name and address of the contractor, subcontractor, grantee, Department of Defense activity or other organization *(corporate author)* issuing the report.

2a. REPORT SECURITY CLASSIFICATION: Enter the overall security classification of the report. Indicate whether "Restricted Data" is included. Marking is to be in accordance with appropriate security regulations.

2b. GROUP: Automatic downgrading is specified in DoD Directive 5200.10 and Armed Forces Industrial Manual. Enter the group number. Also, when applicable, show that optional markings have been used for Group 3 and Group 4 as authorized.

3. REPORT TITLE: Enter the complete report title in all capital letters. Titles in all cases should be unclassified. If a meaningful title cannot be selected without classification, show title classification in all capitals in parenthesis immediately following the title.

4. DESCRIPTIVE NOTES: If appropriate, enter the type of report, e.g., interim, progress, summary, annual, or final. Give the inclusive dates when a specific reporting period is covered.

5. AUTHOR(S): Enter the name(s) of author(s) as shown on or in the report. Enter last name, first name, middle initial. If military, show rank and branch of service. The name of the principal author is an absolute minimum requirement.

6. REPORT DATE: Enter the date of the report as day, month, year; or month, year. If more than one date appears on the report, use date of publication.

7a. TOTAL NUMBER OF PAGES: The total page count should follow normal pagination procedures, i.e., enter the number of pages containing information.

7b. NUMBER OF REFERENCES: Enter the total number of references cited in the report.

8a. CONTRACT OR GRANT NUMBER: If appropriate, enter the applicable number of the contract or grant under which the report was written.

8b, &c, & 8d. PROJECT NUMBER: Enter the appropriate military department identification, such as project number, subproject number, system numbers, task number, etc.

9a. ORIGINATOR'S REPORT NUMBER(S): Enter the official report number by which the document will be identified and controlled by the originating activity. This number must be unique to this report.

9b. OTHER REPORT NUMBER(S): If the report has been assigned any other report numbers *(either by the originator or by the sponsor)*, also enter this number(s).

10. AVAILABILITY/LIMITATION NOTICES: Enter any limitations on further dissemination of the report, other than those imposed by security classification, using standard statements such as:

(1) "Qualified requesters may obtain copies of this report from DDC."

(2) "Foreign announcement and dissemination of this report by DDC is not authorized."

(3) "U. S. Government agencies may obtain copies of this report directly from DDC. Other qualified DDC users shall request through _____."

(4) "U. S. military agencies may obtain copies of this report directly from DDC. Other qualified users shall request through _____."

(5) "All distribution of this report is controlled. Qualified DDC users shall request through _____."

If the report has been furnished to the Office of Technical Services, Department of Commerce, for sale to the public, indicate this fact and enter the price, if known.

11. SUPPLEMENTARY NOTES: Use for additional explanatory notes.

12. SPONSORING MILITARY ACTIVITY: Enter the name of the departmental project office or laboratory sponsoring *(paying for)* the research and development. Include address.

13. ABSTRACT: Enter an abstract giving a brief and factual summary of the document indicative of the report, even though it may also appear elsewhere in the body of the technical report. If additional space is required, a continuation sheet shall be attached.

It is highly desirable that the abstract of classified reports be unclassified. Each paragraph of the abstract shall end with an indication of the military security classification of the information in the paragraph, represented as *(TS), (S), (C), or (U)*.

There is no limitation on the length of the abstract. However, the suggested length is from 150 to 225 words.

14. KEY WORDS: Key words are technically meaningful terms or short phrases that characterize a report and may be used as index entries for cataloging the report. Key words must be selected so that no security classification is required. Identifiers, such as equipment model designation, trade name, military project code name, geographic location, may be used as key words but will be followed by an indication of technical context. The assignment of links, rules, and weights is optional.

NOTICES

When Government drawings, specifications, or other data are used for any purpose other than in connection with a definitely related Government procurement operation, the United States Government thereby incurs no responsibility nor any obligation whatsoever; and the fact that the Government may have formulated, furnished, or in any way supplied said drawings, specifications, or other data, is not to be regarded by implication or otherwise as in any manner licensing the holder or any other person or corporation, or conveying any rights or permission to manufacture, use, or sell any patented invention that may in any way be related thereto.

Copies of this report should not be returned unless return is required by security considerations, contractual obligations, or notice on a specific document.

AIR FORCE/56780/30 April 1975 — 300

FOREWORD

This report was prepared by the Petroleum Refining Laboratory, Department of Chemical Engineering, College of Engineering at The Pennsylvania State University under Contract F33615-73-C-5101. This project was initiated under Project No. 7343 "Aerospace Lubricants," Task No. 734303 "Fluid Lubricant Materials." This work was administered under the direction of the Air Force Materials Laboratory, Air Force Systems Command, Wright-Patterson Air Force Base, Ohio with Mr. George Morris (MBT) as Project Engineer.

This report covers work conducted from 1 May 1973 through 30 April 1974; it was submitted by the authors 15 June 1974. They are E. Erwin Klaus, Elmer J. Tewksbury, Michael Charles, and Arun Bose.

This technical report has been reviewed and is approved for publication.

Larry L. Fehrenbacher

Larry L. Fehrenbacher, Major, USAF
Chief, Lubricants and Tribiology Branch
Nonmetallic Materials Division

ABSTRACT

Oxidation studies with a variety of fluids at high temperatures are presented. These studies emphasize the evaluation of oxygen tolerance of the fluids as opposed to conventional tests measuring the stable life or induction period of fluids. The tests are conducted at 500°C. in a glass apparatus. Test fluids comprise an ester and several naphthenic and paraffinic mineral oils (3 to 77 centistokes at 100°F.) Oxygen assimilation rates are measured using gas chromatographic methods. Temperature-programmed gas chromatography using an internal standard is used for the quantitative evaluation of the oxidized product. Temperature measurements are being made for both the liquid and the vapor space in the reaction zone. Equipment variations are discussed which allow the variation of the temperature in the vapor phase. The effect of the volatility of the fluid and of the volatile oxidation products on the rate of oxygen assimilation is determined. The presence of these materials in the oil is shown to cause an apparent retardation of the reaction between an oil and oxygen after an initial oxidation period. Test conditions necessary to optimize the relationship between temperature control of the vapor phase and the degree of oxidation in the liquid phase are suggested. Procedures for the recovery and analysis of the debris formed at the wear surfaces in a four-ball wear tester are presented. A lubrication model based on metal-fluid interaction in the concentrated contact is proposed. The effects of temperatures, lubricant, and atmosphere are considered. Environmental conditions in the concentrated contact are shown to be capable of providing fluid degradation products. These products can then react with metals or metal oxides to produce organometallic material. A material balance used to quantify the lubrication debris recovered is discussed. Atomic absorption spectrophotometry is used to obtain the metal content of the various fractions of the wear debris. The metal and metal-containing compounds are shown to include oil-soluble organometallic compounds, free metal, metal oxides, and extractable organometallic material. A method to identify iron oxide in the presence of iron is presented. Some preliminary data on the effect of several materials on the wear behavior of steel-on-titanium and titanium-on-titanium are presented. Bulk modulus measurements for some Spec. MIL-H-83282 type fluids are given.

TABLE OF CONTENTS

TABLE OF CONTENTS (Continued)

LIST OF ILLUSTRATIONS

LIST OF ILLUSTRATIONS (CONT'D)

LIST OF ILLUSTRATIONS (CONT'D)

LIST OF ILLUSTRATIONS (CONT'D)

LIST OF ILLUSTRATIONS (CONCLUDED)

LIST OF TABLES

LIST OF TABLES (Continued)

LIST OF TABLES (Concluded)

I. FLUID AND LUBRICANT STUDIES

A. SUMMARY. Studies have been continued to understand better the interaction of lubricants and working fluids and the environment in which these materials must function. Studies involving the reactions taking place at the wear surfaces under conditions of elastohydrodynamic and boundary lubrication will aid in the formulation of lubricants to give optimum performance in a given application. Mechanism studies involving the degradation of fluids and lubricants are necessary to the development of methods to qualitatively and quantitatively measure the abilities of various fluids to function under given conditions.

The oxidation of liquid lubricants at high temperature is investigated in this study. Oxygen assimilation rates have been measured for several fluids, employing gas chromatographic techniques. Oxygen absorption is determined by analyzing samples from the exit gas stream and comparing them with the samples of inlet gas. Air is used as the oxidizing medium in a single-pass arrangement. A bath temperature of 500 $\pm$ 3°F is used as the heating source of the fluids with an air flow rate of 5.0 $\pm$ 0.5 liters per hour for all tests conducted. These tests are conducted in all glass apparatus. These data, along with data from previous studies, are used to correlate oxidative characteristics of the fluid with their physical properties.

Oxygen absorption values have been determined for several fluids which possess a wide range of properties. The viscosities of these fluids range from 3.22 to 76.9 centistokes at 100°F. The chemical types of the fluids include a synthetic diester, two paraffinic super-refined mineral oils and three naphthenic super-refined mineral oils. Temperature-programmed gas chromatography is employed in the determination of the distillation ranges of the mineral oils before and after oxidation. The composition of the degraded ester was evaluated by temperature-programmed gas chromatography using tridecane as an internal standard to give quantitative results.

Liquid column chromatography is used in the separation of the oxidized mineral oils into their respective oxidized and unoxidized fractions. Infrared spectroscopy is used to check the separation obtained in these procedures. Temperature measurements are made for the liquid and vapor space in the reaction vessel during the oxidation reaction using copper-constantan thermocouples.

The effect of volatility of the fluid and the volatile oxidation products is demonstrated. The effect of the control and removal of volatile oxidation products from the reaction vessel is also shown to produce data with much less scatter and less temperature variations within the reaction vessel. Small concentrations of nonreactive volatile products, for example, water, are found to dissolve in the reacting fluid and decrease the solubility of oxygen in the fluid. The removal of these products is shown to restore the level of oxygen assimilation from a low value to a higher value. The presence of those materials in the oil is used to explain the apparent retardation of the reaction between an oil and oxygen after an initial short period. No evidence is

found to support the theory that natural inhibitors are formed during the reaction.

A lubrication model has been proposed based on the metal-fluid interaction in the concentrated contact. The effects of temperature, lubricant, and atmosphere have been considered for this proposed model. A surface film was observed in and around the concentrated contact area of the bearings. After wear is encountered, evidence of the oxide film originally present on the bearing surface and organometallic product produced in the wear process are found in the system. In the case of nonreactive lubricants the formation of metal oxides in the wear debris is observed. The presence of other polar materials appears to produce organometallic wear debris as a result of chemical reaction at the bearing surface with either the metal oxide surface films or the freshly wiped clean metal surfaces. Careful tests in the absence of oxygen in the atmosphere or fluid, produce both metal oxide and organometallic material indicating the presence of relatively large quantities of oxide debris most probably produced by the wiping action of the bearing surfaces.

A material balance is used to quantify the lubrication debris from the four-ball wear tests. Atomic absorption spectrophotometry has been used to obtain the metal content of the various fractions of the wear products. The metal and metal-containing compounds found in the debris analysis include oil soluble organometallic compounds, free metal, metal oxides, and extractable organometallic material. Indentification of both iron and iron oxide in the wear particles is based on the relative solubility of these materials in an acridine-inhibited hydrochloric acid. The iron oxides have been dissolved in the inhibited hydrochloric acid for atomic absorption spectroscopic analysis (AAS). Finally the metallic wear debris can be dissolved in mineral acid and evaluated by AAS. The total weight loss of the four ball specimens as measured by a microbalance represents the total wear debris to be accounted for in the four fractions including all of the metallic wear products. In general, the metal lost from the balls and the wear products found in the analysis agree to $\pm$ 12 percent.

It is not clear from these data whether the organometallic compounds result from reactions between components of the lubricants and iron or iron oxide. It appears that in the case of wear in an inert atmosphere that at least some or most of the reactions occur between the clean metal surface and the lubricant components. There is evidence that the environment in a four-ball wear tester at the conjunctions includes temperatures on the metal surface approaching the melting point of the metal.

Some preliminary data on the wear behavior of steel-on-titanium and titanium-on-titanium in a four-ball wear tester using halogenated fluids and zinc, sulfur, and phosphorus-containing additives in a mineral oil are included. Preliminary oxidation data on several gas turbine oils and some experimental silicone fluids are presented. Bulk modulus values for several Spec MIL-H-83282 type fluids have been determined.

B. HIGH TEMPERATURE OXIDATION OF SOME ORGANIC LIQUIDS. The most severe limitation to the use of mineral oils and esters as lubricants at elevated temperatures is the deterioration of the fluid due to oxidation. At temperatures above 400°F, the inhibitors available provide, at best, a short induction period and/or a reduced oxidation rate for some modest time period after the stable life. Essentially all of the accepted oxidation tests in widespread usage are designed to evaluate changes that occur within the stable life or induction period. These test methods are not directly applicable to high temperature use without a critical analysis to demonstrate limits of error where oxidation rate is the prime measurement.

Mineral oils and synthetic esters have been used extensively as lubricants and functional fluids in the moderate to high temperature range in aircraft engines and aeronautic and astronautic hydraulic systems. There is a need for the development of reliable testing methods for evaluation of these fluids at temperatures where the test time exceeds the fluid stable life. Non conformity of testing methods to rigid standards give rise to the lack of reproducibility in the data obtained from these tests. This also allows for the tailoring of testing methods to provide desired results for a given fluid. The lack of a proper understanding of the parameters and variables involved in these testing methods and the data obtained from these tests could result in faulty interpretation of the data.

The objective of this study is to investigate the variables involved in the oxidation of lubricating oils at high temperatures to obtain a better understanding of the reaction. Another goal of this study is to be able to account for the characteristics of the oxidation reaction at high temperatures in physical terms. Possible improvements in the testing procedures and in the collection of oxygen assimilation data are other goals of this study.

1. Apparatus and Procedures. The apparatus used in this study for the oxidation of oils consists basically of an oil reservoir through which air is bubbled as the oxidizing and stirring medium for the oil. The oil is heated by a constant-temperature bath. The exit gas stream from the oxidation tube is passed through cold traps to remove the condensibles before the gas is collected for analysis in a gas chromatograph. A flow diagram of the apparatus is shown in Figure 1. This is a modification of the single-pass oxidation test system used in the Petroleum Refining Laboratory for high-temperature oxidation of lubricating oils. A temperature of 500 $\pm$ 3°F is maintained in the constant-temperature bath. Air is used as the oxidizing medium at a flow rate of 5 $\pm$ 0.5 liters per hour. Electrical heat is provided to the thermostatically controlled constant-temperature bath.

Air for the system is obtained from the laboratory air supply at 80 p.s.i.. Prior to use in the oxidation test, the air is dried by passage through a tower packed with Drierite. A calcium chloride-Drierite tube serves as a visual check on the efficiency of the drying tower. The pressure of the air stream is reduced by two reducing valves in series set to give a final pressure of about nine pounds per square

inch. A manifold in the air line provides for the use of multiple oxidation tests.

The dried air is metered through individual manometer-style flow-meters. The air is metered by passing the total flow through a stainless steel hypodermic capillary tubing seven inches long and 0.026 inch in diameter, and then measuring the pressure drop across the capillary. The pressure drop across the capillary is measured on a standard oil-filled U-tube manometer. Air flow rates are calibrated in terms of pressure drop as indicated by the difference in height of the manometer fluid levels. The dried air is then bubbled through the fluid charge at a fixed rate of five liters per hour.

The fluid charge is placed in the reservoir of an all-glass assembly, comprising an oil reservoir and condenser. The air is added to the fluid through a capillary tube at the bottom of the oil reservoir. The gas passes through the fluid and the gas space above the liquid and then through the exit tube to the cold traps as shown in Figure 2. Three sizes of oil reservoirs are provided to allow significant changes in the oil-air volume ratio. All three sizes include the same depth of oil and therefore the same air-oil contact time and area of air-oil interface. The tubes are 450 millimeters long and the diameter of the lower portion is 38 millimeters for the regular, 22 millimeters for the semi-micro and 14 millimeters for the micro. The air inlet line is thick-walled six-millimeter o.d. glass tubing which extends to the bottom of the reservoir.

The condenser or gas space above the liquid can also be changed to provide a water condenser, an air condenser, and an electrically heated jacket. The latter condition is achieved by wrapping the air condenser with insulated nichrome wire, over which is placed a covering of asbestos webbing to insulate it from the surroundings. Current is supplied to the nichrome wire and controlled through a Variac. The top of the fluid reservoir which extends above the bath is also insulated with asbestos. To aid in more efficient removal of volatiles, the direction of the exit port is changed for some of the tests. The modified apparatus is shown in Figure 3. The three designs for the gas space provide more careful control of the volatile products. Return versus removal of the volatile oxidation products can have a marked effect on the course of the oxidation

The exit gases from the oxidation test are passed through two cold traps as shown in Figure 4. The first trap at 32°F was filled with ice and water and the second trap at -109°F was filled with dry ice and acetone. These traps removed most of the condensible materials from the exit gas stream. The exit gas after the second trap is divided into two streams. One gas stream goes to a large gas sampling bottle filled with acidified, saturated salt water. A representative sample is continuously collected in this container during a test run by pumping the saturated salt water out of the bottle at a rate of three milliliters per minute. The second gas stream is led through a long piece of flexible tubing, at the end of which is a section of capillary glass tubing six inches long. The exit gases are exhausted through this line which is kept under two inches of water to assure unidirectional flow of gases from the system.

Samples for oxygen assimilation measurements can also be taken from this line. Gas samples must be taken at a rate equal to or less than the flow rate of exhaust gas through this capillary system. The apparatus used for sampling the exhaust gases consists of a gas burette and a leveling bulb connected by a length of tubing and containing a solution of acidified, saturated salt water. A diagram of this apparatus is shown in Figure 5. Gas is drawn into or pushed out of the burette by lowering or raising the leveling bulb. This apparatus was found to give good, repeatable results for gas chromatographic analyses of the exit gases.

The source of heat is a constant-temperature bath. This bath consists of an aluminum block cast around 14 steel tubes, two inches o.d. and 12 inches long, which are sealed at the bottom end. Strip heaters are clamped to the outside of the aluminum block to provide a heat source. The aluminum block is supported at four corners by ceramic bricks within a metal box and is insulated from the box by two inches of glass wool. The metal box is covered with a transite top which is flush with the top of the tubes. A mixture of plaster of paris and asbestos cement is used to fill the void between the block and the transite top. Construction details are shown in Figure 6.

To provide good thermal contact between the aluminum block and the glass oxidation tubes, a low melting (225°F), lead-bismuth alloy, Cerrobase, is placed in the two-inch steel tubes. The oxidation tubes are held down in the high density molten Cerrobase alloy by an arrangement of three steel bars mounted about one inch above the level of the transite top. A transite U-shaped clamp, placed above the enlargement ridge of the oxidation tube and under two adjacent steel bars, anchors the tube securely in the bath.

The temperature of the bath is controlled by a thermocouple, mounted in one of the center holes of the bath which actuates an indicating pyrometer controller. Eight thermocouples located at different positions in the block enable the measurement of the temperature gradient across the bath from end to end. The thermocouples used are copper-constantan. A single cold junction is employed and the desired thermocouple is obtained by means of a selector switch. Figure 7 shows the relative positions of the thermocouples.

A total of 3,000 watts is available for quick heating, when all heaters are connected in parallel and variacs are set at 100 volts. A wiring diagram of the bath is shown in Figure 8. The bath is located in a hood complete with exhaust fan and full length sliding window for safety.

Before each test run, the oxidation tube is cleaned thoroughly using an acid cleaning solution followed by a water wash and a series of washes and acetone, naphtha, and benzene in that order. The cold traps, are subjected to the latter solvent washes. The tare weight is recorded for the clean dry oxidation tube. The tube is then charged with approximately 200 milliliters of liquid for the regular tube, 65 milliliters for the semi-micro tube and 25 milliliters for the micro tube, and the weight recorded. For tests where liquid samples are taken during the

run, these weights are not recorded because of the difficulties of obtaining a good material balance under these conditions. After the test equipment is assembled, nitrogen is bubbled through the test fluid for 15 minutes at five liters per hour at room temperature to replace all soluble gases with nitrogen. The oxidation tube is then lowered into the bath and the nitrogen flow allowed to continue for an additional 15 minutes to prevent oxidation until the test temperature of the oxidation bath is achieved. The exit gas train, comprising the two cold traps and the gas sampling bottle, is assembled and connected before the oxidation tube is inserted in the bath. After the oxidation tube has been in the bath for 15 minutes, the nitrogen is shut and the air started at 5.0 liters per hour.

During the test run, exhaust gas samples are taken after a half hour and one hour of testing and at hourly intervals thereafter. These samples are analyzed to obtain oxygen assimilation data. Liquid samples are taken in some of the tests to follow property changes as a function of oxygen assimilation. Liquid sampling is done by interrupting the air flow for about one minute. The oil which rises in the air tube is quickly transferred to a sample bottle by removing the air tube. The air flow is resumed as soon as the air tube is replaced. At the end of the test, the air is shut off, the oxidation tube removed from the bath, and nitrogen is bubbled through the tube for about 20 minutes to cool the oil with no further oxidation. The use of nitrogen during the cool-down period also has a safety feature. The nitrogen prevents a build-up of inflammable and explosive mixtures. The traps are sealed and allowed to warm to room temperature. Test times vary over a wide time range but most of the tests used to establish the oxidation characteristics during the early phases of the oxidation reaction are of eight hours duration.

2. Methods of Analysis. Gas analyses are accomplished with a Perkin-Elmer model 154 Vapor Fractometer. A 20-foot column of 0.25-inch outside diameter copper tubing, packed with 5A molecular sieves is used to analyze for oxygen, nitrogen, methane, and carbon monoxide. Another column, 27 feet long and 0.25-inch outside copper tubing, packed with hexamethylphosphoramide on 30-60 mesh Chromosorb P, is used to analyze for carbon dioxide and C_2 through C_6 hydrocarbons. The volatile liquid products were analyzed a 0.25-inch outside diameter column, 20 feet long, packed with β-β′-oxydipropionitrile on 30-60 mesh Chromosorb P. The operating conditions for the instrument with these columns are shown in Table 1. These conditions afford adequate separation of the peaks of the individual components.

For complete identification of all components in the exit gas, two chromatographic units have to be used, one with a 5A molecular sieves column and the other with a hexamethylphosphoramide column. Samples for both instruments are obtained with the gas sampling device described earlier and shown in Figure 4. In taking a sample, the exit line of the exhaust gas is connected to the gas burette by way of a two stopcock mechanism. The gas burette is flushed twice with the gas before a sample is retained. The two stopcock mechanism is used to insure that there is always positive flow from the sampling line.

A portion of the gas sample is introduced directly from the gas samples into the gas chromatograph by means of a constant volume loop on the instrument. A constant volume loop of 200 microliters is used for the 5A molecular sieves column, and one of 300 microliters for the hexamethylphosphoramide column.

Nitrogen is inert to the reaction system, carbon monoxide is formed in small quantities with the percentage of methane being small. The percentage of oxygen absorbed can therefore be determined by comparing the ratio of the area under the oxygen peak to the area under the nitrogen peak in the exhaust gas to the corresponding ratio in an air standard. The calculation is done as follows:

$$\% \text{ Available Oxygen Absorbed} = \left\{ 1 - \frac{\left\{ \frac{\text{area under } O_2 \text{ peak}}{\text{area under } N_2 \text{ peak}} \right\}_{\text{exhaust}}}{\left\{ \frac{\text{area under } O_2 \text{ peak}}{\text{area under } N_2 \text{ peak}} \right\}_{\text{air}}} \right\} \times 100$$

This is done for hourly samples and a plot is obtained of percent available oxygen absorbed versus time. The percentages of methane and carbon monoxide formed are calculated directly from the ratio of the area under the specific peak to the total area under all peaks in the exhaust gas. The areas used in these calculations are corrected using the Relative Thermal Response Value of each component and procedures developed in the Petroleum Refining Laboratory.

The chromatographic peaks obtained from these samples are regular triangular peaks and hence the areas are measured by triangulation. The raw area under the peak is taken as the product of the height of the peak and its width at half the height. The height is measured by a rule to the nearest hundredth of an inch and the width is measured by a seven-power Bausch and Lomb monocular containing a scale in inches. This method is reproducible and easy to perform.

The values of "percentage of oxygen" are easily converted to moles of oxygen in the following manner. The flow rate of five liters of air per hour is reduced to its value at standard temperature and pressure, assuming ideal gas behavior. Room temperature is taken as 25°C and barometric pressure as 734 millimeters of mercury. Standard temperature is 0°C and pressure 760 millimeters of mercury

$$\text{STP flow rate} = \frac{734 \times 5 \text{ liters} \times 263\,^{\circ}\text{K}}{760 \times 298\,^{\circ}\text{K} \times 1 \text{ hour}}$$

$$= 4.26 \text{ liters/hour}$$

$$\text{Number of moles of oxygen per hour} = \frac{4.26 \times 0.2095}{22.14}$$

$$= 0.0403 \text{ mole oxygen/hour}$$

The number of moles of oxygen absorbed at any time is the product of the number of moles of oxygen supplied and the percentage of oxygen adsorbed. The total amount of oxygen absorbed is calculated as the sum of the instantaneous hourly values.

An F and M Scientific Company Temperature-Programmed Gas Chromatograph, Model 700 is used in the evaluation of the oils and their oxidation products. This instrument affords both isothermal and temperature-programmed capabilities. In the temperature-programmed mode, compounds boiling as high as 950°F can be analyzed. It is a dual column instrument, which tends to reduce or eliminate the problem of baseline drift experienced in single-column units. Baseline drift problems are minimized by comparing the substrate bleeding in the test and reference columns. The instrument is equipped with a tungsten wire thermal conductivity detection system.

The columns used are two feet of stainless steel tubing of 0.125 inch outside diameter and 0.055 inch inside diameter, packed with silicone rubber on a substrate of diatomaceous earth. Helium is used as the carrier gas at a flow rate of 60 cubic centimeters per minute. The instrument is programmed at a rate of 13.5°F per minute from 122° to 608°F. Sample size is usually two microliters, injected into the instrument with a Hamilton 10-microliter syringe. The complete operating conditions are shown in Table 2.

For quantitative analysis on samples, tridecane ($C_{13}H_{28}$) is used as an internal standard in approximately 15 percent (by weight) solutions in the oil samples. This standard and the operating conditions were chosen on the basis of previous work done in this laboratory (AFML-TR-70-304, Part III). The peaks obtained are sometimes irregularly shaped, hence the areas under the peak were measured by a weighing method. Each peak was cut out precisely from the chromatogram and weighed on a Metler Gramatic balance to five decimal places.

The average distillation range for each of the five oils used was determined by a chromatographic technique. These oils all gave very broad smooth peaks on the recorder chart. For temperature correlation, a mixture of straight chain hydrocarbons of known boiling point is used as a standard. The hydrocarbons used are tridecane, $C_{13}H_{28}$ (b.p. 445.7°F); hexadecane, $C_{16}H_{34}$ (b.p. 548.6°F); eicosane, $C_{20}H_{42}$ (b.p. 650°F); and hexacosane, $C_{26}H_{54}$ (b.p. 774°F). The boiling points of these compounds are plotted versus their retention times measured from an air peak. This is a straight line function for a homologous series in adsorption chromatography.

For the broad oil peak, the area is measured carefully with a Keuffel and Esser compensating polar planimeter and the 10 percent and 90 percent elution points determined. From the boiling point correlation above, the 10 percent, 90 percent, and initial boiling points are determined. Typical temperature-programmed chromatograms for an oil, one of the standard and correlation plot are shown in Figures 9 and 10 respectively.

Liquid chromatography involves the separation of unoxidized or paraffinic portion of the oils from the oxidized portion. This is achieved by percolation of the oil through a dual-packed, silica gel-alumina chromatographic column.

A glass column (0.75-inch o.d.) is packed with approximately 50 grams of fully activated grade F20, 80-200 mesh Alco Alumina on the bottom, and approximately 250 grams of fully activated 28-200 mesh Davidson Silica gel on the top. The Silica gel is activated at 260°C for 16 hours and the alumina at 400°C for 16 hours.

Approximately 100 milliliters of pure n-pentane are allowed to percolate through the column after which approximately 15 milliliters of the oxidized oil mixed with 15 milliliters of n-pentane are added and allowed to percolate. Pure n-pentane is used to elute the paraffinic portion. The n-pentane is added until a fraction of pure n-pentane is obtained from the bottom of column. The oxidized products on the column are eluted with approximately 200 milliliters of diethyl ether followed by methanol, until essentially pure methanol is obtained at the bottom of the column. The desired products are obtained from the eluted solvent product by evaporation of the solvents.

Infrared spectroscopy is used to check the chemical groups present in the oxidized oil. The instrument used is a Perkin-Elmer Model 137 Infracord Spectrophotometer. All samples are evaluated without solvent dilution as a thin film between two sodium chloride plates.

3. Factors Affecting the Reproducibility of Results.

a. Temperature Control. The temperature of the bath is maintained at 500°F with a maximum deviation of ± 3°F. High temperature oxidation of a lubricant proceeds at an appreciable rate which doubles with a temperature rise of approximately 18°F. A total change in temperature of 6°F could therefore cause a measureable change in reaction rate.

b. Control of Air Flow Rate. The air flow rate is controlled by an oil filled manometer at a rate of 5.0 ± 0.5 liters per hour. This corresponds to a 10 percent deviation. In terms of moles of oxygen supplied to the system, it corresponds to a minimum of 0.0363 mole per hour and a maximum of 0.0443 mole per hour. This variation is caused by changes in pressure in the system during the oxidation, especially during violent bumping of the liquid. The flow rate requires frequent adjustment during a test run when bumping is occurring.

c. Analytical Methods. Recorder response in the gas chromatograph has been found to vary randomly and unpredictably. This variance is probably due to changes in output voltage of the batteries in the recorder circuit and by changes in line voltage. It has been found that these changes can vary over a 15-minutes period. To compensate for these changes, an air standard is included in each set of runs made on the instrument.

Another variance in results stems from the use of Relative Thermal Response Values. These values were calculated for one set of conditions on the gas chromatograph. Since these conditions are difficult to simulate exactly, there would be slight error when these values are used. However, these variances would be evident in methane and carbon monoxide percentage only since oxygen percentages are measured against air standards.

Evaluation of fluid properties involves qualitative and quantitative analysis of liquid products and their boiling ranges by temperature-programmed gas chromatography. Previous studies (AFML TR-70-304, Part III) have indicated that the factors affecting the analysis of compounds by temperature-programmed gas chromatography are column length, packing weight, bridge current, program rate, starting oven temperature, and carrier gas flow rate. The use of an internal standard provides a reproducible reference point for quantitative as well as qualitative analysis.

The packing material used in the silicone rubber column is commercially prepared. The solid support is Chromosorb P, a thoroughly washed diatomaceous earth, 60-80 mesh, with the stationary phase being a methyl silicone rubber, GE SE-30. These are packed in a 2-foot long piece of stainless steel, of 0.055-inch inside diameter and 0.125-inch outside diameter. A hand-held vibrator is used to aid in close and uniform packing of the columns. Matched pairs of columns with equal weights of packing are used so that liquid losses are matched in the columns.

The use of dual columns reduces the excessive baseline drift experienced in single column units by equalizing the loss of liquid substrate at high oven temperatures. The maximum operating temperature of the columns is about 620°F, above which there is excessive thermal degradation of the liquid substrate. This sets an upper limitation on the boiling points of compounds eluted by the column under a given set of conditions. This causes a buildup of any high boiling (>950°F) compounds injected into the column over a period of time. If the unknown sample is always charged to the same column the buildup of low volatility liquid will cause a high differential bleed rate and result in baseline drift. To balance the effect of this buildup, sample injection is alternated between the matched pair of columns. In this study, the oven temperature is programmed at a rate of 13.5°F per minute, from 122° to 608°F, with a carrier gas flow rate of 60 cubic centimeters per minute.

The mineral oils used do not lend themselves to quantitative analysis. The chromatograms of these samples are very broad peaks which extend over most of the temperature range and exclude the use of an internal standard. For temperature correlations on these samples an external standard is used, which consists of a mixture of normal paraffins boiling between 450° and 775°F. A homologous series gives a straight-line relationship between boiling point and retention time in adsorption chromatography. Retention times are measured from an air peak for correlation with mineral oil peaks. The 10 percent, 90 percent and initial boiling points are determined using this correlation as described earlier. A certain degree of error is incorporated in these

values, due to the uncertainty of a constant reference point, since an internal standard was not used.

The ester, di-2-ethylhexyl sebacate, exhibits a narrow boiling range and hence is ideal for qualitative analysis. Tridecane, $C_{13}H_{28}$, is used as an internal standard in homogeneous solution with the ester of approximately 15 percent by weight. A two-microliter sample of this mixture is injected into the chromatograph, and allowed to be eluted at the operating conditions. The resulting peaks are carefully cut off and weighed to obtain a ratio of the areas. If a constant weight of sample is injected each time, the amount of unreacted ester of a sample of oxidized ester is the simple ratio of the areas under the ester peak for that sample to the corresponding area for the original unoxidized ester. Since constant weight injection is difficult to perform with a microliter syringe, the area under each ester peak is reduced to a common standard. The ratio of area of the tridecane peak to the weight percent of tridecane is determined for the standard solution containing the unoxidized ester. This is a constant for identical weights of solution with the same concentration of tridecane. This would not be true if the sample contains any compounds which elute at the same time as tridecane. No such compounds are observed in these analyses. For oxidized samples, the ratio of peak area to weight percent of the tridecane is found. The correction factor for the ester peak of that particular sample is given by the ratio of the area to weight ratios of tridecane in the unoxidized and oxidized samples. The corrected area under the ester peak is given by the following:

$$\text{Corrected Area} = \left\{\begin{array}{c}\text{Raw Area of Unoxidized} \\ \text{Ester Peak in} \\ \text{Degraded Fluid}\end{array}\right\} \times \frac{(\text{area/weight \%})^{C_{13}}_{\text{standard fluid}}}{(\text{Area/weight \%})^{C_{13}}_{\text{oxidized fluid}}}$$

The percentage of ester degraded is calculated as follows: percent ester degraded $= 100 \left(1 - \frac{\text{corrected area ester in oxidized oil}}{\text{area of ester in standard}}\right)$. The percentage of products formed are also calculated in the same way. The amount of high boiling (>950°F) products formed could be estimated by the difference in the total corrected area of ester and products in the degraded fluid and area of ester in the standard fluid

4. Quantitative Oxidation Studies. Most conventional oxidation tests are designed to determine the effectiveness of oxidation inhibitors in providing an induction period during which there is little or no oxidation reaction. In these tests, the requirements for maintaining repeatable test conditions include adequate mixing of the fluid and saturation of the fluid with dissolved oxygen. Since there is little or no reaction during these tests, the test repeatability is not dependent to any significant degree on variables such as air rate, contact time, and air-oil contact area. It is possible, therefore, to provide standard repeatable test conditions for oxidation stable life with a minimum of specified test conditions beyond test temperature, nominal fluid volume and air rate.

If a significant rate of oxidation does occur, test repeatability is far more difficult to achieve. When oxidation does occur, the oxidation rate is a function of oxygen solubility in the liquid, liquid volatility in the air space, the diffusion rate of oxygen through the air-oil interface, the area of the air-oil interface, the contact time between the air bubble and the oil, the temperature of the system, the partial pressure of the oxygen at the air-oil interface, and the solubility of the oxygen in the oxidized oil. The dependence of oxidation rate on these variables increases the experimental problems in achieving test reproducibility. Repeatability for the determination of oxidation rate under oxidation conditions can be achieved by a careful control of all of these variables. To add a more complete understanding of oxidative damage to the fluid, the concept of oxygen tolerance is defined as the oxidative deterioration, i.e. the changes in viscosity, neutralization number, sludge formation, and corrosion, calculated on the basis of moles of oxygen assimilated per mole or unit volume of fluid. The combination of oxidation rate and oxygen tolerance will yield a useful life for the fluid under these high temperature oxidizing conditions in the same manner as stable life studies indicate a useful life in the lower temperature ranges.

a. Air-Oil Contact. In a diffusion limited reaction, the area across which the reactant diffusion takes place becomes a limiting factor. In a typical oxidation test the air is bubbled through the test fluid at a given rate and at a constant temperature. The area of air-oil contact in this type of test, becomes the total area of the surface of the air bubbles in the oil at any one time. The rate of bubble formation (bubbles per minute) times the residence time of each bubble (minutes) times the area of the bubble surface (centimeters square) results in the critical area of contact.

The area of contact between the air and the oil is a function of the number of bubbles rising in the fluid in unit time, the size of the bubble and the life of the bubble. The life of the bubble is the length of time the bubble resides in the oil. The bubble size is a function of the diameter of the air tube, the surface tension of the fluid and to a lesser extent the air flow rate. For a given flow rate of air through a fluid, the area of contact increases with decreasing bubble size, and increasing bubble life. The number of bubbles rising in the fluid in a given time depends on the size of the bubble and the air flow rate.

For the fluids tested, the exact bubble size can be calculated by counting the number of bubbles per unit time at a given air rate. This information will provide a volume per bubble and the bubble surface determined by assuming the bubble to be a sphere. These tests should be determined with a test fluid designed to match the viscosity of the test fluid at 500°F and the surface tension of the test fluid using the actual oxidation equipment. The description and physical properties of the test fluids are shown in Tables 3 and 4. MLO 7710 is a synthetic diester, di-2-ethylhexyl sebacate. The mineral oils range from a fairly high viscosity, high boiling oil to a low viscosity, low boiling oil. Three of the mineral oils are naphthenic, MLO 7625, MLO 7797, and MLO 7685.

The other two mineral oils are paraffinic, MLO 7789 and MLO 7478. These oils were chosen for their wide range of volatility and viscosity characteristics. The viscosities of these fluids at the test temperature of 500°F were calculated using the ASTM method for prediciton of viscosities. These values are listed in Table 5.

The viscosities of all of the test fluids are low at 500°F and the volatility or vapor pressure relatively high. The properties of normal heptane at 100°F tend to simulate the test fluid properties at 500°F. (Normal heptane, with a viscosity of 0.523 centistoke at 100°F, was chosen as the fluid to simulate the average fluid conditions at 500°F.) The high temperature oxidation test conditions were simulated with n-heptane at 100°F using standard test equipment and air rate. The life of the bubble in n-heptane was on the order of one second. The number of bubbles flowing through the fluid in one minute was 300 with the air flow rate at five liters per hour. The bubbles were counted in a five-second period using a stop watch. Ten separate counts were taken to determine the average. The average for the five-second period was 25 bubbles. Assuming spherical bubbles, the bubble diameter was determined to be 8.1 millimeters corresponding to an interfacial area of 206 square millimeters per bubble. Since there is an average of five bubbles in the fluid at any one time, the interfacial area due to the bubbles is 1030 square millimeters. This corresponds to a bubble diameter of 9.8 millimeters at the test temperature of 500°F assuming ideal gas behavior. The surface area of the bubble corresponding to this diameter is 302 square millimeters making the interfacial area due to the bubbles 1510 square millimeters. This bubble area plus the liquid surface in the oxidation tube gives the average interfacial area available for diffusion of oxygen into the oil during the oxidation, using a 2.5 millimeter i.d. air inlet tube.

The area of the air-oil interface is increased if the bubble size is decreased at constant flow rate. The bubble size may be decreased by providing a means of obstruction in the bubble path which causes the bubble to break up or by the use of an air filter which distributes the air as a series of small bubbles in the fluid. In one test run, di-2-ethylhexyl sebacate was oxidized in a tube packed with short lengths of six millimeter glass tubing. The oxygen assimilation results on this test are compared with the oxidation of the ester in an open tube in Figure 11. The fluid height was the same in both tests. The test in the packed tube consumed considerably more oxygen than the one in the open tube. The rates of oxygen absorption for the two tests are shown in Figure 12. In a simulated experiment air was bubbled through normal heptane in the packed tube at room temperature. The air bubbles were observed to break up into a series of smaller bubbles, some of which became trapped in the packing for varying lengths of time. The increase in oxidation rate is therefore the result of increased interfacial area and increased bubble life.

Previous tests conducted at the Petroleum Refining Laboratory (WADC-TR-55-30, Part IV) show that if the air-oil interfacial area is continually increased at a test temperature of 500°F, the oxidation rate increases sufficiently to consume all of the oxygen in the air flowing

through the reacting fluid. This level of reaction rate can be achieved with mineral oils and esters of the types used in this study. In order to make meaningful comparisons of oxidation rates at elevated temperatures such as 500°F, it is desirable to choose test conditions so that the most stable fluids show some oxygen assimilation and the least stable fluids use less than the total available oxygen in the air used. For comparison of oxidation rates at 500°F an air rate of five liters per hour dispersed with a 2.5 millimeter i.d. air tube provides the desired relative oxidation rates for the fluids used in this study. The larger bubbles in the open tube show a minimum change in interfacial area for the variations of test conditions studied. The oxidation of oils is often accompanied by the formation of sludge which sometimes collects at the tip of the air inlet tube. Such a condition would decrease the number of bubbles produced by an air sparger. The effect would be less severe for the capillary air inlet used in this study. The high air flow rate in the single capillary tends to keep the discharge end of the tube clear of sludge.

The time of contact of the air bubble and oil is a function of the height of fluid in the reservoir, the bubble size, and the density and viscosity of the fluid. The height of fluid in the oxidation tube is the length of the bubble path. The bubble size and the density and viscosity of the fluid together determine the velocity with which the bubble will rise in the open tube. The rate of oxidation of an oil increases with an increase in contact time of the air bubble and oil. For a given flow rate of air in a fluid, the contact time of the air and oil may be increased by increasing the height of fluid charged to the apparatus. The effect of increased fluid height is illustrated by a series of tests conducted previously at the Petroleum Refining Laboratory (WADC-TR-55-30, Part IV). One test was conducted with a charge of 100 milliliters in a regular oxidation tube using a 2.5 millimeter i.d. capillary air inlet tube. The charge for another test was 800 milliliters in a series of four oxidation tubes, each containing 200 milliliters of fluid and utilizing a 2.5 millimeter air inlet tube in each unit. The fluid is di-2-ethylhexyl sebacate inhibited with 0.5 weight percent of phenothiazine. The oxygen assimilation results from these two tests are shown in Figure 13. In the test with 800 milliliters of fluid, the exit gas from the first oxidation tube is passed through a cold trap to remove the condensible vapors and then used as the charge to the second tube. This process is repeated between the second and third and the third and fourth tubes. The length of the bubble path in the test fluid for this test is eight times that of a test with a charge of 100 milliliters of fluid. The average percentage of oxygen absorbed by the test fluid with eight times the bubble path is 3.7 times that of the short path test. The reason for this nonlinearity in oxygen assimilation as a function of contact time of the bubble is the decrease in the partial pressure of oxygen with increased contact time. During the test with the long fluid path, the partial pressure of oxygen is decreased by oxidation and the formation of gaseous reaction products.

A comparison of Figures 11 and 13 shows the effect of the oxidation inhibitor on the reaction. The high rates of oxygen assimilation experienced with the increased bubble path have some of the

same disadvantages as the use of smaller bubbles to increase reaction rate. Increased areas of air-oil interfaces and increased contact time have the same effect on partial pressure of oxygen. The bubble path for the standard test conditions used in this study provides the desired oxidation rates and test repeatability.

The driving force for the diffusion of oxygen into the oil during an oxidation reaction is the concentration gradient across the air-oil interface. This concentration gradient is a direct function of the partial pressure of oxygen in the air bubble. There is a reduction of partial pressure of oxygen as the bubble of air rises in the fluid. This reduction is uniform and does not present a problem in reaction control. The diffusion of volatile products into the air bubble at random times causes irregular pulses in the partial pressure of oxygen in the air bubble and in the total pressure of the reaction. This condition is observed from its effect on the flow rate during a reaction where the volatile products are not allowed to escape without refluxing. The flow meter which measures air rate showed sudden and abrupt changes and required adjustments to maintain a flow rate of 5.0 liters of air per hour. This problem involving volatile products will be discussed further in a later section.

The rate of flow of air through the reacting fluid determines the amount of oxygen available for reaction in unit time. The number of bubbles rising in the oil in unit time is determined by the size of the bubble and the air flow rate. Increasing flow rates result in increasing reaction rates. However, the relationship of oxidation rate and air flow rate is not linear. This is due to bubble interaction at high flow rates. There is a tendency to increasing bubble size and collision and coalescing of the bubbles to form larger bubbles thus decreasing the air-oil interfacial area. A series of tests performed at the Petroleum Refining Laboratory investigated the effect of increasing flow rate on the rate of oxidation. Air flow rates of up to 30 liters per hour were used in the oxidation of inhibited di-2-ethylhexyl sebacate using a sintered glass air filter. One set of these tests was performed in an open tube and the other in a tube packed with glass beads. The results of these tests are compared in Figure 14. The rate of oxidation increases at a decreasing rate as the flow rate of air is increased, however the rates do not show a limiting value for air flow rates of 30 liters per hour. The test in the packed tube shows a lower rate of oxidation than the test in the open tube. This is the opposite effect exhibited by a packed tube experiment shown in Figure 11. Whereas the larger bubbles produced by the capillary air line are broken up by the packing and trapped for periods of time, the smaller bubbles from the air filter collect on the packing surface and coalesce into larger bubbles

The goal of an oxidation test to evaluate fluids at high temperature is to produce relative oxidation rates at a given temperature or as a function of temperature that can be related to practical high temperature systems. Such tests over the range of fluid types and temperatures should produce oxidation rates of less than 100 percent but more than one percent of the available oxygen assimilated In order to minimize the experimental error a relatively constant air-oil

interface is desirable. The use of an air rate of five liters of air per hour entering the fluid through a 2.5 millimeter inside diameter glass capillary tube appears to provide a nearly constant air-oil interface with a measurable reaction rate for all fluids evaluated at 500°F and an indication of less than 100 percent oxygen assimilation at temperatures of 600°F.

It appears that this type of test apparatus and procedure could be calibrated and related to the kinetics of the oxidation reaction by the use of a calibration technique using fluids with established kinetics to measure the relative effects of diffusion on the kinetics. From the data available it appears that a substantial increase in the air-oil interface would not be desirable because at the high values of interfacial area most of the lubricants tested will use almost all of the oxygen available at 500°F. The trends indicated here are predicted by the study but not specifically determined. Further specific work in this area of data correlation is required.

b. Solubility of Oxygen in the Fluid

(1). The Role of Fluid Properties. The solubility of oxygen in mineral oils and organic acid esters shows a slight increase with increasing temperature. Increasing molecular weight and viscosity level of the liquid decreases oxygen solubility. If there is no reaction between the dissolved oxygen and the fluid, maximum oxygen solubility is achieved at the temperature at which the test fluid exhibits a vapor pressure of approximately 60 millimeters mercury absolute. Generally, oxygen concentration in mineral oils and esters is limited at high temperatures by the rate of reaction between the fluid and the dissolved oxygen. The point at which measured oxygen solubility versus temperature falls below a straight-line relationship indicates that point at which the rate of oxygen reaction with the fluid exceeds the rate of oxygen diffusion into the liquid phase.

Another significant problem affecting the solubility of oxygen in liquids is the presence in the liquid and/or gas phase above the liquid of other gaseous components. In the case of oxidation of mineral oils and esters the volatile oxidation products such as water, carbon monoxide, carbon dioxide, and volatile organic oxidation products all act to reduce the solubility level of oxygen in the fluid. This reduced solubility limit then acts to reduce the concentration of oxygen for the reaction thereby affecting reaction rate.

(2). Assimilation of Oxygen by the Fluids. In this study several oils were oxidized at 500°F with air bubbled through the fluid at five liters per hour. These fluids exhibit a wide range of physical properties. Viscosities range from 3.22 to 76.9 centistokes at 100°F. Tables 3 and 4 list the physical properties of these fluids. The mineral oils exhibit wide boiling ranges which make quantitative liquid product analysis by gas chromatographic techniques difficult. The synthetic diester exhibits a narrow boiling range and quantitative analysis of the liquid product was performed by temperature-programmed gas chromatography using tridecane as an internal standard. Hourly samples of the exit gas were analyzed by gas chromatographic techniques

for oxygen assimilation data. The percentage of oxygen assimilated by the fluid is determined by comparing the composition of the inlet and exit gas streams.

The average volatility characteristics of each of the fluids under the conditions of oxidation were determined by a simple method. The stripping action of the flow of air through the fluid during oxidation was simulated by the use of nitrogen at 5.0 liters per hour at the test temperature in the oxidation apparatus. Two tared cold traps were connected to the exit gas line from the oxidation in such a way that the flow of the gas stream could be directed through either trap while the other is removed for weighing. Both cold traps were maintained at -109°F by dry ice and acetone. The cold traps were alternated during the experiment and the weight of the fluid removed by stripping was obtained at 1, 3, 5 and 7 hours for each of the fluids. The results of these tests are shown in Figure 15. The lowest viscosity mineral oil, MLO 7685, lost the most fluid due to stripping, with 3.80 weight percent stripped over after three hours The highest viscosity mineral oil, MLO 7625, showed no measurable loss of fluid due to stripping after seven hours of testing.

The distillation ranges of these mineral oils were than determined by temperature-programmed gas chromatography. A two microliter sample of the oil was injected into the chromatograph and the instrument programmed from 122° to 608°F at a rate of 13.5°F per minute. The area of the resulting chromatograph was carefully measured and the 10 and 90 percent elution points determined. By comparison with the normal boiling point-retention time relationship for a series of normal paraffins of known boiling points, the temperatures of the 10 and 90 percent elution points along with the initial boiling point were determined. The results of these determinations for the five mineral oils are shown in Table 6. These results are in agreement with the trends of volatility of the fluids observed in the stripping of the oils by nitrogen.

Each oil was then oxidized at 500°F with air bubbling through the fluid contained in a semi-micro tube at 5.0 liters per hour. A heated jacket was used to aid in the removal of the volatile reaction products from the reaction vessel with a minimum of bumping. The exit gases were analyzed at hourly intervals. The percentages of oxygen absorbed are listed in Table 7 for the pure mineral oils. These values are plotted as a function of time in Figures 16, 17, 18, 19 and 20. Oxygen absorption values are observed to increase with the volatility of the fluid in most cases. The fluid with the lowest volatility, MLO 7625 showed essentially a constant percentage of oxygen assimilation as a function of test time The fluids exhibiting high volatility characteristics, for example MLO 7685, gave an exaggerated maximum value of oxygen assimilated after one hour of oxidation and then the assimilation rate decreased sharply to a fairly steady value after approximately four hours of reaction time. The 10 percent boiling point of each fluid was plotted against the percentage of oxygen absorbed at four hours. The curve is shown in Figure 21. The oils seem to follow a general trend of increased oxygen absorption with volatility The 10 per cent boiling point appears to give a better indication of the volatility of the fluid

than does the initial boiling point, because the initial boiling point may represent only very small concentrations of volatile materials. An example of this is shown by the distillation ranges of the heavy naphthenic mineral oil, MLO 7625 which exhibited a difference of 204°F between the initial and 10 percent boiling points.

The low viscosity naphthenic mineral oil, MLO 7797 exhibited lower oxygen absorption values than were expected on the basis of its volatility characteristics. This oil was not as well refined as the other oils tested and may contain small concentrations of polar impurities which act as natural inhibitors. These compounds, however, could not be detected readily by conventional analytical methods.

The rates of oxygen absorption for the five oils are shown in Figures 22, 23, 24, 25 and 26. These rates of oxidation, calculated on the basis of moles of oxygen absorbed by one mole of fluid show that the two paraffinic oils MLO 7789 and MLO 7478 have absorbed the most moles of oxygen per mole of fluid in this series. This interpretation of the data, however, does not present a true picture of the reaction. This method implies that the fluid deterioration is directly related to oxygen assimilation on a mole for mole basis. In a diffusion limited liquid phase oxidation, oxidation of primary, secondary, and tertiary oxidation products appear to be involved in the overall oxidation reaction. The use of moles of oxygen per mole of fluid would certainly be a better indication of the quantity of fluid affected in a vapor phase oxidation. In general the higher the reaction temperature in liquid phase oxidation the larger the fraction of molecules of liquid oxidized from a given quantity of oxygen reacted. In the temperature range of 400° to 500°F for high boiling liquids, three to five moles of oxygen may react on the average with one mole of hydrocarbon or its decomposition products.

The diffusion limited nature of the oxidation in the liquid phase may be responsible for the type of reactions described here. In a diffusion limited system, the molecules of oil are not contacted on an equitable basis by the molecules of oxygen. The reaction is localized in a small area surrounding the air bubbles. The degree to which new fluid from the bulk moves toward the reaction site and reacted molecules move toward the bulk depends on the mixing in the system. Quantitative studies with di-2-ethylhexyl sebacate have shown that the mixing in the system does not approach such equity in the distribution of molecules. For calculated rates of more than one mole of oxygen per mole of ester, the analysis of the degraded fluid shows that a very small fraction of a molecule of ester is degraded. The mole per mole interpretation of the data is misleading as a representation of the oxidation reaction in that it includes the bulk fluid in the reaction scheme and is not sensitive to reactions of primary and secondary reaction products with oxygen. The moles of oxygen reacted as a function of 200 milliliters of liquid represents a better comparative measure of oxidation than a mole for mole basis This method of presentation of data (Figures 16 to 20) is based on the differences in the inlet and exit concentrations of oxygen in the oxidizing gas and does not make any assumptions about the fluid or the mechanism of the reaction. It is therefore deemed appropriate for this type of comparative study of diffusion limited systems.

The products of the oxidations of these mineral oils were separated into oxidized and virgin fractions by liquid column chromatography. The fractions obtained from these columns were checked by infrared spectroscopy to ascertain when good separation was achieved. An example of the separation achieved is shown by the infrared spectra of the low viscosity naphthenic mineral oil, MLO 7685. Figures 27, 28, and 29 show the spectra of the original oil, the virgin fraction and the oxidized fraction, respectively. A comparison of the spectra of the original oil and the virgin fraction of the degraded fluid shows that there is an absence of a peak at 12.7 microns in the virgin portion which is the only difference in the two figures. This peak corresponds to the frequency of an aliphatic side chain which may have been removed by oxidation. The spectrum of the oxidized fraction shows the presence of alcohol, carbonyl and double bonded compounds. This spectra shows separation was achieved by the use of the liquid column chromatography. The virgin fraction of the oil was analyzed by temperature-programmed gas chromatography and the initial, 10 percent and 90 percent boiling points determined. These results are shown in Table 8 along with the initial boiling point of the oxidized product of the three most volatile fluids. These data show an increase in the initial boiling point of all of the fluids oxidized. This increase in initial boiling point after oxidation is the result of the combined effect of the stripping action of the flow of air through the oil and the vapor phase oxidation of light ends. These data also show that the separation of the fluids by percolation through a liquid column removes low boiling oxidation products. This is shown by the differences in initial boiling point before and after chromatographic separation of the oils.

(3). The Role of Oxidative Deterioration. The oxidation of lubricating oils is accompanied by the formation of a variety of volatile and nonvolatile products. It has been shown in previous studies that in the oxidation of super-refined mineral oils at 500°F, about 80 percent of the oxygen absorbed by the oil goes toward the formation of volatile products. These products are principally water (60 percent), the gases carbon dioxide and carbon monoxide (20 percent), and lesser quantities of volatile acids. The liquid products, including the volatile acids accounted for 20 to 24 percent of the oxygen adsorbed with products such as ketones, aldehydes, acids, alcohols and esters.

In this study, the amount of volatile products being stripped out of the reaction vessel into the cold traps was measured during the oxidation of the high boiling naphthenic mineral oil, MLO 7625. The weight of the volatile products was obtained in the same manner described earlier for the stripping operation with nitrogen. The weight percentage of the volatile products collected was determined after 1, 3, 5 and 7 hours of reaction. The values obtained are shown in Figure 30. The volatile products exhibited a rapid build-up during the first four hours of reaction after which the quantity of volatile products in the fluid remained about the same.

The oxygen assimilation curves generally decreased from an initial high value to a lower value after approximately four hours. The production of these volatile products probably affected the rate of

diffusion of oxygen into the oil.

The oxygen absorption values for two consecutive test runs with di-2-ethylhexyl sebacate, MLO 7710, are compared in Figure 31. An experiment was conducted to investigate the effect of removal of these volatile products on the oxygen assimilation by the fluid. The pure ester was oxidized for five hours. The oxidized product was then subjected to reduced pressure using a vacuum pump for about 12 hours to remove the volatile oxidation products. The pressure in the apparatus was restored to atmospheric by allowing nitrogen into the oxidation tube. The degassed product was then oxidized for an additional five hours. The oxygen assimilation values for these two tests are shown in Figure 32. These data show that the removal of the dissolved volatile products from the fluid restored the oxygen assimilation values to the original level. It should be noted that nonvolatile oxidation products are not removed by this process. The high level of oxygen absorption for the degassed, oxidized fluid is short lived and the oxygen assimilation rate decreases to a lower value. The shorter increment of high oxygen assimilation rate with oxidized fluid is probably due to the presence of reactive oxygenated molecules in the fluid which react to build up rapidly the concentration of volatiles in the fluid necessary to affect diffusion of oxygen into the oil. The effect of vacuum stripping on the degradation of the liquid product is shown Figure 33. There is evidence of increased degradation in the fluid after the fluid is degassed. The volatile products in the fluid may also be removed by stripping the fluid with a flow of nitrogen. An oxidized ester was stripped by nitrogen flowing at five liters per hour for one hour at room temperature and gave a 0.03 percent loss in weight. When this fluid was further subjected to vacuum stripping for five hours there was a 1.01 percent loss in weight.

The effect of these small concentrations of volatile products was further elucidated in a series of test runs with the heavy naphthenic mineral oil, MLO 7625. The fluid was oxidized for a total of eight hours at 500°F (test run number 9). The product of this test was subjected to vacuum stripping for twelve hours and then oxidized for an additional eight hours (test run number 10). The oxygen assimilation values for these two test runs (number 9 and 10) are shown in Figures 34 and 35. A low rate of oxidation was recorded for the fluid from which the volatile products were removed (test run number 10), however, the shape of the curve is similar to that of the original. The level of the oxygen assimilation curves is subject to changes within the reaction vessel due to bumping and the resultant temperature change and to analytical error due to variation in the signal to the gas chromatograph recorder.

The errors due to signal problems with the gas chromatograph recorder are the most difficult to determine and eliminate. On any given day the concentration of oxygen could be determined to $\pm$ 3 percent of the determined value. However, due to long time changes in the gas chromatograph, directional drifts in the level of the entire set of oxygen values measured for a given system could change as much as seven percent over the year during which data were taken with the same chromatographic unit.

Oxygen absorption values as a function of test time may vary as

much as ± 10 percent from the smooth curve because of the problems of bumping and the resultant temperature control for tests using an air condenser. Tests using a heated air space show less than ± 6 percent variation of individual points from the smoothed curve. The differences between the data points obtained in the cases of the air condenser and the heated gas space provide a good indication of the problems involved in thermal control of the test system.

In order to obtain gas samples for exhaust gas analysis that fall within these error tolerance limits it is necessary to take the gas samples under carefully controlled conditions. The gas samples taken through the capillary must be taken at a flow rate somewhat below that of the total exhaust gas from the reaction to avoid leaks and contamination from room air.

Since the removal of the volatile products from the fluid restored the oxygen assimilation level to its original value or close to it, the shape of the curve of oxygen assimilation appears to be the result of the production and subsequent build-up of small concentrations of these volatile products in the fluids. To check the validity of this theory, the original oil was oxidized for eight hours in test number 16 and a 50:50 mixture of the oxidized product and the original stock was prepared and oxidized further for eight hours (test number 17). The oxygen assimilation values for these two test runs (number 16 and 17) are shown in Figures 36 and 37. These data show that for the mixture containing the oxidized oil, including the volatile products (test run number 17), the initial high level of oxygen absorption was not observed.

This effect of oxidized products on the level of oxygen assimilation of the fluid has been observed by numerous investigators. There is little evidence of attempts to determine the cause of the decreased rate of oxidation with time. Suggestions have been made that the reduced oxidation rate may be due to the formation of natural inhibitors as oxidation products during the reaction. If this is the case, the effect of the inhibitor could be shown for very small concentrations of the inhibitor in the oxidized stock. A mixture of 10 percent of oxidized oil in virgin stock was prepared and oxidized in test run number 18. The oxygen assimilation values are shown in Figure 38. There is essentially no difference in the values for this test from those from the oxidation of the pure oil in test number 16. The product of test run number 18 was subjected to vacuum stripping for 12 hours and then oxidized for an additional eight hours in test run number 19. The results, in Figure 39, show that the level of oxygen assimilation rose to essentially the original level exhibited by the virgin stock. The shape of the curve follows the trend obtained by the oxidation of the virgin stock. The level of oxygen absorption rose to a high value and rapidly decreased to a lower steady value. The decrease to the lower value is decidedly more rapid for the degassed, degraded fluids than for the virgin stock. The shape of these curves could also result from the oxidation of easily oxidizable materials in the oil. To investigate this theory, the product of the reaction in test run number 19 was subjected to liquid column chromatography, where the liquid product was percolated through alumina to separate the unoxidized fraction from the oxidized fraction of the oil. The

unoxidized fraction of the oil was then oxidized for eight hours in test run number 20. The oxygen assimilation values shown in Figure 40 are almost identical to those of the virgin stock and the 10 percent oxidized oil in the virgin stock. The percolation of the degraded fluid is also an effective degassing procedure. A check run was made with the virgin fluid in test run number 21. The results of this test are shown in Figure 41. The oxygen absorption curve for this test is similar to those of tests number 16, 18 and 20.

The series of test runs 16 through 21 has shown that the shape of the oxygen absorption curve is probably a result of the production and build up of small concentrations of volatile products in the fluid. The removal of these products appears to restore the level of oxygen absorption to its original level. No evidence has been found to support the theories that natural inhibitors are formed as reaction products during the oxidation of lubricating oils or that easily oxidizable components in the oil are oxidized rapidly at the beginning of the reaction. These data have shown that the addition of oxidized fluid to the virgin stock in quantities sufficient to provide enough volatile products to affect diffusion of oxygen into the oil, would inhibit the oxidation at high temperatures, by reducing the rate of diffusion of oxygen into the oil.

c. System Temperature

(1). The Effect of the Exothermic Reaction. The oxidation of a lubricating oil is an exothermic reaction. The amount of heat evolved depends on the extent of reaction between the oil and oxygen. At high temperatures, the heat generated by the oxidation reaction affects the system temperature appreciably. Temperature measurements were made in the vapor and liquid phases during the oxidation of a low boiling naphthenic mineral oil MLO 7797. The low boiling naphthenic oil was selected to include significant liquid and vapor phase reactions. The temperatures were measured with copper-constantan thermocouples. The thermocouple in the liquid phase was placed in the path of the air bubbles. Two separate tests were conducted for a system with a heated jacket and one with an air cooled condenser. Figure 42 shows the temperature in the liquid phase for the two tests as a function of time. The corresponding values for the vapor phase temperature are shown in Figure 43.

These measurements were made by first bubbling nitorgen through the oil until a steady state temperature was attained. This temperature was attained within twenty minutes and recorded as the temperature at zero time. It can be noted that the temperature of the fluid with nitrogen mixing but no reaction is 484°F or 16°F below the constant-temperature bath. The cooling effect noted from a flow rate of five liters per hour of nitrogen is assumed to be a combined function of the heating of the cold nitrogen by the oil and the limited heat transfer through the glass tube from the 500°F bath.

The magnitude of the temperature increase when air is substituted for nitrogen is indicative of the extent of reaction. However, it should be noted that these temperatures are measured in a non-equilibrium

system where heating and cooling forces operate simultaneouly. There is an initial increase of 8.5°F for the reaction with the heated jacket and an increase of 4.4°F for the reaction with the air cooled condenser. The lower temperature of the test with the air cooled condenser is due to the cooling effect of the refluxing condensable products for which the bulk liquid must resupply the sensible and latent heat of vaporization of these condensed vapors. The temperatures of the test with the air cooled jacket also show fluctuations. These are caused by collection of liquid drops in the condenser and the nonuniform return of these materials to the liquid reservoir. All of the temperatures recorded are representative of system temperature at a specific time. It is not feasible to draw a smooth curve through the points. The temperatures recorded for the test with the heated jacket show less variation because of the substantial reduction of refluxing and bumping in the system. This reduction of the cooling effect gives a temperature increase for the test liquid that is approximately that due to the heat of reaction.

The vapor temperatures in Figure 43 show trends similar to the liquid temperature. A temperature increase of 8°F was recorded for the reaction in the gas phase with the air cooled condenser compared with an increase of 59°F in the gas phase for the test with the heated jacket. However, the vapor temperatures in the air condenser are subject to cooling and condensation at the condenser wall.

The cooling effect of these condensed vapors and the heat loss at the condenser wall is dramatized by the difference in vapor temperatures with the heated jacket and air condenser system. The heated jacket was maintained at about 212° to 214°F, to prevent the condensation of water and other equally volatile products on the walls. The jacket, therefore, served to reduce substantially heat loss at the condenser wall. The temperatures measured in this vapor space for the system with the heated vapor space were generated from the heats of reaction of vapor phase oxidation.

(2). Effect of the Heated Jacket. The use of the heated jacket on the gas space in the oxidation tube promotes the removal of volatile products. This system design substantially decreases the loss of heat through the condenser walls. The resultant high vapor temperatures increase the vapor phase reaction rates. The vapor temperature is 220°F higher in apparatus with the heated jacket than in the apparatus with the air condenser. The reduction of reflux from the condenser also affected the temperature of the liquid resulting in a temperature increase of 3°F. This temperature increase is in agreement with the differences in temperature and oxidation rates noted between oxidation tests with and without excessive bumping from condensation.

These differences in liquid and vapor temperature appear to have a significant effect on the rate of assimilation of oxygen by the fluid. The major increase in oxygen assimilation appears to occur in the vapor phase. The high boiling naphthenic mineral oil, MLO 7625 was oxidized at 500°F in one test with an air condenser and the other with a heated jacket. The comparison of oxygen assimilation values for these two tests is shown in Figure 44 The test with the heated jacket consumed

50 percent more oxygen than the one with the air-cooled condenser. The difference in liquid phase temperatures is approximately 4°F which would predict a 22 percent increase in rate if the reaction were kinetically controlled. This would attribute about 28 percent of the reaction to vapor phase oxidation. To illustrate this point further similar tests were run with di-2-ethylhexyl sebacate. The results of these tests are shown in Figures 45 and 46. There was a dramatic increase in the amount of oxygen absorbed by the ester in changing from the air condenser to the heated jacket. The heated jacket test consumed about 2.6 times as much oxygen as the air condenser test. The degradation of the ester was monitored by temperature-programmed gas chromatography. The fraction of unoxidized molecules remaining in the degraded fluid was calculated for hourly samples and plotted as a function of time in Figure 47. These results show that the test with the heated jacket was 1.2 times as severe as that in the air-cooled condenser. The remainder of reaction which occurred is therefore due to the oxidation of primary and secondary reaction products in the vapor phase.

The vapor pressure of the mineral oil MLO 7625 and di-2-ethylhexyl sebacate are about the same. In both cases little vapor phase oxidation is anticipated because of the low vapor pressure (10 to 15 mm Hg) of the original fluid at 500°F. The increase in vapor phase oxidation in both cases is due to the primary oxidation products that are more volatile than the original material. The ester decomposition in the liquid phase generally yields a C_8 olefin which would be volatile at the test temperature. The primary liquid phase oxidation product of the mineral oil is probably no more volatile than the original mineral oil. Secondary oxidation products of the mineral oil may produce volatile products. The relative increase in oxygen uptake in the case of the heated gas space does correlate well with the relative amounts of volatile oxidation products produced in the liquid phase.

For most tests performed with the air-cooled condenser on the ester and mineral oils, an average of 30 percent of oxygen was absorbed by the fluids. The temperature profile of the reactions suggests that little vapor phase reaction occurred under these circumstances. The 30 percent of oxygen absorbed is therefore attributed to liquid phase oxidation of the fluids. The remainder of the absorbed oxygen is attributed to vapor phase oxidation of volatile oil and volatile reaction products. On this basis it was calculated that an average of 0.019 mole of oxygen or 47.5 percent of the absorbed oxygen reacted in the vapor phase during the oxidation of the ester. From the liquid product analysis in Figure 47 and previous data (Table 9), it was determined that an average of 0.0065 mole of volatile reaction products (average molecular weight 175) was available in the vapor phase for reaction. This corresponds to 3.0 mole of oxygen reacting with each mole of reactant. Di-2-ethylhexyl sebacate is a high boiling ester. Therefore the vapor phase reactants would involve essentially no original ester. The multiple reaction of intermediate products is substantiated by the dramatic increase in the production of carbon monoxide and carbon dioxide. The percentages of carbon monoxide in the exit gases of the two tests with di-2-ethylhexyl sebacate are compared in Figure 48. The percentage of carbon monoxide in the heated jacket test is 5.4 times as much as that in the test with

the air condenser. (Due to experimental difficulties carbon dioxide determinations were not done in this experiment.) The increase in production of carbon monoxide which is a product of incomplete oxidation indicates multiple oxidation of a hydrocarbon or oxygenated molecules.

In the series of mineral oils tested, it was determined that a small percentage of the virgin fluid was removed by the stripping action of the air flow (Figure 15). Using these values and the assumption that 30 percent of the available oxygen was due to liquid phase oxidation, it was determined that one mole of the vaporized fluid reacted with or consumed about one mole of oxygen in the initial oxidation reaction of each of the oils.

These results show that the major differences measured in the tests with the heated jacket was in the vapor phase oxidation of the fluids and their reaction products. The heated jacket, while offering better control of some of the reaction variables, shifted the emphasis of the reaction from the liquid to the vapor phase. High temperature oxidation tests with heated vapor space may be misleading as a basis for relative oxidation stability or oxidation rate. It can be seen that the oxygen assimilation can be changed substantially by vapor phase oxidation. The effect of low volatility products, if any, formed by the vapor phase oxidation provides an unknown effect on the liquid product and the liquid phase oxidation.

(3). The Effect of Geometry. The geometry of the test system is an important consideration in the interpretation of data from an oxidation test. In this study, three different sizes of oxidation tubes were used; regular, semimicro and micro. Approximately the same height of liquid in the test tube was maintained with fluid charges of 200 milliliters in the regular tube, 65 milliliters in the semimicro tube and 25 milliliters in the micro tube. The inside diameters of the three tubes are 34, 18, and 10 millimeters, respectively. The air inlet tube has an outside diameter of eight millimeters. This allows an annular space of 13, 5, and 1 millimeters, in the regular, semimicro and micro tubes respectively, between the wall of the oxidation tube and the air tube. The average air bubble diameter from the standard air tube was determined to be 9.8 millimeters. In test systems where the annular space is smaller than the diameter of the air bubble, the shape of the bubble is distorted and the time of rise is altered. In extreme cases such as the micro test, the formation of large bubbles by coalescence has been observed. In the micro apparatus the bulk of the fluid is forced to provide a good contact with the air-oil interface. That is, the rising bubble tends to fill the annular space except for a thin film of liquid on each tube wall. The degree of mixing and the overall geometry in the micro test provides for much better diffusion per unit volume of liquid than is the case in the other two tests.

The rate of diffusion of oxygen into the oil would be the same for the same bubble size, bubble contact time and temperature. These factors are essentially the same for the full size and semimicro tests. In the case of the micro test the time of contact may be about twice that in the other two tests and, in addition, fluid mixing and the thin

layer of fluid between the bubble and the tube walls should tend to favor a higher reaction rate than in the other two tests. The same amount of oxidation in smaller liquid volumes should also cause a more rapid buildup of volatile oxidation products which may reduce the driving force for the diffusion of oxygen into the oil. The vapor phase oxidation effect has been shown to be important in these high temperature oxidation tests. The size of the vapor space is not significantly different in the three tests. The liquid-vapor space interface does differ significantly. It is assumed that the mechanism of transfer to the vapor phase is primarily volatility and entrainment. The role of the excess air is to sweep away continuously the volatile molecules as they leave the liquid surface, and to contribute to the entrainment of less volatile material into the gas space and thereby contribute to vapor phase oxidation. Entrainment loss should increase with the reduction in free surface of the test tube and the outside diameter of the air tube. The vapor phase oxidation effect should therefore increase in order from the regular to the semimicro to the micro test.

To determine the overall effect of these factors affecting oxidation rate as a function of test system size and geometry, a series of runs in the regular and semimicro test systems was made using di-2-ethylhexyl sebacate. The results of these tests are shown in Figure 49. The data show an increase rate of oxidation for the semimicro test over the regular test based on percent of the oxygen assimilated. It should be emphasized that the di-2-ethylhexyl sebacate shows a substantial component of vapor phase oxidation in the tests previuously described. It appears that the increase in total oxidation reaction in the semimicro test over the regular test is probably due primarily to the vapor phase oxidation component. The oxidation rate for these tests is shown on Figure 50 based on moles of oxygen reacted per mole of fluid. In this comparison the increased oxidation rate for the semimicro test is more apparent. The moles of oxygen per mole of fluid is three times as high in the semimicro test as in the regular test but the rate of reaction is about four times as high. These comparative tests were evaluated in a third way as shown in Figure 51. In this case the percentage of unreacted di-2-ethylhexyl sebacate was determined by temperature-programmed gas chromatography. The semimicro test on this basis appears to be about 1.3 times as severe as the regular test based on the percent of original ester oxidized. It should be emphasized that this analysis applies only to the liquid phase product remaining in the test tube after the test. These three evaluations of oxidation imply that the amount of vapor phase oxidation both primary and secondary is very high in these tests. The data indicate further that there is probably a higher percentage based on the charge of the liquid in the semimicro test that is vaporized and entrained into the vapor phase than is the case with the regular test. The relatively high component of vapor phase oxidation is shown by other tests on di-2-ethylhexyl sebacate conducted in this series.

A comparison between oxidative severity in the semimicro and micro oxidation test procedures has been carried out with a paraffinic mineral oil, MLO 7789. An eight-hour test time has been used in this comparison at 500°F and an air rate of five liters per hour as shown in Figure 52. In general the paraffinic mineral oil shows about the same rate of oxidation in the liuqid phase but less vapor phase oxidation than

the diester used to compare the regular and semimicro tests. The semimicro test for the ester and paraffinic mineral oil compare very well as shown by Figures 49 and 52 and 50 and 53, respectively. The comparison of the oxygen assimilated shows clearly a higher rate in the micro than in the semimicro test. The trends are consistent in that the smaller the volume of liquid and the better the air-oil contact with increased volatility loss and entrainment the higher the amount of oxygen assimilated. The higher level of oxygen assimilated in the micro test is also shown in Figure 53 by the 4 to 1 ratio of the moles of oxygen reacted per mole of fluid compared with the semimicro test. The wide boiling range of the paraffinic oil precludes a quantitative evaluation of the remaining virgin fluid after the test by simple temperature-programmed gas chromatography. The similar trends between the regular and semimicro test, and the semimicro and the micro test show a consistent and significant trend based on the geometry of the test system.

d. Products of Oxidative Degradation. A complete identification of the products formed during the oxidation of uncatalyzed di-2-ethylhexyl sebacate at 500°F is discussed in AFML-TR-70-304, Part III. A list of these products is shown in Table 9. Of the products identified, 2-ethylhexyl perlagonate is produced in the largest percentage. Other products identified are 2-ethyl-1-hexene, 2-ethyl-1-hexanol and mono-2-ethyl-hexyl sebacate. The olefin 2-ethyl-1-hexene is stripped out of the oxidation apparatus along with 2-ethyl-1-hexanol and collected in the hold trap. Other products detected in the condensed vapor are 2-heptene, 3-heptanol and 2-ethyl-1-hexanol.

In this study the liquid product of the oxidation of the ester was analyzed by temperature-programmed gas chromatography and the percentages of unoxidized and 2-ethylhexyl perlagonate determined for hourly samples. To check the reproducibiblity of the results obtained, the percentage of unoxidized ester remaining in the oxidation apparatus during a test run in this study is compared with similar values reported in Table 9. This comparison is made on Figure 54. Figure 55 shows the comparison of the percentages of 2-ethylhexyl perlagonate formed in the two tests. The two curves show generally good agreement for these tests conducted at least one year apart.

No detailed analysis was performed on the liquid product in this study. The exit gases were analyzed at hourly intervals for each test run. The analysis of these gases was done on a Perkin Elmer Model 156 Vapor Fractometer using a 5A molecular sieves column maintained at 100°C to analyze for oxygen, nitrogen, carbon monoxide and methane. A hexylmethylphosphoramide column maintained at 33°C was used to analyze for carbon dioxide and C_2 to C_5 alkanes and alkenes. On the 5A molecular sieves column used, carbon monoxide and methane have almost identical retention times and a mixture of both appeared on one peak with a slight shoulder. The results obtained from this peak are reported as carbon monoxide and methane. However, it is believed that methane comprises a small fraction of the gas.

The analysis of the gaseous products shows small concentrations of carbon dioxide, carbon monoxide and methane, along with traces of C_2

to C_5 alkanes and alkenes. The percentages of carbon dioxide and carbon monoxide-methane produced in the oxidation of di-2-ethylhexyl sebacate at 500°F are shown in Figure 56. There is a noticeable difference in the production of these gases for the oxidation of the ester and the oxidation of the mineral oils. In the oxidation of the ester, more carbon dioxide than carbon monoxide-methane is formed. The reverse is true for the oxidation of the mineral oil. The percentage of carbon dioxide and carbon monoxide-methane formed during the oxidation of the heavy naphthenic mineral oil, MLO 7625, is shown in Figure 57. In the oxidation of the ester, carbon dioxide is produced by decarbonxylation of the original ester and ester products of the reaction. In the oxidation of the mineral oils, carbon dioxide is produced by oxidative degradation of the carbon chain. The production of these gaseous products increases with increased oxygen assimilation by the fluid. In the oxidation of the five mineral oils which absorbed different amounts of the available oxygen, the amount of carbon monoxide-methane produced closely followed the oxygen absorption trends. The percentage of carbon monoxide-methane produced in these oxidation tests is listed in Table 10 and plotted in Figure 58. The shapes of the curves for these gases closely resemble those of the oxygen assimilation curves for the respective oils. No carbon dioxide determination was performed on these fluids.

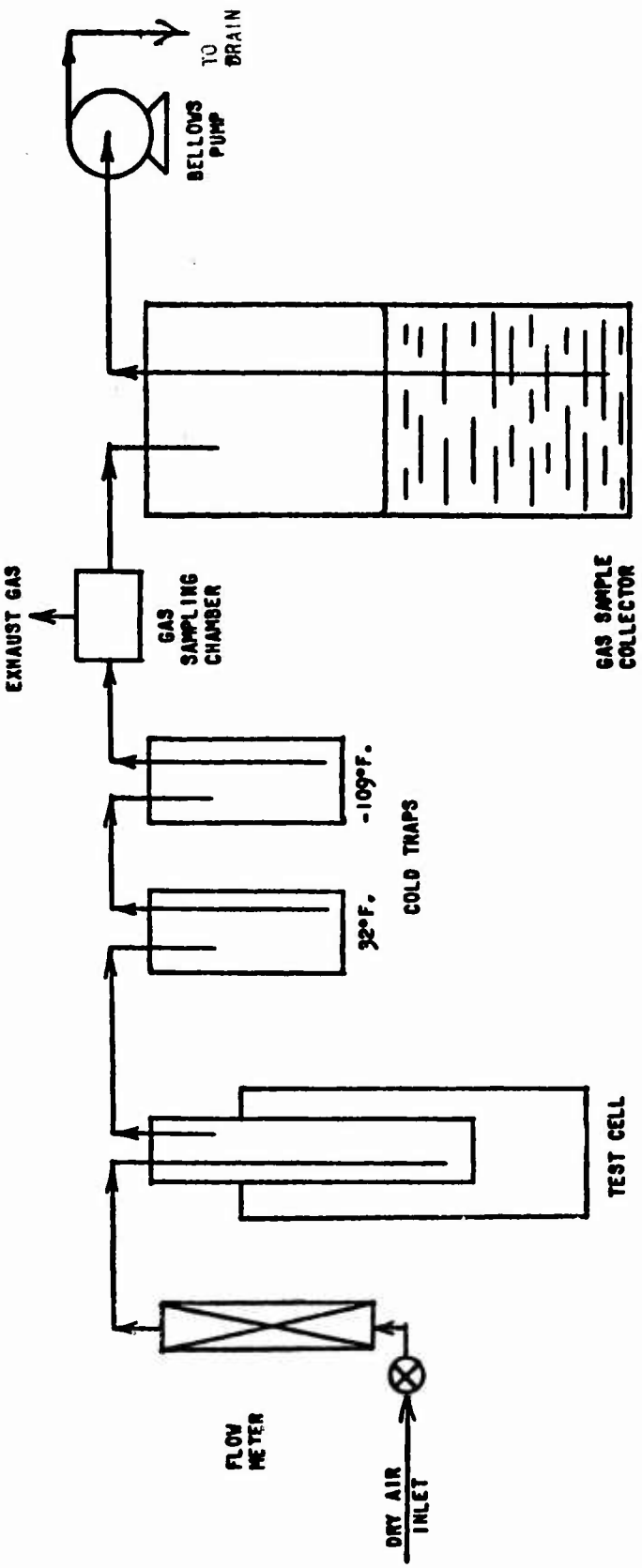

Figure 1. SCHEMATIC DIAGRAM OF OXIDATION APPARATUS

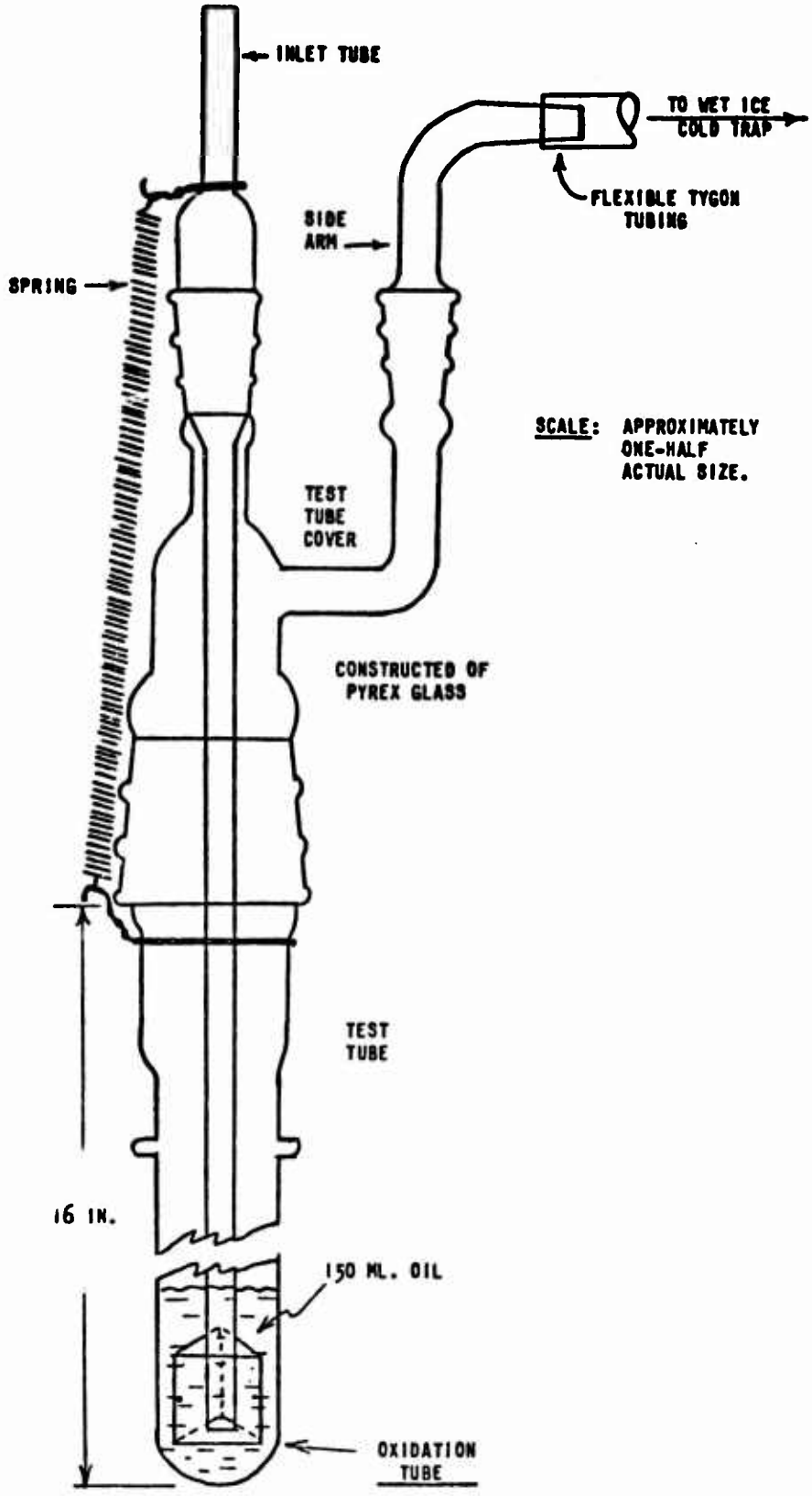

Figure 2. GLASS APPARATUS FOR OXIDATION TESTS

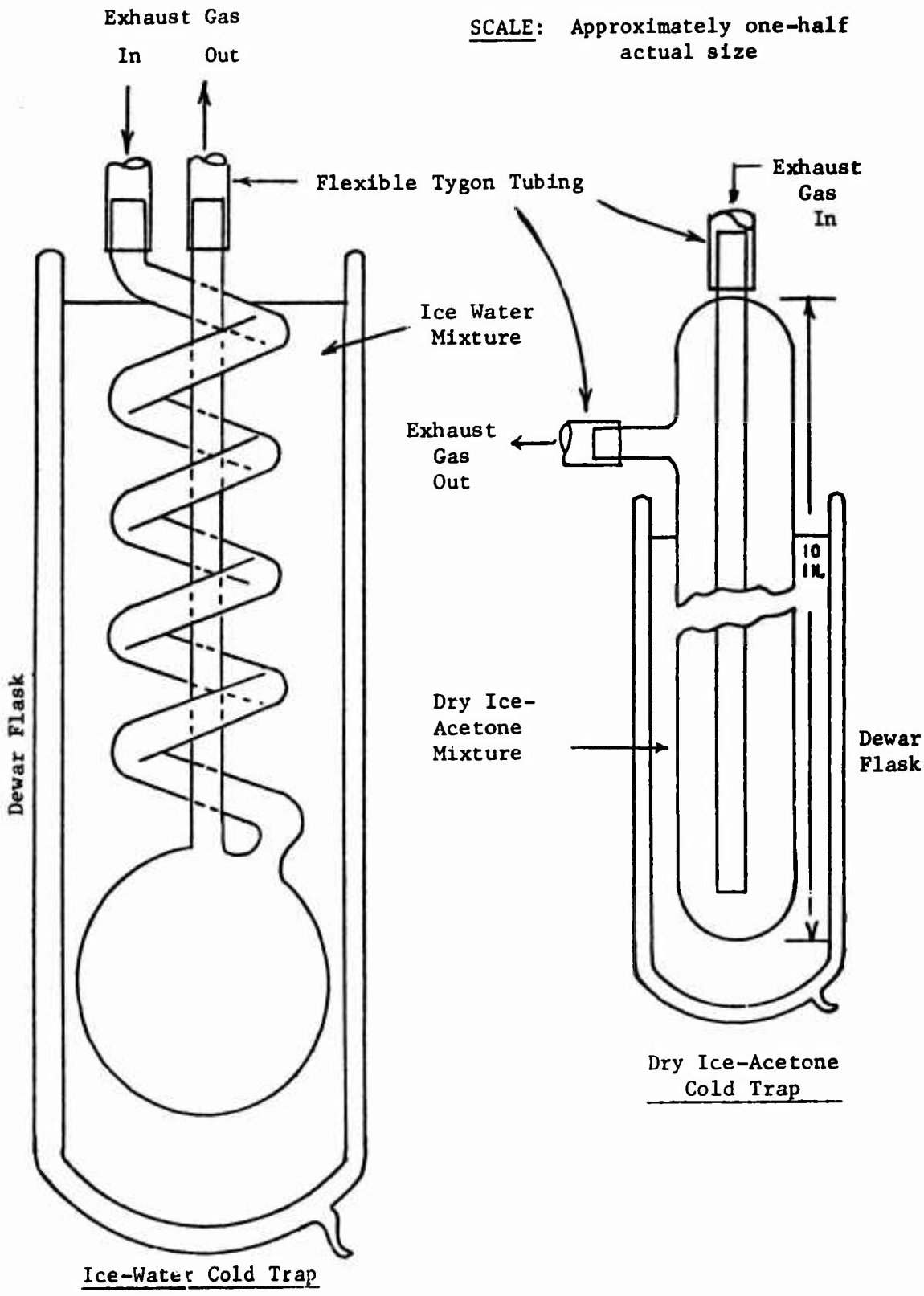

Figure 3. COLD TRAP SYSTEM

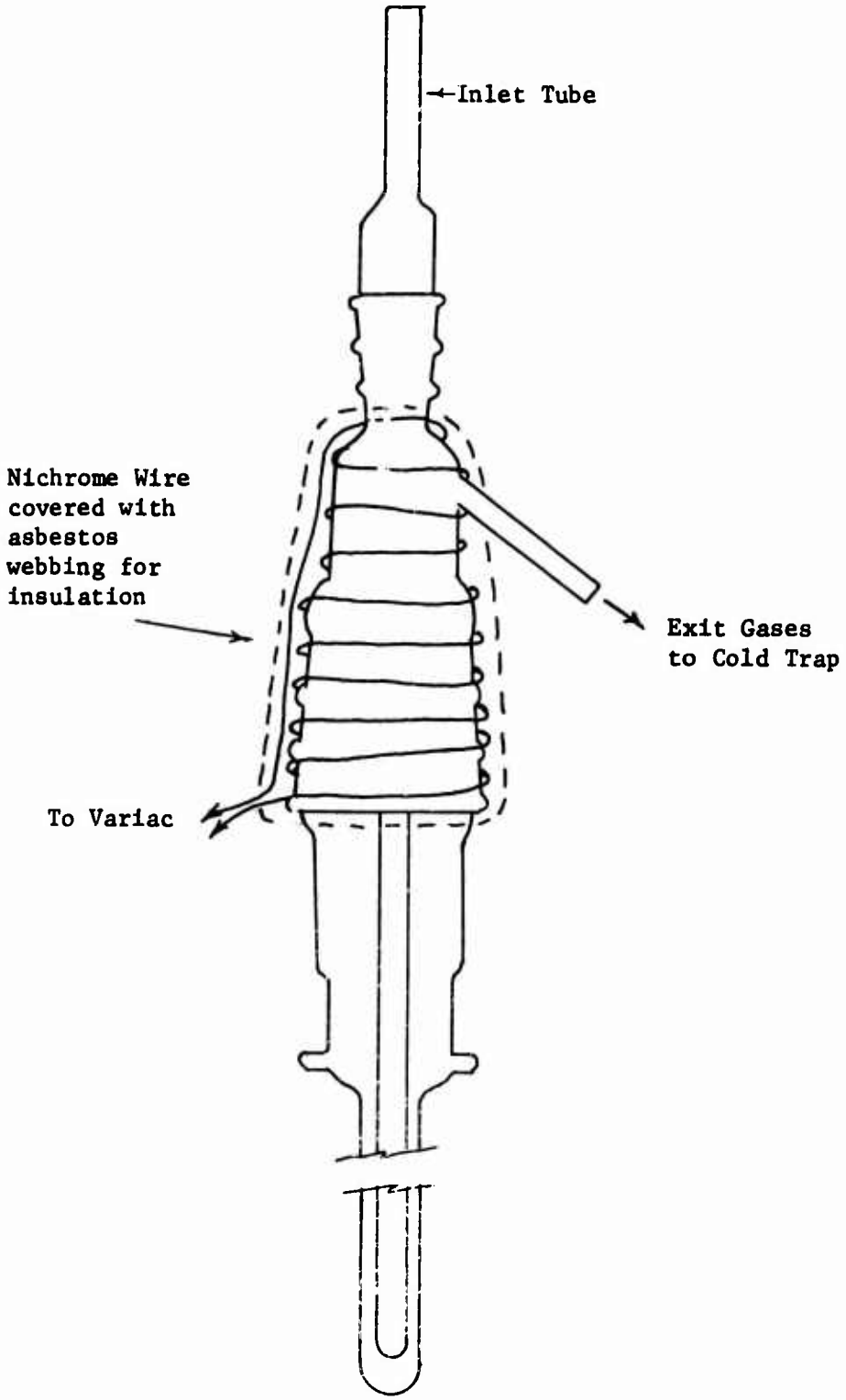

Figure 4. MODIFIED OXIDATION APPARATUS WITH HEATED JACKET

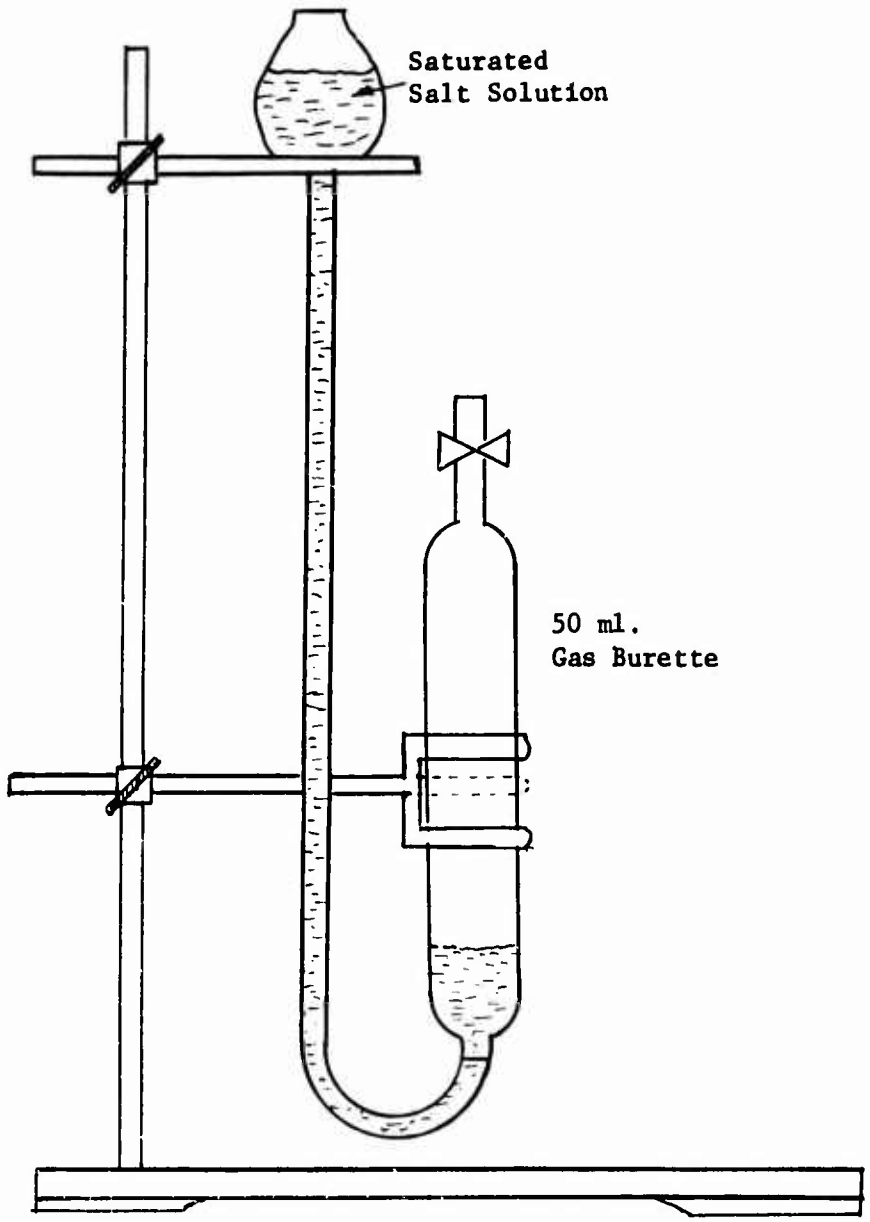

Figure 5. GAS SAMPLING APPARATUS

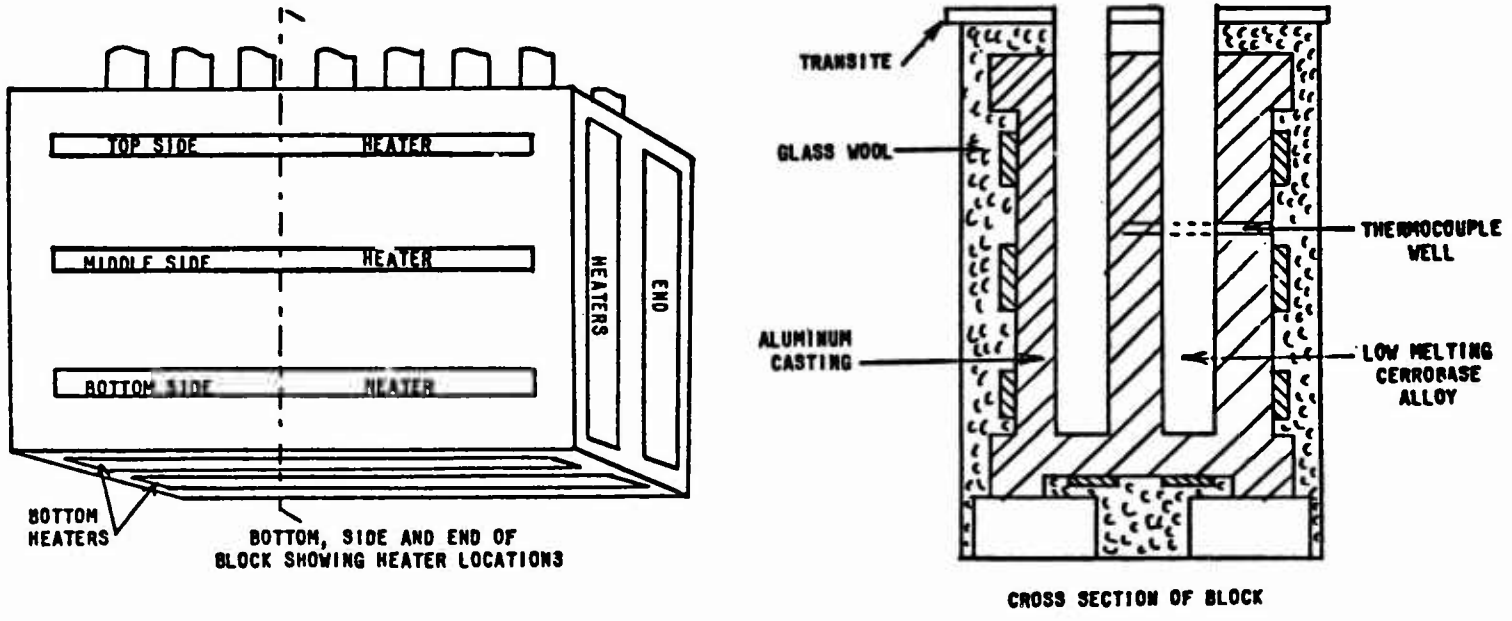

Figure 6. CONSTRUCTION DETAILS FOR HIGH TEMPERATURE OXIDATION BATH

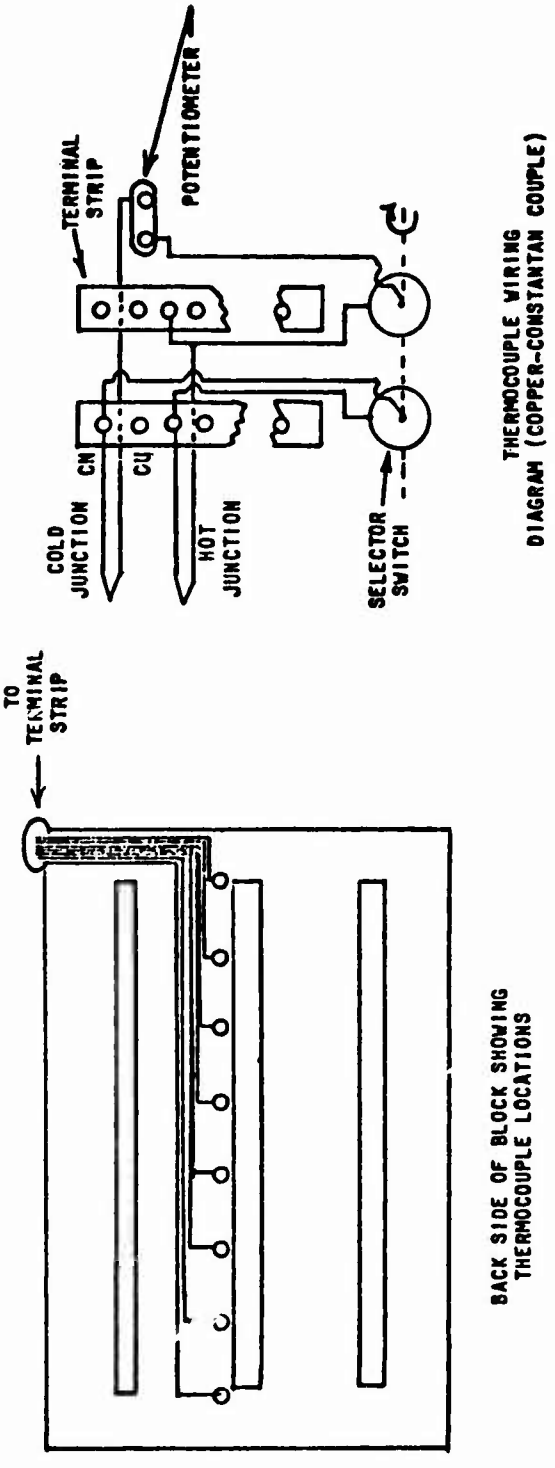

Figure 7. THERMOCOUPLE WIRING DIAGRAM FOR HIGH TEMPERATURE OXIDATION BATH

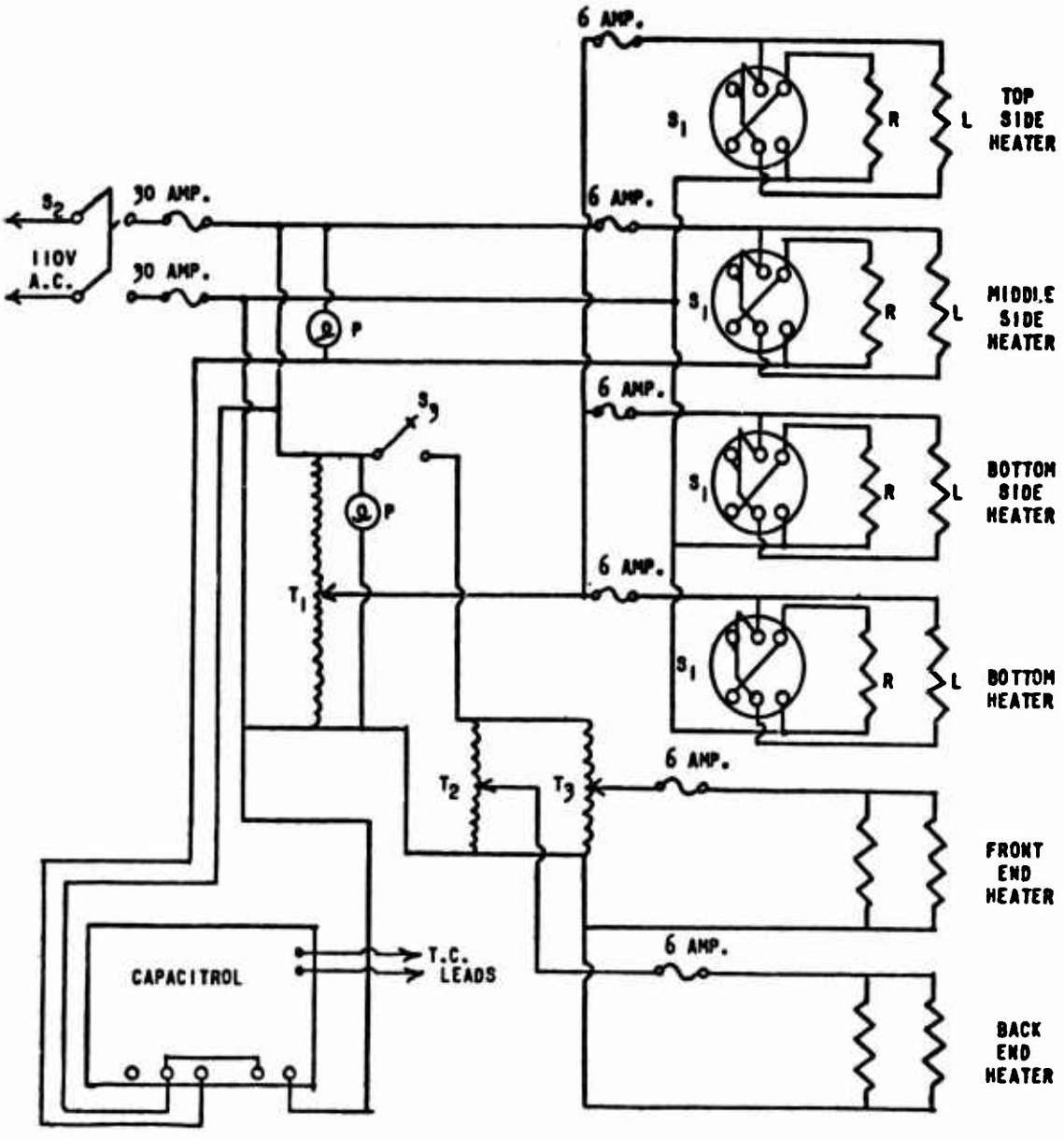

LEGEND:

L = LEFT SIDE OF BLOCK	T.C. = THERMOCOUPLE
R = RIGHT SIDE OF BLOCK	T_1 = TYPE 1000 VARIAC, 18 AMPS., 115V
S_1 = DOUBLE POLE DOUBLE THROW SWITCH	T_2, T_3 = TYPE V-5 VARIAC, 5 AMPS., 115V
S_2 = DOUBLE POLE SINGLE THROW SWITCH	P = PILOT LIGHT
S_3 = TOGGLE SWITCH	HEATERS = 250 WATT STRIP HEATERS

Figure 8. WIRING DIAGRAM FOR HIGH TEMPERATURE OXIDATION BATH

Table 1

OPERATING CONDITIONS FOR PERKIN ELMER
MODEL 154 VAPOR FRACTOMETER

Column	Length, Ft.	Inlet Pressure of Helium psig	Oven Temperature, °C.	Sample Size, µl
5A molecular seives	20	10	100	200
hexamethyl-phosphoramide	27	15	33	300
β-β-oxydi-propionitrile	20	10	100	4

Table 2

OPERATING CONDITIONS FOR
TEMPERATURE-PROGRAMMED GAS CHROMATOGRAPH

Column	Silicone Rubber on 10 percent S.E. 30
Column Dimensions	Stainless Steel tubing, 1/4 inch o.d. 2 feet long
Detector Temperature	626°F.
Injector Temperature	572°F.
Oven Temperature	122°F. to 608°F. at 13.5°F. per minute
Carrier Gas	Helium
Flow Rate	60 milliliters per minute

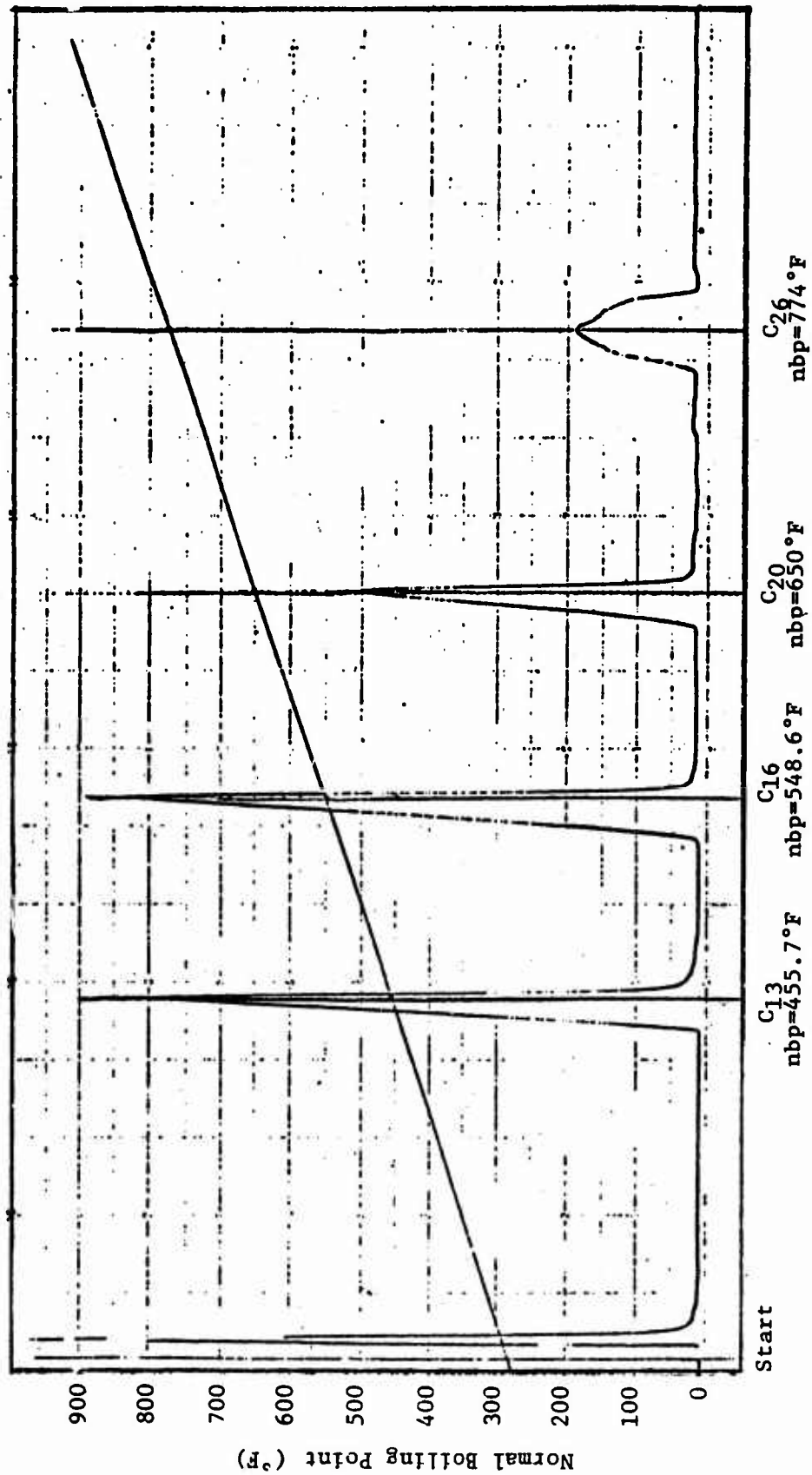

Figure 9. CHROMATOGRAM OF STANDARD MIXTURE OF HYDROCARBONS

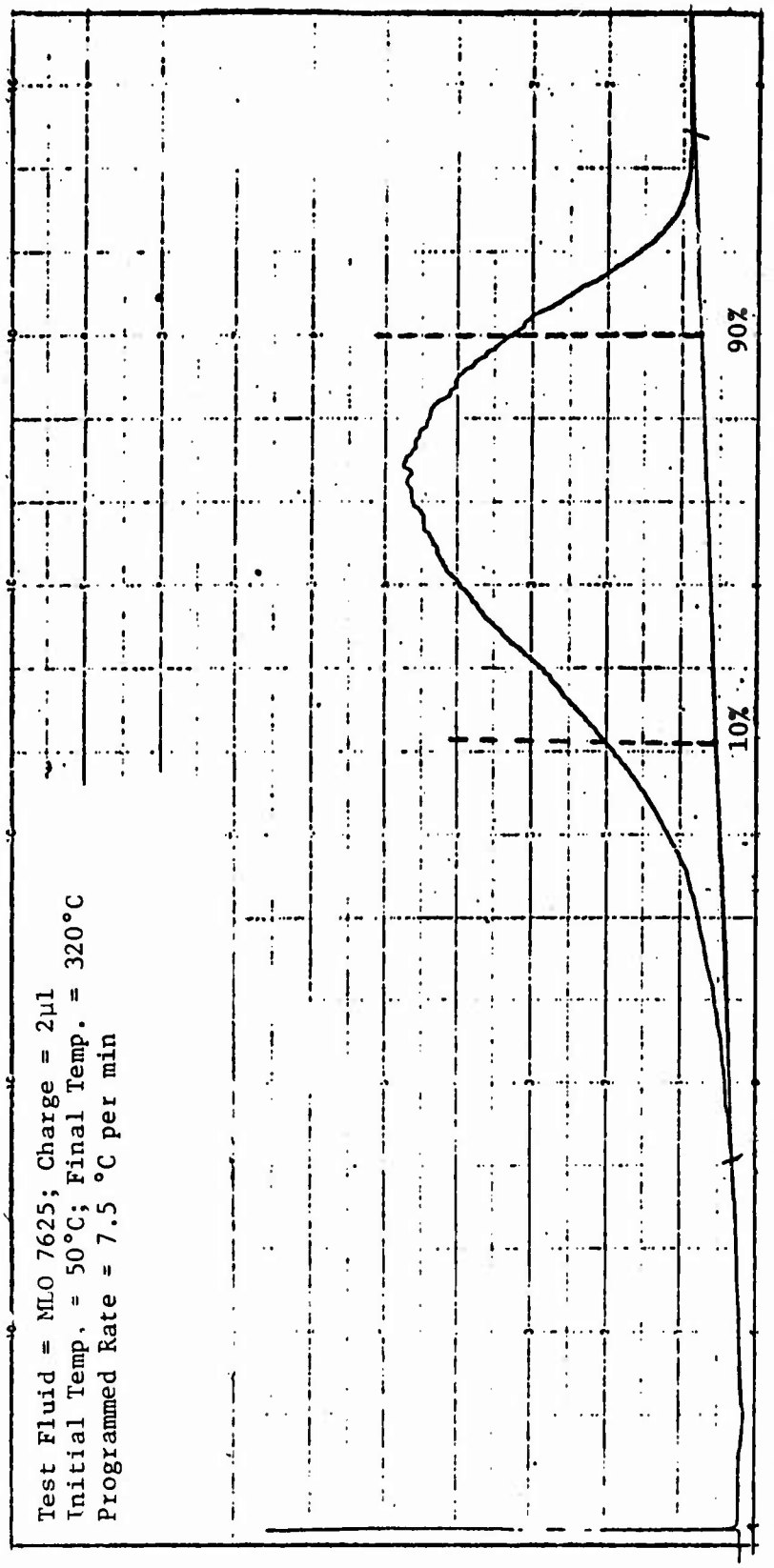

Figure 10. CHROMATOGRAM OF MLO 7625 SHOWING INITIAL, 10 PERCENT AND 90 PERCENT BOILING POINTS

Table 3

DESCRIPTION OF FLUIDS WITH n-d-m ANALYSIS

MLO Number	Fluid Description[1]	Centistoke Viscosity at 100°F.	Weight Percent Carbon Atoms[2]		
			Paraffin Chains	Naphthenic Rings	Aromatic Rings
7710	Synthetic Ester di-2 ethylhexylsebacate	12 6	---	---	---
7625	S R Naphthenic White Oil	76 9	55.2	44.8	0.0
7789	S R Paraffinic White Oil	13.1	68.7	31.3	0.0
7478	S.R Paraffinic White Oil	12.4	70.4	29.6	0.0
7797	S.R. Naphthenic White Oil	8.93	47.3	50.5	2.2
7685	S R Naphthenic White Oil	3 22	37.3	61.1	1.6
n-heptane	Pure hydrocabon	0.523	100.0	---	---

(1) S.R. = Super-Refined

(2) Calculated using the n-d-m method of vanNess and vanWeston.(Aspects of the Constitution of Mineral Oils, Elsevier Publ. Co., New York (1951).

Table 4

PHYSICAL PROPERTIES OF FLUIDS

Fluid Descriptions Shown in Table 3.

MLO Number	Centistoke Viscosity at 100°F.	Centistoke Viscosity at 210°F.	Viscosity Index	Astm Slope (100°-210°F.)	Refraction Index, n_D^{20}	Density, gm/ml at 60°F.	Molecular Weight (1)
7710	12.6	3.32	154	0.700	1.4510	0.916	426
7625	76.9	8.14	76	0.768	1.4820	0.885	430
7789	13.1	3.11	110	0.763	1.4637	0.838	331
7478	12.4	3.35	119	0.687	1.4616	0.835	332
7797	8.93	2.27	62	0.840	1.4752	0.869	262
7685	3.22	1.24	51	0.856	1.4620	0.846	182
n-heptane	0.523	--	--	--	1.3876	0.687	100

(1) Calculated from viscosity data using the method of Hirschler ("Molecular Weights of Viscous Hydrocarbon Oils; Correlation of Density with Viscosities," J. Inst. Petrol. 32, 133 (1946).

Table 5

PREDICTION OF FLUID VISCOSITIES AT 500°F.

Fluid Descriptions Shown in Table 3.

Fluid Designation	Viscosity at 210°F., cs.	Calculated Visc. at 500°F., cs. (1)
MLO 7710	3.32	0.82
MLO 7625	8.14	1.09
MLO 7789	3.11	0.73
MLO 7478	3.35	0.84
MLO 7797	2.27	0.565
MLO 7685	1.24	0.42

(1) Calculated from procedures compiled by L. T. Eby ("Tables for Determination of ASTM Slope and Prediction of Viscosities," Chem. Div., Standard Oil Devel. Co., July 21, 1946.

Test Fluid: MLO 7710, Di-2-ethylhexyl sebacate (12.6 cs at 100°F)
Test Condition: Temperature = 500 ± 3°F, Air Rate = 5 ± 0.5 l/hr
Fluid Charge as Indicated in Regular Tube with Air Cooled Condenser

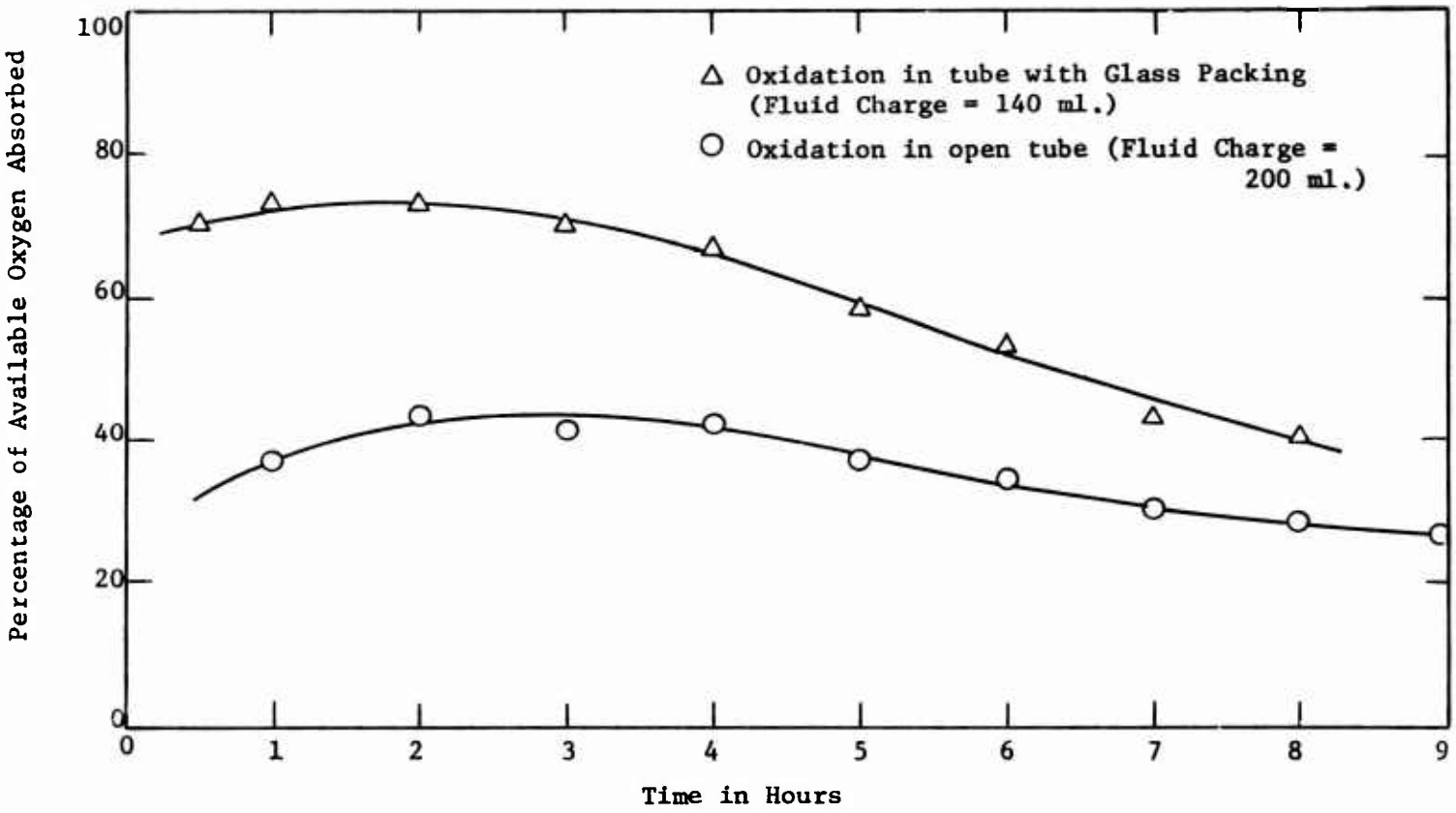

Figure 11. EFFECT OF AIR-OIL CONTACT AREA ON OXYGEN ABSORPTION

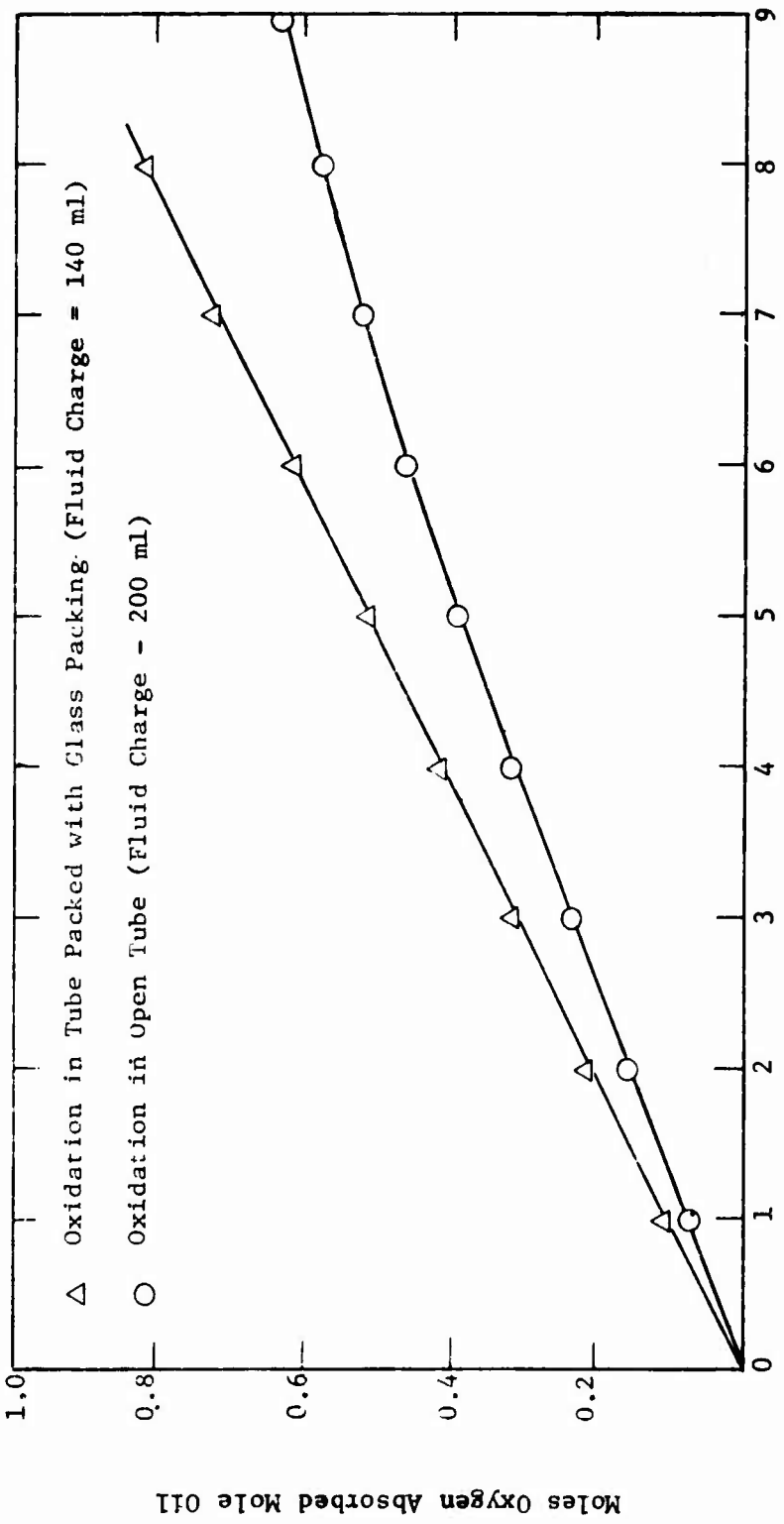

Figure 12. EFFECT OF AIR-OIL CONTACT ON RATE OF OXYGEN ABSORPTION

Data taken from WADC-TR-55-30; Part IV.
Test Temperature = 500 ± 5°F.; Air Rate = 10 ± 1 l./hr.; and Test Time = 6 Hours.
Test Fluid = Di-2-Ethylhexyl Sebacate + 0.5 Wt.% Phenothiazine.
O = Test Conducted with 100 ml. of Fluid in regular tube with air cooled condenser.
Δ = Test Conducted by passing air through four regular oxidation tubes in series, each tube containing 200 ml. of fluid.

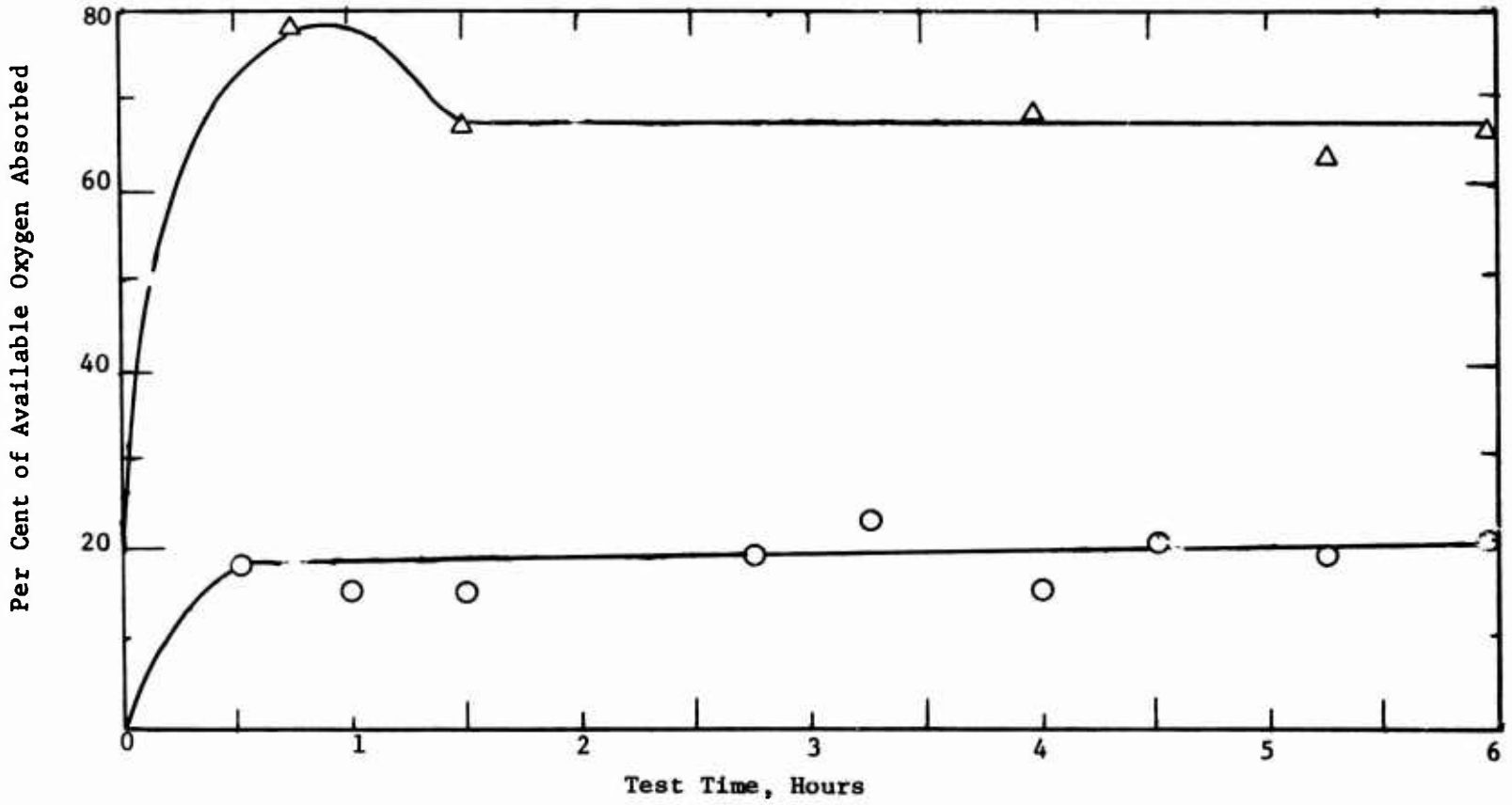

Figure 13. EFFECT OF TIME OF OXYGEN-FLUID CONTACT ON OXIDATION AT 500°F.

Data Taken from WADC-TR-55-30, Part IV.
Test Conditions: Test Temperature = 500 ± 5°F., Fluid Charge = 50 ml.; Test Time = 6 hr., Air Rate as Indicated; Air Distributor = Fine Porosity Sintered Glass Filter; 2600 cm^2 of cm Diameter Glass Beads Used to Increase Surface Area Where Indicated

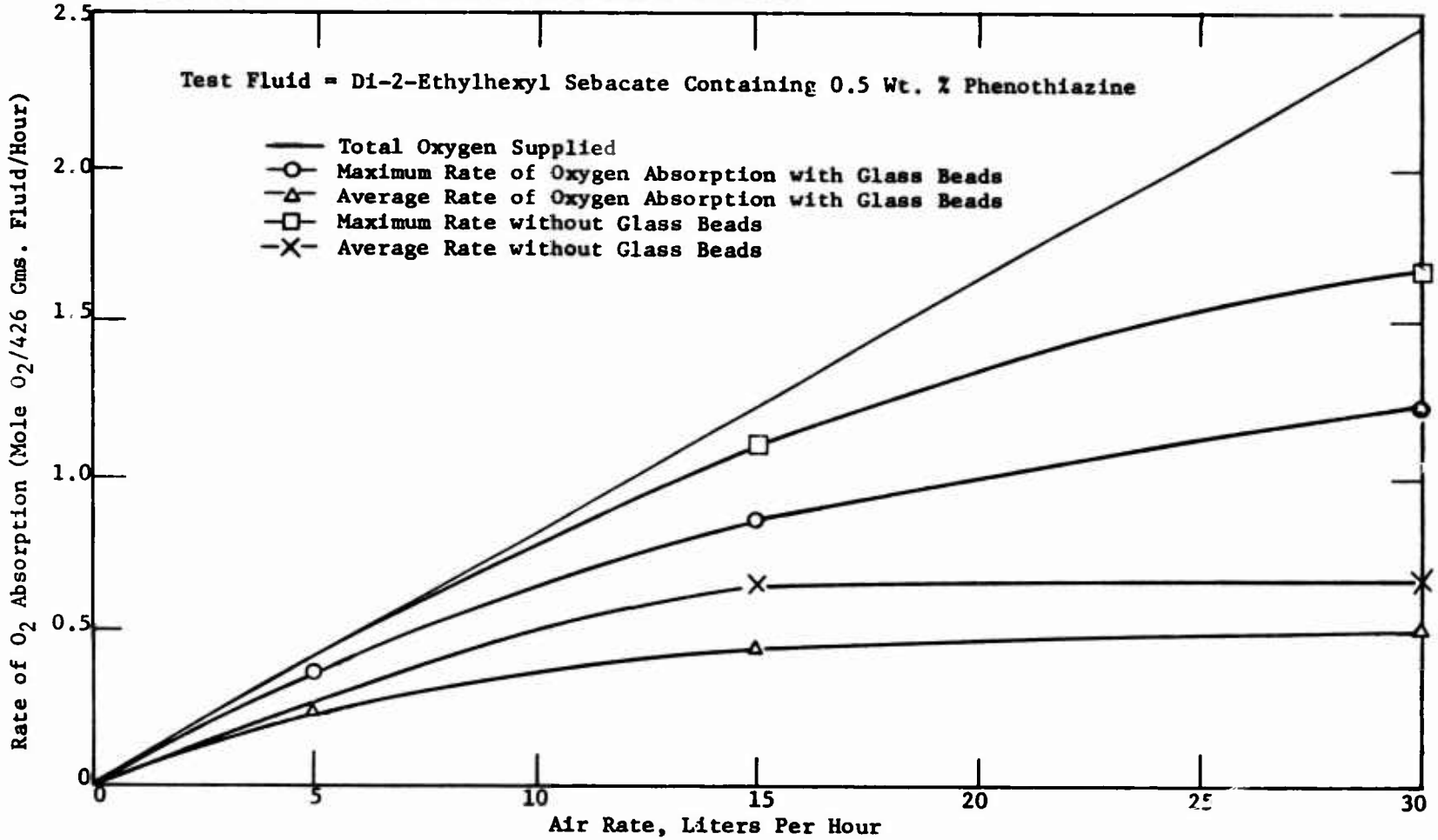

Figure 14. OXYGEN ASSIMILATION AS A FUNCTION OF AIR-OIL CONTACT

Test Fluid: As Indicated
Test Conditions: Temperature = 500 ± 3°F., Nitrogen at 5 1/hr
Charge = 65 ml in a Semi Micro Tube with an Air Cooled Condenser
Fluid Description Shown in Table 3.

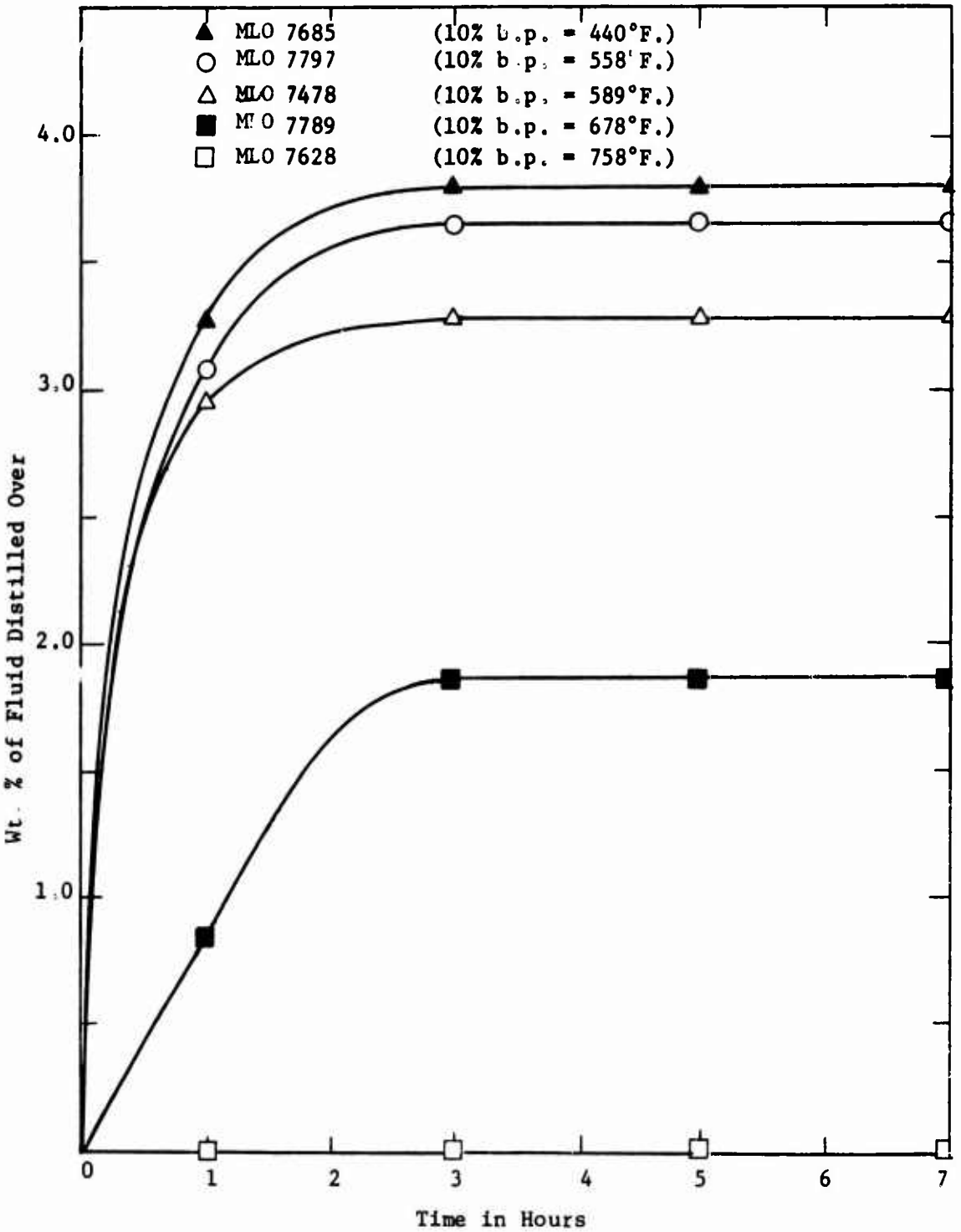

Figure 15. Volatility of Test Fluids

Table 6

DISTILLATION RANGES OF TEST FLUIDS BEFORE OXIDATION

Determined by Temperature-programmed Gas Chromatography
Fluid Descriptions Shown in Table 3.

Fluid Designation	Initial Boiling Point (°F)	10% (wt.) Boiling Point (°F.)	90% (wt.) Boiling Point (°F.)
MLO 7625	554	758	958
MLO 7789	568	678	803
MLO 7478	427	589	840
MLO 7797	392	558	722
MLO 7685	382	440	612

Table 7

PERCENTAGE OF AVAILABLE OXYGEN ABSORBED BY THE FLUIDS

Fluid Descriptions Shown in Table 3.

Sample Time, hrs.	Fluid Designation 7625	7789	7478	7797	7685
0.5	33.36	40.02	64.32	42.65	73.88
1	31.40	44.21	74.31	45.23	93.95
2	31.57	44.28	72.00	48.30	87.27
3	37.11	43.54	49.82	42.39	75.47
4	34.07	37.13	46.64	43.67	68.95
5	31.16	37.60	44.11	36.59	69.92
6	32.20	39.02	41.15	39.22	68.99
7	35.08	37.37	46.93	38.27	64.54
8	--	38.45	43.42	36.60	62.51
Average	32 24	40.20	53.63	41.44	73.94

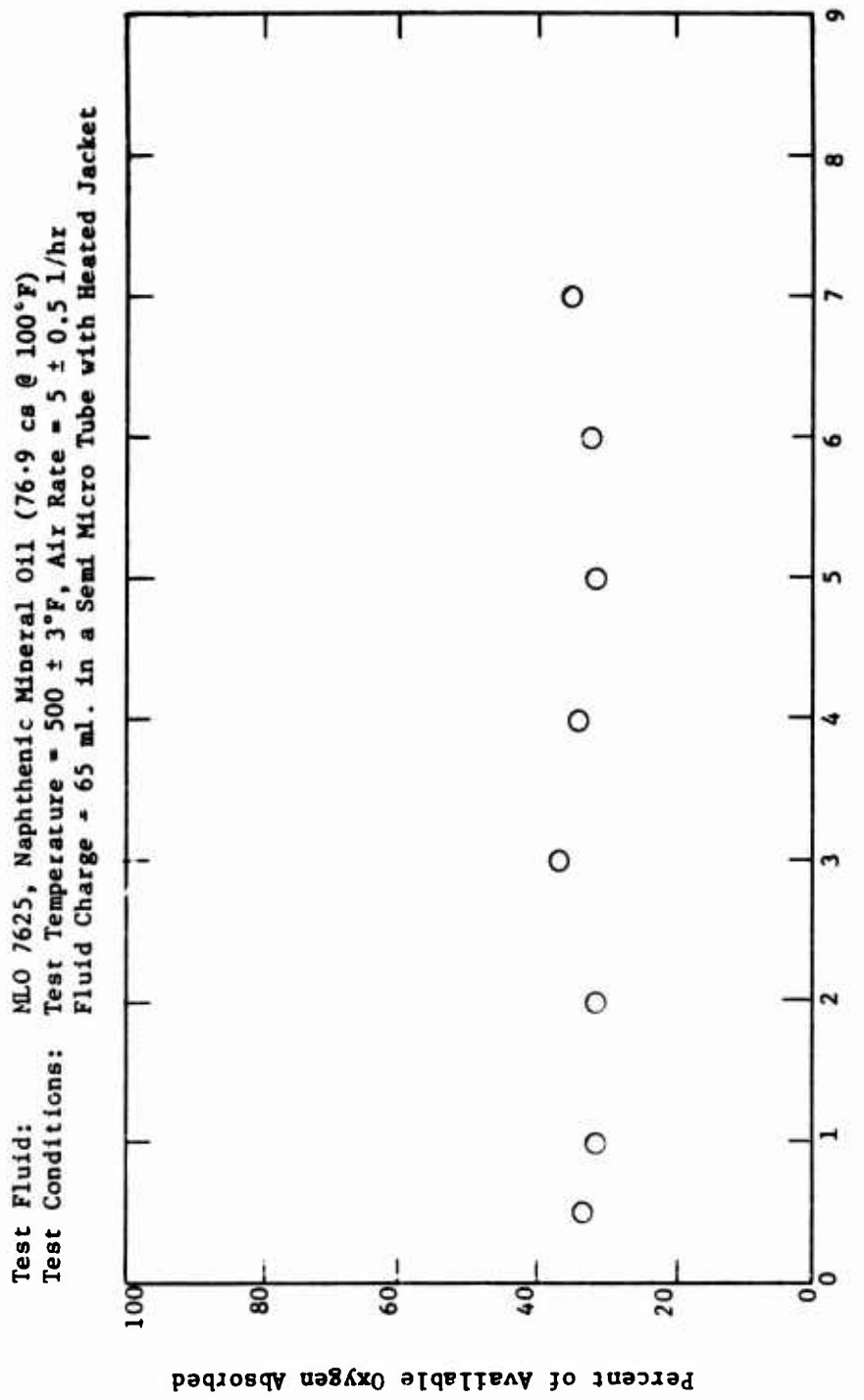

Figure 16. OXIDATION ASSIMILATION MEASUREMENTS FOR MLO 7625

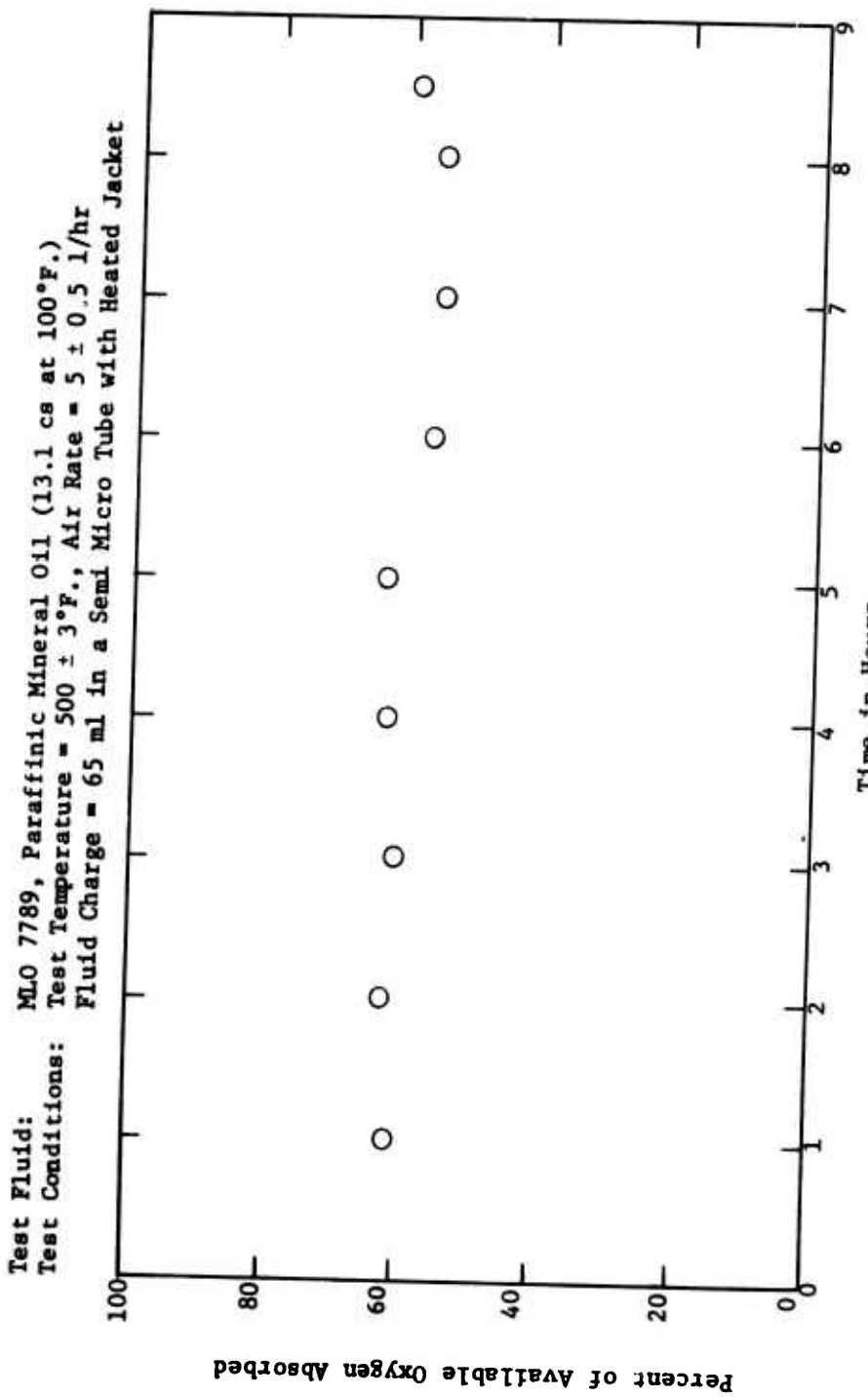

Figure 17. OXYGEN ASSIMILATION MEASUREMENTS FOR MLO 7789

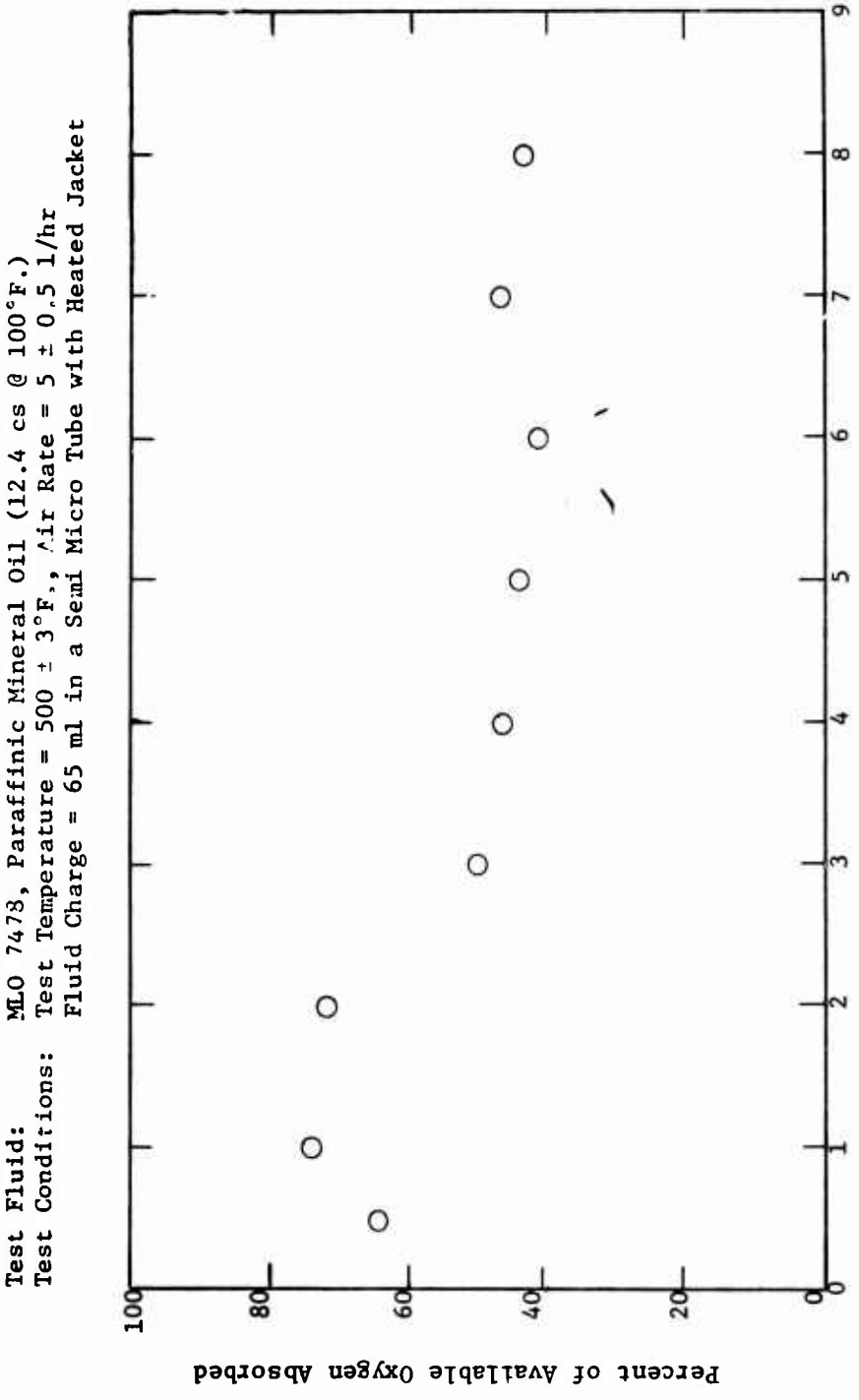

Figure 18. OXIDATION ASSIMILATION MEASUREMENTS FOR MLO 7478

Test Fluid: MLO 7797, Naphthenic Mineral Oil (8.93 cs @ 100°F.)
Test Conditions: Test Temperature = 500 ± 3°F., Air Rate = 5 ± 0.5 l/hr
Fluid Charge = 65 ml in a Semi Micro Tube with Heated Jacket

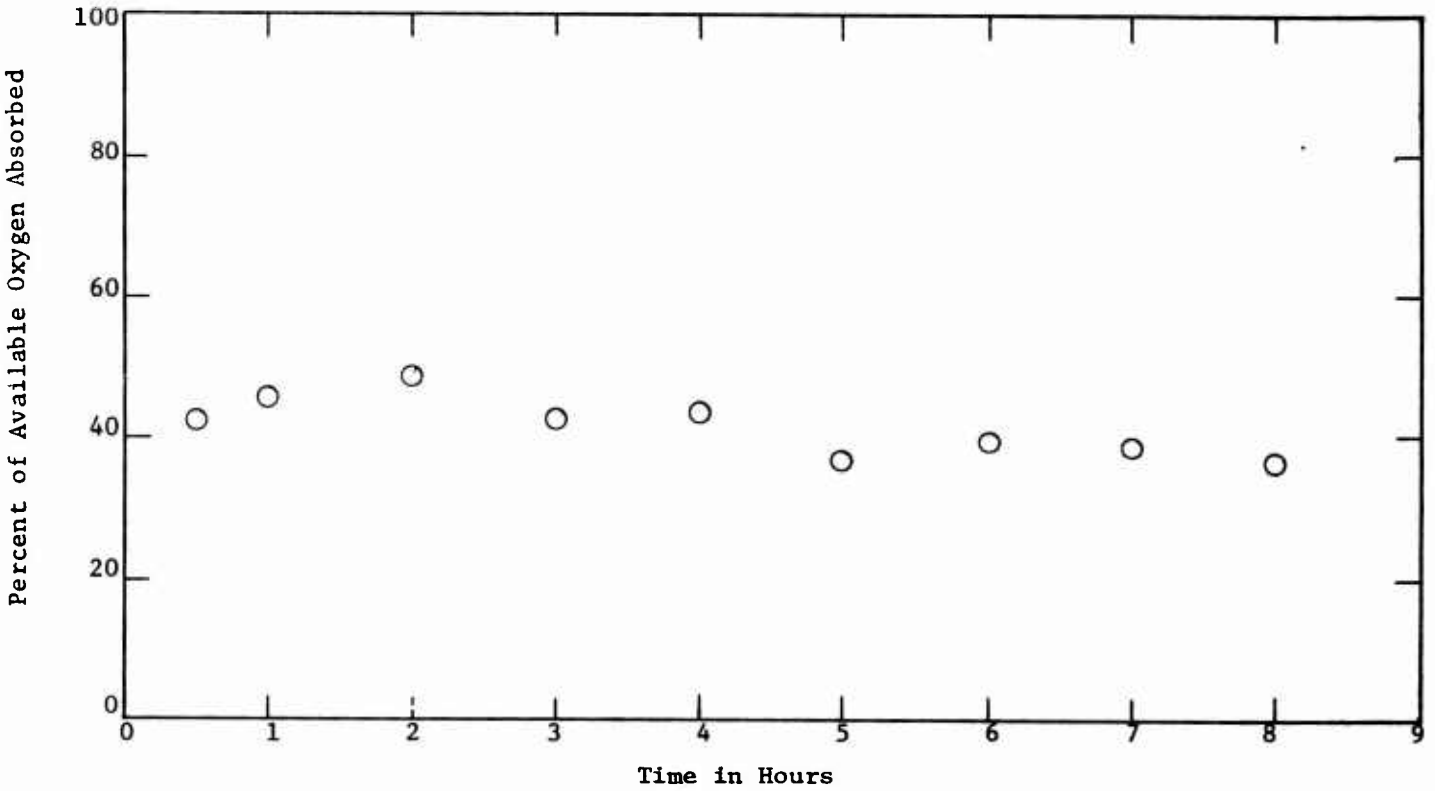

Figure 19. OXYGEN ASSIMILATION MEASUREMENTS FOR MLO 7797

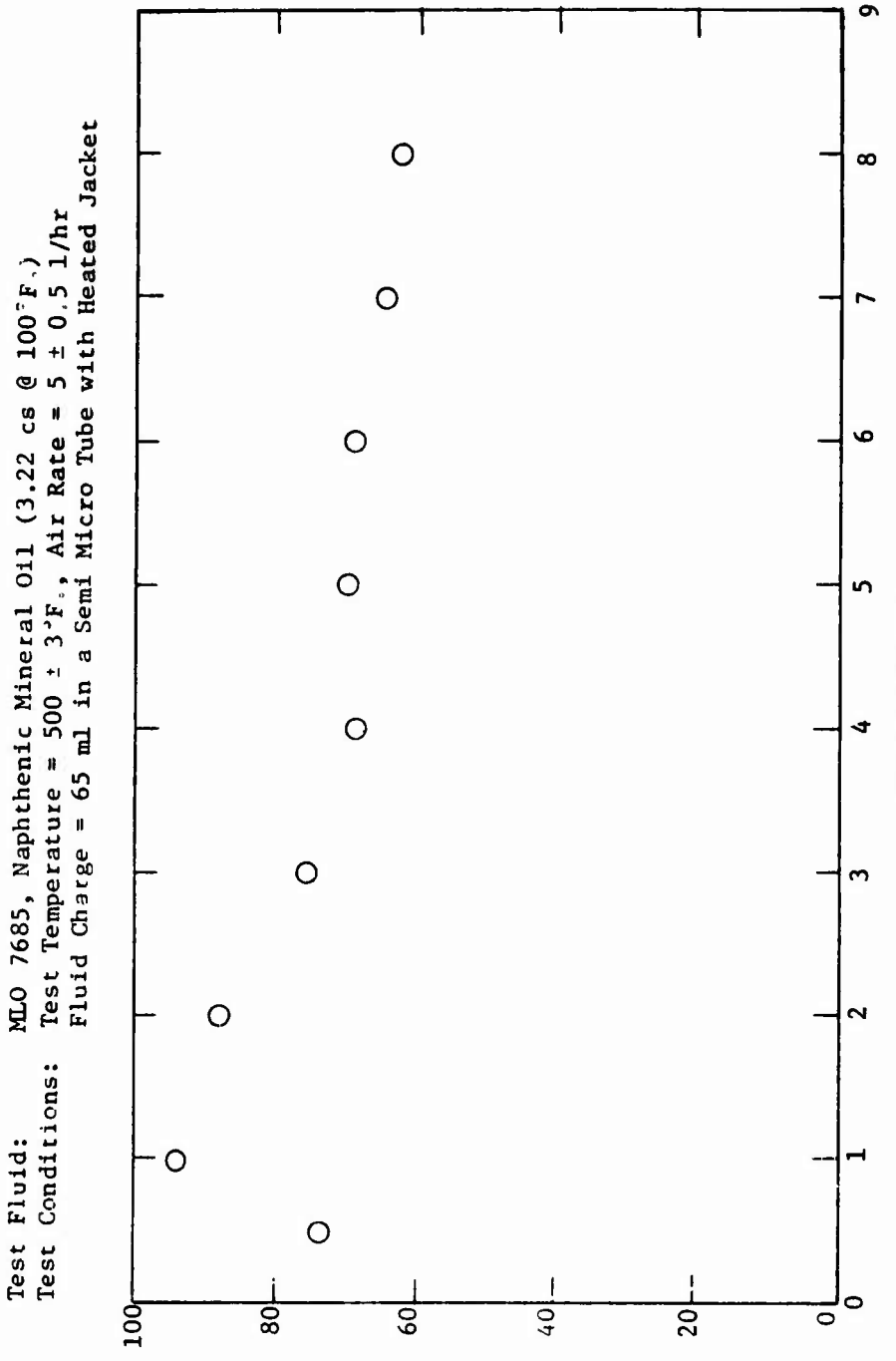

Figure 20. OXYGEN ASSIMILATION MEASUREMENTS FOR MLO 7685

Test Conditions: Test Temperature = 500 ± 3°F., Air Flow = 5 ± 0.5 l/hr
Fluid Charge = 65 ml in a Semi Micro Tube with a Heated Jacket
Fluid Description Shown in Table 3

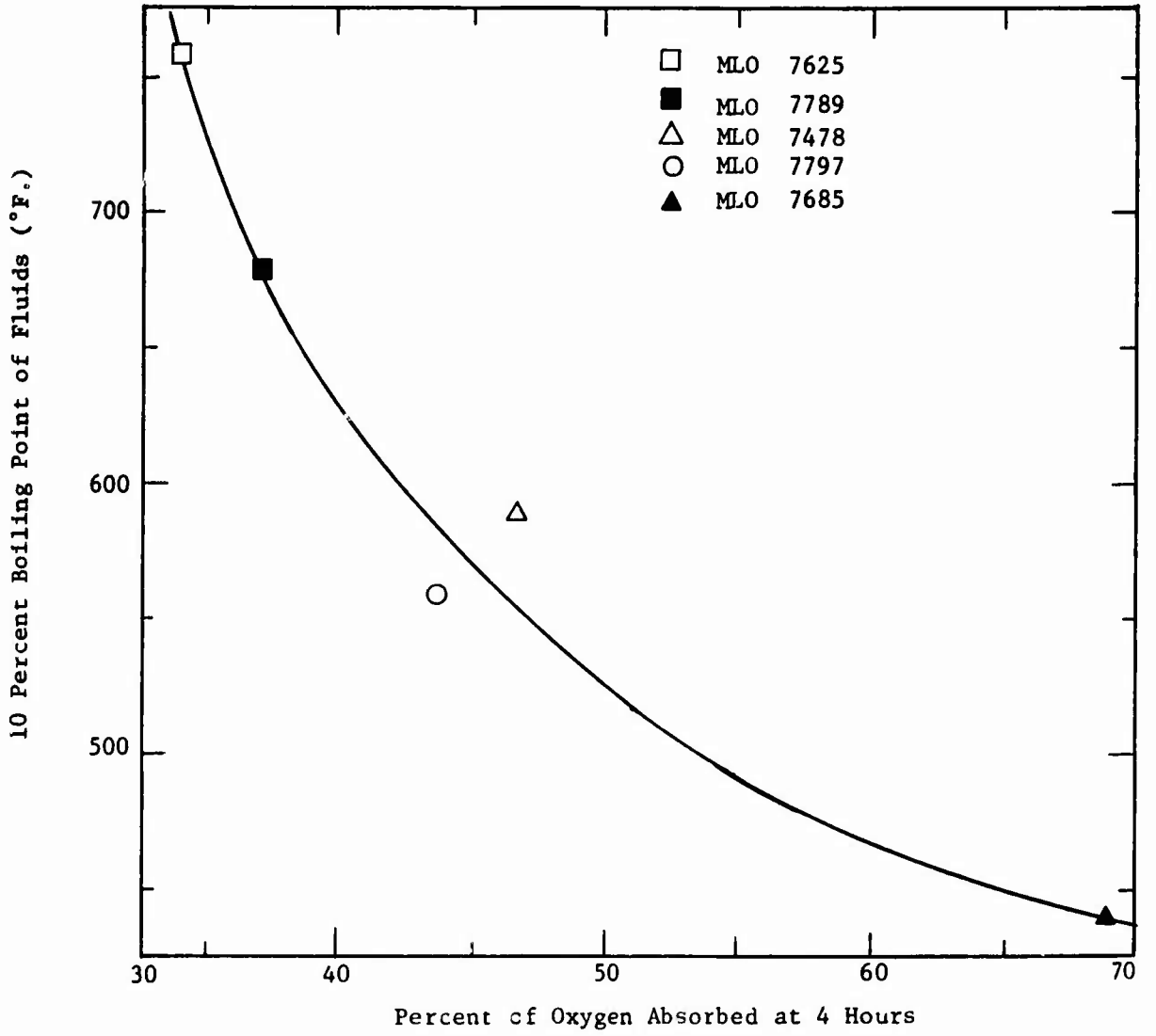

Figure 21 RELATIONSHIP OF OXYGEN ABSORPTION AT FOUR HOURS TEST TIME WITH 10 PERCENT BOILING POINT

Test Fluid: MLO 7625, Naphthenic Mineral Oil (76.9 cs at 100°F.)
Test Conditions: Test Temperature = 500 ± 3°F., Air Rate = 5 ± 0.5 1/hr
Fluid Charge = 65 ml in a Semi Micro Tube with Heated Jacket

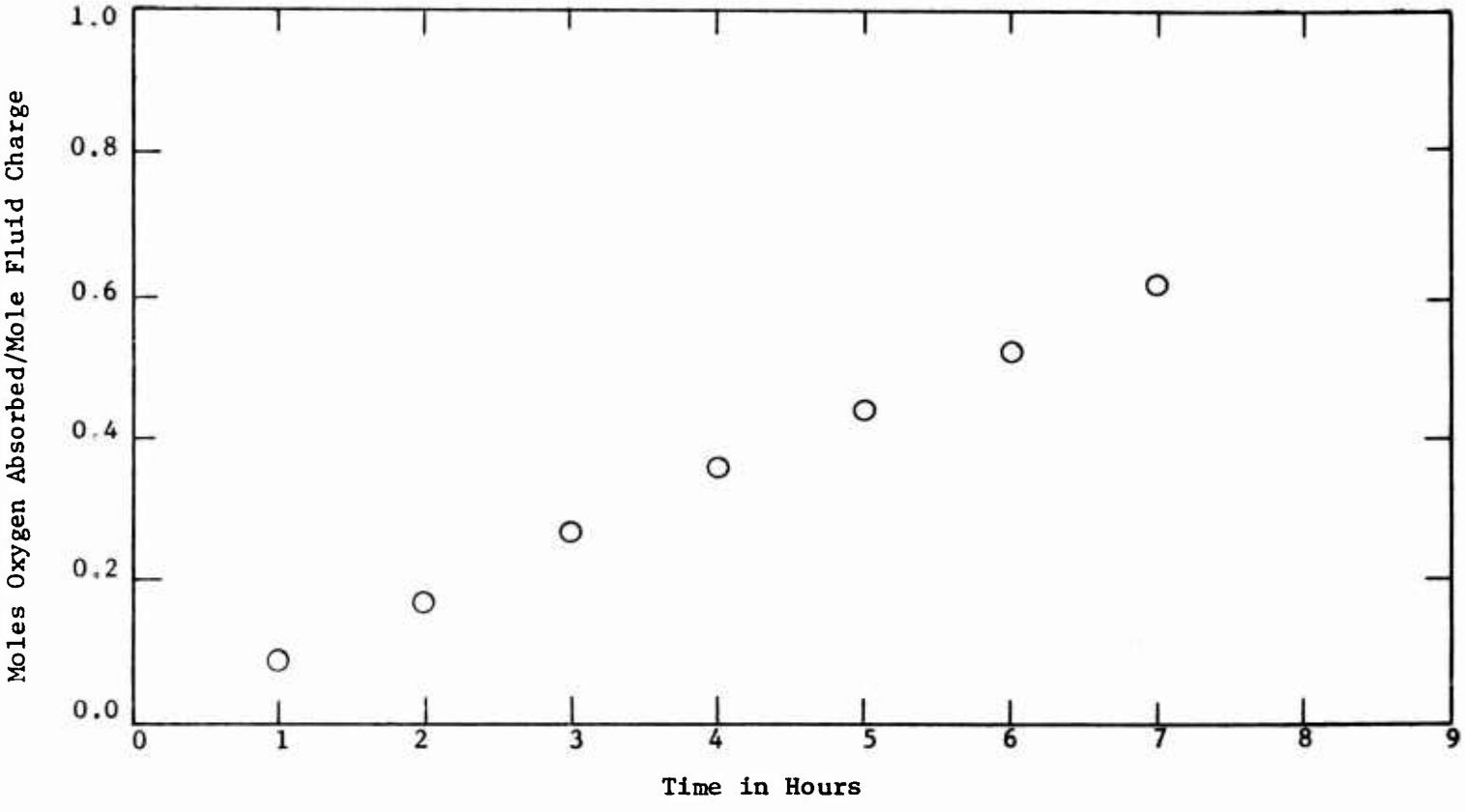

Figure 22 TOTAL OXYGEN ABSORBED BY MLO 7625

Test Fluid: MLO 7789, Paraffinic Mineral Oil (13.1 cs at 100°F.)
Test Conditions: Test Temperature = 500 ± 3°F , Air Rate = 5 ± 0.5 1/hr
Fluid Charge = 65 ml in a Semi Micro Tube with Heated Jacket

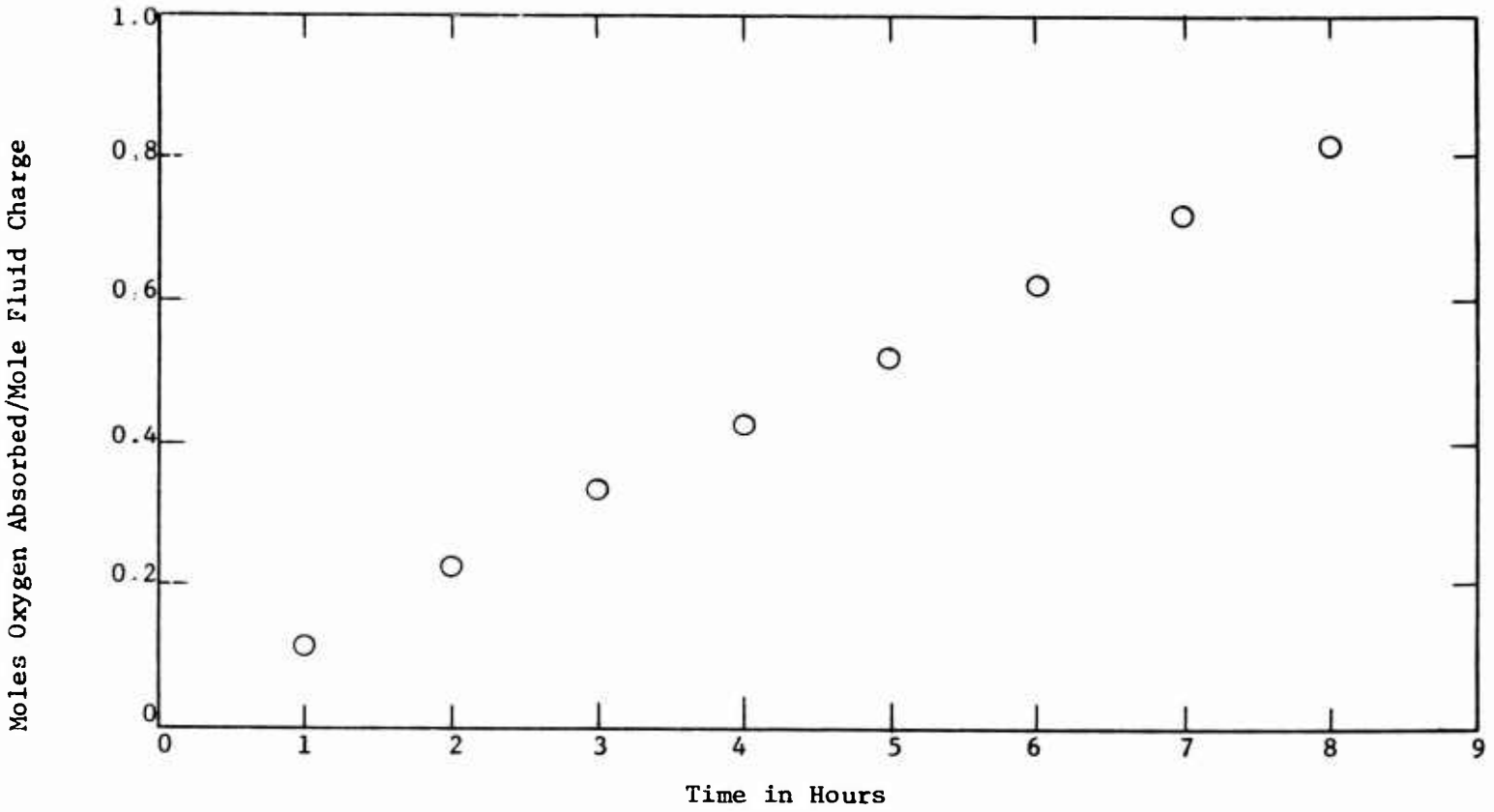

Figure 23 TOTAL OXYGEN ABSORBED BY MLO 7789

Test Fluid: MLO 7478, Paraffinic Mineral Oil, (12.4 cs at 100°F.)
Test Conditions: Test Temperature = 500 ± 3°F., Air Rate = 5 ± 0.5 1/hr
Fluid Charge = 65 ml in a Semi Micro Tube with Heated Jacket

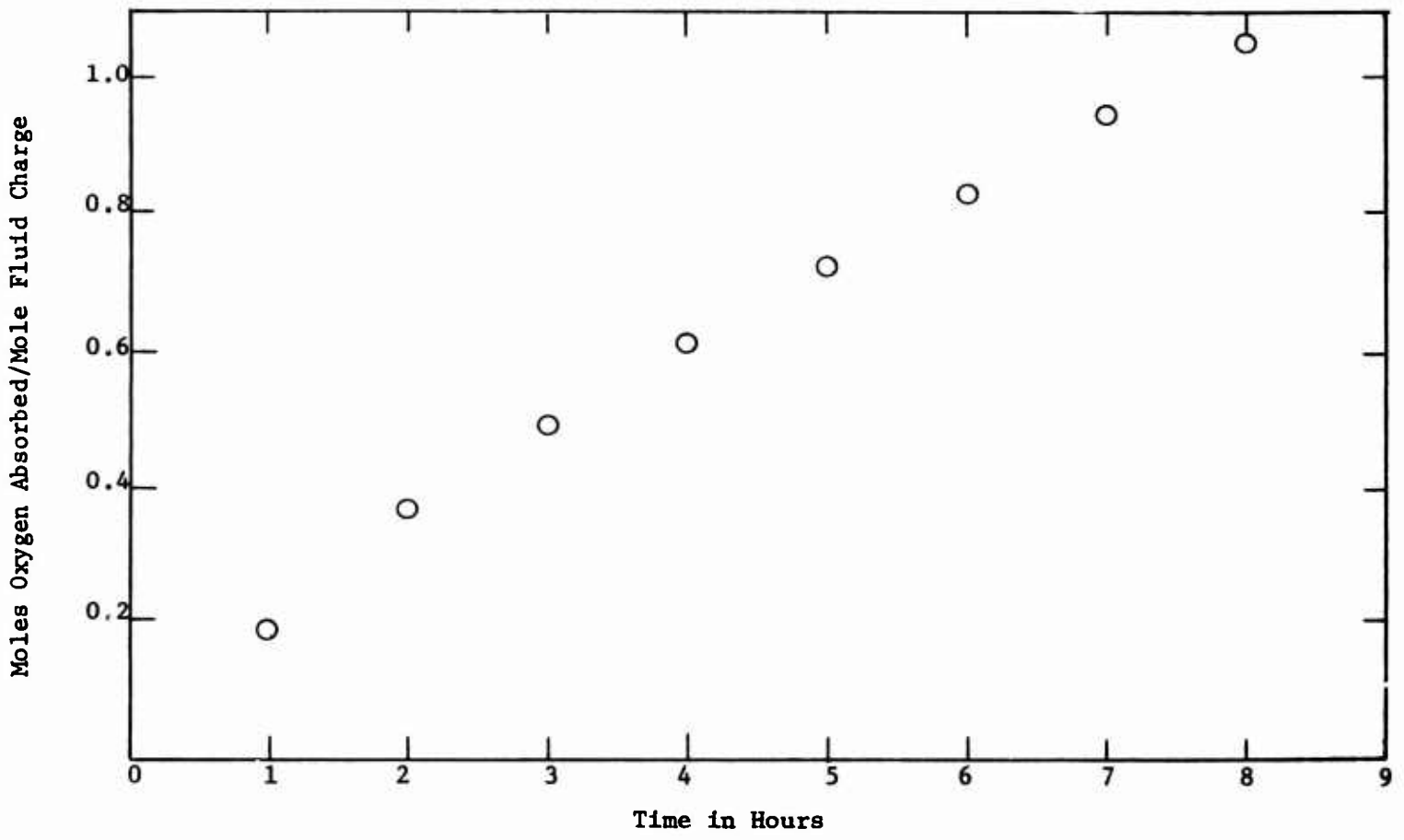

Figure 24. TOTAL OXYGEN ABSORBED BY MLO 7478

Test Fluid: MLO 7797, Naphthenic Mineral Oil (8.93 cs @ 100°F.)
Test Conditions: Test Temperature = 500 ± 3°F , Air Rate = 5 ± 0.5 l/hr
Fluid Charge = 65 ml in a Semi Micro Tube with Heated Jacket

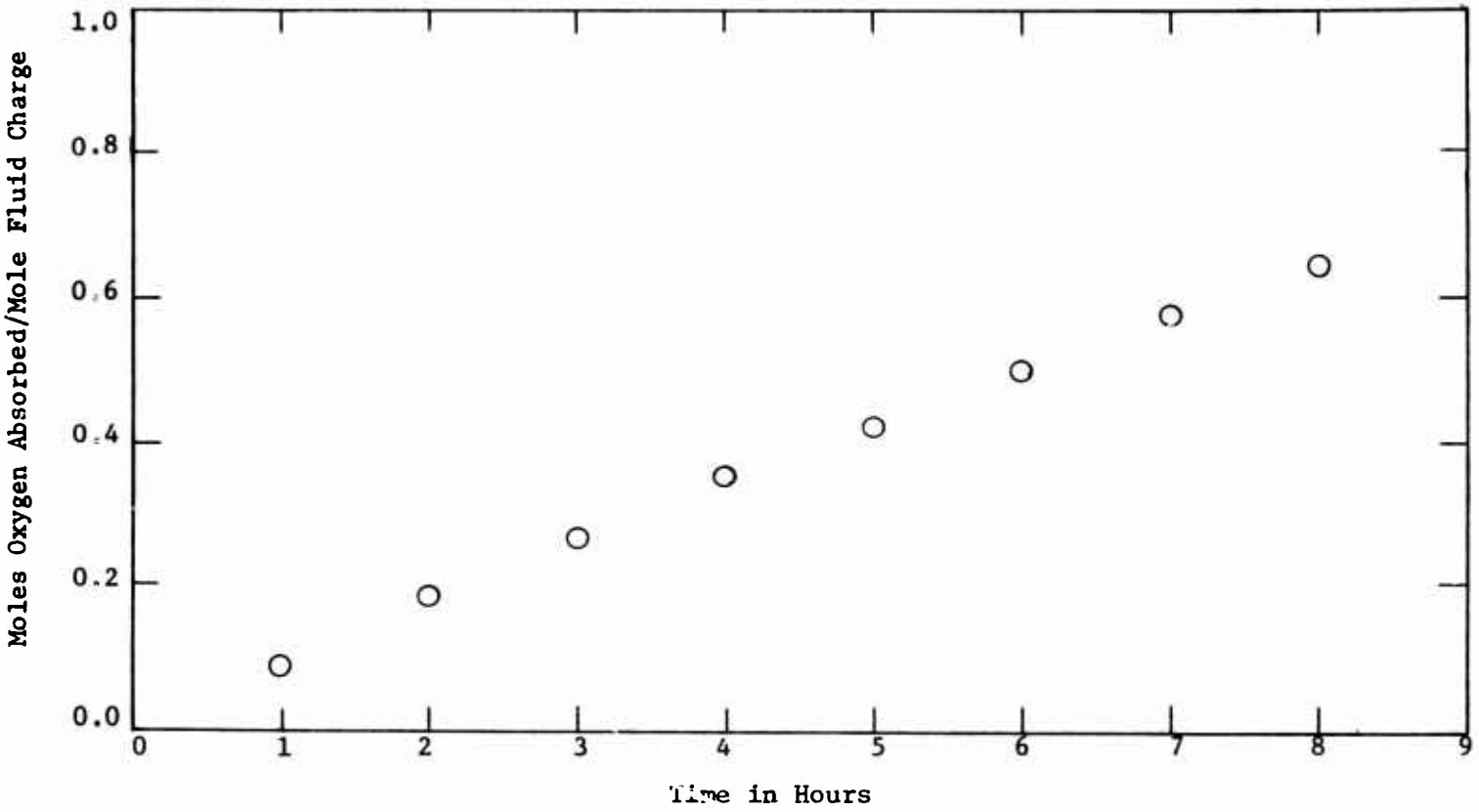

Figure 25. TOTAL OXYGEN ABSORBED BY MLO 7797

Test Fluid: MLO 7685, Naphthenic Mineral Oil (3.22 cs @ 100°F.)
Test Conditions: Test Temperature = 500 ± 3°F., Air Rate = 5 ± 0.5 1/hr
Fluid Charge = 65 ml in a Semi Micro Tube with Heated Jacket

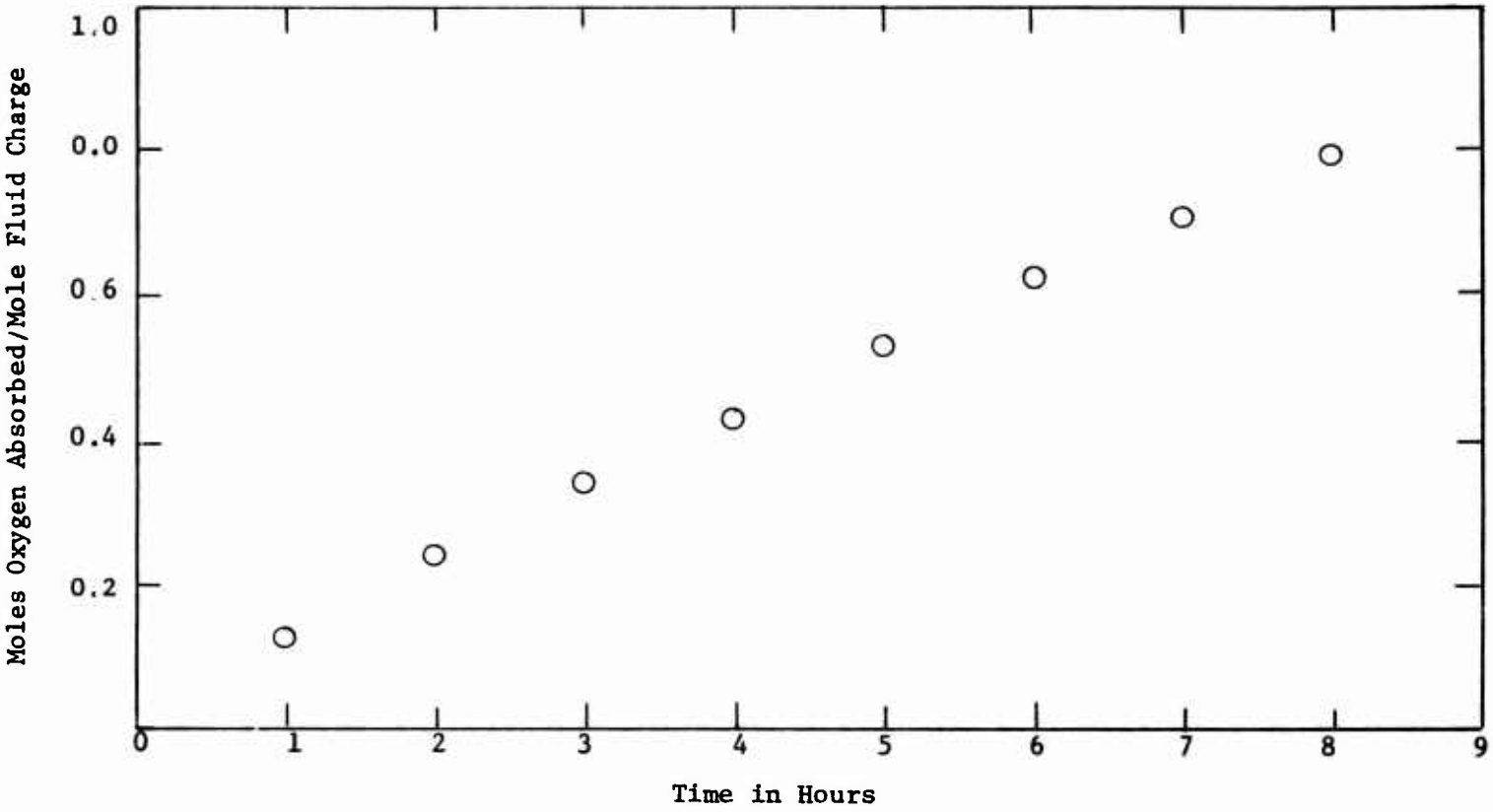

Figure 26. TOTAL OXYGEN ABSORBED BY MLO 7685

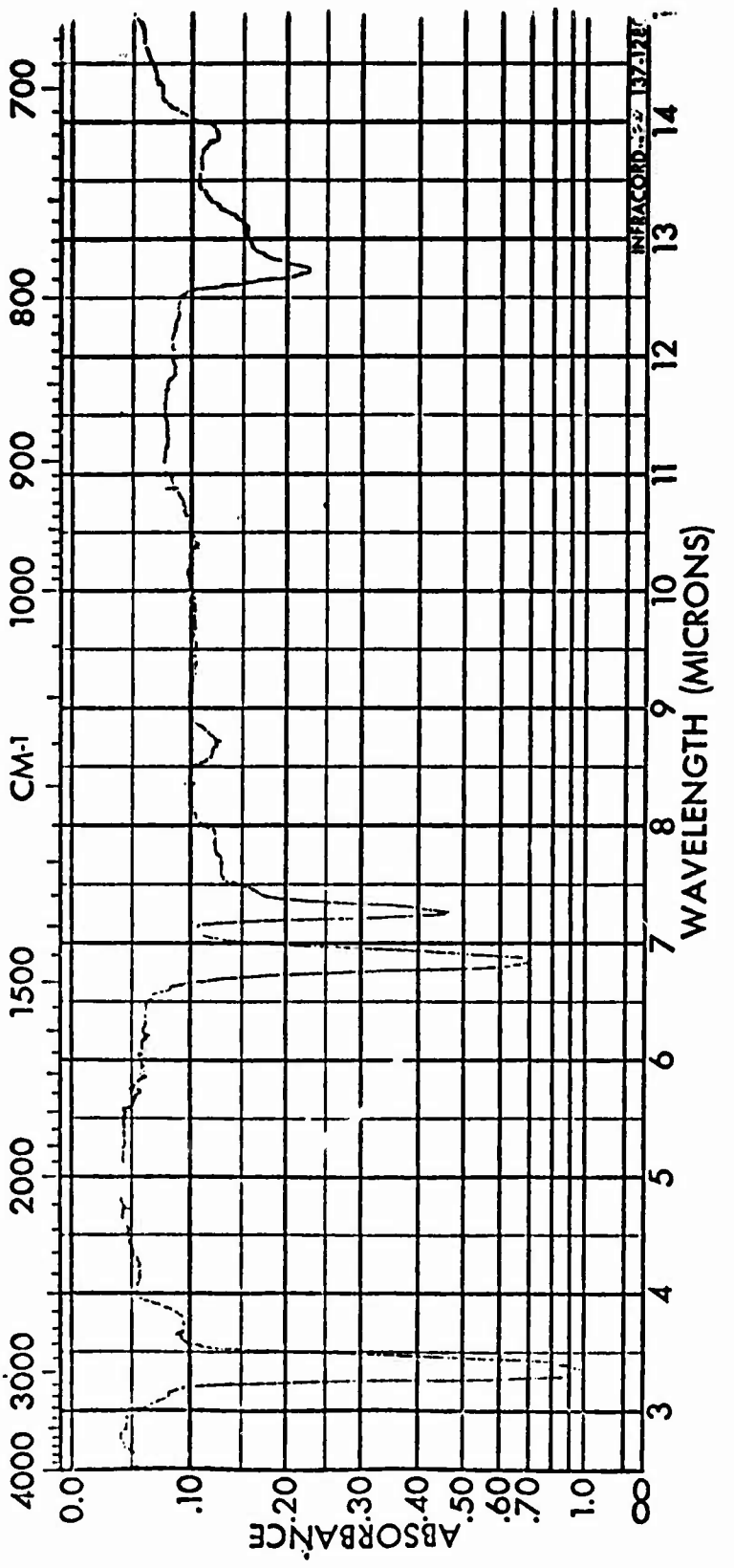

Figure 27. INFRARED SPECTRUM OF UNOXIDIZED MLO 7685

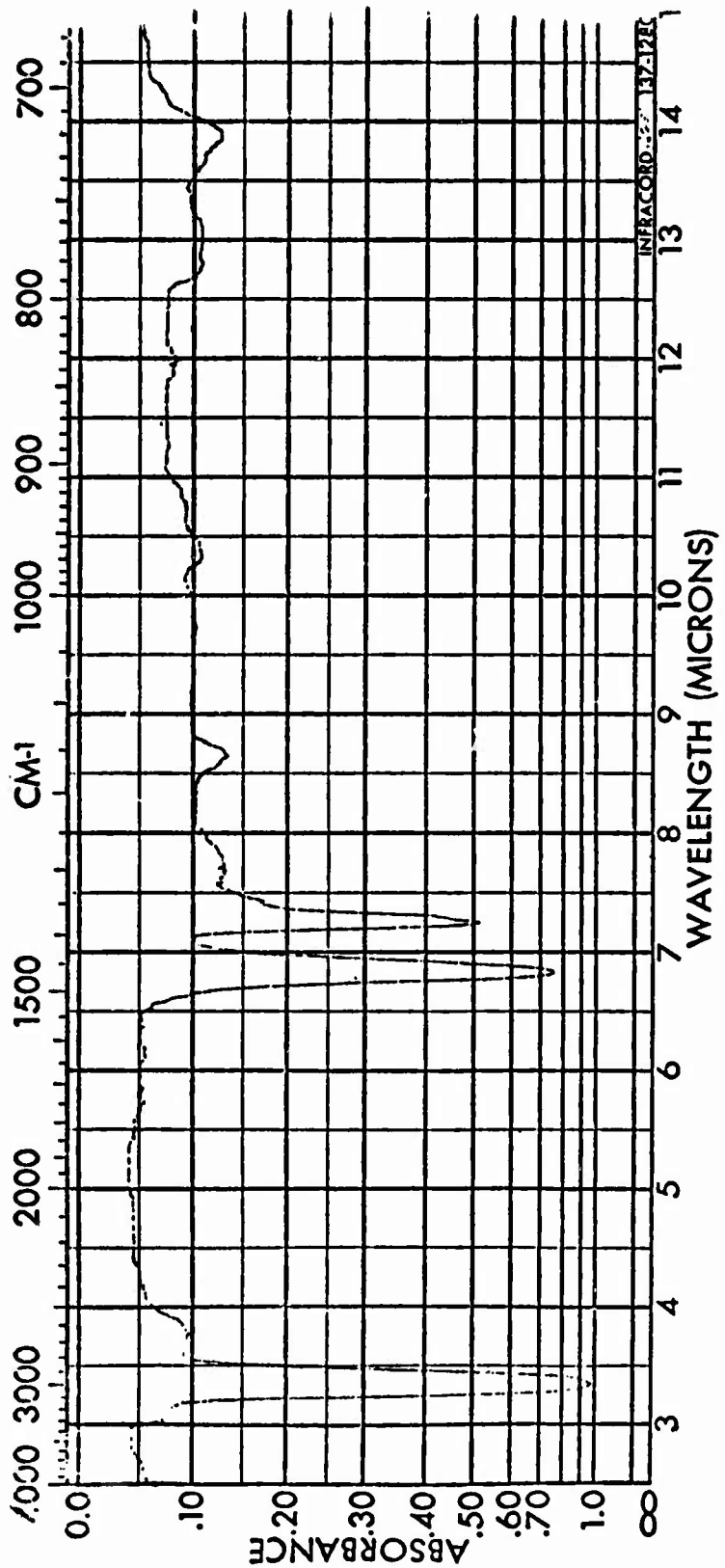

Figure 28. INFRARED SPECTRUM OF PENTANE FRACTION FROM OXIDIZED MLO 7685

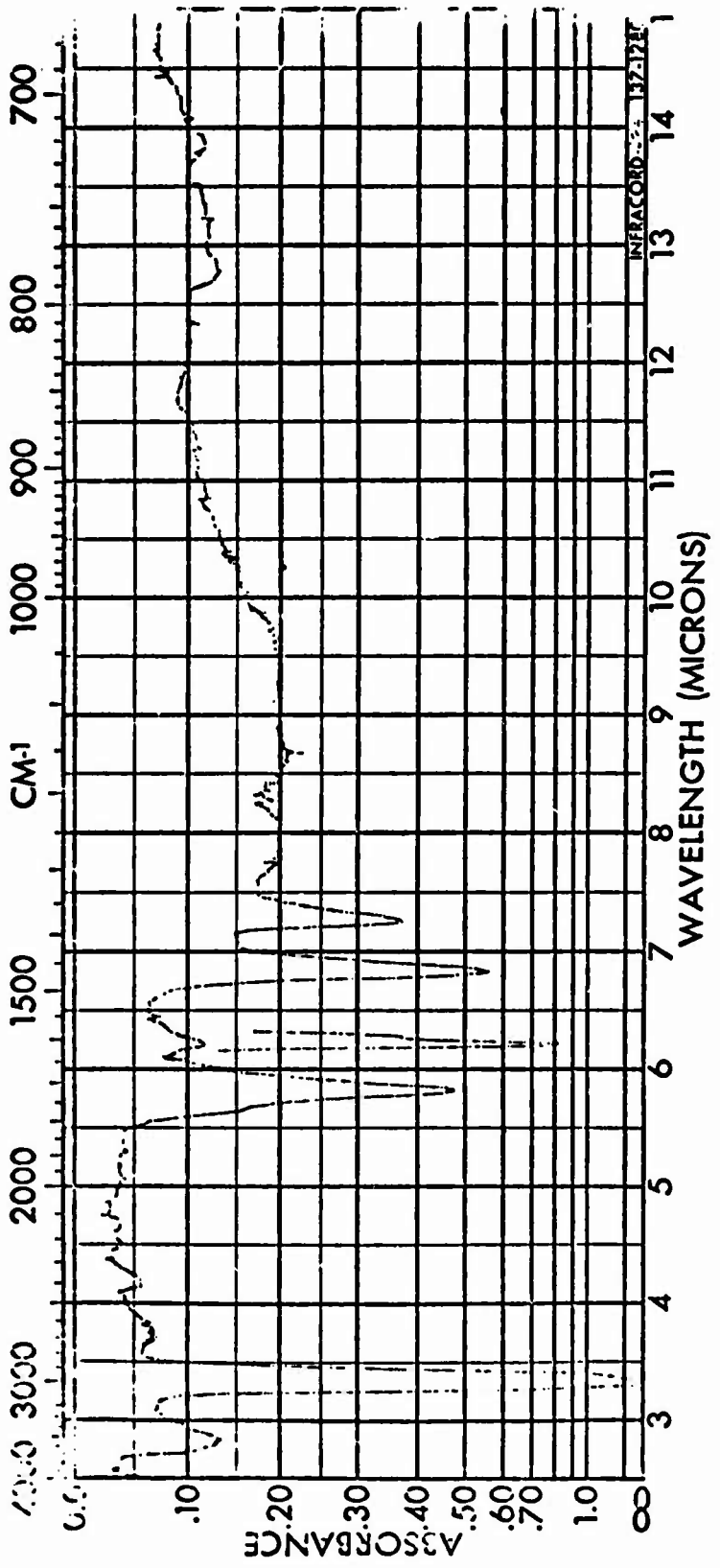

Figure 29. INFRARED SPECTRUM OF METHANOL-ETHER FRACTION FROM OXIDIZED MLO 7685

Table 8

DISTILLATION RANGES OF TEST FLUIDS AFTER OXIDATION

Determined by temperature-programmed gas chromatographic techniques.
Fluid descriptions shown in Table 3

Fluid Designation	Total Oxidized Product	Paraffin Portion of Oxidized Product		
	Initial Boiling Point, °F	Initial Boiling Point, °F.	10% Boiling Point, °F.	90% Boiling Point, °F.
MLO 7625	---	565	732	910
MLO 7789	---	569	673	808
MLO 7478	438	445	587	821
MLO 7797	420	452	558	703
MLO 7685	391	394	445	610

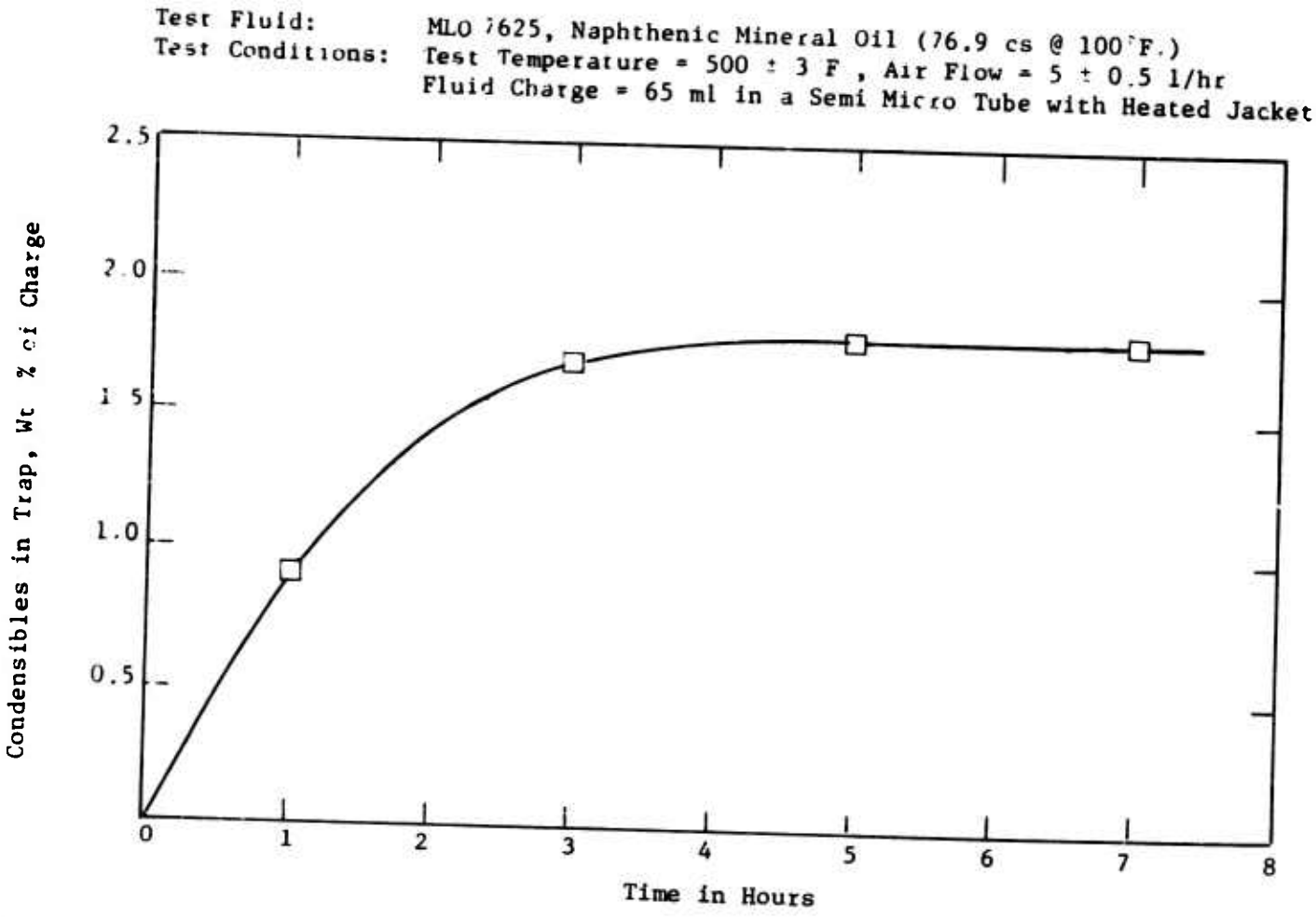

Figure 30. VOLATILE PRODUCTS CONDENSED IN COLD TRAP

Test Fluid: MLO 7710, Di-2-Ethylhexyl Sebacate (12.6 cs @ 100°F.)
Test Conditions: Test Temperature = 500 ± 3°F., Air Rate = 5 ± 0.5 l/hr
Fluid Charge = 200 ml in a Regular Tube with Air Cooled Condenser

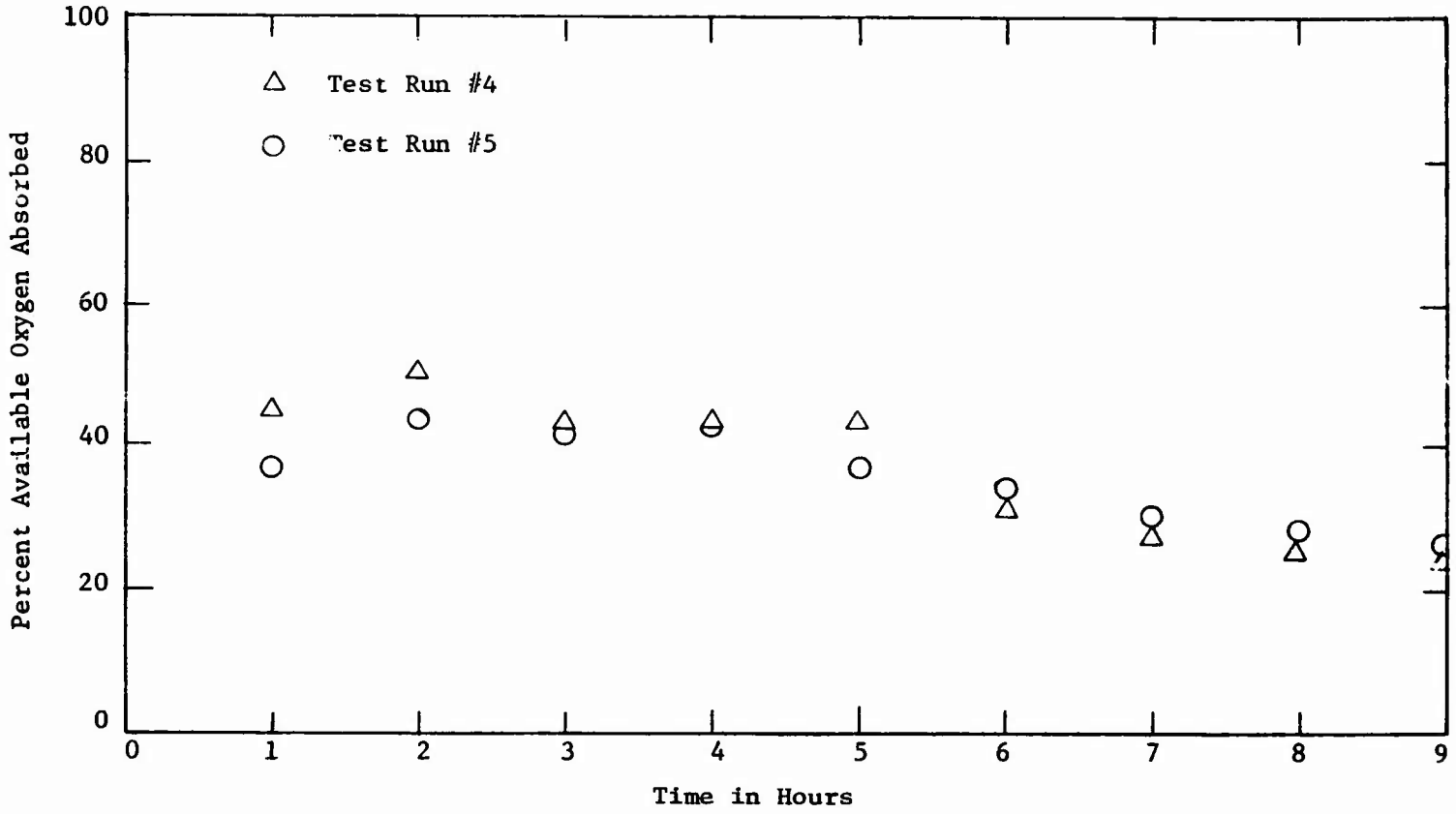

Figure 31. REPRODUCIBILITY OF OXIDATION TEST USING DI-2-ETHYLHEXYL SEBACATE

Test Fluid: MLO 7710, Di-2-Ethylhexyl Sebacate (12.6 cs at 100°F.)
Test Conditions: Test Temperature = 500 ± 3°F., Air Rate = 5 ± 0.5 l/hr
Fluid Charge = 200 ml, Regular Tube with Air Cooled Condenser

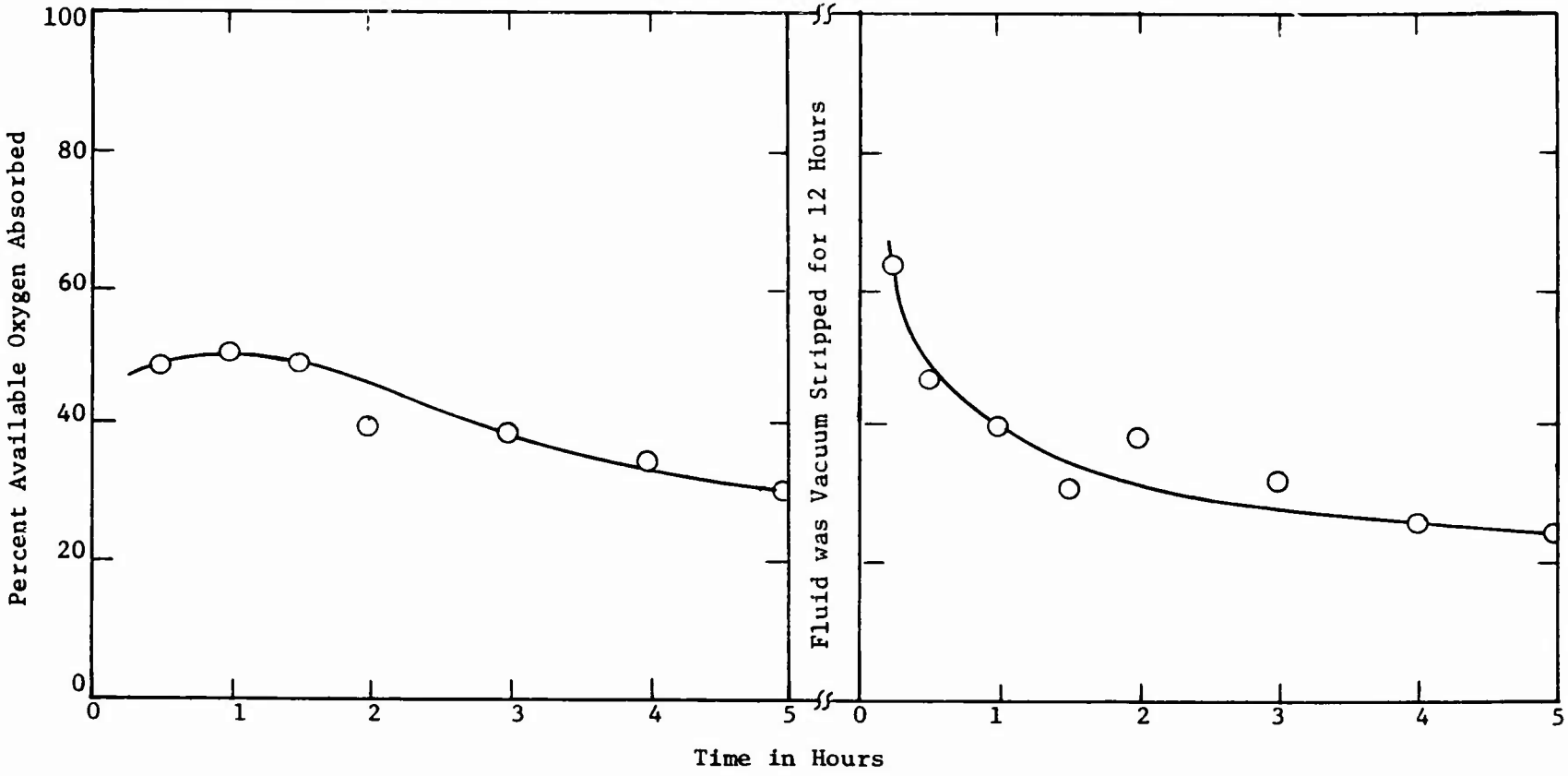

Figure 32. EFFECT OF VACUUM STRIPPING ON THE OXYGEN ASSIMILATION OF MLO 7710

Test Fluid: MLO 7710, Di-2-Ethylhexyl Sebacate (12.6 cs @ 100°F.)
Test Conditions: Test Temperature = 500 ± 3°F., Air Rate = 5 ± 0.5 l/hr
Fluid Charge = 200 ml, Regular Tube with Air Cooled Condenser

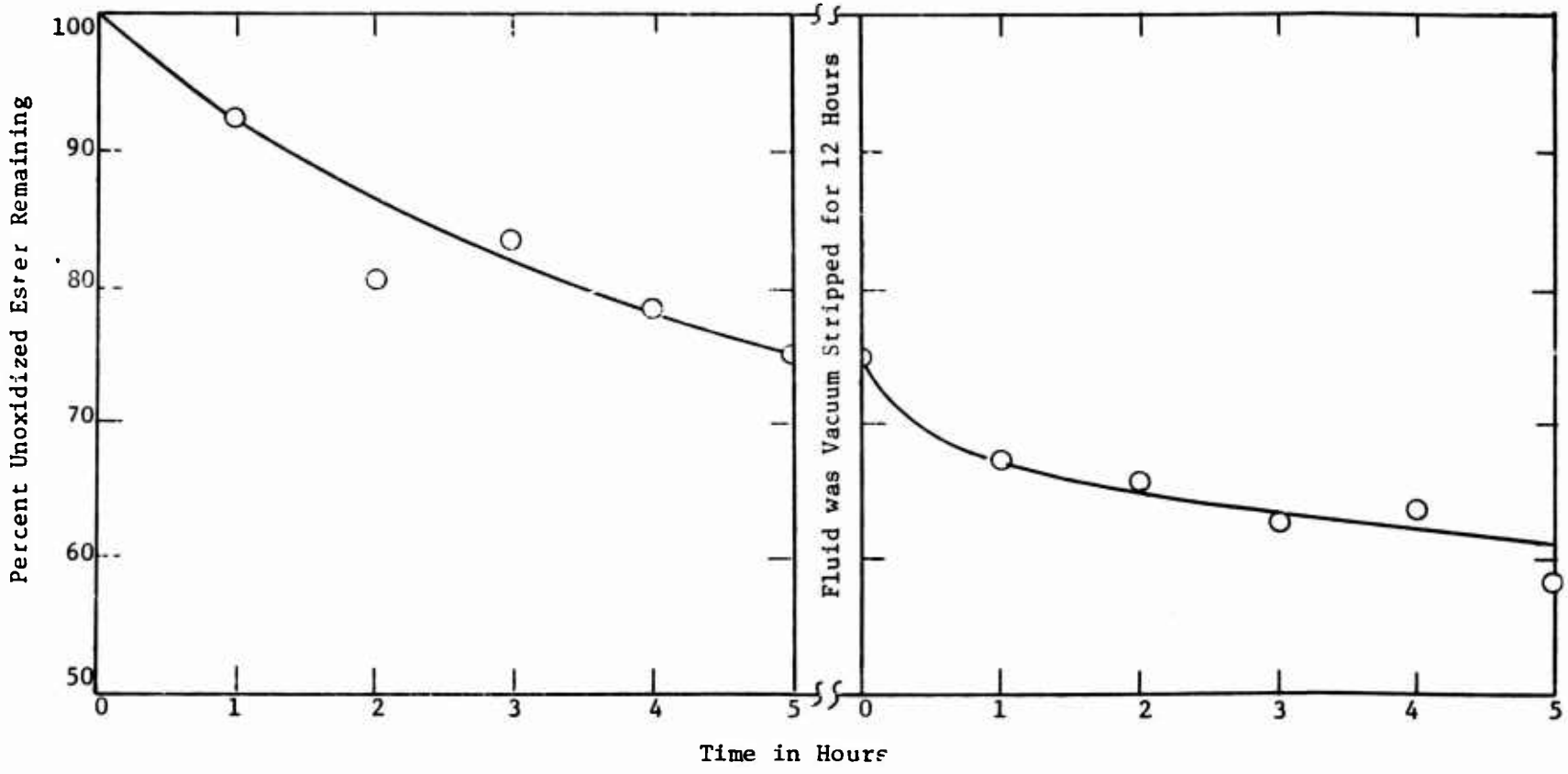

Figure 33. EFFECT OF VACUUM STRIPPING ON THE DEGRADATION OF MLO 7710 DURING OXIDATION

Test Fluid: MLO 7625, Naphthenic Mineral Oil (76.9 cs @ 100°F.)
Test Conditions: Test Temperature = 500 ± 3°F., Air Rate = 5 ± 0.5 1/hr
Fluid Charge = 200 ml in a Regular Tube with Heated Jacket

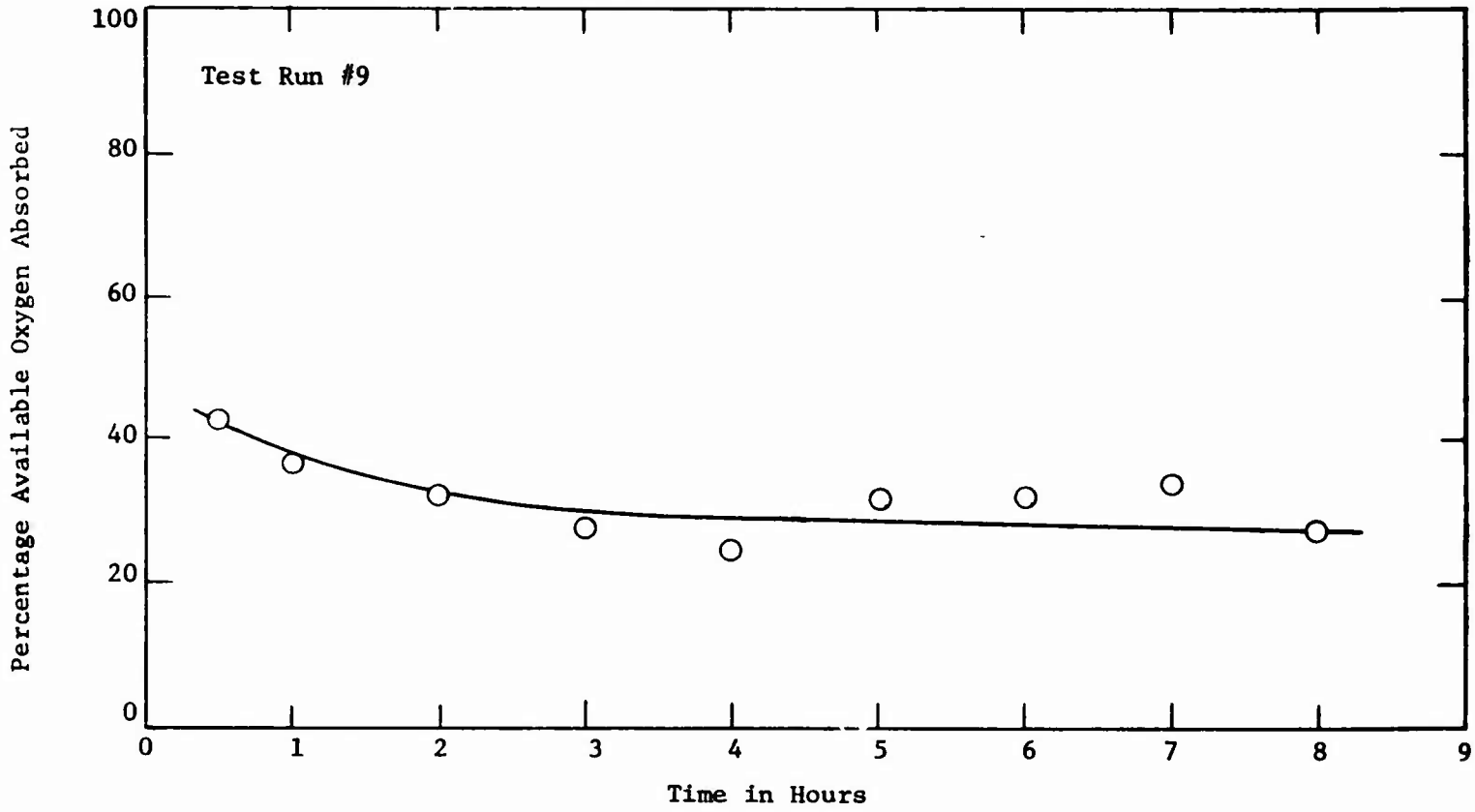

Figure 34. OXYGEN ASSIMILATION MEASUREMENT FOR MLO 7625

Test Fluid: Vacuum Stripped Product from Test Run #9 (Fig. 24)
Test Conditions: Test Temperature = 500 ± 3°F., Air Rate = 5 ± 0.5 1/hr
Fluid Charge = 65 ml, in a Semi Micro Tube with Heated Jacket

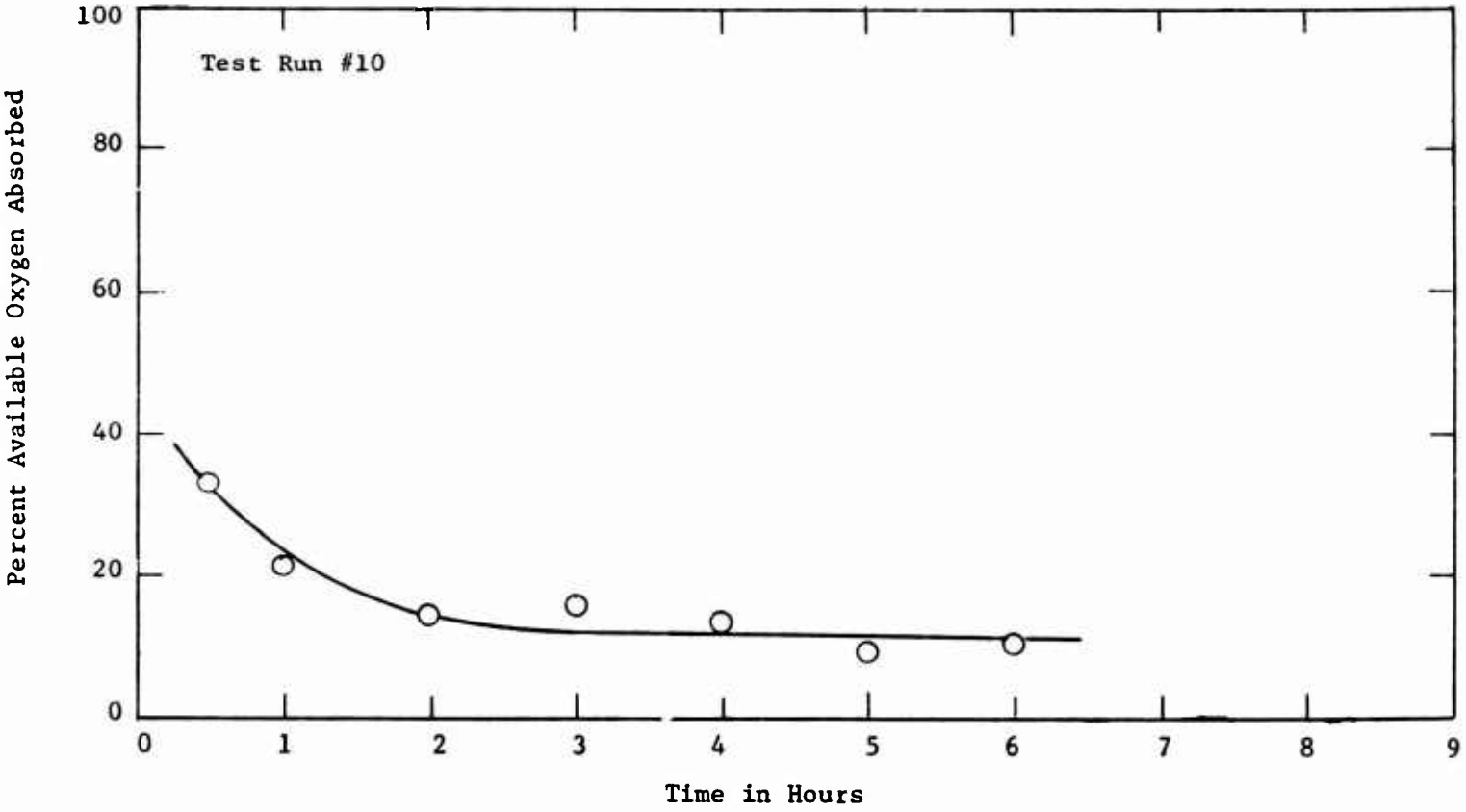

Figure 35. EFFECT OF VACUUM STRIPPING ON OXYGEN ABSORPTION

Test Fluid: MLO 7625, Naphthenic Mineral Oil (76.9 cs @ 100°F.)
Test Conditions: Test Temperature = 500 ± 3°F., Air Rate = 5 ± 0.5 l/hr
Fluid Charge = 65 ml, in a Semi Micro Tube with Heated Jacket

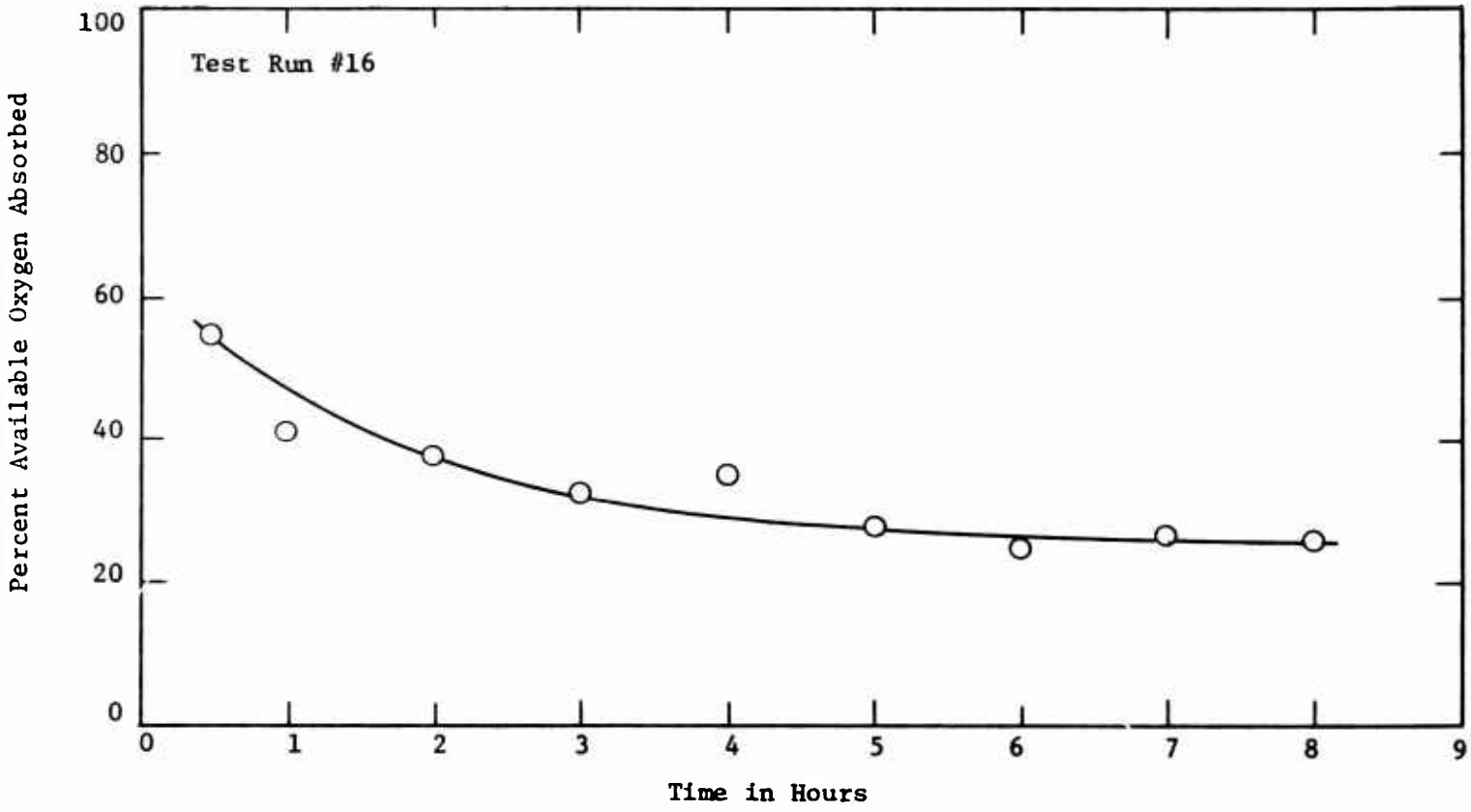

Figure 36 OXYGEN ASSIMILATION MEASUREMENTS FOR MLO 7625

Test Fluid: A 50:50 Mixture of MLO 7625 and Product from Test Run #16 (Fig. 26).
Test Conditions: Test Temperature = 500 ± 3°F., Air Rate = 5 ± 0.5 l/hr
Fluid Charge = 65 ml, in a Semi Micro Tube with Heated Jacket

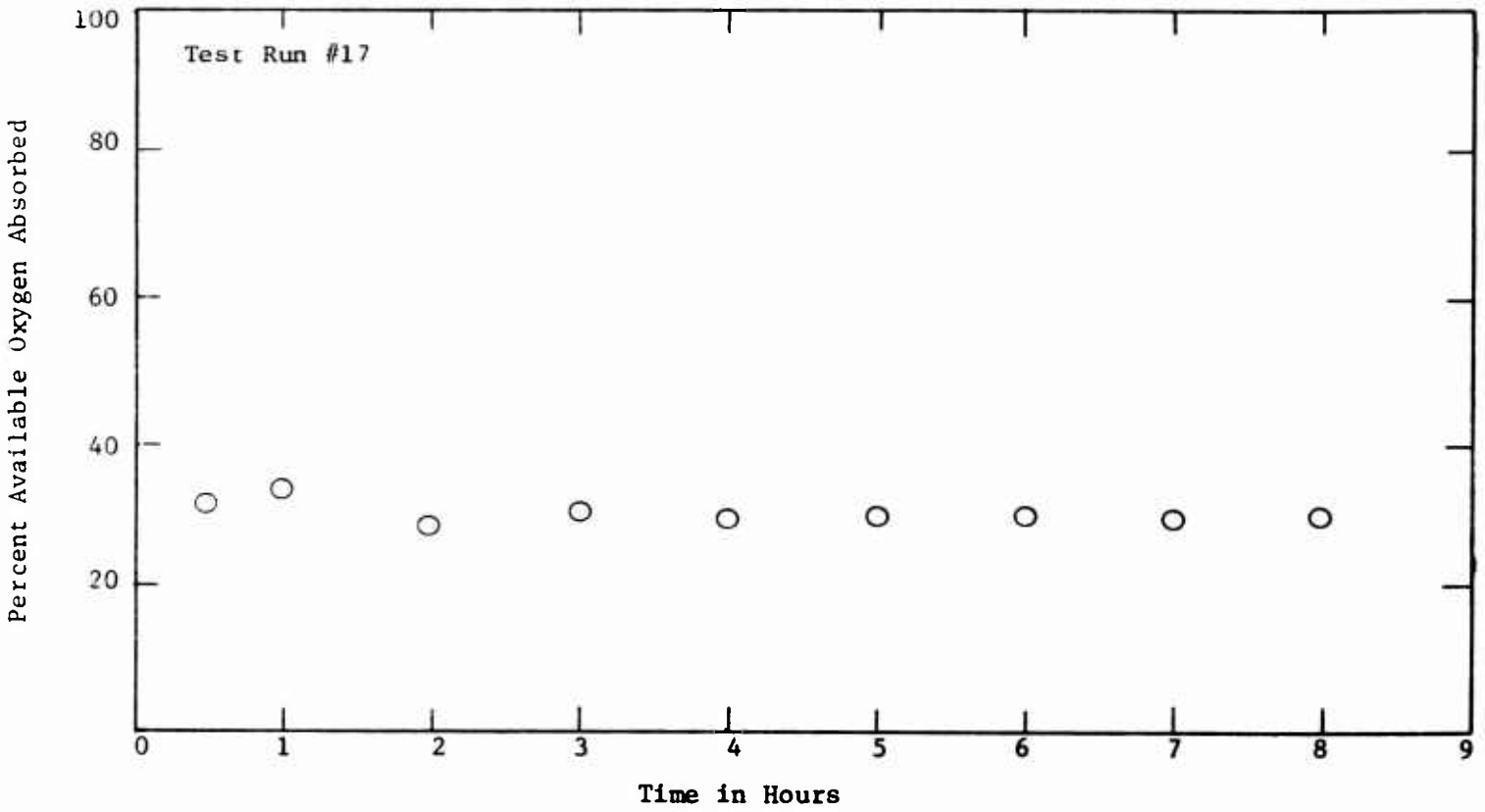

Figure 37. EFFECT OF ADDITION OF 50 PERCENT OXIDIZED PRODUCT ON OXYGEN ASSIMILATION

Test Fluid: A Mixture of 10% of Product from Test Run #17 (Fig. 37) in MLO 7625
Test Conditions: Test Temperature = 500 ± 3°F., Air Rate = 5 ± 0.5 l/hr
Fluid Charge = 65 ml, in a Semi Micro Tube with Heated Jacket

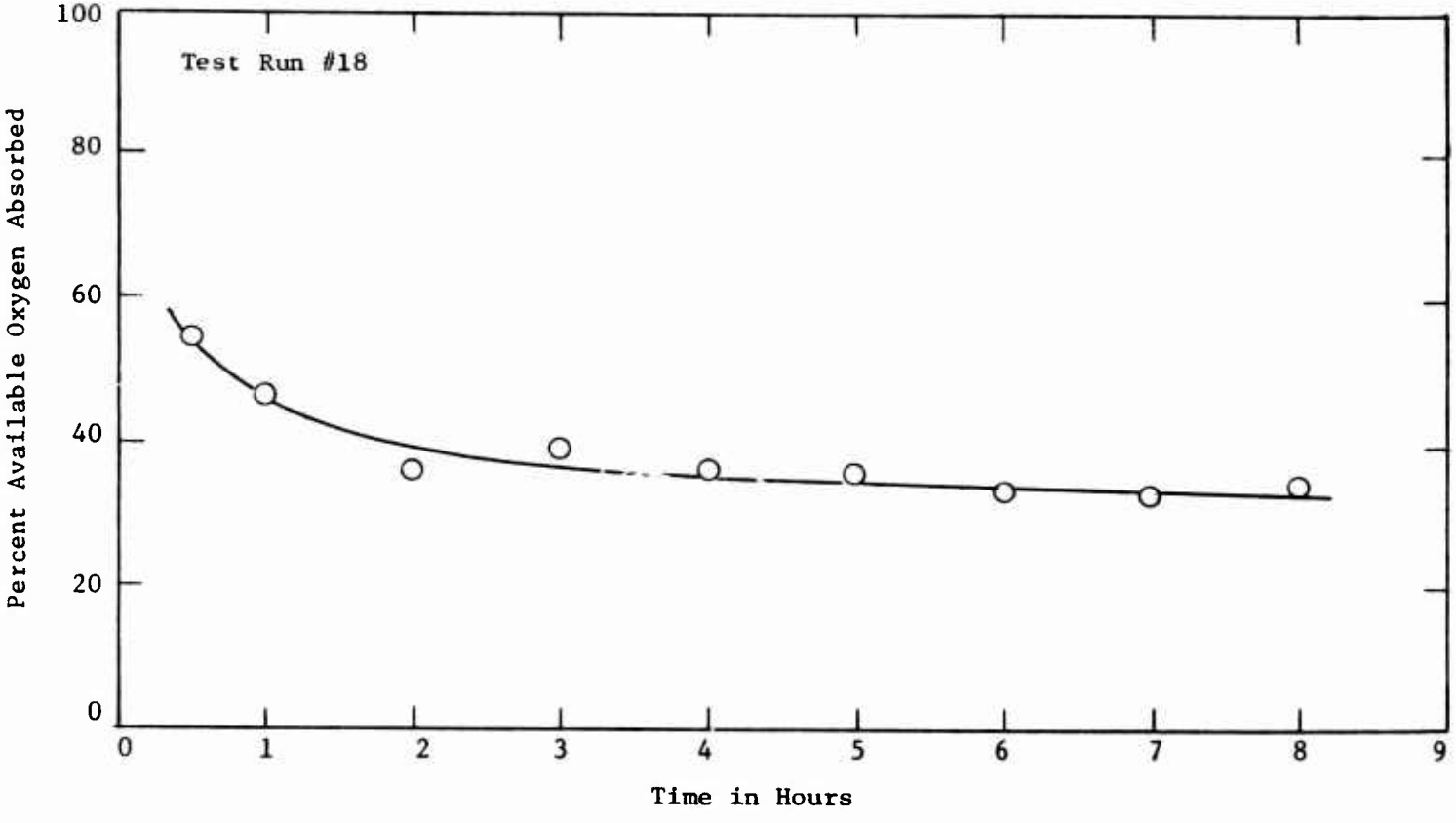

Figure 38 EFFECT OF THE ADDITION OF 10% OF OXIDIZED PRODUCT ON OXYGEN ASSIMILATION

Test Fluid: Vacuum Stripped Product from Test Run #18 (Fig. 38).
Test Conditions: Test Temperature = 500 ± 3°F., Air Rate = 5 ± 0.5 l/hr
Fluid Charge = 65 ml, in a Semi Micro Tube with Heated Jacket

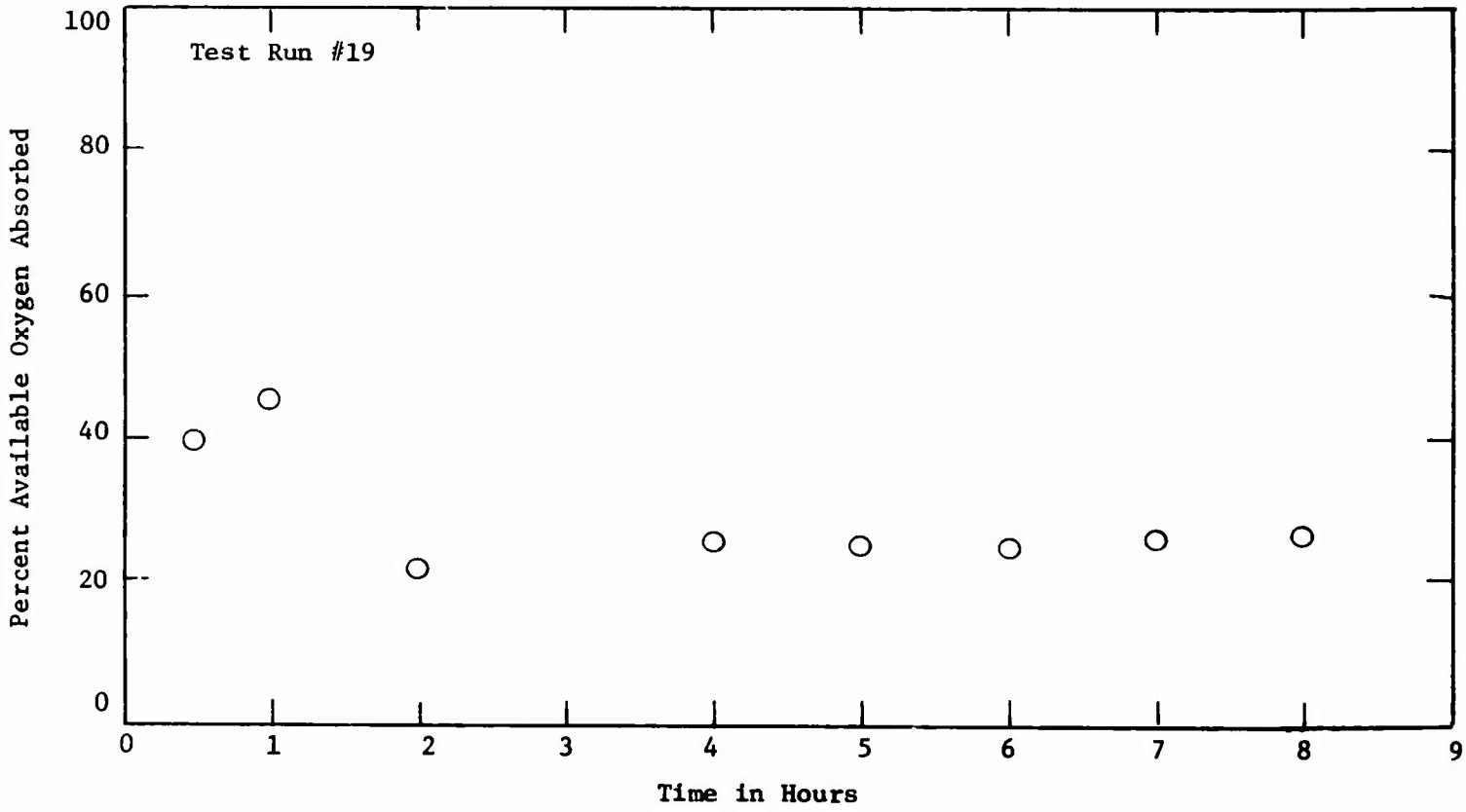

Figure 39. EFFECT OF VACUUM STRIPPING ON OXYGEN ABSORPTION

Test Fluid: Product of Test Run #19 (Fig. 39), Percolated Through Alumina
Test Conditions: Test Temperature = 500 ± 3°F., Air Rate = 5 ± 0.5 1/hr
Fluid Charge = 65 ml, in a Semi Micro Tube with Heated Jacket

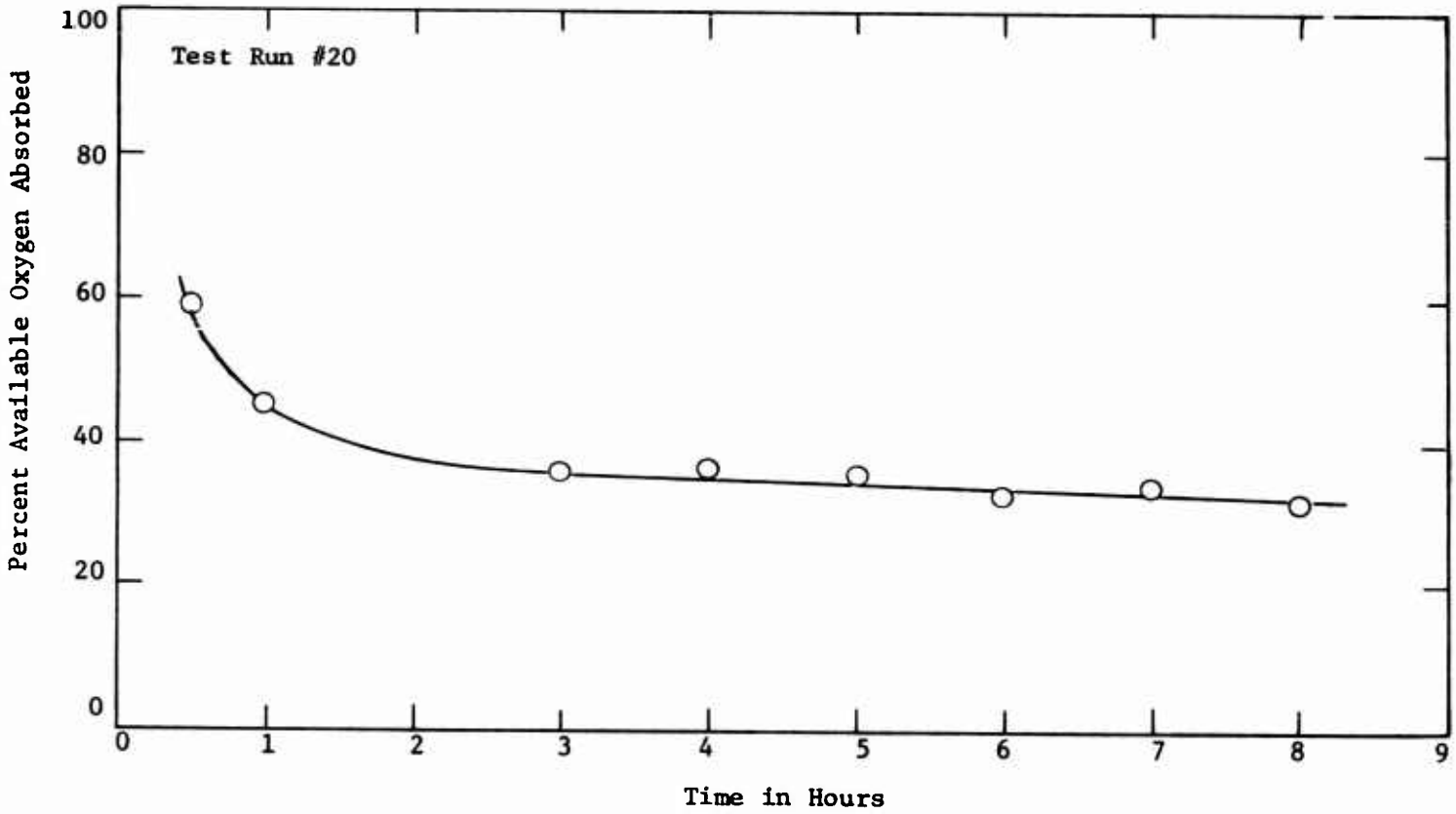

Figure 40. OXYGEN ASSIMILATION OF UNOXIDIZED FRACTION OF PRODUCT FROM TEST RUN #19 (FIG. 39)

Test Fluid: MLO 7625 Naphthenic Mineral Oil (76.9 cs @ 100°F.)
Test Conditions: Test Temperature = 500 ± 3°F , Air Rate = 5 ± 0.5 l/hr
Fluid Charge = 65 ml, in a Semi Micro Tube with Heated Jacket

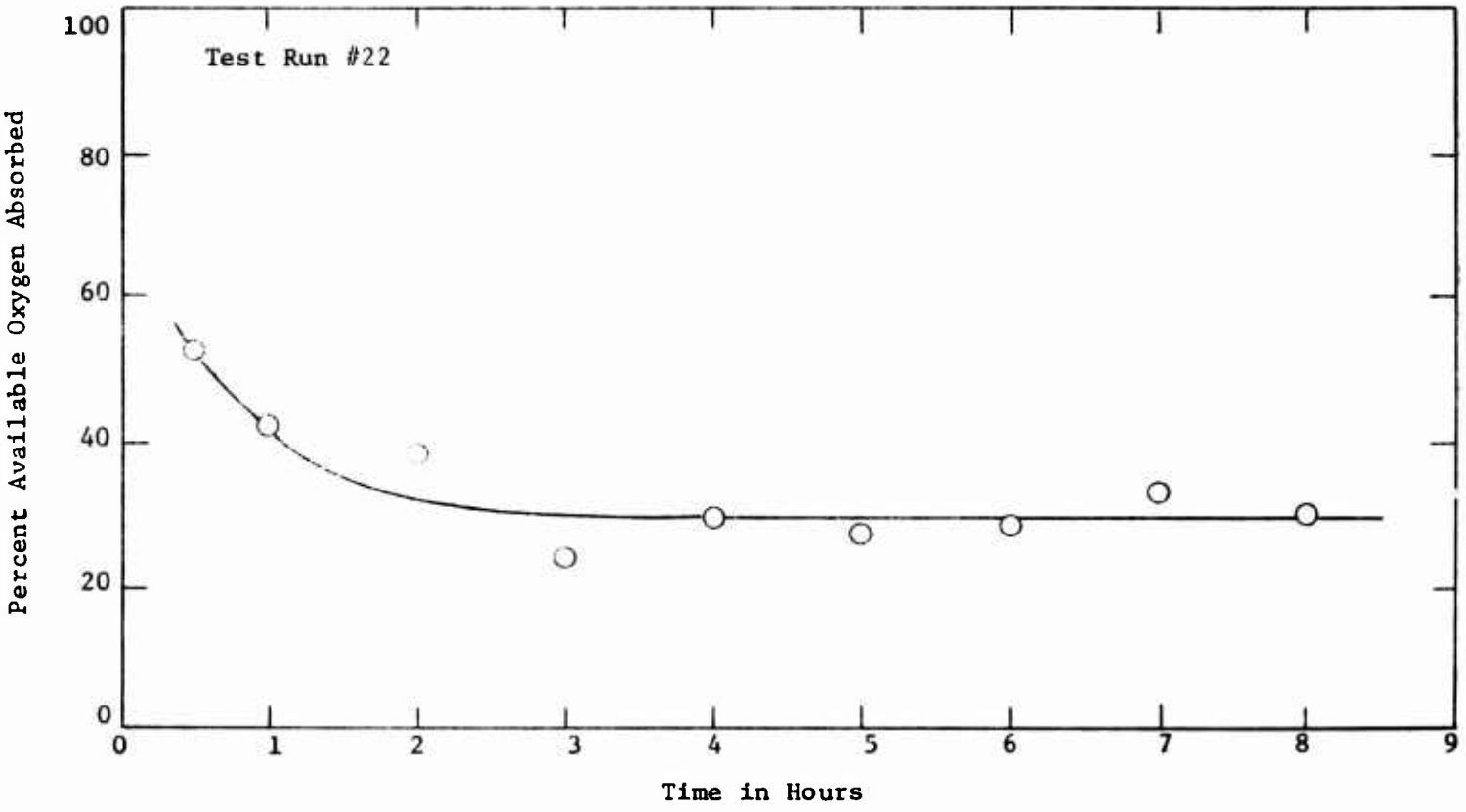

Figure 41. OXYGEN ASSIMILATION MEASUREMENTS FOR MLO 7625

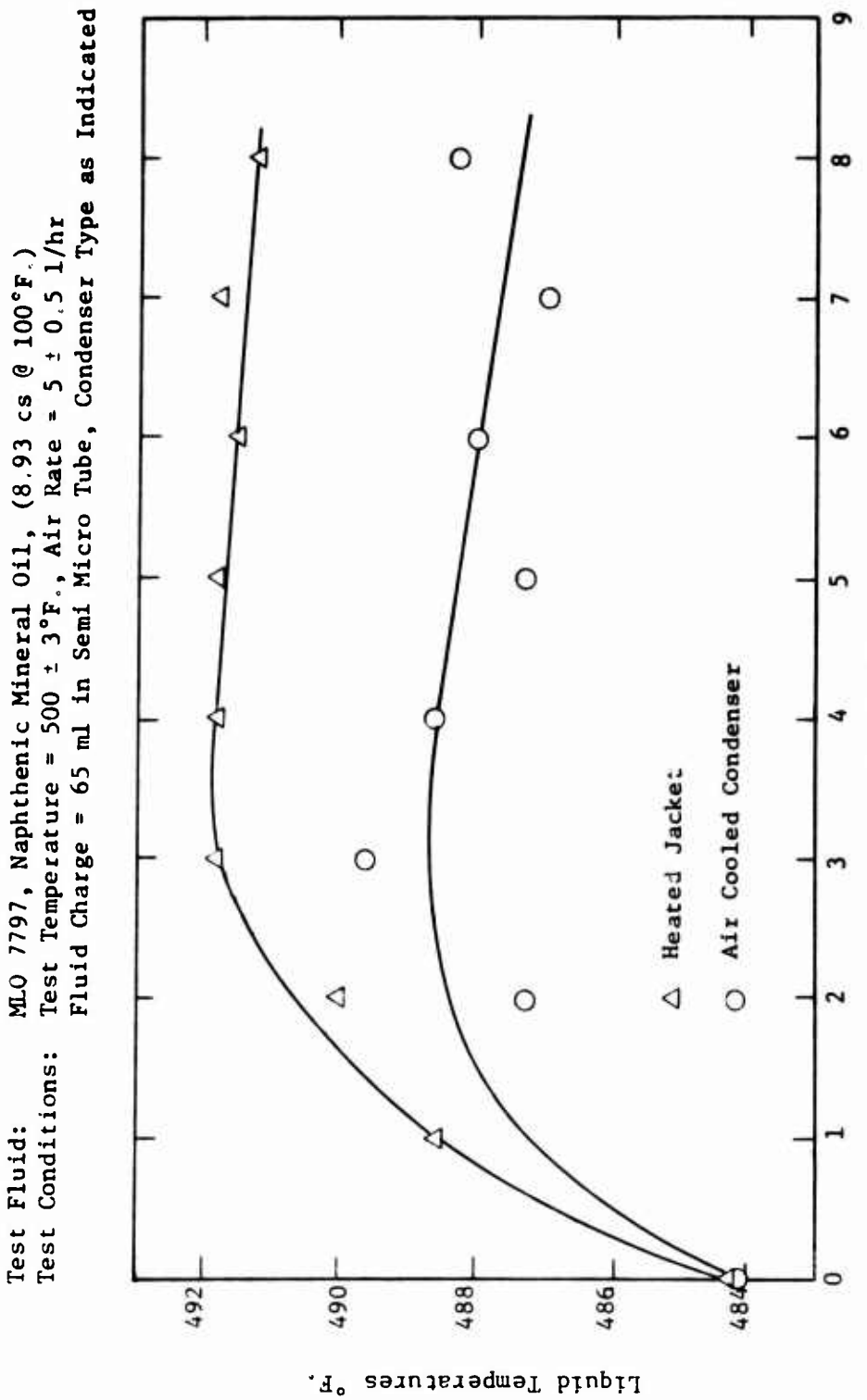

Figure 42. LIQUID PHASE TEMPERATURES FOR OXIDATION TEST USING MLO 7797

Test Fluid: MLO 7797, Naphthenic Mineral Oil (8.93 cs at 100°F.)
Test Conditions: Test Temperature = 500 ± 3°F., Air Rate = 5 ± 0.5 l/hr
Fluid Charge = 65 ml in a Semi Micro Tube with Condenser Type as Indicated

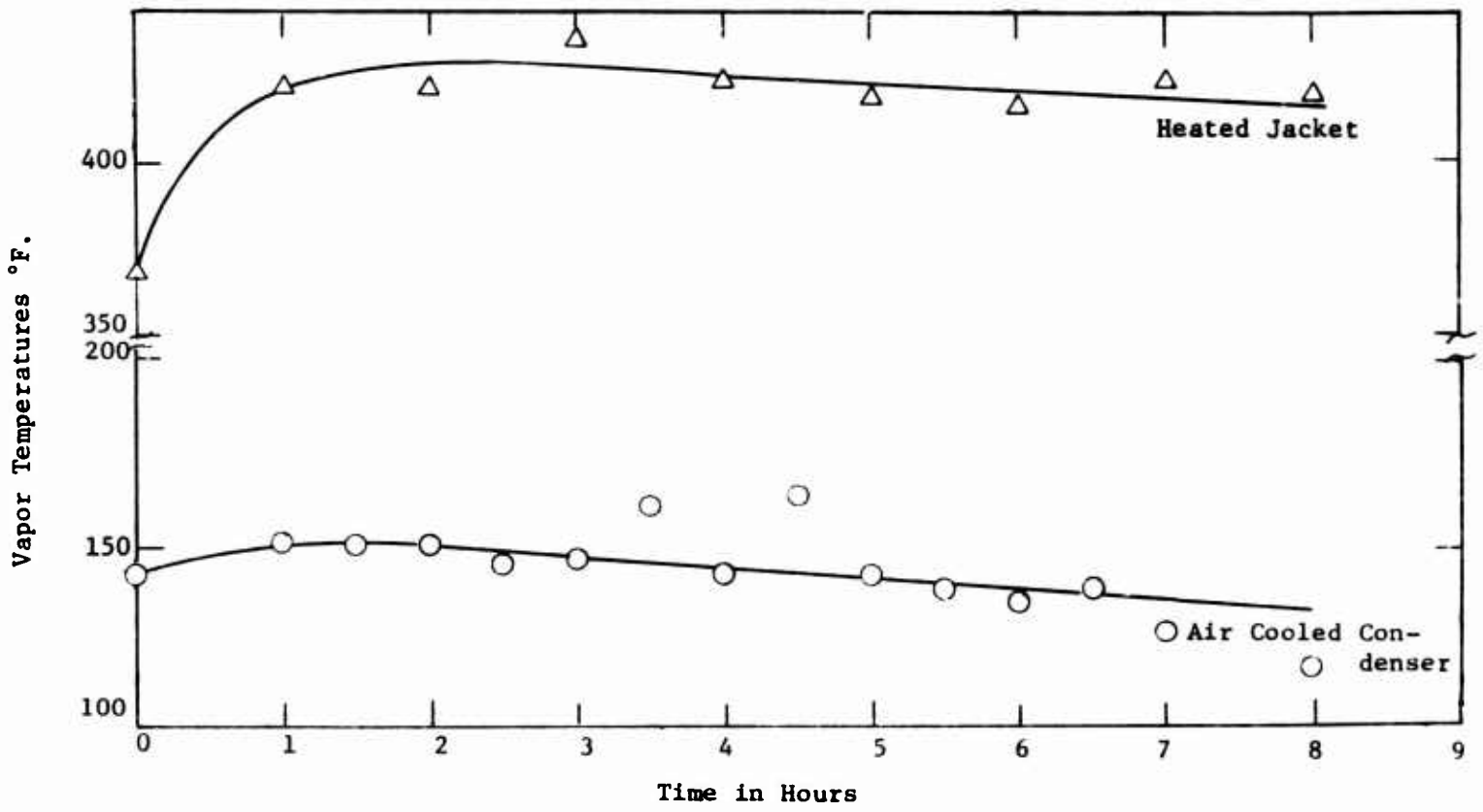

Figure 43 VAPOR PHASE TEMPERATURES FOR OXIDATION TEST USING MLO 7797

Test Fluid: MLO 7625, Naphthenic Mineral Oil (76.9 cs @ 100°F.)
Test Conditions: Test Temperature = 500 ± 3°F., Air Rate = 5 ± 0.5 l/hr
Fluid Charge = 200 ml in a Regular Tube with Condenser Type as Indicated

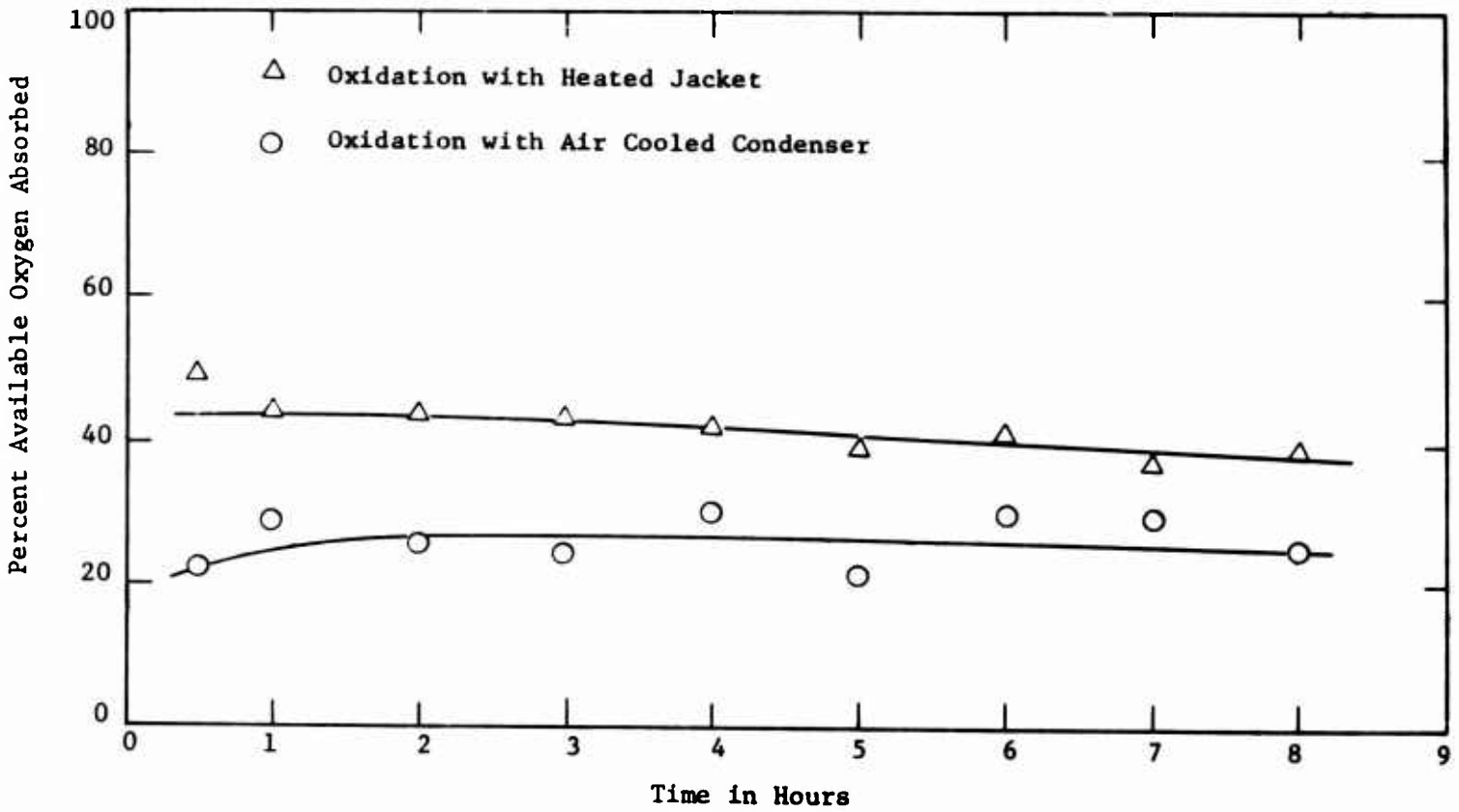

Figure 44. THE EFFECT OF THE HEATED JACKET ON OXYGEN ASSIMILATION

Test Fluid: MLO 7710, Di-2-Ethylhexyl Sebacate (12.6 cs @ 100°F.)
Test Conditions: Test Temperature = 500 ± 3°F., Air Rate = 5 ± 0.5 1/hr
Fluid Charge = 65 ml in Semi Micro Tube with Condenser Type as Indicated

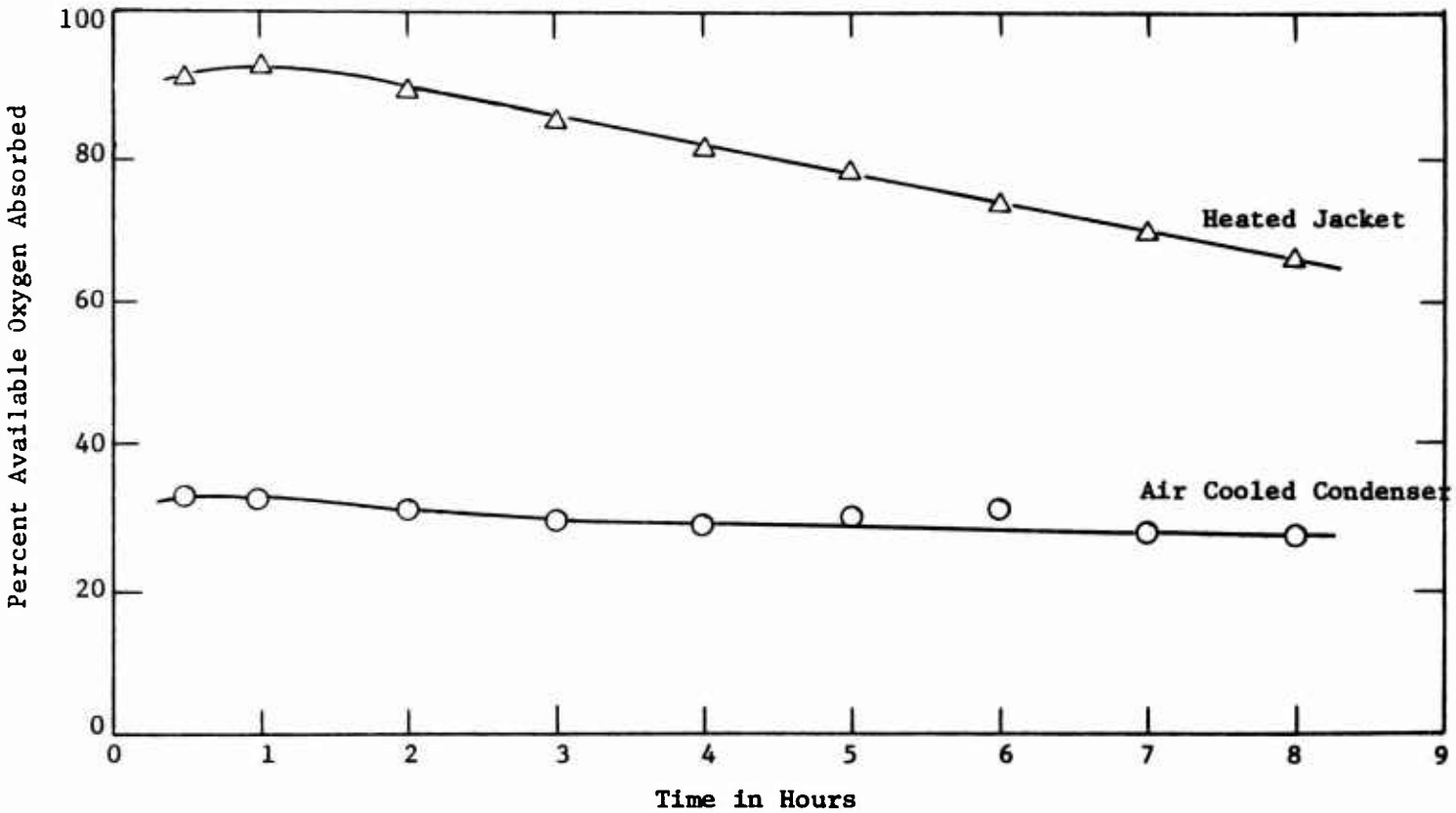

Figure 45. EFFECT OF HEATED JACKET ON OXYGEN ASSIMILATION

Test Fluid: MLO 7710, Di-2-Ethylhexyl Sebacate (12.6 cs @ 100°F.)
Test Conditions: Test Temperature = 500 ± 3°F., Air Rate = 5 ± 0.5°F.
Fluid Charge = 65 ml in Semi Micro Tube with Condenser Type as Indicated

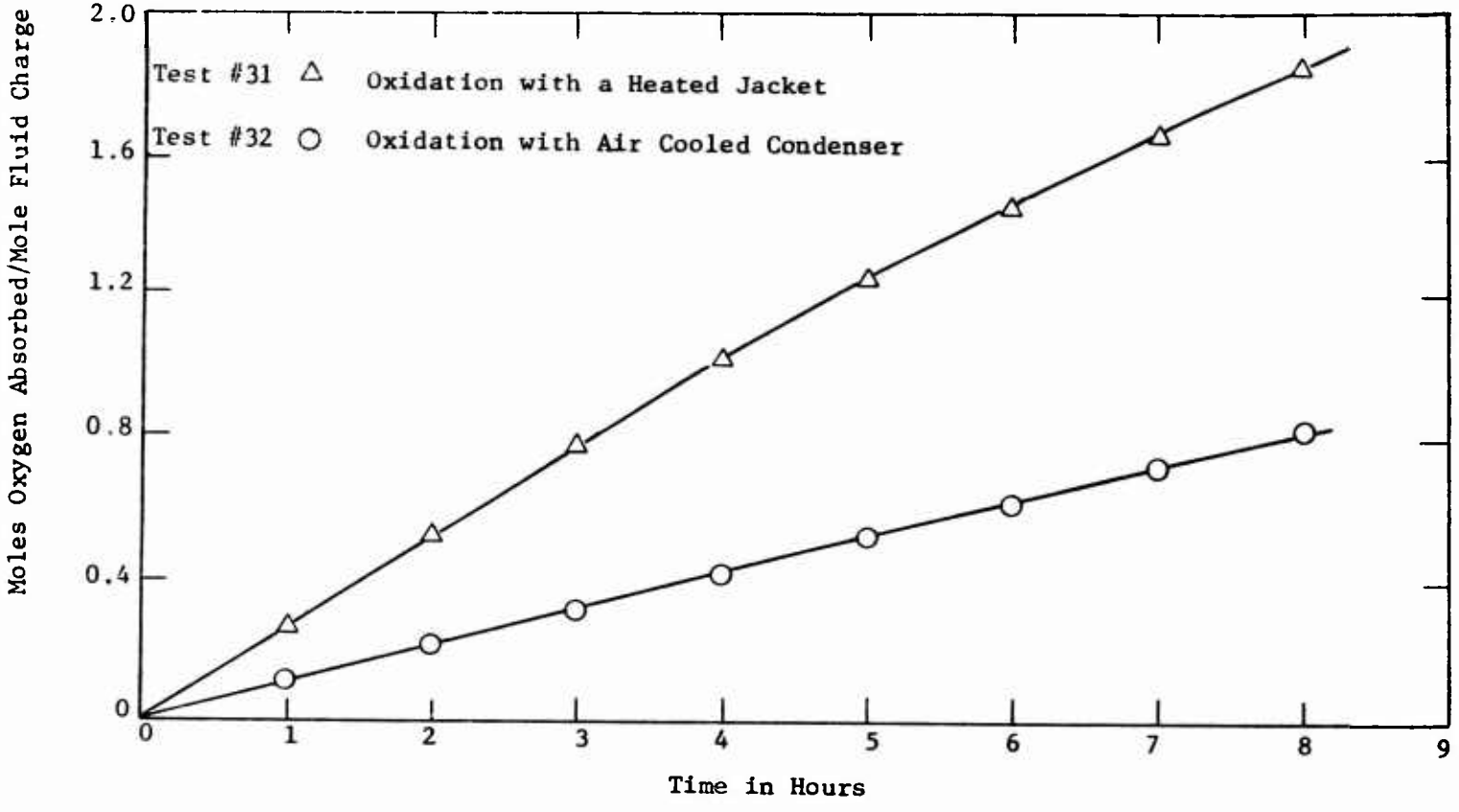

Figure 46. EFFECT OF HEATED JACKET ON RATE OF OXYGEN ASSIMILATION

Test Fluid: MLO 7710, Di-2-Ethylhexyl Sebacate (12.6 cs @ 100°F.)
Test Conditions: Temperature = 500 ± 3°F., Air Rate = 5 ± 0.5 1/hr
Fluid Charge = 65 ml in Semi Micro Tube with Condenser Type as Indicated

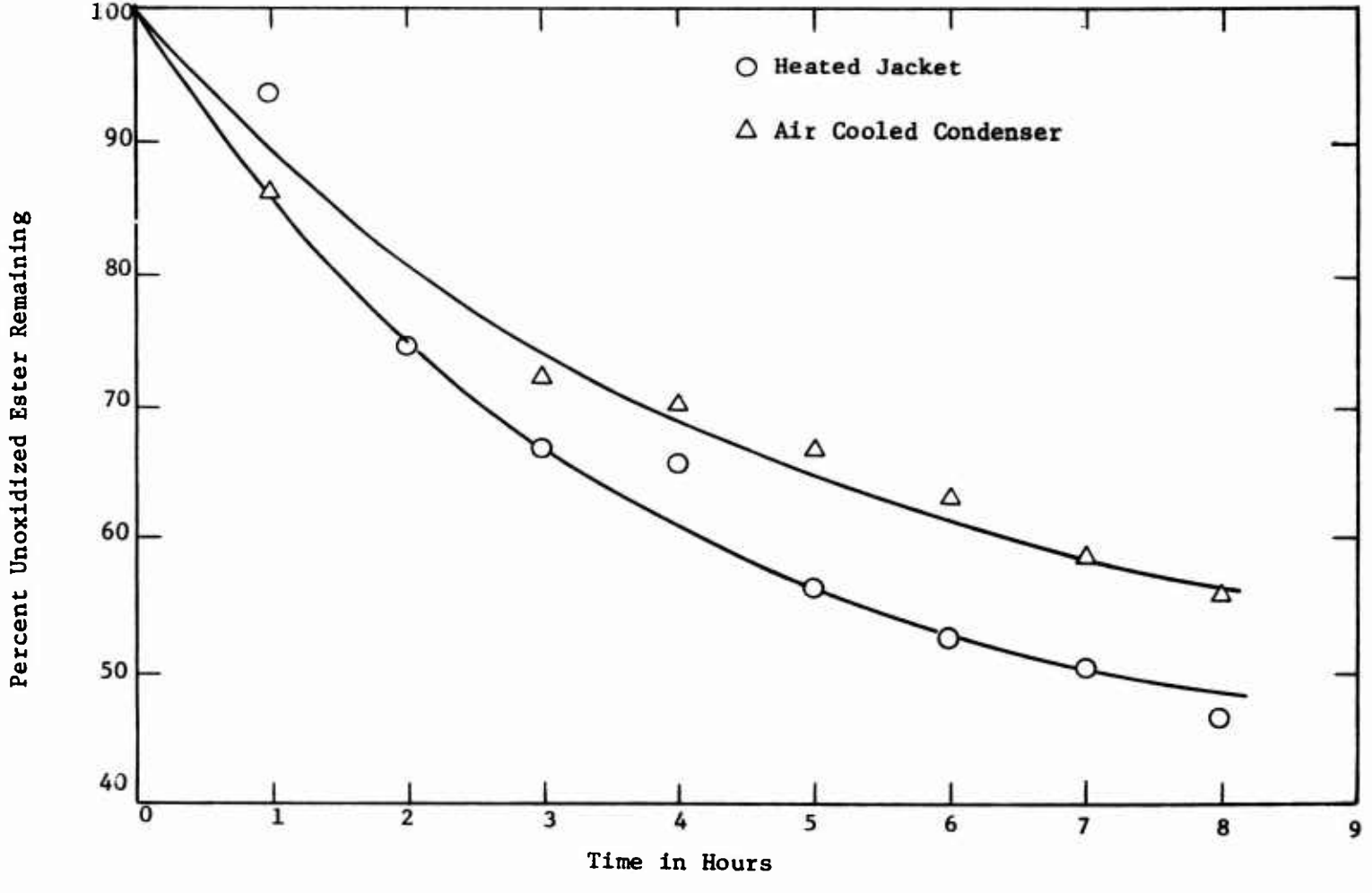

Figure 47. EFFECT OF HEATED JACKET ON DEGRADATION OF FLUID

Test Fluid: MLO 7710, Di-2-Ethylhexyl Sebacate (12.6 cs @ 100°F.)
Test Conditions: Test Temperature = 500 ± 3°F., Air Rate = 5 ± 0.5 l/hr
Fluid Charge = 65 ml in Semi Micro Tube with Condenser Type as Indicated

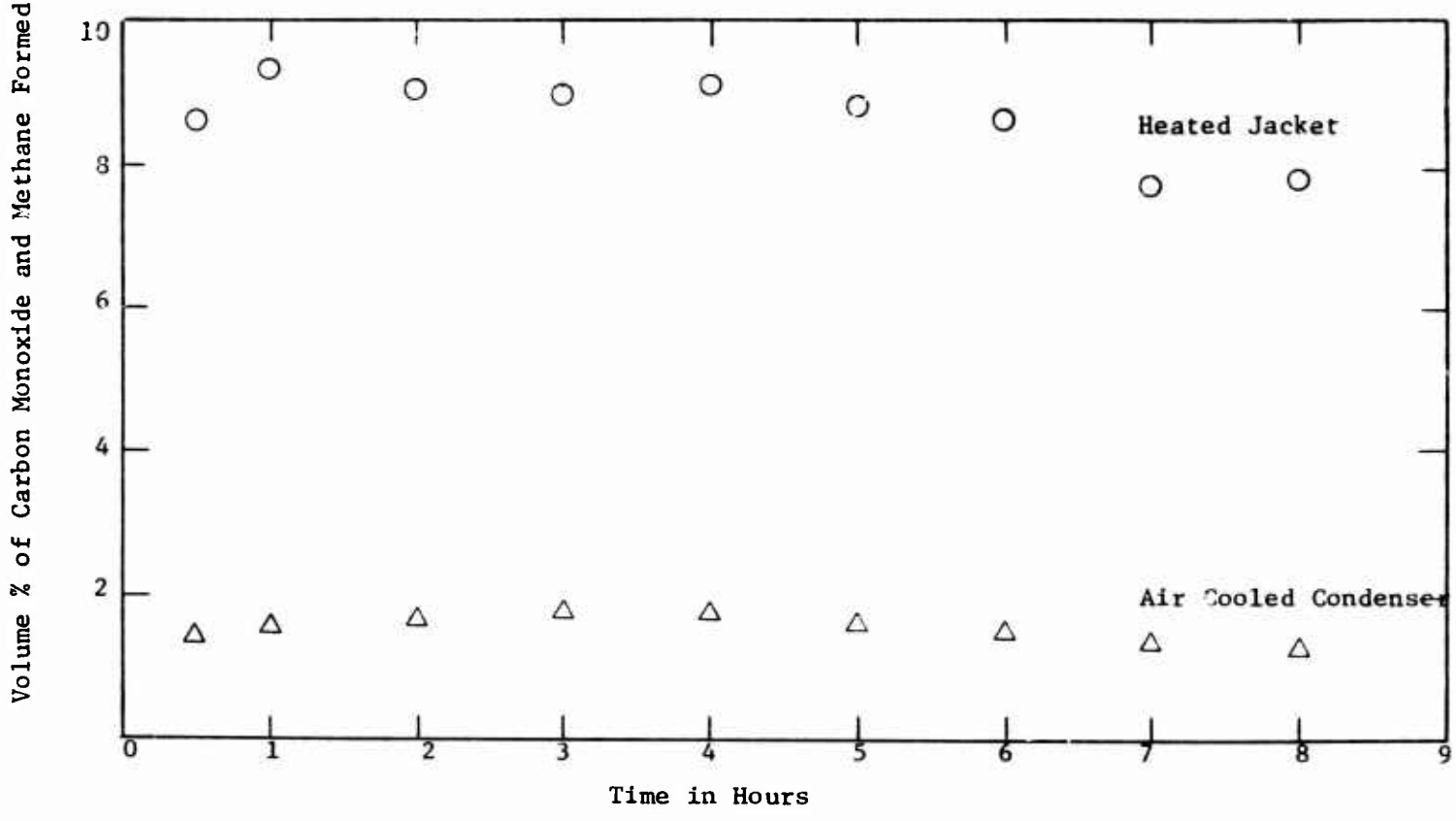

Figure 48. VOLUME PERCENT OF CARBON MONOXIDE AND METHANE FORMED IN THE OXIDATION OF DI-2-ETHYLHEXYL SEBACATE

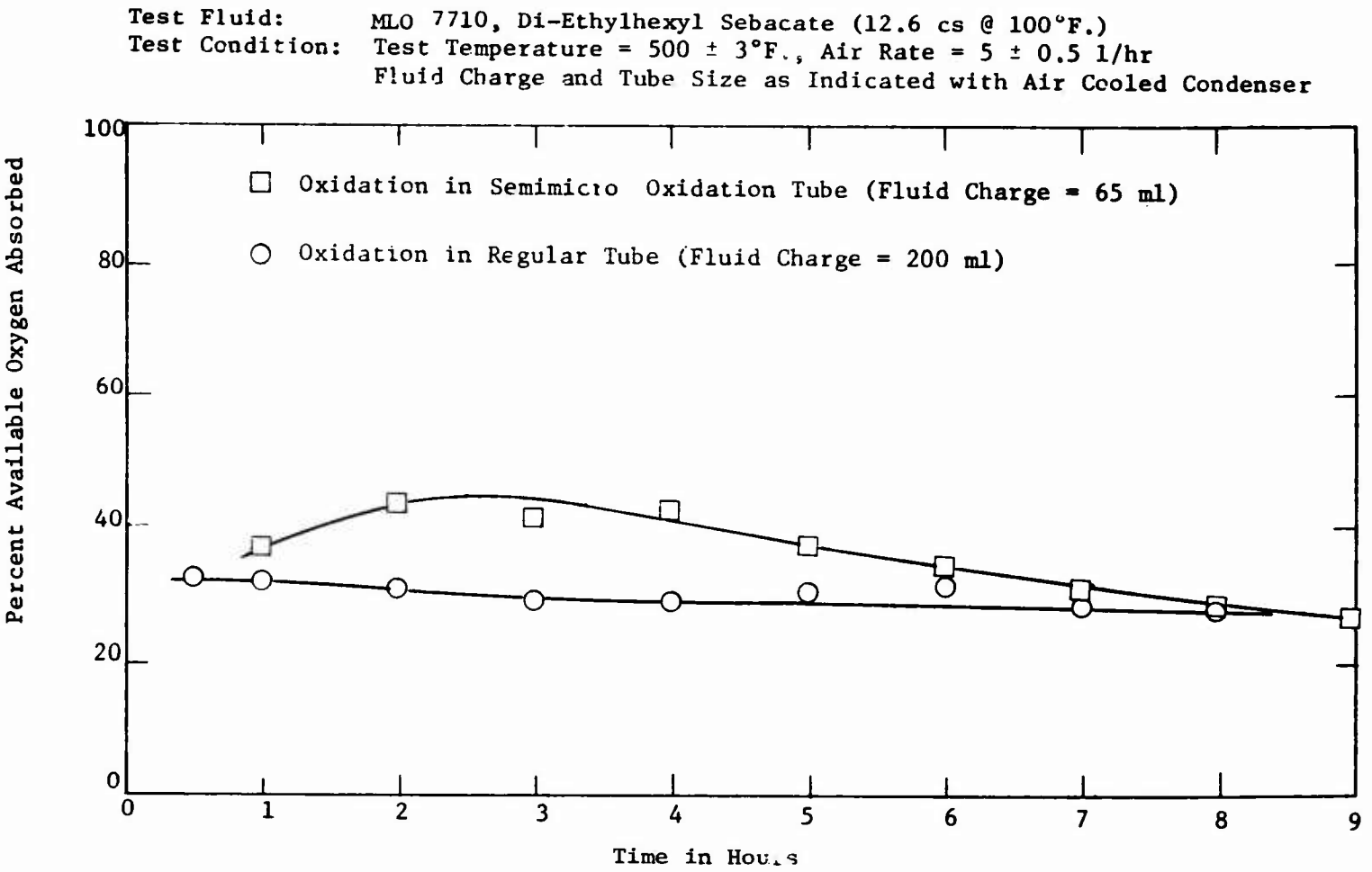

Figure 49. EFFECT OF GEOMETRY ON OXYGEN ASSIMILATION OF MLO 7710

Test Fluid: MLO 7710, Di-2-Ethylhexyl Sebacate (12.6 cs @ 100°F.)
Test Conditions: Test Temperature = 500 ± 3°., Air Rate = 5 ± 0.5 l/hr
Fluid Charge and Tube Size as Indicated, and Air Cooled Condenser

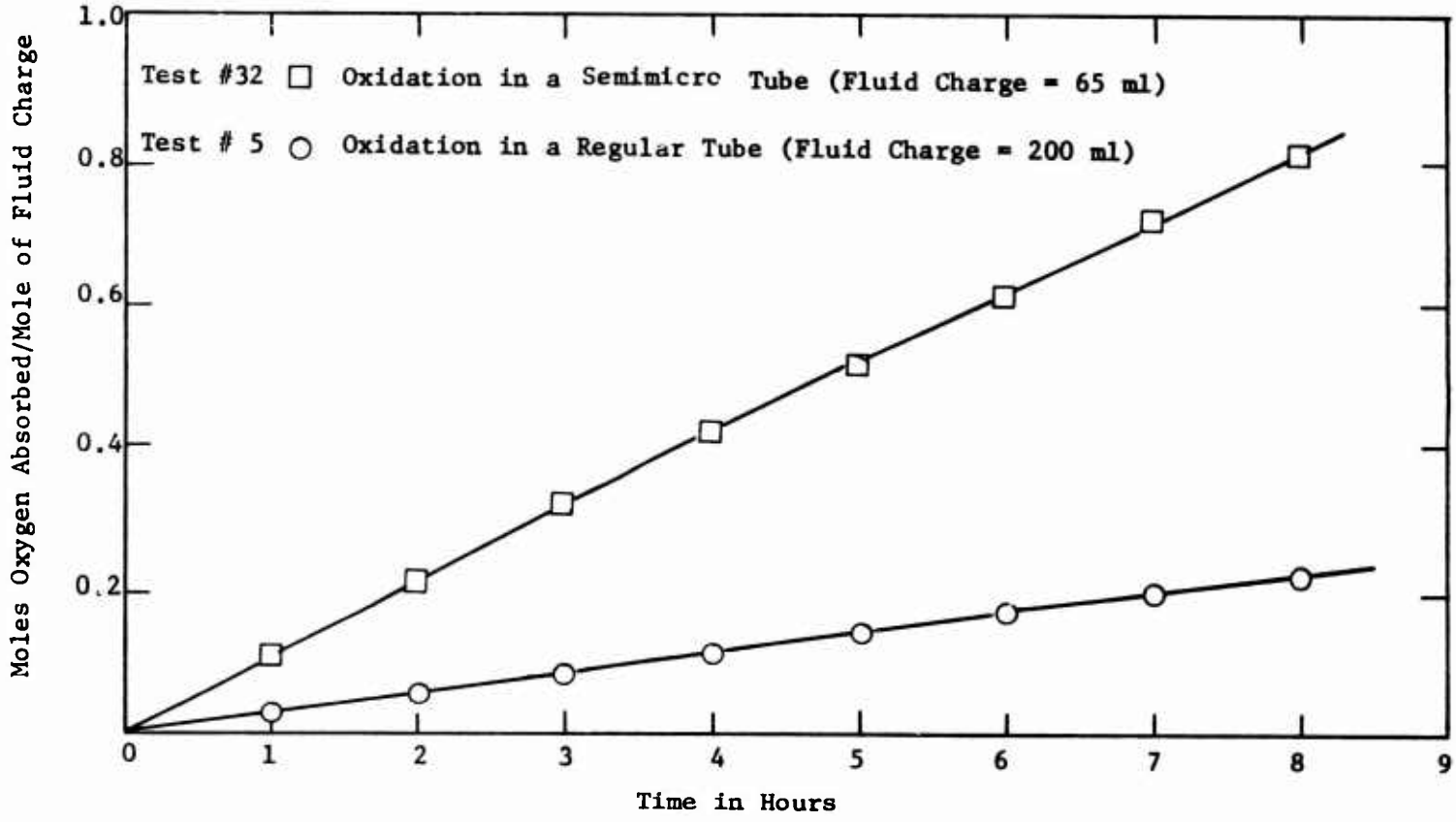

Figure 50. EFFECT OF GEOMETRY ON THE RATE OF OXYGEN ASSIMILATION

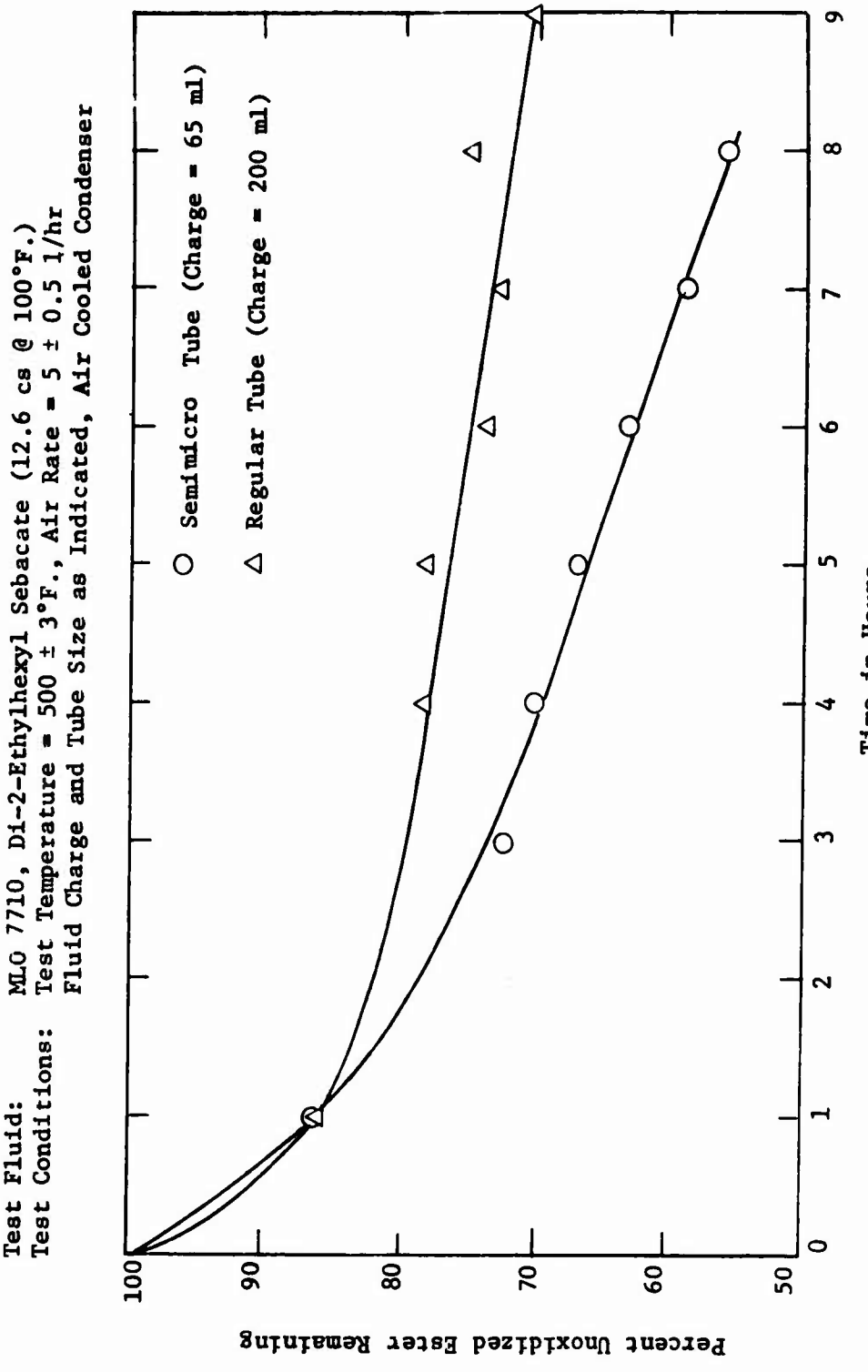

Figure 51. EFFECT OF GEOMETRY ON DEGRADATION OF TEST FLUID

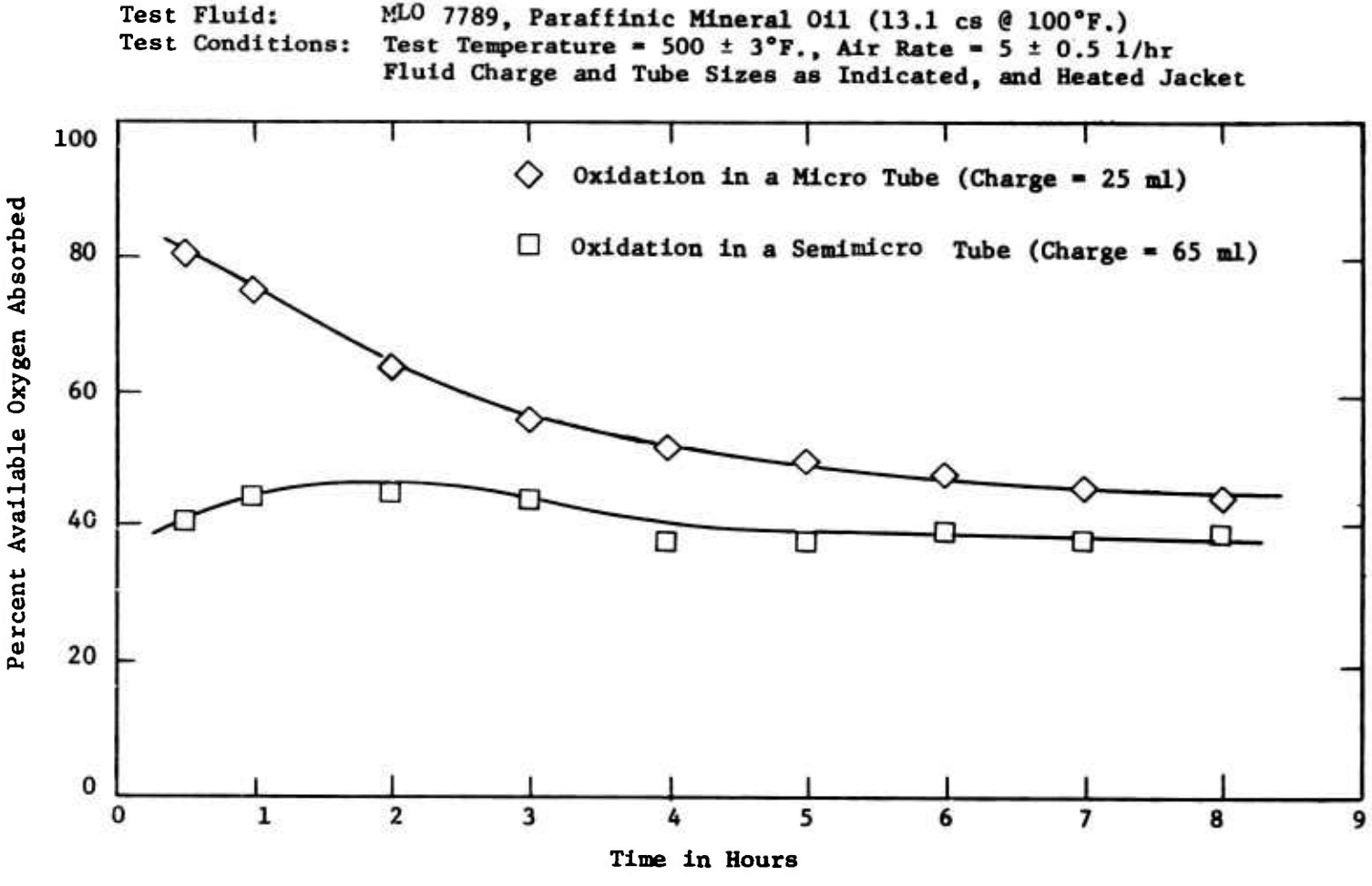

Figure 52. THE EFFECT OF GEOMETRY ON THE OXIDATION OF A PARAFFINIC MINERAL OIL

Test Fluid: MLO 7789, Paraffinic Mineral Oil (13.1 cs @ 100°F.)
Test Conditions: Test Temperature = 500 ± 3°F., Air Rate = 5 ± 0.5 l/hr
Fluid Charge and Tube Size as Indicated, and Heated Jacket

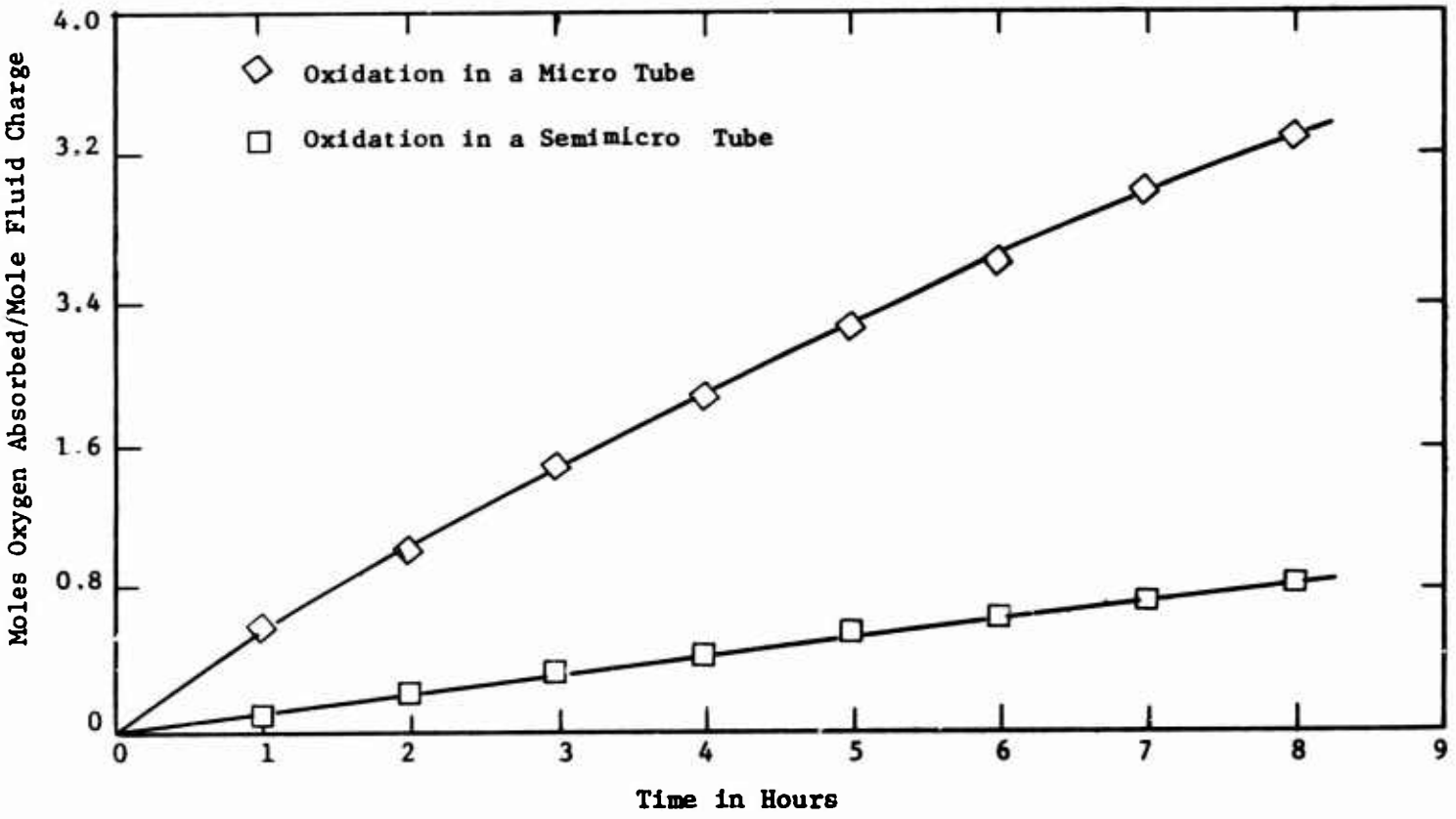

Figure 53. EFFECT OF GEOMETRY ON RATE OF OXYGEN ASSIMILATION OF A PARAFFINIC MINERAL OIL

Table 9

ANALYSIS OF THE LIQUID PRODUCTS FROM AN UNCATALYZED OXIDATION TEST ON DI-2-ETHYLHEXYL SEBACATE AT 500°F.

Data Taken from Reference AFML-TR-70-304, Part III.

Analyses Conducted by Temperature-Programmed Gas Chromatography Using a Two-Foot Silicone Rubber Column with Tridecane as Internal Standard. Reaction Product Classification by Structure, Normal Boiling Point, or Normal Boiling Point Range.

Liquid Products from an Oxidation Test Conducted Under the Following Test Conditions: Test Temperature = 500 ± 3°F.; Test Time as Indicated; Catalyst = None; Air Rate = 5 ± 0.5 Liters per Hour; Fluid Charge = 100 ml. Prior to the Start of the Test, the System is Purged with Helium. The Air Line is then Connected and the Test Started.

Oxidation Test Time, hr.	0.0	1.0	2.0	3.0	4.0	5.0	6.3	7.2	9.5	10.0
Neutralization No. of Liquid Product (mg. KOH/ g. oil)	0.1	1.9	4.6	6.3	7.7	10.0	11.8	15.6	17.5	17.9
	Chromatographic Analysis of Liquid Product, g. per 100 g. Diester									
2-Ethyl-1-Hexene		Trace[a]	Trace	Trace	---	---	---	---	---	Trace
360° - 380°F.[b]		0.1	0.1	0.3	0.5	0.2	0.8	1.0	1.0	1.1
419°F.		---	---	Trace	Trace	---	---	---	---	0.2
477°F.		Trace	Trace	0.2	0.3	---	---	---	---	0.4
500°F.		---	Trace	0.2	0.2	---	---	---	---	0.3
531°F.		Trace	0.1	0.2	0.2	---	---	---	---	0.2
558°F.		Trace	0.1	0.2	0.2	---	---	---	---	0.2
2-Ethylhexyl Pelargonate		3.1	4.0	4.5	5.3	4.6	4.9	4.8		5.1
626°F.		0.1	0.2	0.4	0.5	---	---	---	---	0.7
680° - 750°F.[c]		---[d]	1.1	1.4	1.8	1.6	2.9	4.3	4.0	4.2
Di-2-Ethylhexyl Sebacate	100.0	92.6	84.1	81.7	73.7	71.1	66.3	63.9	59.8	57.6
860°F.		0.5	0.6	0.5	0.5	---	---	---	---	0.3
>950°F.[e]		3.6	9.7	10.4	16.8	22.5	25.1	26.0	30.4	29.7

[a] Trace less than 0.05 grams per 100 grams diester.

[b] The alcohol 2-ethyl-1-hexanol elutes with this fraction.

[c] Mono-2-ethylhexyl sebacate elutes with this fraction.

[d] This fraction elutes over a 70°F. range and concentrations less than 0.3 grams per 100 grams diester are difficult to determine accurately.

[e] Concentration value obtained by difference.

Test Fluid: MLO 7710, Di-2-Ethylhexyl Sebacate (12.6 cs @ 100°F.)
Test Conditions: Test Temperature = 500 ± 3°F., Air Rate = 5 ± 0.5 l/hr
Fluid Charge = 200 ml, in a Regular Tube with an Air Cooled Condenser

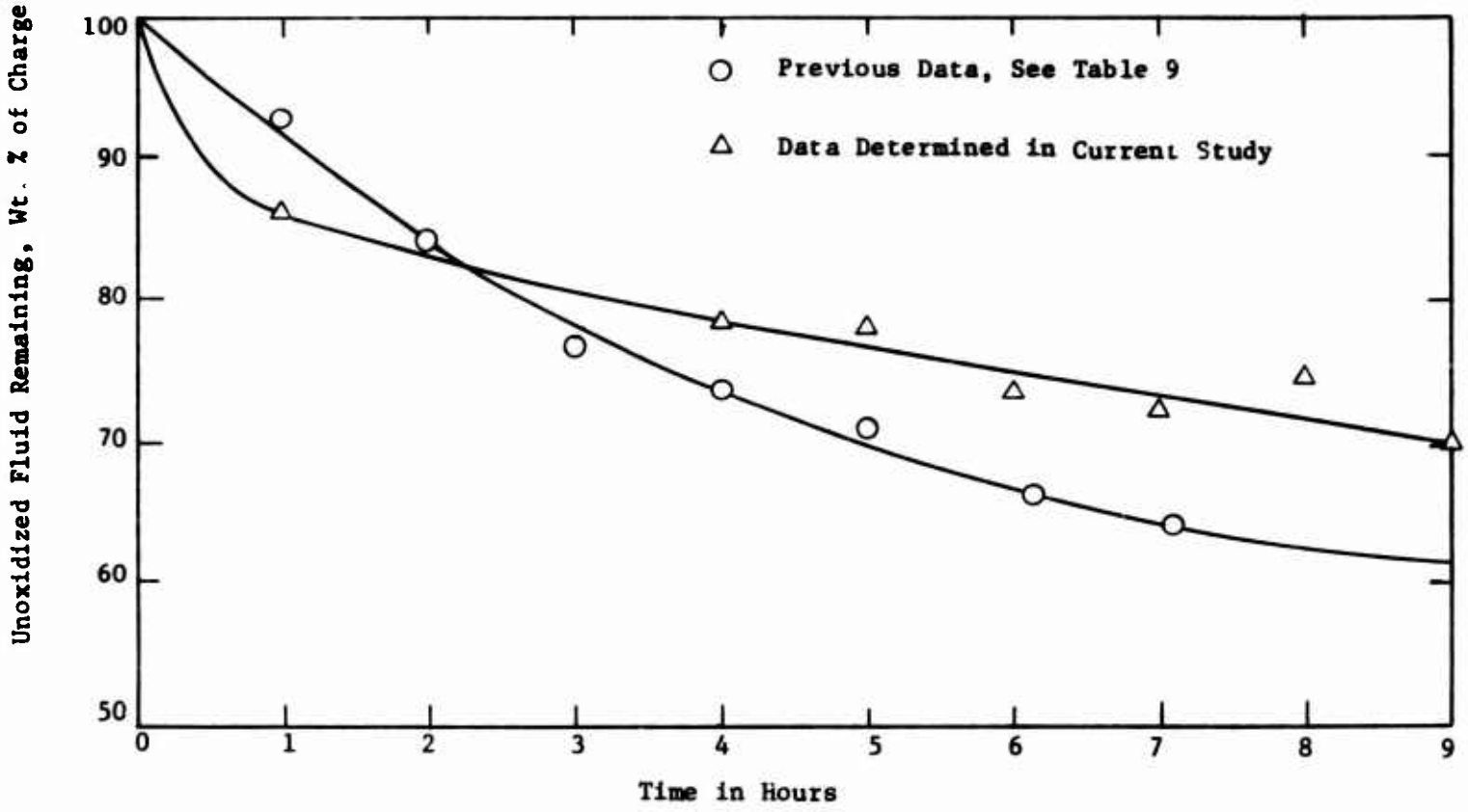

Figure 54. FLUID DEGRADATION FOR OXIDATION OF DI-2-ETHYLHEXYL SEBACATE

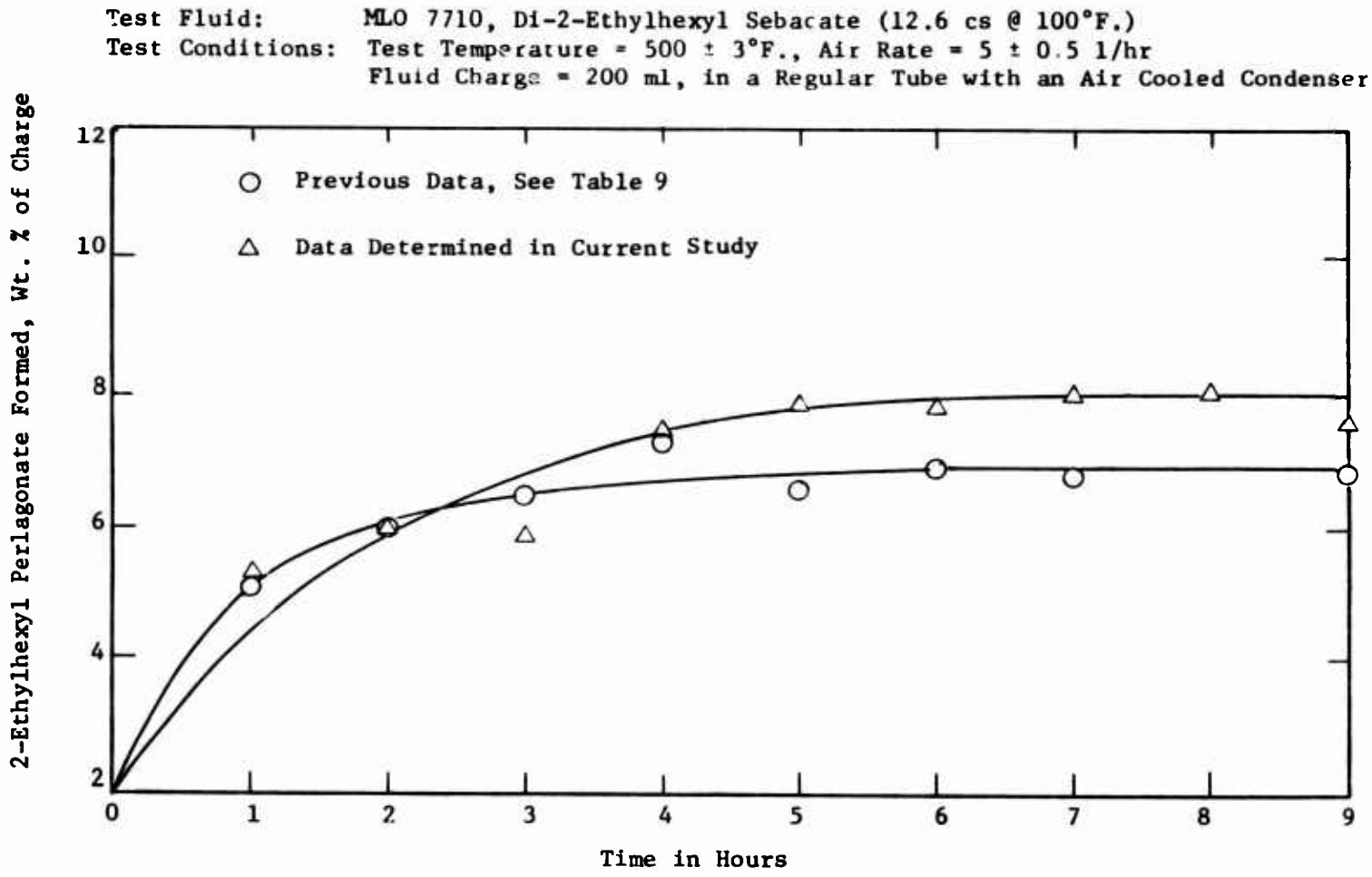

Figure 55. FORMATION OF 2-ETHYLHEXYL PELARGONATE DURING OXIDATION OF DI-2-ETHYLHEXYL SEBACATE

Test Fluid: MLO 7710, Di-2-Ethylhexyl Sebacate (12.6 cs @ 100°F.)
Test Conditions: Test Temperature = 500 ± 3°F., Air Rate = 5 ± 0.5 l/hr
Fluid Charge = 200 ml, in a Regular Tube with an Air Cooled Condenser

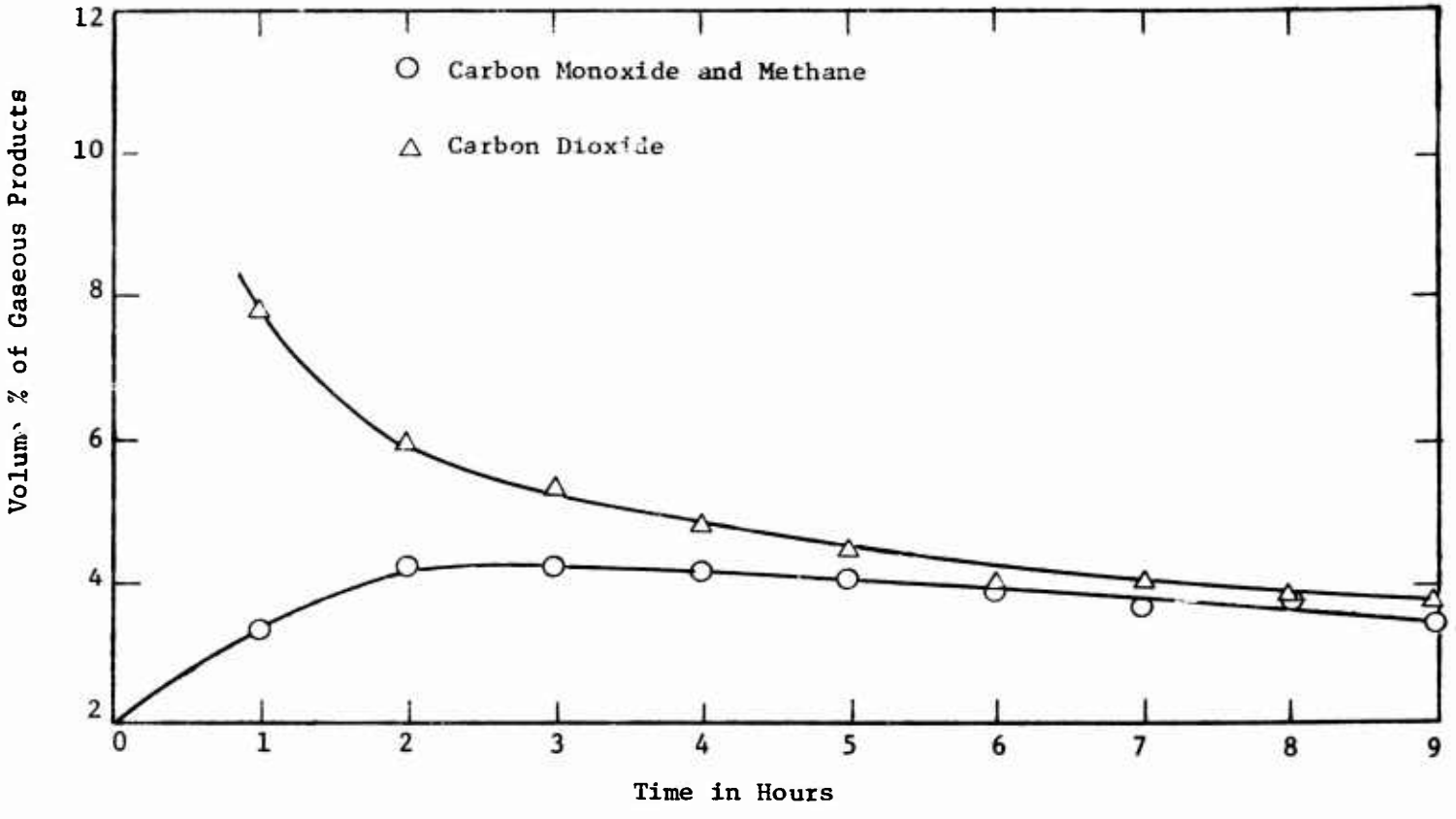

Figure 56. FORMATION OF NONCONDENSIBLE GASEOUS PRODUCTS

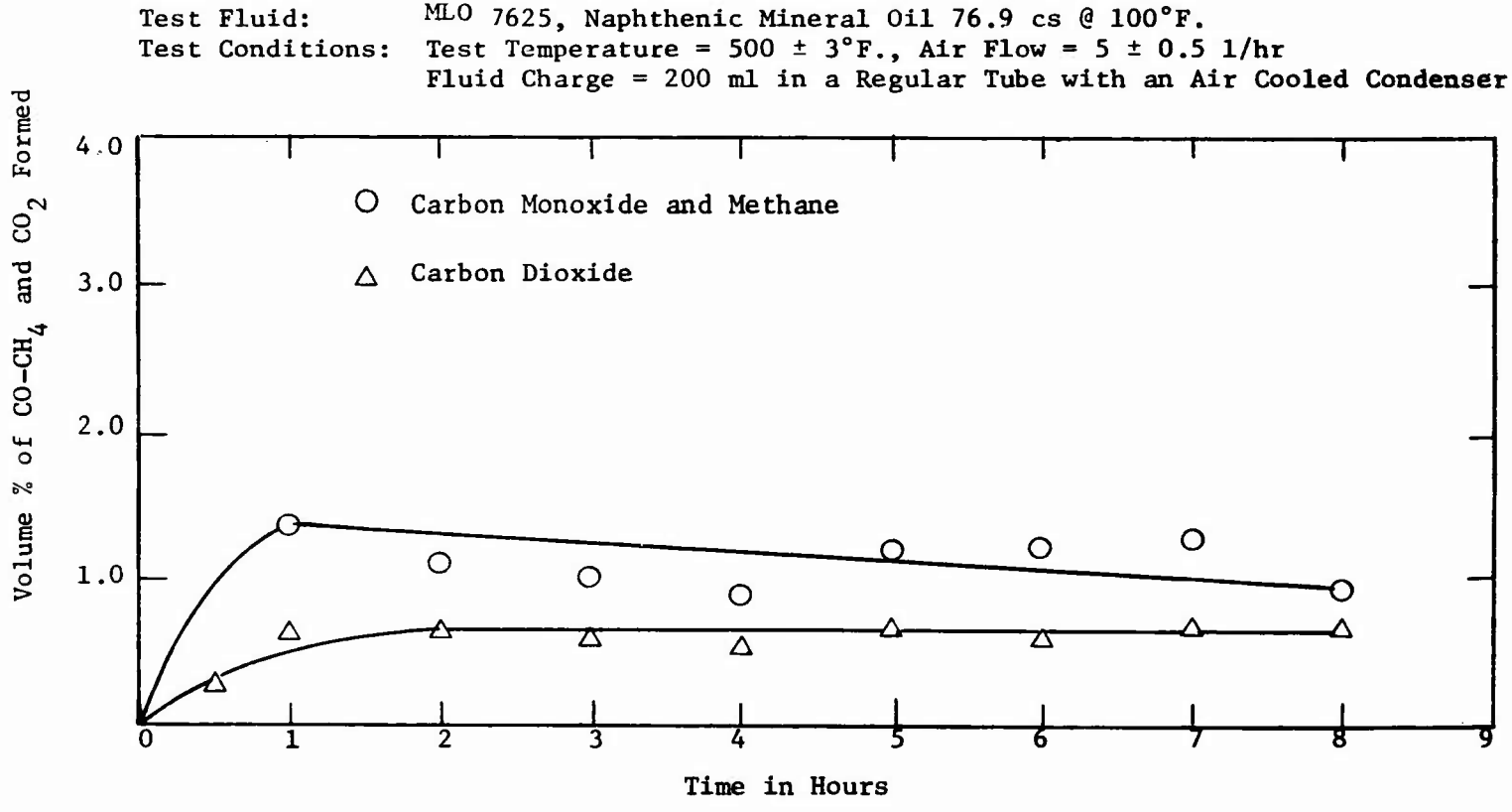

Figure 57. FORMATION OF NONCONDENSIBLE GASEOUS PRODUCTS

Table 10

PERCENTAGE OF METHANE AND CARBON MONOXIDE PRODUCED
IN THE OXIDATION OF MINERAL OILS

Fluid Descriptions Shown in Table 3.

Sample Time, hrs.	Fluid Designation 7625	7789	7478	7797	7685
0.5	1.08	1.32	2.42	1.26	4.88
1	1.14	1.81	4.58	1.85	8.02
2	1.04	2.03	4.42	2.19	7.54
3	1.57	2.10	2.49	1.97	6.16
4	1.54	1.72	2.38	1.87	5.27
5	1.54	1.88	2.13	1.43	5.73
6	1.55	1.61	1.93	1.81	5.61
7	1.73	1.38	2 17	1.64	5.86
8	--	1.89	1 93	1.74	4.68

Test Fluid: As Indicated
Test Condition: Test Temperatures = 500 ± 3°F., Air Rate = 5 ± 0.5 l/hr, Charge = 65 ml in a Semi Micro Tube with Heated Jacket

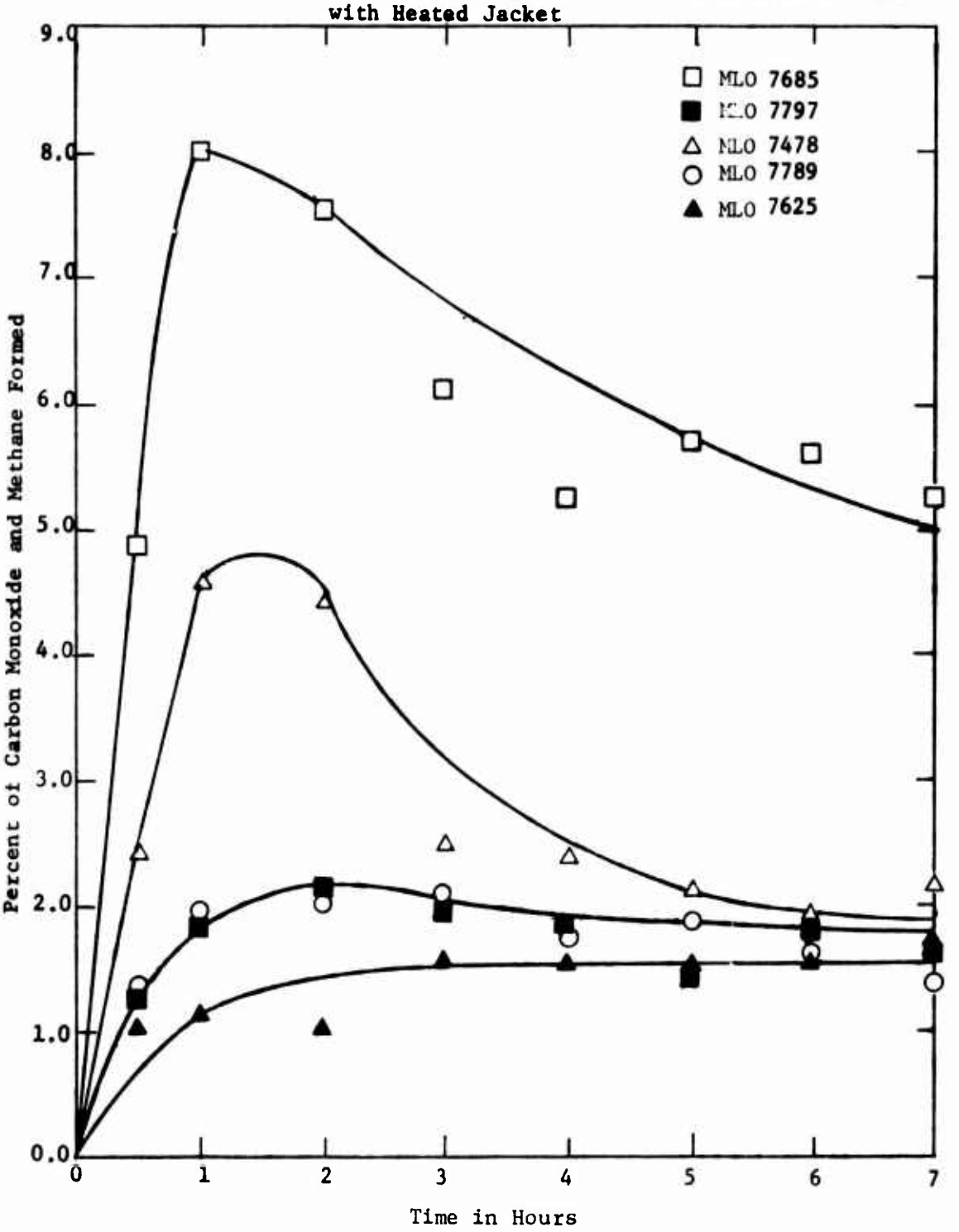

Figure 58. CARBON MONOXIDE-METHANE PRODUCED IN THE OXIDATION OF MINERAL OILS

C. STUDIES OF CHEMICAL REACTIONS IN BOUNDARY LUBRICATION. Boundary lubrication has become increasingly important in recent years due to the general increase in bea.ing loading and design in both industrial and aerospace technology. In most cases lubricant degradation is observed as a result of boundary conditions. The principal result of this lubricant degradation is the formation of insoluble sludge. The boundary lubrication process comprises chemical reactions at localized high temperature zones involving the lubricant components and the metal surface. The sludge is a result of these chemical reactions at the wear site.

Sludge formation is generally associated with poor lubricant performance. Some investigators have recently suggested a friction polymer (sludge) mechanism as an effective method of improving elastohydrodynamic lubrication (EHD) by providing surface rheology different from bulk viscosity properties.

The object of this study is to determine the conditions under which the sludge is formed in boundary lubrication. The concept of friction polymer in EHD lubrication has been included in this study. It has been shown in previous static studies that the organometallic portion of the sludge is strongly adsorbed on the wear site and may be an effective film to prevent further wear. The film thickness has been assumed to be within the elastohydrodynamic range.

The second object has been to distinguish between the behavior of a reactive and a nonreactive lubricant. To establish a reaction mechanism as the most important step in the wear reactions, the effects of surface temperature, catalysis and reactions in the system must be considered. A study of fluid oxidation suggests a method by which oxygen may react with the fluid to produce a lubricant oriented sludge rather than a metal oxide. Oxidation reactions for typical mineral oils and esters become rapid at temperatures above 400°F. The reaction of oxygen with the lubricant in which it is dissolved will tie up the oxygen chemically before reactions with the metal surface take place. A better definition of the conditions favoring organic or organometallic sludge formation due to chemical reaction should aid in future investigations of the boundary lubrication mechanism.

1. Apparatus and Procedure for Collecting and Analyzing Reaction Products in a Wear Test. A modified Shell four-ball wear tester and an atomic absorption spectrophotometer were used to obtain data for this study. The test results are then applied to a lubrication model for boundary lubrication conditions.

a. The Shell Four-Ball Wear Tester. A diagram illustrating the essential working parts of a wear tester is shown in Figure 59. The range of lubrication studied by the conventional four-ball tester is in the elastohydrodynamic and boundary regions. As the wear progresses in a four-ball wear test, the bearing area increases and the unit loading decreases Thus the boundary conditions become less severe approaching elastohydrodynamic lubrication. The main advantage of the four-ball wear tester is that the surface finish of the bearings is not a test variable. Fresh surfaces are continuously exposed to the lubricant during a test.

The test cup containing the liquid lubricant is open to the atmosphere in a conventional Shell four-ball wear tester. A controlled-atmosphere version of this wear tester incorporates a liquid seal surrounding the ball pot. This allows the imposition of any desired atmosphere over the lubricant during the test. This liquid seal allows motion of the ball pot about the axis of the rotating ball. The seal between the atmosphere shield and the spindle housing is not gas tight. Therefore, a constant flow of the test atmosphere from the enclosed space to the room is maintained. This positive flow rate prevents counter diffusion. A diagram is presented in Figure 60.

The controlled atmosphere is supplied to the ball pot by a system shown in Figure 61 for tests under a nitrogen or argon atmosphere and by the system shown in Figure 62 for runs in an air atmosphere. When air is used, it is first reduced from line pressure to about three psig. It is then filtered through calcium chloride to remove any moisture. The gas flow rate to the ball pot is regulated by a needle valve preceding the capillary restriction. The pressure drop across the capillary restriction is measured by a differential manometer. When a nitrogen or argon atmosphere is used, the gas bottle is connected to the supply system at a point near the vibrational damper on Figure 59. The gas pressure is reduced at the gas bottle to a pressure of about three psig.

All the tests for this study have been conducted within the following conditions:

Test time	= 10 to 150 minutes;
Test temperature	= 167° or 400°F;
Speed	= 600 r.p.m. (≈40 cm/sec sliding velocity);
Load	= 1, 4, 10, 20 or 40 kg;
Atmosphere	= dry air at 0.7 liter/hour, nitrogen at 4.8 liters/hour, or argon at 4.8 liters/hour; and
Bearings	= 52-100 steel, PRL batch Nos. 14 and 15; 0.5 inch diameter.

The 52-100 steel balls are supplied by SKF Industries with a tolerance of $\pm$ 0.25 x 10^{-4} inch in diameter. The composition of these balls is shown in Table 11

Table 11

Composition of 52-100 Bearing Steel

Element	Weight Percent
Carbon	0.95-1.10
Manganese	0.30-0.50
Phosphorus	0.025 Max.
Sulfur	0.025 Max.
Silicon	0.2-0.35
Chromium	1.2-1.5
Iron	Remainder

The Shell four-ball wear tester is standardized by comparing the wear properties of a series of standard fluids under well defined test conditions Super-refined mineral oils were used to evaluate the overall procedure and wear specimens.

A new set of ball bearings is used for each wear test. The balls are first cleaned with pyridine, scrubbed with tissue paper, rinsed with naphtha and acetone followed by air drying. The balls are not touched by hand after the cleaning procedure.

Three balls are locked in the test pot and the fourth is placed in the spindle. The ball pot, prior to loading, has been cleaned using the same procedure described for the balls. About 20 milliliters of test fluid is charged to the pot. The quantity of fluid assures complete coverage of the balls in the ball pot and the contacts between the rotating and stationary balls for the complete test.

The assembled ball pot is placed on the heater and the thermocouple leads are connected. The entire assembly is then placed on the ball pot mounting bearing and the restraining spring is connected. The desired temperature is set on the temperature controller and the heat is turned on. When the test fluid reaches the test temperature, the lever arm containing the desired load is lowered gently from the no-load to the load position. The ball pot is centered beneath the spindle to assure even distribution of the load on the three lower balls. This is checked by placing a level on the lever arm. The motor is started and the test is allowed to run for the desired time.

In the case of an air atmosphere, 20 milliliters of test fluid is charged directly to the ball pot and dry air at the rate of 0.7 liters per hour flows through the ball pot continuously during the test. The system is depicted in Figure 62.

In the case of a nitrogen or argon atmosphere, the flow system during the tests is the same as for dry air. The total atmosphere control system does include provisions for degassing the fluid and gas saturation of the lubricant prior to charging to the ball pot. The conditioned liquid charge can then be added to the ball pot without exposure of the test fluid to the laboratory atmosphere. A diagram of

the system is shown in Figure 61. A complete test using the controlled atmosphere system includes the following steps.

First, the wear tester pot is cleaned and set up for the wear test. The desired test atmosphere at the designated rate is run through the system for five minutes to replace the air with the test atmosphere. The test fluid is placed in the graduated degassing tube and heated to about 180°F. Valve B is opened and valves A and C are closed. A vacuum of about 25 millimeters of mercury is applied to the fluid for about twenty minutes until the formation of bubbles ceases. Valve A is opened slowly and valve B is closed to bring the system to atmospheric pressure. When the system has reached atmospheric pressure, valve C is opened to purge the wear tester of air. The test atmosphere is bubbled through the system for about twenty minutes at a rate of 4.8 liters per hour. The fluid charging tube is lowered in the fluid as shown in Figure 61 and approximately 20 milliliters of the conditioned fluid is charged to the pot. When the fluid has been charged, the tube is raised above the fluid level to allow the test atmosphere to flush the pot continuously during the wear test. The free space above the ball pot is about 0.0708 liter at any time. It was found that a gas flow rate of 0.08 liter per minute or 4.8 liters per hour provides a positive flow through the test pot and a positive leak through the spindle bearing system thereby creating the maximum pressure drop that can be contained by the liquid seal surrounding the ball pot.

Wear scar diameters are measured with a microscope containing a calibrated scale in the ocular lens. Measurements are made so that a strip of light is continuous in intensity throughout the diameters on the axis parallel to the striations. If the wear scars are not circular, the diameters are measured both parallel and perpendicular to the striations and are averaged. In both cases, the scar diameters of the three stationary balls are averaged. The spindle ball halo width is also measured and recorded.

b. Atomic Absorption Spectroscopy. The principle of atomic absorption spectroscopy and its application to analysis of metals has been described in detail in previous reports. Briefly a liquid sample is converted into an atomic vapor by a flame and irradiated by a light from a source whose emission lines are those of the metal being sought. The absorption of the light by the vaporized sample is related to the concentration of metal in it.

The atomic absorption spectrophotometer used in this study is model 303 Perkin-Elmer Corporation instrument. It was used in conjunction with the Perkin-Elmer automatic null recorder readout and a Servo/riter II Potentiometric Recorder, Model PS01W64, made by Texas Instruments. Basically, the Model 303 is a double beam single detector instrument. The light beam from the spectral source is split by a rotating chopper. Half of the beam is used as a reference beam while the other half passes through the sample flame. Both halves pass through the monochromator, enter the detector and are compared. The ratio of the intensities of the two beams is related to the metal concentration in the sample, and is read out as a percent absorption on the recorder chart as shown in

Figure 63. A block diagram of the instrument is shown in Figure 64.

The procedure used in operating Model 303 Atomic Absorption Spectrophotomer is presented in previous reports Briefly, the proper source lamp is installed in the instrument and the standard conditions are set. The source lamp is an Intensitron lamp and is approximately ten percent more sensitive in absorption and qualitatively less noisy than an iron cathode lamp.

Since diluted oil samples caused frequent fouling of the single slot standard burner head, a three slot boiling burner head was used. This burner head increases sensitivity by approximately ten percent by increasing the flame cross-section and the gas flow rate.

A calibration curve is developed by using a series of standard solutions in the atomic absorption spectrophotomer. A typical trace is shown in Figure 63 and the calibration curve is shown in Figure 65. The correct aspiration rate for a given viscosity of solution is also determined by calibrating with solutions of known viscosity. These solutions were made by diluting super-refined paraffinic mineral oil (viscosity at 100°F - 13.1 cs.) with pyridine according to the blending procedure given in ASTM viscosity temperature chart D-341-43 followed by experimental confirmation in the laboratory using modified Cannon-Fenske viscometers. The calibration curve is presented in Figure 66. The aspiration rate is measured using a five-millimeter graduated cylinder and noting the amount injected for one minute.

The pyridine used in this study was redistilled in the laboratory. The redistilled pyridine, blank oil specimens, and filter papers were all tested for iron content. No iron was found within detectable limits.

c. Analysis of Wear Debris. The wear debris, after a test, is filtered quantitatively and the total amount of debris is noted. This debris is then divided into various factions by solvent treatment and analyzed for metal by atomic absorption. The portion of the debris soluble in pyridine has been shown to be an organic metallic product (soluble metal) and the remaining portion which is insoluble in pyridine and soluble in hydrochloric acid solution has been referred to as insoluble metal. The test oil is also analyzed for metal content and this organometallic product has been called oil soluble metal.

(1). Filtration and Weighing. A metricel (0.45 micron) filter paper has been found to be very good for determining quantitatively small amounts of debris. The filter paper is pretreated by filtering 50 milliliters of naphtha solvent through the unit. The pretreated paper is then dried at 90°C for one hour and cooled for one hour in a dessicator, until a constant weight is achieved The weighings are made on a Mettler model 2750 B6, semimicro, analytical balance. The heating and cooling is repeated until two successive weighings are within 0.05 milligram of each other. By averaging these final two weights, the tare weight of the paper is obtained. The tared filter papers are stored in planchets in a dessicator and covered until use

To assure equal treatment for a blank, two pieces of cleaned and tared filter paper are placed in the filtration apparatus. This unit is a 47 millimeter diameter pyrex filter holder. The top paper will collect the insoluble material while both papers will be exposed to the soluble componenets, i.e. oil and solvent.

The first step in the analysis is to separate the oil insolubles from the oil-soluble portion. For this system, petroleum naphtha with an end point of 260°F is used as the solvent. Organometallic products as well as the organic materials insoluble in the mineral oil will remain insoluble in the naphtha diluted solutions. In fact there is a slight trend to precipitate borderline solubility products of these two classes with the naphtha. The naphtha soluble material provides a source of the metal-containing compounds soluble in the oil.

The procedure for the determination of oil-soluble metal starts with the four-ball test pot following a wear test. Two filter papers, for reasons mentioned earlier, are placed in the filter apparatus. A centrifuge tube is placed under the filter to collect the test fluid. When the test pot is cooled to room temperature, the lock nut is removed. The test oil is transferred from the pot to the filter funnel by means of a ten-milliliter pipette. After the oil has passed through the filter paper, the centrifuge tube is removed and the filter assembly connected to the Erlenmeyer flask connected to a water aspirator. The ball pot parts are then rinsed thoroughly with naphtha. A wash bottle fitted with a 0.45 micron continuous filtration assembly is used for the naphtha rinse. The balls are rinsed with naphtha with the help of a rubber policeman to wash debris from around the wear scar. The ball pot itself, the spindle ball, the transfer pipette, and all equipment that comes into contact with the oil and debris during the washing procedure is rinsed. The filter papers are then rinsed with 200 milliliters of naphtha to remove entrained oil. The filter funnel is carefully lifted from the filter papers and the filter edges are rinsed using a five-milliliter syringe. Care is taken not to rinse any loose debris over the edge of the top filter paper. This step is important since entrained oil can usually be attributed to filter edges. The total naphtha rinse is then evaporated to one sixth of its volume and tested for iron. Planchets are again used to store the used filter papers. The same system of heating, cooling and weighing is used to obtain the weights of the filter papers as was used for the tare weights.

The top or sample filter paper contains the insoluble material while the bottom or blank filer paper has been subjected to the same oil and solvent treatment. If the papers are now dried and weighed in the manner previously described, the blank paper should give little or no change over the original tare weight. For a successful test, the maximum change for the blank paper is +0.10 to -0.10 milligram. A larger weight gain indicates transfer of the insoluble material to the blank paper and indicates an unsatisfactory separation. When the weight of the blank paper falls within the prescribed limits, the weight change noted is added to or substracted from the final weight of the sample filter paper to determine the actual amount of insoluble deposit.

(2). Separation of Wear Debris and Preparation of Sample Fractions. Basically the insoluble wear debris from the four-ball test is separated into two samples for analysis: a) organometallic wear products soluble in pyridine, and b) organometallic products insoluble in pyridine along with the iron-iron oxide particulates soluble in hydrochloric acid solution.

(a) Organometallic Sample Preparation. Pyridine has been found to be a good solvent for organometallic wear products. The sample filter paper after weighing is placed in a flask with 20 milliliters of pyridine. The sample filter is basically made of cellulose triacetate which is soluble in pyridine. Gentle heating and stirring were used to speed the dissolving process. When the solution cooled, it was filtered through a high retention filter paper with a polypropylene filter paper 10 micron porosity as a backup in the filter apparatus. The polypropylene filter paper was placed under the high retention filter paper to prevent any lint or dust from being carried into the solution. The presence of lint and other particulates will cause problems in the flow rate through the capillary aspiration system in the atomic absorption unit. Both filter papers used in this step are insoluble in pyridine. The residue was rinsed with 10 milliliters of pyridine. After recording the total volume of filtrate collected, it is placed in a small sample bottle for analysis by atomic abosorption.

The high retention filter paper now holding basically metal and metal oxide particulates was again placed in a flask with 20 milliliters of pyridine and a second extraction with pyridine was conducted using the same procedure. The residue now contains primarily metal chips and/or its oxide.

(b) Iron-Iron Oxide Sample Preparation. A solution of six normal hydrochloric acid was used to dissolve the metal-metal oxide. The high retention filter paper containing the metal was placed in a 50-milliliter flask along with 20 milliliters of six normal hydrochloric acid. It was heated and stirred until the filter papers were reduced to a pulpy mass. The solution was cooled to room temperature and filtered again through the high retention paper with a polypropylene filter beneath it. Ten milliliters of six normal hydrochloric acid solution was used to rinse the filter papers. After recording the total volume of filtrate collected, it was placed in a small sample bottle for subsequent atomic absorption analysis.

(c) Naphtha Rinse Portion. The total naphtha rinse solution was evaporated to about one sixth of its volume and the final volume measured. A 10-milliliter sample of this solution was mixed with an equal volume of super-refined paraffinic mineral oil (MLO 7789) to impart the desired viscosity. The solution was placed in a bottle for atomic absorption analysis.

(d) Oil Soluble Metal Sample Preparation. The test oil collected in the centrifuge tube was diluted with redistilled, filtered pyridine and kept in a sample bottle for atomic absorption analysis.

(3). Metal Analysis. The samples, thus collected, are now read for atomic absorption analysis for metal content.

(a) Analysis of Iron in Organometallics. Standards for organometallic iron analysis were prepared by mixing pyridine with the soluble-iron-in-oil-standards supplied by Cannon Instrument Co., State College, Pa. The soluble-iron-in-oil-standard concentrations were 100, 75, 50 and 25 p.p.m. by weight of iron. The pyridine diluted standards were prepared to provide the same viscosity level for analysis and were 10, 7.5, 5.0 and 2.5 p.p.m. (by weight of iron) concentration. Unknown samples in pyridine solution and equivalent viscosity levels are compared with the known standards in pyridine solution in the atomic absorption unit. Two unknown solutions are followed by two known standards in the atomic absorption unit to assure proper aspiration rate and burning in the analyzer.

The deflections of the standard solutions from the zero parts per million line are a measure of the percent absorption for those standards. Similarly, the deflections of the experimental samples from the zero solution line are a measure of the percentage absorption for the unknowns. Thus the metal concentration can be found from the calibration curve of absorbance versus concentration prepared from the standards. This relationship is linear up to 20 p.p.m. by weight of iron. The two metal concentrations obtained for each sample are averaged to get the final value and converted to milligrams of metal by weight.

(b) Analysis of Iron in the Iron-Iron Oxide Fractions. The iron standards for the acid samples were made by dissolving iron powder (electrolytically pure grade) in six normal hydrochloric acid solution. The iron standard concentrations were 10.0, 5.0, 2.5, 1.25 p.p.m. of iron by weight.

The actual procedure for determining iron in HCL solution is the same as for the pyridine in the oil sample. Water-base iron standards were aspirated, followed by two water-base unknowns, followed by the reference standards, etc. This sequential procedure was followed until each unknown water-base iron sample had been measured twice.

(c) Analysis of Iron in Test Oil. The residual oils were diluted with pyridine and analyzed for iron in the same way as the other organic samples. In all cases the reference standards were used between tests for the unknown samples.

(d) Analysis of Iron in Naphtha Rinse. Analysis of the naphtha rinse for iron required a third set of calibration standards. To match the aspiration rate of the naphtha rinse materials, naphtha is used to dilute the standards supplied by Cannon Instrument Co., State College, Pa. Analyses were made in the same way as described for the two other solvent systems (HCL and pyridine). The naphtha rinse was found to contain no iron; hence the naphtha fractions were not measured for metal content in later runs. Because of the inherent drift and noise level in the instrument, a new calibration curve was plotted for each set of unknowns aspirated. This was the reason for running the standards with each set of experimental samples. Two metal concentrations obtained for

each sample were averaged to get the final value in all cases. The deviation for the pyridine samples was within ± 0.01 percent and for the acid samples was within ± 0.04 percent.

(4.) Accuracy, Limitations and Reproducibility. The major factors affecting the reproducibility of the debris analysis are the quantitative transfer of the wear debris from the ball pot to the analysis system, sample preparation and the basic machine characteristics of the atomic absorption unit.

The washing procedure of the wear debris presents practical problems to optimize the sensitivity of measurements. Extra care was taken to minimize any loss of the debris from the ball pots. The problems of consistency in washing the debris improved with experience. The limits of error in the atomic absorption unit can be influenced by sample viscosity, the solvent burning characteristics and the basic machine characteristics.

The viscosity determines the rate of sample injection into the flame. The fluid is drawn into the burner by a constant pressure of approximately 0.4 psia across the nebulizer and the Teflon capillary tubing. It is important to match the viscosity of the reference and unknown samples. Before each run, the sample aspiration rate was noted for one minute using a five-milliliter graduated cylinder and comparing with the reference plot. The reference plot was made by aspirating samples of known viscosity found theoretically by the procedure given in ASTM D-341-43 and followed by laboratory confirmation of the samples using modified Cannon-Fenske viscometers.

The burning characteristics of the solvents were eliminated as a significant error by using the same solvent system in the standardization samples and the unknowns. In addition, the air-fuel ratio was adjusted to provide optimum response for the standard solutions before evaluating the unknowns.

The atomic absorption spectrophotometer was optimized for maximum absorption by adjusting the wave length, aligning the burner head in the beam path and adjusting the aspirator. Necessary dilution of the sample to keep the metal concentration in the proper range for precision measurements in the atomic absorption spectrophotometer multiplies the percentage error by the dilution factor. This factor was constant since dilution of all samples was made to the same extent.

Atomic absorption spectrophotometer precision, method of sampling and transfer of debris affect the overall reproducibility of the tests. Within these limits, the overall reproducibility was found to be ± 10 percent.

2. Boundary Lubrication Studies. The process of wear and lubrication under boundary conditions appears to be very complex. The process probably involves an interaction between the bearing surfaces, and a component or components of the lubricant including additives, polar impurities, and dissolved gases from the environment in the bearing system. Very high localized surface temperatures are generated at the concentrated contact. The local high temperatures

exercise considerable influence on the wear characteristics under boundary conditions. These temperatures promote chemical reactions involving bearing surfaces, oxygen and the lubricant components. Attempts have been made to identify the polar components as thermal or oxidative decomposition products of the lubricant base stock. Such reactions at the concentrated contact have been found to produce a deposit on and around the wear scar area. Attempts have been made to isolate this deposit by its selective solubility in pyridine and to identify the constituents in this deposit. It is suspected that this reaction product may affect the wear characteristics as the wear progresses. This product may remain preferentially adsorbed on the wear site and provide a protective coating on the bearing surfaces. The rheology of this product might provide an elastohydrodynamic component to mitigate further wear. By carefully choosing test conditions, the present work has been designed to study these system variables, reactions and reaction products.

a. Calibration and Standardization of the Wear Tester. The four-ball wear tester is standardized by comparing the wear properties of a series of well defined lubricants. The object of this study is to calibrate the conditions of the tester and the quality of the test specimens. These calibration tests are summarized in Table 13. Superrefined mineral oils are used as the test fluids over the conventional load range.

b. Effect of Temperature and Atmosphere on the Wear Performance of Steel. Experiments were designed to find the effect of bulk reaction temperature and gaseous environment over the test fluid on the wear performance of standard 52-100 bearing steel balls. Superrefined mineral oils and a dibasic acid ester were used for this study. Fluid properties are presented in Table 12. To effect a controlled atmosphere, the procedure described previously was employed. The results of this study are summarized in Table 14. An interesting fact shown by these data is that temperature has an apparent influence on the wear performance of a mineral oil. Wear is low under a nominal nitrogen atmosphere at a bulk fluid temperature of 167°F. Tank nitrogen has been found by a gas chromatographic method to contain typically about 0.5 volume percent oxygen. The consequent lower wear under a nitrogen atmosphere than under an air atmoshpere at the same temperature and condition of sliding indicate that oxygen plays an important role in boundary lubrication reactions. Lower wear at a bulk temperature of 400°F with uninhibited super-refined mineral oils is a definite indication of a temperature dependent fluid-oxygen reaction. This reaction appears to remove free dissolved oxygen otherwise available to the reaction site.

Dissolved oxygen as a lubricity additive available from air produces the highest wear at a bulk temperature of 167°F in the test system. At this temperature oxygen solubility is high and reactivity with the fluid low. This provides a high concentration of dissolved oxygen to act as a corrosive lubricity additive. On the other hand, higher wear results under a nominal nitrogen atmosphere at 400°F. The temperature dependent oxygen-fluid interaction probably removes the dissolved oxygen to a level below that necessary for satisfactory boundary lubrication reactions. It appears that for nonadditive superrefined mineral oils, an optimal oxygen concentration is necessary to

provide minimum wear. The oxygen concentration of conventional compressed nitrogen seems to approximate the optimal value at a temperature of 167°F. The behavior of the diester, on the other hand, is different. The wear characteristics of the diester are more directly a function of temperature and appear to be less dependent on oxygen concentration.

c. Wear Debris Analysis and its Relation to Reacted Metals. Boundary lubrication involves a chemical reaction. The reaction products have been collectively termed wear debris. This wear debris was analyzed to identify the major types of wear products.

A set of experiments was designed to produce wear debris which could then be separated and analyzed. The quantitative measurements of the metal concentration have been determined by atomic adsorption spectroscopy. Separation of the debris and subsequent sample preparation and analysis have been described in an earlier section. Super-refined mineral oils and a dibasic acid ester have been used in these tests. Fluid properties are presented in Table 12. Results of these analyses are summarized in Table 15.

A material balance was used to quantify the wear debris from the four-ball wear tests. The same principle of debris analysis was employed with one main difference. The bearings were weighed before and after tests and the weight of metal loss as found by weight difference was correlated with metal present in the various fractions of the wear debris. The metal bearings were cleaned as usual and placed on a metal planchet for weighing. The weighings were made on a semi-micro analytical balance. The ball bearings and the metal planchet were weighed, followed by a weighing of the planchet alone. The difference in weight gives the weight of the ball bearings. The same procedure was applied after the test using the cleaned balls but without touching the balls by hand. Care was taken to maintain the balance pan in a level position. The overall difference in weight gives the minimum total metal loss from the bearing surfaces. The cleaning procedure, was not severe enough in these studies to remove all of the varnish and corrosive products. The majority of the deposits were removed by this cleaning technique. Results of this study are presented in Table 16. The total metal loss as found by bearing weight differences agrees well with the sum of the metal concentration found in pyridine soluble and insoluble wear debris. The relationship between wear scar diameter and total wear debris, pyridine soluble compounds containing metals, and pyridine insoluble metallic compounds is presented in Figures 67, 68, and 69, respectively.

Lubricant additives are a class of compounds which when added to a base stock impart certain new properties or enhance desirable properties originally present in the base stock. Additives of many types have been made to meet diverse lubrication needs. These additives are polar materials and interfere with each other and with oxygen as the preferentially adsorbed molecules on the metal surface.

Super-refined mineral oil MLO 7789 was mixed with one weight percent 2,6 di-tert-butyl-4-methyl phenol (Parabar 441); MLO 7625 was mixed with one weight percent 4,4'-methylene-bis-2,6-di-tert-butyl phenol (Ethyl 702) and the diester base stock was mixed with 0.5 weight

percent phenothiazine. Four-ball wear tests were conducted with these inhibited fluids in a test atmosphere of dry air at 0.7 liter per hour. The ball bearings were weighed before and after all tests to determine a material balance. Results on the evaluation of these inhibited fluids are presented in Table 17. A marked difference is observed in the values of the organometallics (metal soluble in pyridine). The organometallic debris formed by the inhibited fluids MLO 7710 and MLO 7625 is less by a factor of 10 compared to the comparable product formed by uninhibited fluids. The organometallic value for inhibited MLO 7789 is a factor of 1.6 lower compared to the uninhibited fluid. Pyridine insoluble metal oxide wear debris for the uninhibited mineral oils is higher than for the inhibited fluids. The wear characteristics of the ester fluid appear to follow a different trend.

It has been found that for the super-refined mineral oils, the wear levels are low in two types of systems. These are a nominal nitrogen atmosphere contaminated with 0.5 volume percent oxygen run at 167°F and and air atmosphere at 400°F.

Data on the solubility of various gases inhibited and uninhibited super-refined mineral oils are discussed in previous reports. These data show that the oxygen solubility in a super-refined mineral oil increases with increasing temperature up to temperatures where oxidation of the mineral oil becomes a significant reaction. By the time the bulk temperature reaches 390°F, the oxidation rate exceeds the rate of diffusion through the air-oil interface. For nitrogen, however, the solubility increases with increasing temperature until the temperature is reached at which the fluid exhibits a vapor pressure of 50 millimeters of mercury or higher. It appears that nitrogen is inert and does not participate in the lubrication reaction.

Oxygen solubility values from previous studies are shown in Table 18 as a function of wear scar diameter and plotted in Figure 70. From the data shown on Table 18 and Figure 70, it can be seen that an oxygen level of 0.53 p.p.m. by weight is effective in producing low wear in lubrication reactions for the super-refined paraffinic stock. The air atmosphere (20.8% O_2) appears to give corrosive wear due to an excess of active oxygen. A level of 0.5 percent oxygen from the compressed nitrogen cylinder, on the other hand, still functions as an effective lubricity additive. Thus, dissolved oxygen behaves as a concentration-sensitive antiwear additive in super-refined mineral oils. The oxygen solubility values are presented in Figure 71, as a function of organometallic material, metal oxide and metallic (pyridine insoluble) debris (Table 19). It can be seen that the formation of the total wear debris decreases with decreasing oxygen to the point of minimum wear. The pyridine insoluble (metallic) wear debris then increases below the point of minimum wear. It is apparent that this increase in metallic debris below the point of minimum wear represents a change in wear mechanism. The organometallic formation as an indication of the lubrication reactions does not change even in this new wear region. It is apparent that this organometallic reaction becomes limited by the amount of organic reactant available. The increase in metallic particles is indicative of seizure in the concentrated contact. The decreasing wear observed with increasing temperature with mineral oils appears to be primarily due to the dissolved oxygen

level control by the fluid oxidation. Oxygen appears to be the most effective lubricity additive in test systems involving lubricants containing less polar constituents than oxygen.

At 167°F the oxygen that remains dissolved in the bulk fluid from an air atmosphere is enough to produce corrosive wear. At 400°F there is a rapid rate of fluid oxidation, thus increasing the concentration of polar oxygenated products but decreasing the amount of dissolved oxygen. It appears that these products of oxidation are also polar and reactive at the high temperatures existing at the sliding contacts. It appears that all lubricity additives are sensitive to concentration as well as to relative polarity. The increased wear in a nominal nitrogen atmosphere at 400°F indicates lubricity additive concentrations below the minimum for effectiveness. The 0.5 volume percent oxygen present in a nitrogen cylinder is involved in the fluid oxidation at this temperature and assimilated by the fluid faster than its rate of diffusion to the metal surface. This oxidation process, therefore, consumes enough oxygen to reduce the concentration below the value for minimum wear. The net effect is the production of an increasingly "inert" environment at the wear surface. Well documented studies demonstrate high wear with increasing chemical inertness of the bearing-lubricant system. Very high friction and even welding have been reported. It appears that the wear in this portion of the system is probably controlled by seizure. The super-refined paraffinic mineral oil produces wear levels that are higher than the super-refined naphthenic mineral oil. This indicates a lower sensitvity of the naphthenic stock to oxygen concentration. The probable reason for the reduced oxygen concentration effect is the presence in the naphthenic stock of significant quantities of polar impurities which dominate over the dissolved oxygen in adsorption on the bearing surface. A similar relationship has been shown for oxygen concentration versus wear for super-refined mineral oil containing tricresyl phosphate antiwear additive. In this fluid system the effect of oxygen concentration is eliminated.

It has been shown that the apparent dependence of wear on fluid viscosity is essentially related to the impurity levels in the fluid. Superrefining removes large amounts of these impurities. It has been determined that polar impurities are harder to remove from high molecular weight fluids than from low molecular weight fluids. On this basis the low molecular weight paraffinic stock should have less polar impurities than the naphthenic stock. The difficulty of removing impurities from the higher molecular weight oil MLO 7625 than from MLO 7789 is reflected in the viscosity-wear trends.

Organic debris formed by the wear process is determined to be the difference between the total debris weight and the sum of the metals in the organometallic and metallic fractions. The organic debris formed by the mineral oils is generally lower than similar values for the ester fluid. Organic debris in almost all cases exceeds the metallic debris by a factor of 2 to 10. The two cases shown where the organic debris is of the same order of magnitude as the metallic debris or even less are believed to represent cases of major weighing errors. In both cases with the ester and mineral oil check determinations are available to indicate

that the error appears to be in the weight of the total debris.

The wear behavior of the ester base stock follows a trend different from that of the mineral oils. For a given bulk temperature the wear does decrease with decreasing oxygen concentration. There is no indication of a minimum wear value such as that found with the mineral oils. The wear keeps decreasing with decreasing oxygen concentration to the lowest oxygen concentrations attainable with this system. The wear level is affected by bulk temperature at any level of oxygen concentration. The increase in bulk temperature level appears to increase thermal degradation of the ester and thereby provide an excess of polar corrosive products. The result of increased bulk temperature at any oxygen concentration is an increase in wear. Oxygen solubility in esters has been studied and discussed in previous reports. These values were given in microliter/milliliter of fluid. These values can be converted to ppm (by weight) by the use of equation [1].

$$\text{ppm (Wt.)} = (S_T)\ (\mu L/ml)_T \qquad [1]$$

where:

$$S_T = \frac{(\text{mol wt. of gas})}{(22.4)\ (\text{Fluid density})_T}$$

The fluid density versus temperature relationship is linear. From values available in the literature and equation [1], values of oxygen solubility in the ester have been converted to ppm by weight and are shown in Table 20. Oxygen solubility as a function of wear scar diameter is shown in Figure 72. The oxygen solubility values of the ester are presented in Table 21 and Figure 73 as a function of pyridine-soluble wear debris. A trend to lower debris formation with decreasing oxygen can be observed at both 167° and 400 F operating temperatures. Thermal instability with increasing temperature is reflected in higher generation of wear debris at 400°F. The load in the bearing system also appears to exert some influence on thermal degradation of the ester. Increased load also increases the wear level of the uninhibited diester fluid. The same characteristic trend of decreasing wear with decreased oxygen concentration can be observed. The oxygen chemically combined in the ester coupled with a low threshold of thermal degradation provides adequate reactivity at the bearing surface without oxygen from the atmosphere. The corrosivity of the ester degradation products appears to keep the general wear level higher than the minimum values obtained with mineral oils at optimum levels of dissolved oxygen

The primary degradation products of the ester include corrosive organic acids that increase the wear through a chemical corrosion mechanism. Presence of high temperature, metal surface and oxygen appears to accelerate this degradation. Studies conducted previously (AFML-TR-70-304, Part III) indicate that a significant amount of sebacic acid is found in the thermal decomposition products of the ester. That work also shows a lower level of stability for the first ester group in the diester. The oxidative and thermal degradation of the ester produced similar types of degradation products. It appears oxidation conditions lower the temperature over thermal conditions at which the primary products are formed. The pyridine-

soluble organometallic material appears to represent the products of reaction of the metal surface with ester degradation products The ester degradation products and free dissolved molecular oxygen are the two principal competing polar materials in this system.

The wear performance of the ester inhibited with phenothiazine is different from that of the uninhibited fluid. The organometallic debris values for the uninhibited fluid are higher by a factor of 10 than those for the inhibited fluid. This indicates that the presence of phenothiazine reduced the lubrication reaction with the steel. It is not clear how the phenothiazine affects the wear level. Phenothiazine does provide a stable life for the ester fluid. The phenothiazine also appears to become involved in the reaction with metals in static corrosion tests. The degradation of the inhibited ester produces the same type of products upon oxidation as that of the uninhibited ester (AFML-TR-70-304, Part III). In static corrosion tests the phenothiazine becomes involved in the formation of metal corrosion products which in turn form a varnish-like coating on the metal surface (organometallic debris in wear tests). This coating prevents or reduces further metal corrosion even at high acid numbers. This same type of reaction may be responsible for the lower organometallic debris in the inhibited ester wear tests.

Four-ball wear tests were performed according to the standard procedure with the ester (MLO 7710) inhibited with phenothiazine (PRL 3207) and a combination of phenothiazine and tricresyl phosphate (PRL 3462). An air atmosphere was used. Results are presented in Table 22. The corresponding wear scar values for the uninhibited fluid are also given. The effectiveness of TCP in reducing the wear level of ester fluids is shown in this comparison. The effectiveness of TCP an antiwear additive is related to preferential adsorption on the bearing surface followed by chemical reaction with the metal during boundary lubrication. It appears that the additive effectiveness is a function of polarity. That is, the active ingredients in the tricresyl phosphate adsorb on the bearing in preference to oxygen or any other component present in the fluid. As a result, the reaction taking place at the bearing surface is between the acid phosphate and the metal. This iron phosphate layer supports the load adequately and reduces wear.

Debris analyses show that the total oil insolubles cannot be accounted for by considering only iron and iron oxide. To effect a good material balance, it is necessary to consider the involvement of the lubricants, its impurities and the decomposition products in the formation of the wear debris. High oxygen concentration available at or near the wear surface results in high wear A corrosive mechanism appears therefore as the probable mechansim Iron oxide formation and oxygen-lubricant interactions are the primary reactions occurring. The products of the oxygen-lubricant reactions subsequently react with the bearing surface to form the organometallic compounds. It appears that a characteristic role played by the organometallic material is to provide a protective coating on the bearing surface against further corrosive attack. It is clear that a high concentration of dissolved oxygen in the lubricant fosters high wear. The preferential reaction of the same amount of dissolved oxygen with the fluid provides less wear. The reasons for this difference are not clear. The reaction of the oxygen with iron and

lubricant in the vicinity of the rubbing surfaces is faster because of higher temperatures. This route may remain reactive until the organometallic reaction occurs. Multiple oxidation reactions on a hydrocarbon, for example, render this route less corrosive.

It has been shown by qualitative observations, that a sludge-like material was generated when the lubricants were evaluated in the four-ball wear tests. These sludge-like materials form at low bulk temperatures of 167°F in one-hour tests. Even under low-bulk temperatures, high surface temperatures exist at the rubbing surfaces. This system also differs from the static oxidation or thermal tests since wear in a four-ball tester always generates metallic debris. This debris may vary in particle size depending on the test conditions and the lubricant. These wear particles are generated from subsurface bearing metal under an inerting oil blanket. Further, the metal particles are probably hot and reactive and much of the iron oxide found may be formed after the wear particle is removed from the bearing. The quantitative measurement of the lubrication debris provides an important key to the mechanism of lubrication. These data also aid in understanding practical lubrication problems.

d. Composition of Lubricant Debris. The complex reaction in boundary lubrication between lubricant components, bearing surfaces and oxygen generates reaction products which are difficult to characterize. However, a semiquantitative analysis of the debris may be compared with fluid-metal interactions from static oxidation and corrosion tests. This might suggest a series of reaction steps and potential reaction products. The organometallic component of the debris has been shown to be the result of the thermal or oxidative decomposition products of the test fluid at or near the concentrated contacts and the subsequent reactions of these products with the bearing surface. The inorganic or the pyridine-insoluble portion of the debris may range from iron chips to iron oxide as oxygen availability increases. It is clear though, from the wear debris analyses that under all conditions studied, the wear debris consisted of metal-oxygen and organic material. Simple material balance data indicate this to be true. The separation of wear debris into several fractions by solubility and reactivity indicates that in all cases, there is at least some unreacted metal, metal oxide and organometallic material. It is suspected, although it cannot be shown conclusively, that in advanced stages of wear-debris formation, an organic sludge is also a common constituent. The purpose of this study is to estimate the extent of free metal, metal oxide and organometallic material in the wear debris as a function of lubricant composition, load and temperature.

Acridine-inhibited hydrochloric acid selectively dissolves iron oxides but has little effect on iron. An attempt was made to find the rate of dissolution of iron oxide and iron in an acridine-inhibited hydrochloric acid. For this purpose about 0.5 grams of iron powder was weighed into each of seven 100-milliliter beakers. A 30-milliliter sample of freshly prepared acridine-inhibited hydrochloric acid solution was added to each of the seven beakers. The products of these tests were then filtered through 0.45 micron filter paper after reaction times of 1, 5, 10, 15, 20, 25, and 30 minutes. A polypropylene filter paper was used beneath

each filter. The solvent was 4.25N with respect to hydrochloric acid and 0.007 molar with respect to acridine. The filtrates were analyzed in the atomic absorption spectrophotomer to determine the quantity of iron dissolved. A similar test was performed with an oxide of iron (Fe_2O_3). The entire operation was performed at room temperature.

Results of the above tests are presented in Figures 74 and 75 for the rate of dissolution of iron powder and iron oxide respectively. Results shown in Figure 74 indicate that the rate of dissolution of iron powder in acridine-inhibited hydrochloric acid approaches zero asymtotically on the time axis. It is assumed that the powder, on storage, was partially converted to an oxide. It is probably this oxide concentration that was dissolved until it was completely removed after about 15 minutes. After the apparent reaction of the iron oxide no appreciable reaction rate is noted. Figure 75 indicates that the rate of dissolution of iron oxide in acridine-inhibited hydrochloric acid increases with time and is proportional to the concentration of the reactants. The data point at 30 minutes appears to be an experimental error incorporated during filtration or dilution. It could also be from the hydrolysis of the ferric chloride and retention of part or the hydroxide on the filter paper during filtration.

These findings were next applied to separate and quantify the oxides of iron, unreacted iron and organometallic material in the wear debris obtained from the four-ball wear tests. Three wear tests were performed - one each under air, nitrogen, and argon atmospheres using the same super-refined paraffinic mineral oil (MLO 7789). The load, test duration, speed and bulk fluid temperature were maintained at the same level for each of these tests. The major variable was, therefore, the gaseous environment over the test fluid. The amount of oxygen in the gaseous environment represents the major change in the reactive ingredients in the test system. The tank nitrogen was contaminated with 0.5 volume percent oxygen. The oxygen contamination of tank argon could not be determined chromatographically because of similar relative thermal response values. The analysis furnished by the supplier of the argon was accepted. According to this analysis the oxygen in the tank argon is 20 ppm (by weight).

The wear tester was set and tests were performed according to the standard test procedure. For nitrogen and argon atmospheres, the same procedure of degassing and gas saturation of the fluid prior to a test was employed. The same procedure of fluid charging and maintaining a vapor blanket over the test fluid was followed. For the test under air atmosphere, the fluid was charged directly to the ball pot. After these tests were over, the oil insolubles were collected by filtration. The debris was next treated with pyridine to dissolve the organometallic compounds. The portions remaining after the dissolution of the organometallic material were next treated for the selective extraction of the oxides of the iron from the unreacted metal. The organometallic compounds were separated by the procedure described earlier The filter papers now holding the insoluble debris were placed in 100-milliliter flasks and 20 milliliters of freshly prepared acridine-inhibited hydrochloric acid solution was added to each. The solution was 4.25N with respect to hydrochloric acid and 0.007 molar with acridine Reaction times were 60 seconds with mild stirring. The flask contents were then

filtered using a 0.45 micron metricel filter paper with a polypropylene filter paper beneath it. The residue was rinsed with 10 milliliters of the solution. The volume of the filtrate was noted and then kept in a sample bottle for analysis of metal concentration by atomic absorption. This represents the quantity of the metal oxide in the debris. The residue left on the filter paper was basically unreacted metal. This was dissolved in 6N hydrochloric acid solution in the same way described previously and filtered. The volume of the filtrate was recorded and then kept in a sample bottle for analysis. This represents the unreacted metallic contents of the debris. Thus, the pyridine insoluble portion of the debris was separated by the solubility method into two fractions. The selective solubility characteristics of iron oxide in an acridine-inhibited hyrochloric acid solution was applied to achieve this separation.

The samples were next analyzed by atomic absorption spectroscopy. These data are presented in Table 23. It can be seen that with increasing oxygen availability, the composition of the metallic wear changes from iron to iron oxides. Conversely, with decreased oxygen availability, a trend towards unreacted metal can be observed.

The acridine-inhibited hydrochloric acid extraction did separate the oxides from the wear debris and show substantially different reaction rates with iron and iron oxides. The increased amount of oxide formed with increased oxygen availability suggests a direct oxygen-bearing surface interaction. The part of the dissolved oxygen that did not react with the fluid may have reacted with the steel wear surfaces to form the oxides. At the temperature of the studies, the oxygen reacts rapidly with steel. Thus, at increasing oxygen concentration, the amount of wear increases with increasing corrosion of the wear surfaces by molecular oxygen. The rate of organometallic material generation also appears to be a function of the oxygen concentration. The organometallic values increase by a factor of approximately two when the atmosphere over the test fluid is changed from argon to nitrogen (with 0.5 percent oxygen) to air.

e. Wear Debris Formed in Sequential Tests. This section describes successive tests that have been conducted on the same metal surface with a "run-in" test preceding the test of principal interest. These tests have been called sequential tests. The same procedures and analytical techniques for debris analysis that have been applied to the single run tests have been applied to the second portion of the sequential test. Test discussed in the earlier sections are referred to as original tests when compared with sequential tests.

(1). Theoretical Analysis of Surface Temperature. Temperature has a considerable influence on the wear characteristics of the mineral oil or esters. Thermal and oxidative decomposition of the test fluids to produce reactive components are temperature dependent functions. In boundary lubrication systems, these reactive components and oxygen are available for preferential adsorption on the metal surface. The adsorbed materials are then in position to react with the metal surface when the surface temperatures are increased by boundary friction. Such reactions occur at the concentrated contacts even though the bulk fluid

temperature is not high enough to promote a chemical reaction. It is at or near the high temperature bearing surfaces that the reactions appear to take place. The high surface temperatures are of extremely short duration but appear to exercise considerable influence on wear characteristics under boundary lubrication conditions. For example, the surface temperatures appear to be high enough to cause the formation of organometallics, metal oxides, phase changes, and surface melting of the metal. Because of their short duration and localization, direct measurements of these temperatures are difficult. A theoretical estimate is therefore usually sought. These surface temperatures have been termed flash temperature or 'hot spot' temperature in the Blok-Archard's flash temperature theory. This theory has been used by many investigators and is applied here to determine the flash temperature. According to this theory, the 'hot spot' temperature can be estimated by the following equation:

$$T = 0.435\beta\, NL^{1/2} + T_o \tag{2}$$

where:

$$N = \frac{f\, g_c\, \pi\, P_m}{J\, \delta\, C_p} \tag{3}$$

$$L = \frac{W^{1/2}\, U}{2\, \alpha\, (\pi\, P_m)^{1/2}} \tag{4}$$

The term β is a heat distribution factor and a function of L. L is the parameter introduced to indicate the depth of penetration of the heat below the surface. This equation (2) suggests that the heat has little penetration and is essentially confined to the surface. This theory employs an idealized model of rubbing surfaces between a moving heat source and a stationary body. The terms in equations (2), (3), and (4) are:

T = 'hot spot' temperature, °C,

T_o = ambient temperature, °C,

f = friction coefficient,

g_c = acceleration due to gravity, cm/sec^2

P_m = yield pressure, g/cm^2,

J = mechanical equivalent of heat (4.18×10^7 Joules per calorie),

δ = density, gm/cc,

C_p = specific heat of steel, cal/gm-°C,

W = applied load, gm, and

U = sliding velocity, cm/sec.

The temperature is calculated on the assumption that the heat is generated at the true point of contact and that this heat is conducted away into the bulk of the rubbing members. The equation is developed considering load, sliding speed and type of deformation between moving and stationary elements.

Values of the unknowns for steel-on-steel system for elastic deformation were obtained from the literature*. Using these values and equations (3) and (4), N and L are found to be

$$N = \frac{1.5 \times 980 \times 3.14 \times 7.04 \times 10^{6}}{4.18 \times 10^{7} \times 7.78 \times 0.109} = 916.72$$

$$L = \frac{(40 \times 1000)^{1/2} \times 40}{2 \times .127 \times (3.14 \times 7.04 \times 10^{6})^{1/2}} = 7.12$$

The value of β has been found by the interpolation of the graphical technique given in this theory and is found to be 0.85.

Thus, using equation (2), T for the present study is

$$T = (0.435 \times 0.85 \times 916.72 \times 7.12^{1/2})^{\circ}C + 75^{\circ}C. = 990^{\circ}C.$$

where $T_o = 75^{\circ}C.$ is the bulk fluid temperature and has been considered as the ambient temperature. The hot spot temperatures are obviously high enough to cause chemical reactions between molecules on the contact surface.

Four-ball wear tests were conducted according to the standard wear test procedure. Super-refined mineral oils and the diester were used as the base stocks. The "run-in" test was conducted under the standard operating test conditions of one hour at 167°F and a 40 kg load. After the test, the fluid from the ball pot was filtered into a centrifuge tube. The ball pot assembly was subjected to a thorough cleaning procedure without disassembling any parts. With the stationary balls still locked in position, the ball pot was cleaned with pyridine to remove any soluble organometallic and organic debris. Lint-free paper wetted with pyridine was used to scrubb off the deposits from around the wear scar areas. This was followed by a five minute flush with a high pressure jet of water. The ball pot was held inverted during this flushing by water. This effectively removed the metal particles from the ball pot. This was immediately followed by several rinses with acetone to remove the water. Any residual water, trapped in the ball pot system, was removed by heating to 100°C for ten minutes. This drying

*Furey, M.J., ASLE TRANS., 7, 133-46 (1964)

procedure was followed by further solvent washes with pyridine, naphtha and acetone. The solvents were finally removed by dry air. The spindle ball without being removed from the chuck was also thoroughly cleaned. Any deposit from around the halo area was scrubbed by lint-free paper wetted with pyridine. The same procedure for solvent rinse was used but the flush with water was unnecessary. The ball pot was flushed with water because the metal particles from the wear test would settle at the bottom of the ball pot. Because the balls were left locked in position, the ball pot assembly provided many inaccessable corners which were difficult to clean by a simple washing operation. Removal of the metallic particles and other wear debris from the preliminary "run-in" is necessary to insure that the next test is not adversely influenced by undesirable material left in the system. The ball scars from the preliminary "run-in" were then measured with a microscope without removing the specimens from the ball pot.

The cleaned ball pot assembly and the rotor ball were then used for a test run. The same rubbing surfaces are used with a fresh fluid charge. In the second test in this sequential series, the bearing loads and surface area are essentially constant. In the "run-in" test or a typical test with new balls the load and wear surface changed rapidly during the initial phase of the test. Under such rapidly changing conditions it is difficult to determine how much of the wear debris was formed at each set of test conditions. A comparison of wear debris between the "run-in" test and the second sequential test using the same test conditions and test fluid should show any differences due to the higher initial loadings and surface temperatures in the initial test in the sequence. A series of sequential tests using the same test conditions of bulk temperature, atmosphere, load, and test fluid were studied in this series. Super-refined mineral oils (MLO 7789 and 7625) and the diester MLO 7710 were used in these sequential tests.

After the second run in the sequential tests, the lubrication debris was collected by filtration. The oil insolubes were extracted with pyridine to obtain the pyridine-soluble organometallics. The pyridine fraction and the residue were then analysed for metal concentrations by the atomic absorption technique. The wear scar diameters were measured according to the standard procedure. Data for these sequential tests are presented in Table 24.

The wear characteristics of the diester base stock have been found to depend more on temperature and less on oxygen concentration. The decrease in unit loading and hot-spot temperature in the second test of the sequence should result in a lower rate of generation of the polar fluid decomposition products. This trend is reflected in a lower concentration of pyridine-soluble organometallic compounds for the diester base stock in the second test in the sequence. A comparison of the second and first tests in the sequence in Table 24 and Table 16 shows that the pyridine-soluble organometallic values differ substantially. This comparison is presented in Table 25. The production of pyridine-soluble organometallic materials in the first test is 25 times as high as that in the second test in the sequence. The pyridine-insoluble metallic-oxide wear is higher in the second test than in the first. This

indicates that the wear characteristics of the ester are more dependent on temperature and less on oxygen concentration. The essentially constant unit load and surface temperatures during the second test in the sequence has resulted in a lower rate of generation of polar fluid decomposition products.

It has been observed in the original "run-in" tests that the polar organic acids produced from the thermal fluid decomposition and oxygen are better polar competitors for the bearing surface. The adsorption of polar organic material and oxygen on the metal surface will depend on their relative concentrations. It appears that the polar organic materials are not present in sufficient concentration during the second test in the sequence and as a result oxygen dominated the adsorption process on the bearing surfaces.

The wear characteristics of the mineral oils have been shown to depend on oxygen concentration. Oxygen adsorbs on the surface in the absence of highly polar decomposition products. In case of mineral oils high bulk temperatures and to a lesser extent high surface temperatures promote the formation of polar organic oxidation products. The oxidation products do not appear to be as surface active or as polar as the thermal and oxidative decomposition products of the esters. The trends between the "run-in" test and the second sequential test are the same for the esters and super-refined mineral oils in an air atmosphere. The magnitude of organometallic materials soluble in pyridine is lower in the case of the mineral oil than for the ester. The production of pyridine-soluble organometallic compounds in the "run-in" test with the mineral oil is only 4 to 6 times as high as that in the second test in the sequence. This comparison is presented in Table 25.

Because of the lower surface temperatures existing in the second run in the sequence, the rate of fluid oxidation appears to have been lowered compared with the "run-in" tests. The higher oxygen concentration appears to have resulted in more non-oxygen reaction to produce iron oxide rather than pyridine-soluble organometallic materials.

Wear levels are higher in an air atmosphere than under a nitrogen atmosphere as shown in the second tests in sequence. The wear levels under nominal nitrogen atmosphere are lower in the second tests in the sequence than in the original tests. It appears that the 0.5 volume percent oxygen concentration in the nitrogen gas used is more effective as a lubricity additive because of decreased loading conditions prevalent in the second tests in the sequence. Some of the characteristic differences between the two mineral oils as discussed earlier can be observed again The wear level is lower for the high-viscosity naphthenic stock than for the low-viscosity paraffinic stock These differences have been shown to be related to the relative volatility rather than the viscosity of the stocks. Another possible difference is the presence of polar impurities (natural lubricity additives). The oxygen sensitivity for the wear-oxygen relationship of the naphthenic stock is much lower The presence of polar impurities in the fluids is reflected in the organic debris formed in the wear tests. The naphthenic stock produced much higher organic debris levels than the paraffinic stock. The volatility effect is exhibited in both tests in the sequence. The presence of

polar materials in the higher molecular weight naphthenic stock appears to be responsible for the reduced wear and oxygen effect. Changes in oxygen content do not appreciably alter the basic lubricity reaction mechanism in the sequential tests.

For the ester, the reaction at the bearing surfaces appears to be more a function of the concentration of oxygen and/or organic acid than the relative polarity of the two materials. For the mineral oils, on the other hand, the wear characterisitics appear to depend more on the preferential adsorption of oxygen on the metal surfaces rather than the relative concentrations of oxygen and polar oxygenated materials.

The same base stocks were studied with oxidation inhibitors and the results compared with the same test conditions on the base stocks alone. Tests were conducted under air. The cleaning procedure and analytical techniques used were the same as those described previously. Results of the debris analyses for sequential tests with inhibited fluids are presented in Table 26.

A comparison of the original and second test in the sequence is shown in Table 27. The presence of the inhibitor alters significantly the amount of organometallic product in the wear tests. The organometallic values for all three inhibited fluids in the sequential tests are lower by a factor of 1.5 relative to the corresponding tests on the uninhibited fluids. For the diester, the organometallic debris for the inhibited fluid is higher by a factor of 1.6 than the corresponding values for the uninhibited fluid. For the super-refined paraffinic mineral oil, the organometallic debris value for the inhibited fluid is a factor of 1.2 higher than the corresponding uninhibited fluid in the second test in the sequence. For the naphthenic mineral oil, the trend is reversed and the organometallic values for the inhibited fluid are lower than those of the corresponding uninhibited fluid in the second test in the sequence.

It should be emphasized that in the case of the naphthenic mineral oil without the inhibitor the presence of polar impurities appears to dominate the wear process. Thus, the presence of the inhibitor which would normally emphasize the role of polar dissolved oxygen should have little effect.

Between the two mineral oils, the inhibited paraffinic stock produced more organometallic material than the inhibited naphthenic stock. This may be attributable to the fluid volatility which appears to affect the combined chemical reactivity and removal of the reaction product from the wear surface. The paraffinic stock is more susceptible to oxygen-metal wear reaction. This is reflected in the lower wear values exhibited by the inhibited fluid in the second test in the sequence.

One distinct trend that is evident in the comparison of inhibited and uninhibited fluids is the increased concentration of oil-soluble organometallic material found in wear tests with the inhibited fluids. Such an increase is indicated in spite of a dramatic total reduction in pyridine-soluble organometallic compounds in the same fluid

system compared with the uninhibited fluids. The answer to this problem appears to be found in the role of the anti-oxidant in the overall test system. Static corrosion tests with hindered phenol- and phenothiazine-type oxidation inhibitors show a trend toward altering the metal corrosion characteristics of the base stock. The inhibitors appear to react preferentially with the metal surface to produce soluble organometallic products. The involvement of an acidic phenol in such a reaction is not unexpected.

The reactions between the hindered phenol or the phenothiazine and the metal would appear to be the source of the oil soluble organometallic material. It appears that the reaction takes place at the rubbing surfaces although there is no clear cut proof of this. Static corrosion tests indicate that these additives are capable of the organometallic reaction with the metal surface even at low temperature. The potential for high reaction rates at the elevated temperatures in the sliding contact zone make this area appear to be the source of the reaction. In considering this organometallic reaction based on the contact zone, it is necessary to postulate some adsorption of the inhibitor on the bearing surface for the fluids containing Parabar 441 and phenothiazine. In view of the other wear products it appears that several materials from the lubricant system are involved in the adsorption step, From the increased prominence of the soluble organometallic compounds in the debris from the second test in a sequence, it appears that less severe reaction conditions may be required for this reaction than for the production of the other products noted. It appears for example that the formation of iron oxide is more temperature dependent than the inhibitor-metal reaction.

The behavior of the viscous naphthenic mineral oil containing Ethyl 702 oxidation inhibitor requires special treatment. In this inhibited fluid test series the oil-soluble organometallics were below detection limits. Previous uninhibited fluid tests indicated less wear and a different analysis of wear debris from the super-refined paraffinic mineral oil. This difference was attributed to the presence of polar impurities (natural lubricity additives) in the fluid which appeared to be more polar than the dissolved oxygen. These impurities also appear to be more polar than the Ethyl 702 inhibitor and thereby prevent the reaction of the oil soluble organometallic material. These data provide a consistent explanation for the wear values, the lubrication chemistry at the concentrated contact, and the static corrosion trends noted at moderate temperatures using the same fluids and metal systems.

The presence of an organometallic material has been demonstrated in all tests under sliding conditions. It is interesting to note that corrosion stops after some time with both inhibited and uninhibited fluids. This suggests that the protective coating is still formed and that its formation is not retarded by the inhibitors. Although the coatings formed by uninhibited fluids appear to be much more effective in stopping further corrosion, this could be due to the more limited quantities of polar impurities present which represent the total capability of iron corrosion. It appears that the rate of organometallic

generation is a function of unit load, bulk fluid temperature, availability of 'hot-spot' reaction zones, the presence of other polar impurities such as inhibitors, and the reactivity of the fluids with oxygen. Primary among these variables appears to be temperature for esters and oxygen for mineral oils. The rate of organometallic product generation appears to be very high in the beginning but gradually falling off as more and more constant conditions are established in the concentrated contacts. The polar nature of the organometallics and their adsorption on the bearing surfaces can be demonstrated. The thermal or oxidative decomposition products of the fluids are removed from the oil. As they approach the metal surface they are adsorbed on the surface followed by chemical reactions. It appears that the organometallics are held by chemical bonds to the metal surface and cannot be easily removed by mechanical action. The organometallic materials therefore offer a protective coating to the bearing surface against further corrosive attack. Corrosion falls off with time, probably not because of a lack of corrosive material, but because of a lack of corrodible surfaces. High-wear levels can be generally attributed to the protection offered by the organometallics. In order to be effective to protect the surfaces, it appears that a minimum film thickness has to be achieved. This film should be equal to or greater than the mean separation of the surfaces. Alternatively, elastic deformation of the bearing surfaces is necessary to provide the necessary contact area to maintain a coherent film.

The metal distribution in various phases suggests that the polar decomposition products from the base stocks probably find their way to the bearing surfaces by a diffusion process. For the ester this resistance to diffusion is offered by oxygen versus the polarity of the oxygenated materials.

It appears that the inhibitors perform two functions. First they protect the fluid from oxidation and impart a stable life. Second, their oxidative decomposition products themselves participate in the organometallic reactions. This oxidative decomposition makes the inhibitors become depleted. The depletion rate of the inhibitors appears to depend upon temperature, inhibitor concentration and available active metal surfaces.

f. Analyses of the Oil-Soluble Metal Salts. It has been observed that metals are found in the test oils during the second test in the sequence. Soluble organometallic materials were also found in single tests with some inhibited fluids. It appears that the reasons for the formation of organometallics may be different for the two cases. To obtain further data on oil-soluble organometallic products, some additional four-ball wear tests were conducted according to the standard test procedure. The test fluids from these tests were collected, filtered to remove any solids, and analyzed for metal concentration. The results of these tests are presented in Table 28 for uninhibited fluids and Table 29 for the inhibited fluids.

In all cases the repeat studies of the formation of oil-soluble organometallic material are in excellent agreement with the previous studies where more extensive analysis was done. That is, the

data in Tables 16 and 17 are in excellent agreement with those in Tables 28 and 29. In the formation of oil-soluble organometallic products, static corrosion tests show that primary reaction products only are involved. Secondary and tertiary reaction products result in insoluble products. In the case of an oxygen-poor environment, the presence of oil-soluble organometallics may be attributable to the lack of oxygen for secondary and tertiary reactions. In the case of the second run in a sequence, sufficient oxygen is available but because of the decreased unit load the operating conditions of temperature and pressure are significantly lower resulting in reduced reaction rates in the wear zone. The presence of the oxidation inhibitors in the initial tests also tend to produce oil-soluble organometallic products. Here it appears that the reaction at the bearing surface may actually involve the oxidation inhibitor and, in addition, reaction rates should be reduced by the presence of additonal inhibitor in the fluid. It should be noted that the explanations proposed are consistent with the findings from liquid phase oxidation and static corrosion test results.

g. Catalysis in Boundary Lubrication. Reactions of metals and primary decomposition products of the lubricant base stock have been observed so far. In the dynamic wear system employed in this study clean metal surfaces are continuously produced by the removal of the metal reaction products from the bearing surface. The object of this portion of the study is to evaluate the catalytic activity, if any, by the clean metal surfaces. These active surfaces could produce chemical reactions or changes in the base stock. It has been indicated that high localized temperatures of short duration are typical of concentrated contacts. These temperature peaks are of milli or micro second duration in rolling contacts and should be relatively short in sliding contact where the sliding is not continuous. For the four-ball system where continuous sliding on the stationary balls will maintain a high surface temperature, intermittent operation appears to be a simple way of providing cooling of the bearing surfaces.

The difference between continuous high temperature bearing surfaces and intermittent hot and cold surfaces should demonstrate the difference between thermal and catalytic effects. Catalytic reactions will result from a change in lubricant molecules which will contact clean metal surfaces under experimental conditions. If catalytic activity on the metal surface dominates, then the dissociative adsorption of the lubricant on the surface may produce reactive fragments. These fragments may react with dissolved oxygen to produce organometallics.

Experiments were designed to cool the system for the same time as the heating cycle for exposing the clean metal surfaces. The Shell four-ball wear tester was operated through a Flexopulse set with a 15 second-on 15 second-off cycle. This means the actual rubbing process occurred for 15 seconds followed by 15 seconds of rest to cool the system. For these tests, debris analysis was measured by the usual procedure. The total test time was 120 minutes duration. The actual rubbing occurred for 60 minutes which is comparable to the standard continuous 60 minute runs. An air atmosphere was used with super-refined mineral oils and the diester as the test fluids. Debris analyses for both types of tests were made using standard analytical techniques. Pyridine-soluble

and insoluble fractions were prepared and analyzed. The results for the intermittent operation as shown in Table 30 can be compared with the standard continuous runs in Table 16. These data show that the production of pyridine-soluble organometallics in the continuous tests is three to four times higher than those values for the intermittent runs with mineral oil fluids. The catalytic effect of the metal surface does not appear to be as important as the temperature effect on triboreactions at the bearing surface.

The role of metal surface appears to be limited to high temperature reactions with the fluid or fluid components. The metal does not appear to have an unusual catalytic effect on reaction rates. Wear properties for the continuous and intermittent runs are about the same for a given fluid. Debris analysis tends to show that polar contaminants will affect wear properties more than does catalysis by metal surfaces. In static corrosion tests, it was found that the rate of gas formation was higher in tests containing metals than in metal-free systems. This suggests that reactions between the metal and liquid components will occur on oxide-coated metal surfaces and involve the metal. The role of the metal may therefore be limited to a reactant rather than a catalyst. It can be speculated that the presence of clean metal does not affect greatly the rate of thermal decomposition of the fluids in contact with the surface. The differences between the paraffinic and naphthenic mineral oils in the wear process may be attributed to existing impurities in the fluid or thermally induced reactions at or near the surface.

For the diester, the organometallic values from the continuous tests are higher by a factor of six than in the intermittent test. The conclusions drawn for the mineral oils also appear to apply for the ester. Generally higher metallic oxide debris for the ester suggests that oxygen concentration was high enough in all cases to act as a preferentially adsorbed molecule on the metal surface.

In static corrosion tests with the ester performed with and without metal catalyst, it was found that the neutralization number was lower for a given amount of degradation in the presence of the metal (AFML-TR-67-107, Parts II and III). The reduced neutralization number in this case is indicative of reaction between the acid degradation products and the metal.

h. Particle Sizes of Wear Debris. Particle size and distribution of the wear debris from the four-ball test were measured for both tests in the sequence. The difference between the two tests with a common fluid show the "run-in" on wear particle size. The superrefined mineral oils and the diester base stock were used as test fluids under an air atmosphere.

Four-ball wear tests were conducted according to the standard procedure. The ball pot was allowed to cool to room temperature, shaken vigorously without disassembly, a drop of test fluid was collected, and spread on a microscopic slide. The slide was covered by a watch glass and placed under a microscope. The ocular lens of the microscope contained a calibrated scale on which the smallest unit is 7.6 microns and

measurements can be estimated to 0.76 micron. The length and width of the particles were measured by using this scale as shown in Table 31. The particle area was calculated and is presented in Table 32 as a function of wear scar diameter. Test with the ester and the super-refined paraffinic mineral oil produce particles of about the same size. Super-refined naphthenic stock produced low wear in all cases compared to the paraffinic stock or the ester. It can be seen that the particle size of the wear debris also is low. The ester is more corrosive than the paraffinic stock, but this fact is not reflected by the particle size of the wear debris in a single four-ball wear test. In a test sequence, however, the particle size of the ester debris in the second test is higher than that of the corresponding super-refined mineral oils. For the two super-refined oils, the particle size of the paraffinic stock is higher than for the naphthenic. This order of particle size represents a correlation with the relative corrosivity of the three fluids. The severity during "run-in" tests, probably hides this relationship during a single one-hour test.

In the sequential tests, the particle size is higher in the original tests by a factor of 1.3 for the ester, 1.8 for the paraffinic stock and 1.2 for the naphthenic stock. This appears to be a function of unit loading under the conditions producing the new surface in the wear tester.

The particles were sized and counted in this study by calculating the mean value from eight sample determinations for a given test. This procedure was used for the paraffinic mineral oil. The particle distribution is presented in Figures 76 and 77 for the original and second run in the sequence. The size which represents the highest number of particles in the original test is about twice that value in the second test in the sequence. These values appear to be load related. The gross contact area was determined from the wear scar and halo width diameters. This contact area includes the roto ball track and the wear scar areas of the three stationary balls and represents the maximum probable contact area. The relationship between these contact areas and wear scar diameters is presented in Figure 78. The initial contact area is produced by elastic deformation of the balls under the applied load. These data indicate the amount of corrosion in a particular time based on the area of contacts at that time. It should be mentioned that a larger contact area implies a higher elastohydrodynamic component of lubrication.

i. Wear Rate Studies. It has been observed that the boundary lubrication reactions in all cases generate organometallic compounds that are found preferentially adsorbed on the bearing surfaces. They are probably formed on the bearing surface by chemisorption and have not been removed because of the level of energy required for removal. As more and more organometallic materials are formed, the available surfaces for boundary lubrication reactions diminish. It can be postulated that, with the progress of wear, the surfaces will be covered by the organometallic compounds which will act as a protective film against further corrosive wear. In addition, as the wear-scar size increases

and the EHD film component increases the shearing action as well as cavitational forces on the surface layers decrease.

The various conditions that govern the formation of these organometallics have been discussed in earlier sections. High surface temperatures at the metal surface appears to be one of the most important conditions. This has been observed in the sequential tests. In the beginning of the wear process, the bearing surfaces are "run-in" under the most severe conditions. The high loads and high temperatures diminish with the "run-in" procedure. The decreased unit loading with the progress of wear will generate increasing surface contact area. As a result a nearly constant load and wear may be expected from the latter part of the one-hour wear test in the original test or for all of the second test in the sequence. The experiments discussed in this section have been conducted to determine the validity of this theory.

Four-ball wear tests were conducted according to the standard test procedure for 10, 30, 60, 90, 120, and 150 minutes with the diester base stock. The oil insolubles were collected after each test and the pyridine-soluble and insoluble fractions were prepared and analyzed. Results are presented in Table 33. The relationships of wear scar diameter and pyridine-soluble and insoluble metals with time are presented in Figures 79 and 81. It can be seen that wear rate reaches a constant value after the "run-in" period. Similar data for the super-refined mineral oils MLO 7789 and MLO 7625 are presented in Table 34 and Figures 79, 82, and 83. A log-log relationship of wear scar diameter versus time is presented in Figure 80. The slope of this relationship indicates the wear rate and provides a convenient means to compare lubricant performance.

It can be seen from the ester data that oil-soluble material containing metal is below detection limits after 30 minutes of test. This indicates that the chemical corrosion process taking place in the bearing conjunction has been substantially reduced. The probable factors influencing reaction rate are temperature and sufficient metal to react. As the bearing surfaces are increased in size by wear the unit loading decreases and the possibility of thicker fluid films (EHD component) increases. This trend reduces substantially the surface temperature as well as the tendency to remove surface films by shear or cavitational forces. It should be pointed out that the formation of metal and metal oxide particles do not follow the same reaction-rate path as the chemical corrosion reaction. The higher relative rate of metal particle and metal oxide formation under the milder wear conditions has been noted in all of the tests run in this study. This information would tend to confirm the observation that metal corrosion by organic materials has a strong temperature function. Metal oxide formation appears to proceed at low temperatures with less apparent temperature sensitivity.

It can be seen from the wear data for mineral oils that corrosion is rapid at the beginning of the tests in the same manner described for the ester. The same explanation for the reduced rate of production of metal fluid reaction product with test time applies to the mineral oils as well as the ester.

The contact area versus time relationship is presented in Figure 84. The surface area of contact also increases with time and, with progress of wear, tends to achieve a constant value. A decrease in unit loading is associated with the generation of increasing surface area of contact.

The effect of load on debris formation is presented in Table 35 and Figure 85. These data show that organometallic formation varies directly with load. Within a single test at any load, the change in the rate of formation of organometallic material follows the form of the curves shown in Figure 81, 82, and 83. These latter figures were all determined for a 40 kilogram load.

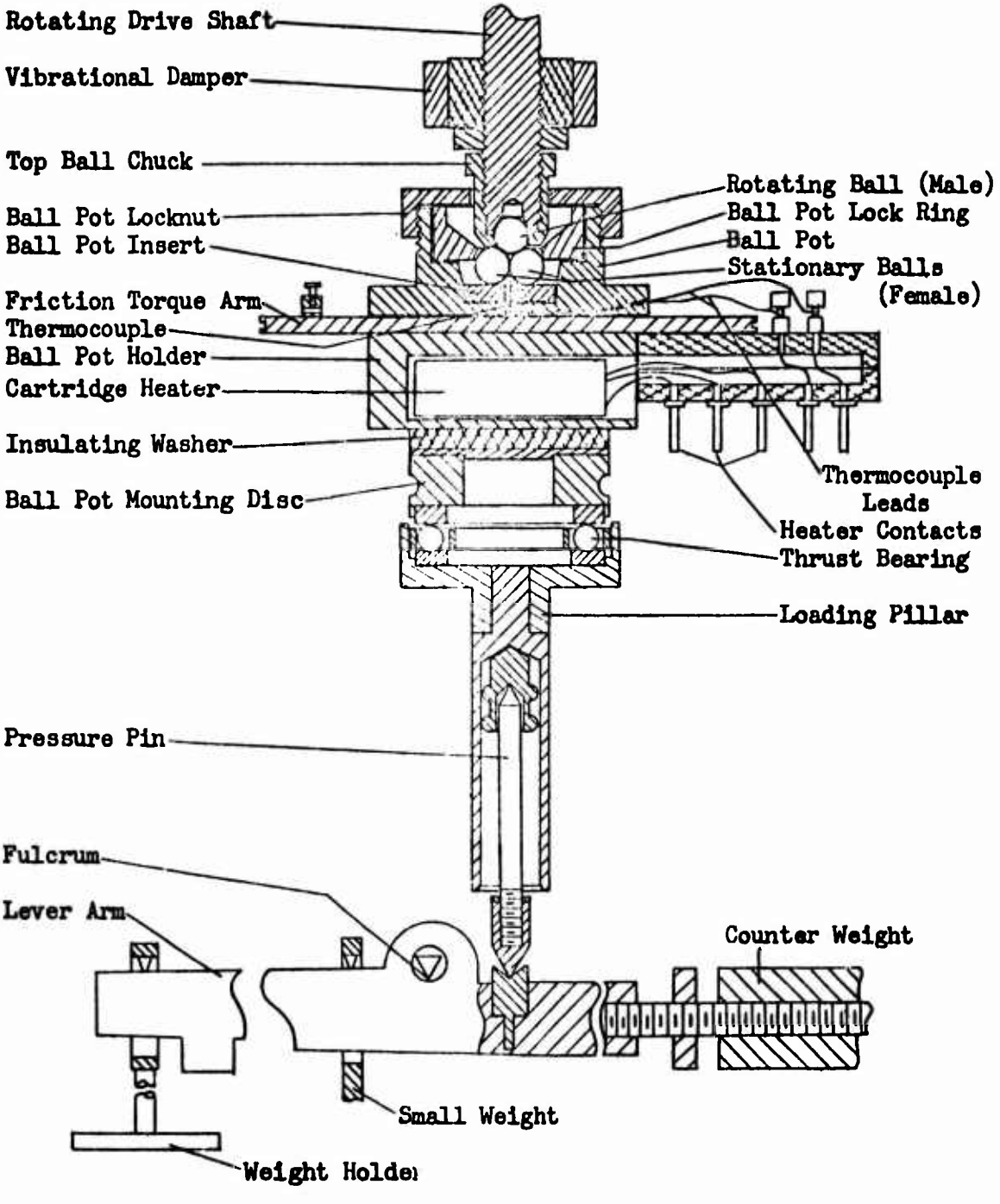

Figure 59. THE SHELL FOUR-BALL WEAR TESTER

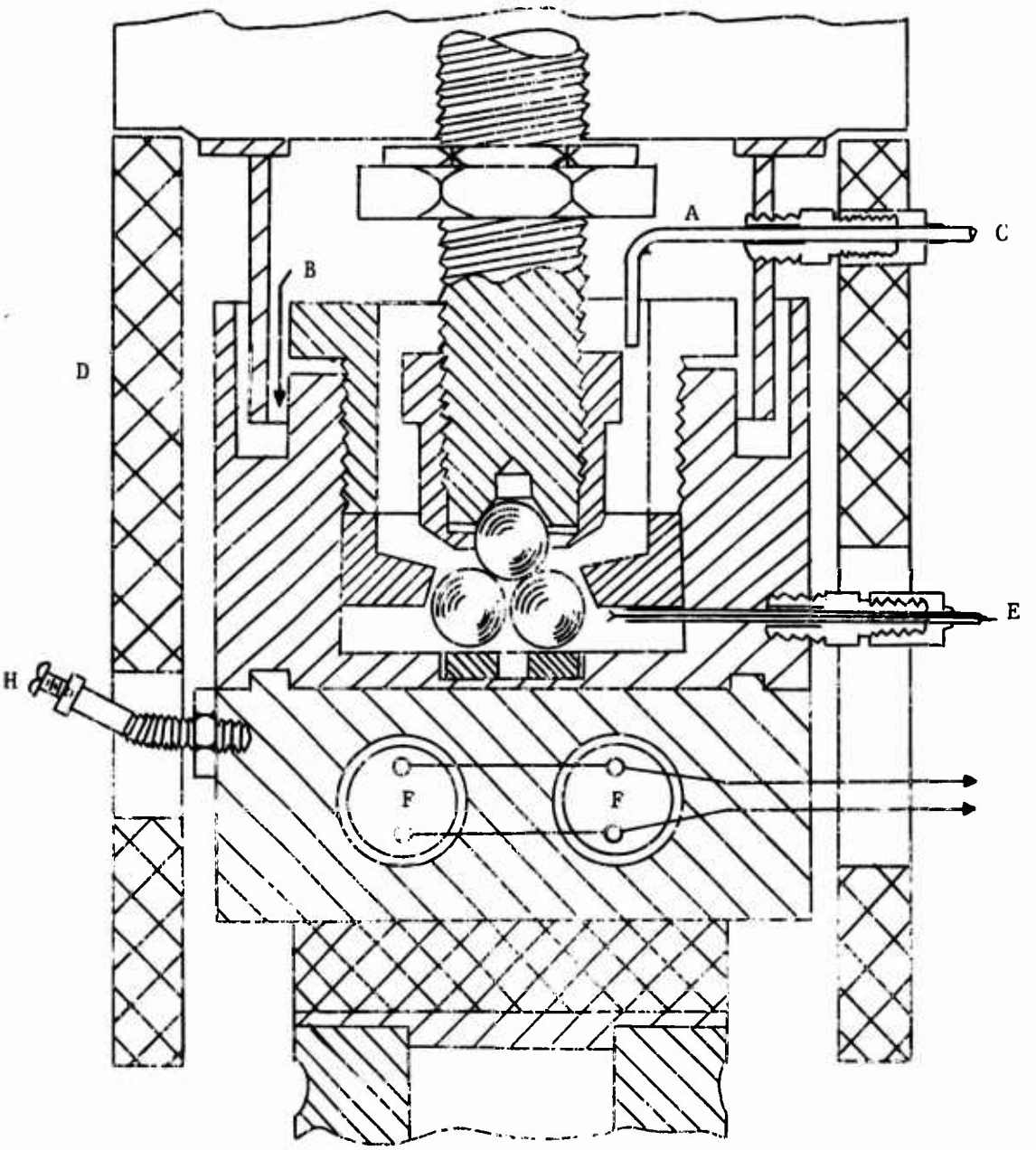

A - Vibrational Damper
B - Liquid Seal
C - Gas Inlet
D - Transite Insulation
E - Thermocouple
F - 200 Watt Cartridge Heater
G - Transite Spacer
H - Friction Torque Arm

FIGURE 60. SHELL FOUR-BALL WEAR TESTER MODIFIED FOR CONTROLLED ATMOSPHERE STUDIES

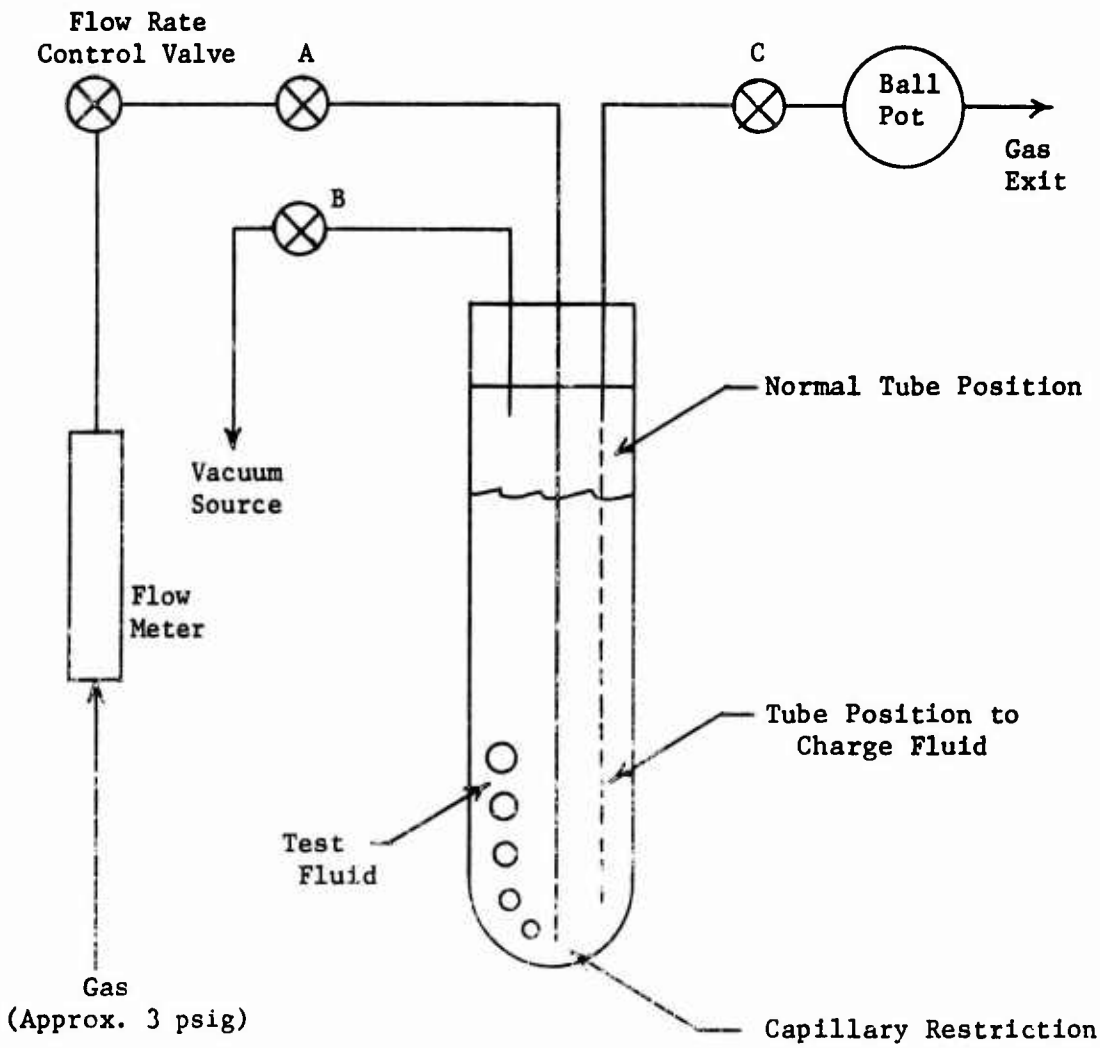

Figure 61. SAMPLE PREPARATION AND CHARGING SYSTEM FOR CONTROLLED ATMOSPHERE FOUR-BALL WEAR TEST

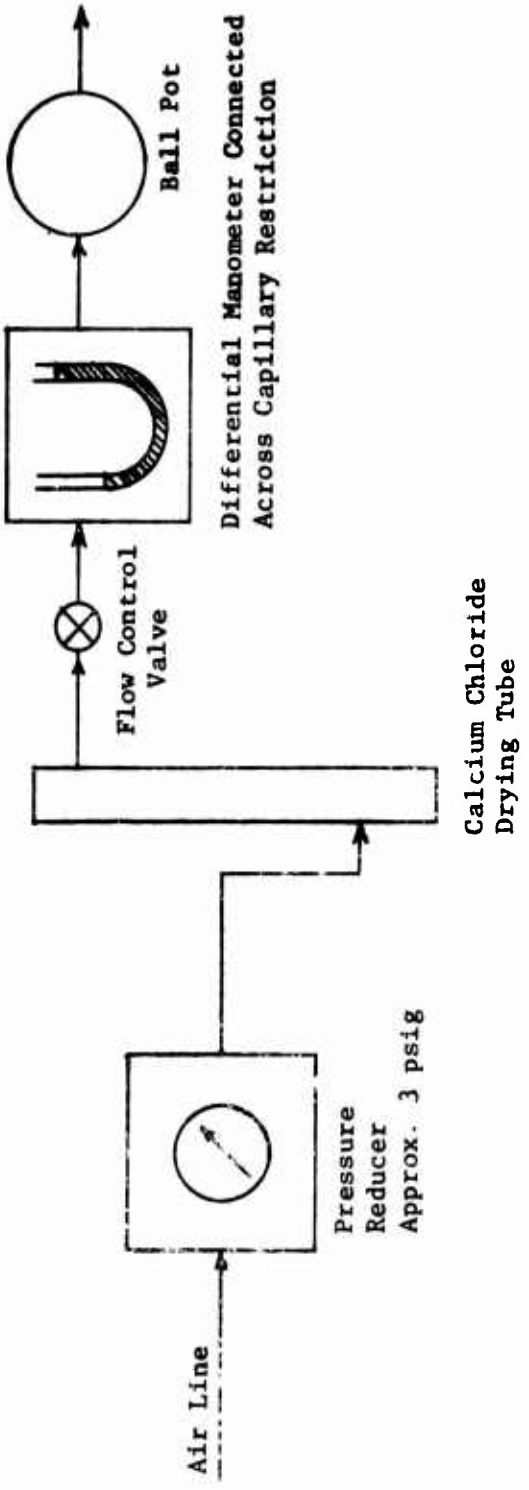

Figure 62. FOUR-BALL WEAR TEST IN AN AIR ATMOSPHERE

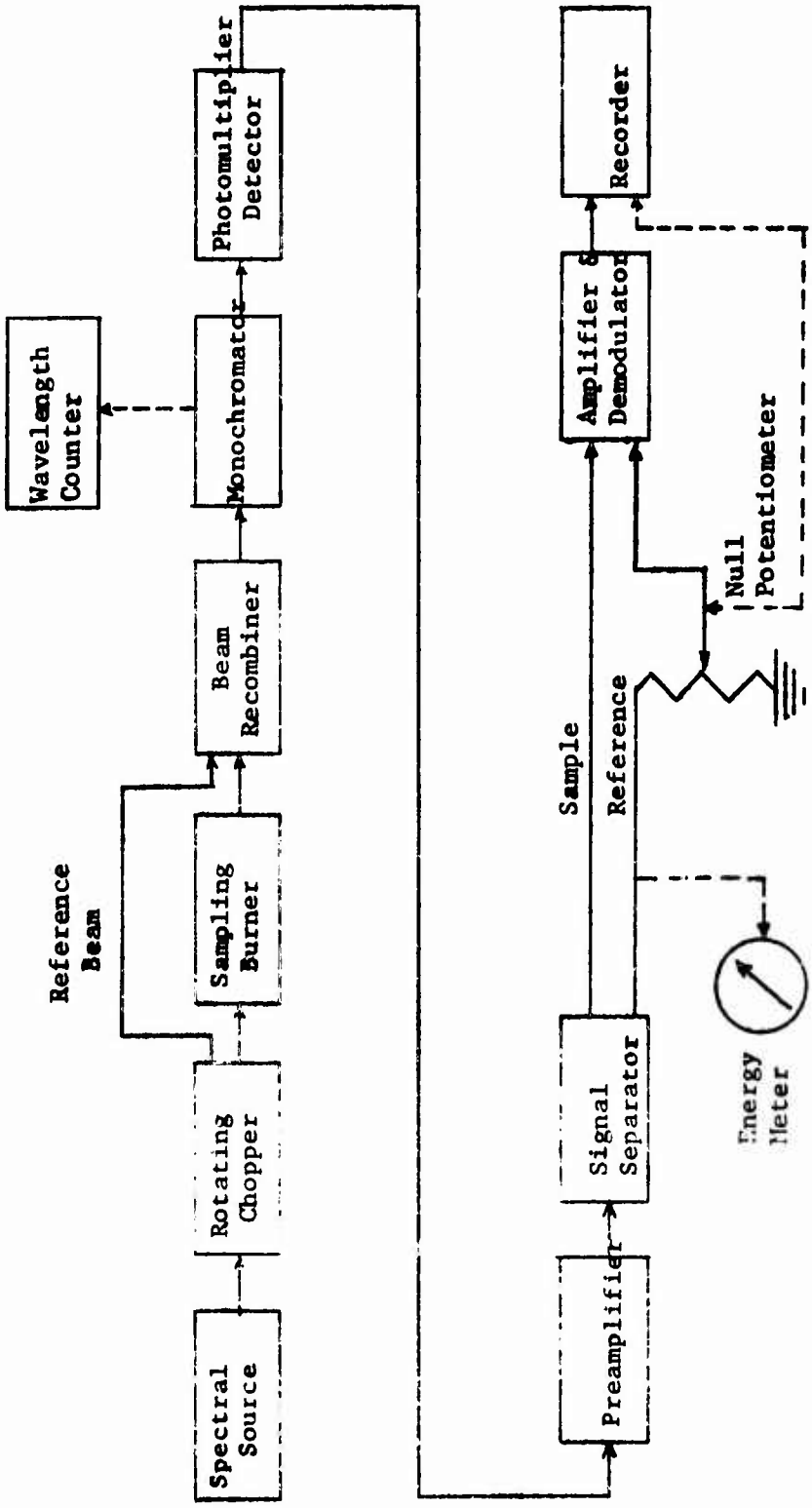

Figure 63. BLOCK DIAGRAM OF THE PERKIN-ELMER MODEL 303 ATOMIC ABSORPTION SPECTROPHOTOMETER

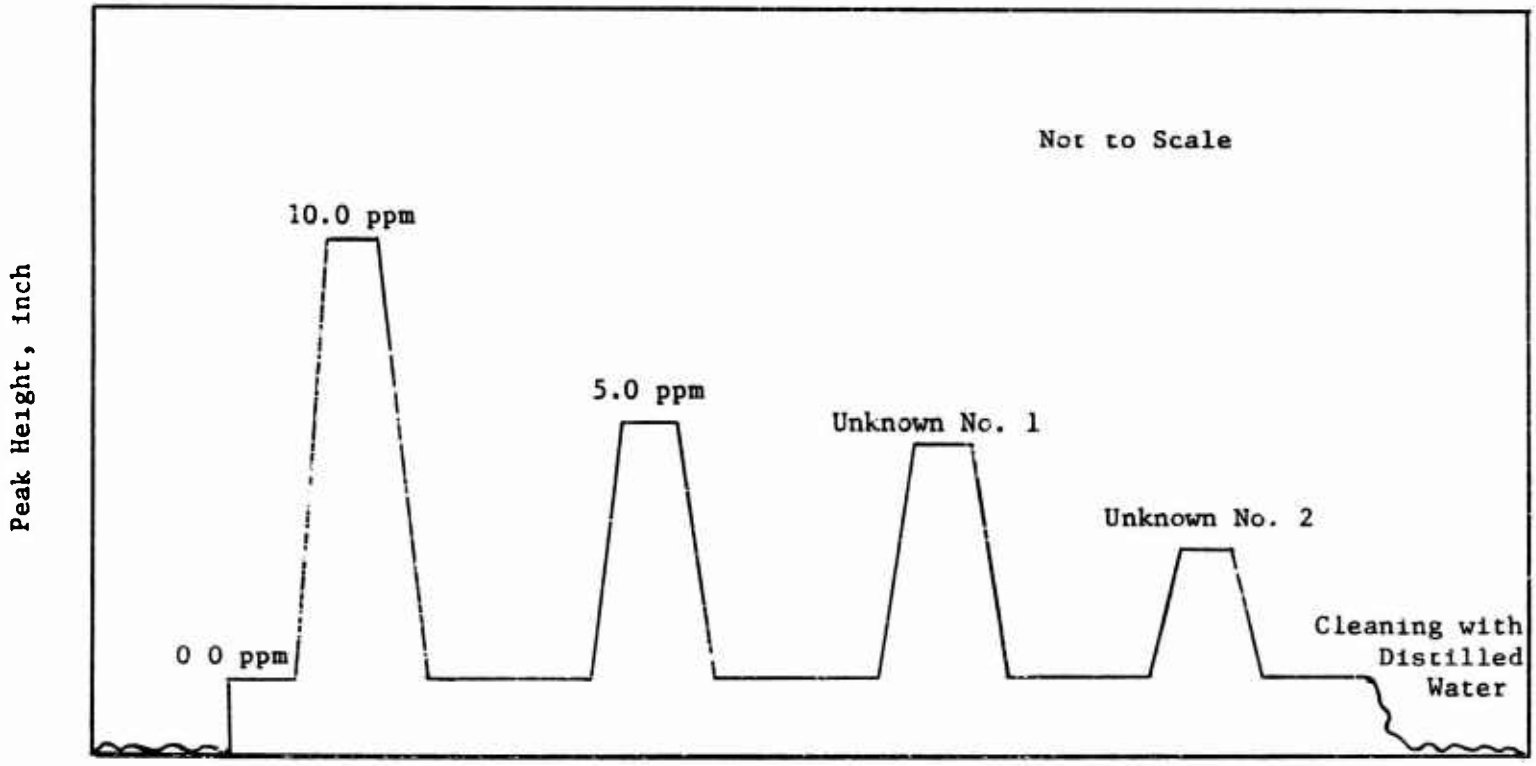

Figure [illegible]. TYPICAL ATOMIC ABSORPTION SPECTROPHOTOMETER TRACE FOR AN IRON DETERMINATION

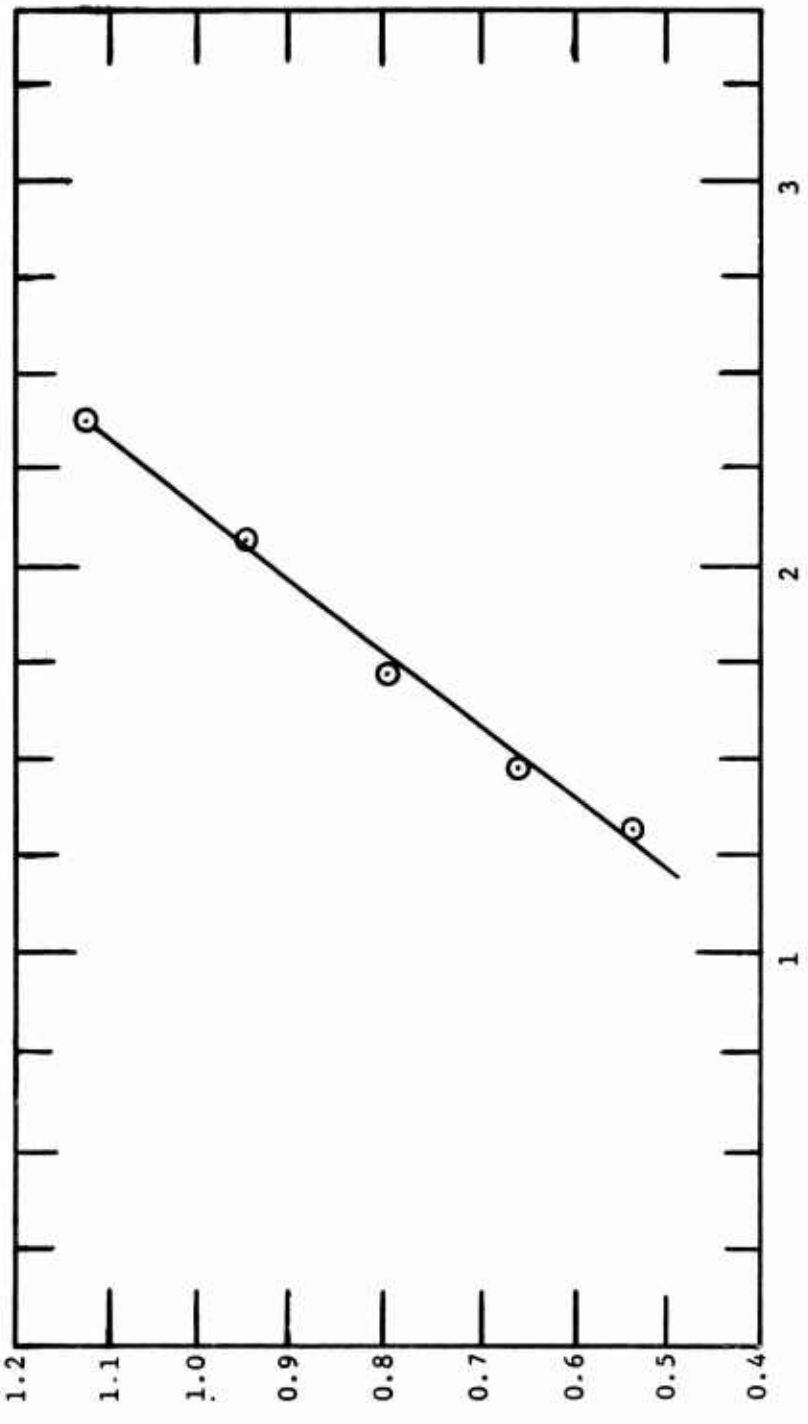

Figure 65. EFFECT OF VISCOSITY ON ASPIRATION RATE IN THE ATOMIC ABSORPTION SPECTROPHOTOMETER

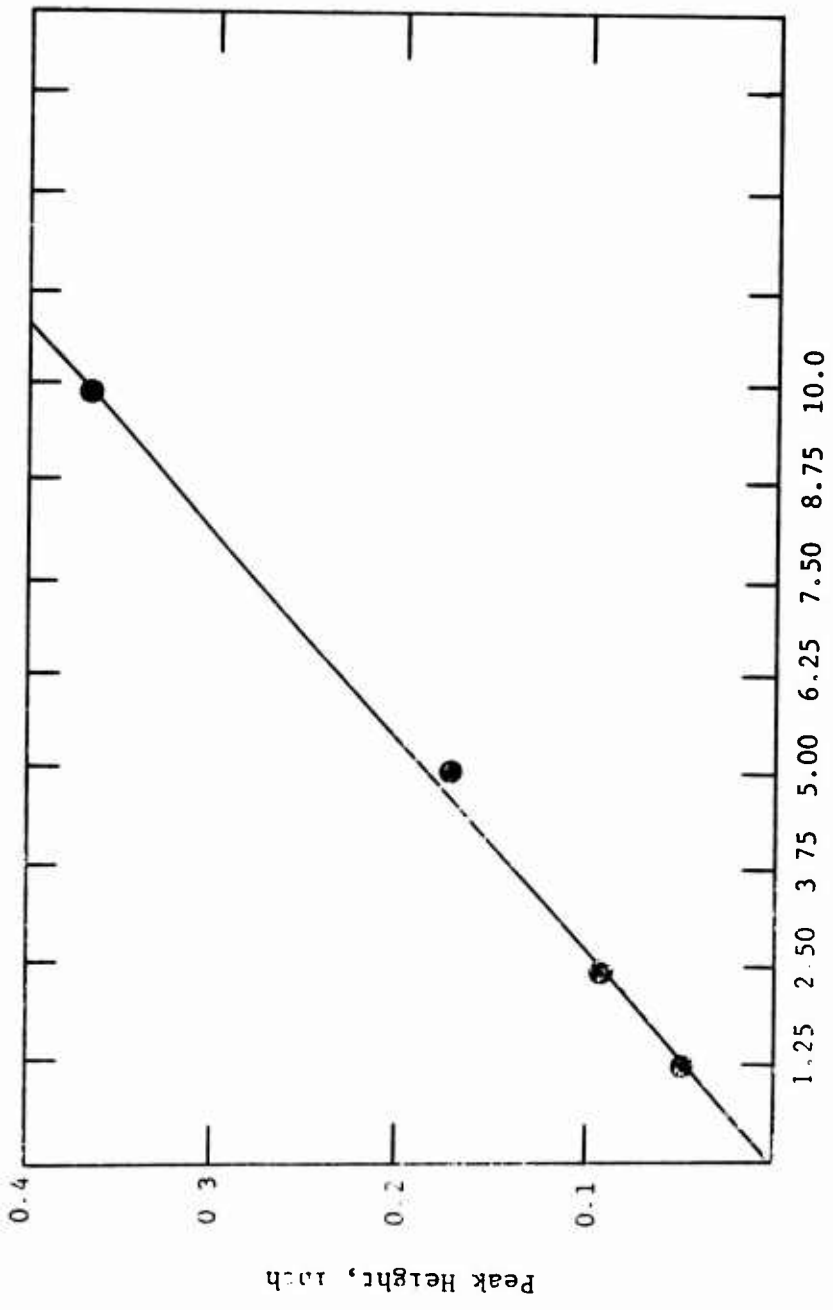

Figure 65 IRON CALIBRATION CURVE FOR THE ATOMIC ABSORPTION SPECTROPHOTOMETER

Table 12

PROPERTIES TYPICAL OF THE BASE STOCKS

Test Fluids: Di-2-Ethylhexyl Sebacate (MLO 7710)
Super-Refined Paraffinic Mineral Oil (MLO 7789)
Super-Refined Naphthenic Mineral Oil (MLO 7625)

Fluid Type, PRL Designation	MLO 7710	MLO 7789	MLO 7625
Viscosity at 210°F., Cs.	3.31	3.11	8.20
Viscosity at 100°F., Cs.	12.6	13.1	77.3
Viscosity Index (ASTM)	155	110	77.4
ASTM Slope	0.703	0.763	0.766
API Gravity, Degrees	---	37.3	28.1
Density, D_4^{20} g./ml.	0.902	0.838	0.883
Refractive Index, n_D^{20}	---	1.4637	1.4823
Calculated Molecular Weight	426	331	430
Hydrocarbon Analysis:			
Wt. % C as Aromatic Rings	---	0.0	0.0
Wt. % C as Naphthenic Rings	---	31.3	41.9
Wt. % C as Paraffinic Chains	---	68.7	58.1
Boiling Point Range at			
760 mm Hg., °F.	795	600-770	800-950

Table 13

PERFORMANCE CHARACTERISTICS OF THE
SHELL FOUR-BALL WEAR TESTER

Four-Ball Test Conditions Include: Test Speed = 600 r.p.m.; Load 1,4 or 10 Kg.; Test Temp. = 167°F.; Test Time = 1 hr.; Fluid Charged = 20 ml.; and Bearings = 52-100 Steel, PRL Batch No. 14.

Test Fluids: Super-refined Paraffinic Mineral Oil (MLO 7789)
Super-refined Naphthenic Mineral Oil (MLO 7625)

Test Fluid	Load, Kg.	Av. Wear Near Scar Diameter, mm.
MLO 7789	1	0.42
	4	0.49
MLO 7625	4	0.34
	10	0.43

Table 14

EFFECT OF TEMPERATURE AND ATMOSPHERE ON WEAR PERFORMANCE OF STEEL

Four-Ball Test Conditions Include: Test Speed = 600 r.p.m.; Load = 10 or 40 kg.; Test Temp. = 167°F.; Test Time = 1 hr.; Fluid Charged = 20 ml. and Bearings = 52-100 Steel, PRL Batch No. 14.

Test Fluids: Super-refined Paraffinic Mineral oil (MLO 7789)
Di-2-Ethylhexyl Sebacate (MLO 7710)

Test Fluid	Test Atmosphere	Load Kg.	Temp, °F.	Av. Wear Scar Diameter, mm.
MLO 7789	Dry Air at 0.7 l./hour	10	167	0.48
MLO 7789	Dry Air at 0.7 l./hour	10	400	0.40
MLO 7789	Nitrogen at 4.8 l./hour	10	167	0.32
MLO 7789	Nitrogen at 4.8 l./hour	10	400	0.43
MLO 7710	Dry Air at 0.7 l./hour	10	167	0.55
MLO 7710	Dry Air at 0.7 l./hour	10	400	0.70
MLO 7710	Nitrogen at 4.8 l./hour	10	167	0.46
MLO 7710	Nitrogen at 4.8 l./hour	10	400	0.68
MLO 7710	Nitrogen at 4.8 l./hour	40	167	0.70
MLO 7710	Dry Air at 0.7 l./hour	40	167	0.79

Table 15

RESULTS OF DEBRIS ANALYSIS AS FOUND BY
ATOMIC ABSORPTION SPECTROSCOPY

Four-Ball Wear Test Conditions Include: Test Speed = 600 r.p.m.; Load = 10 or 40 kg.; Test Temp = 167°F.; Fluid Charged = 20 ml.; Test Atmosphere = Dry Air at 0.7 liter per hour or Nitrogen at 4.8 liters per hour; Test Time = 1 hr.; and Bearings = 52-100 Steel, PRL Batch No. 14.

Test Fluids: Di-2-Ethylhexyl Sebacate (MLO 7710)
Super-refined Paraffinic Mineral Oil (MLO 7789)
Super-refined Naphthenic Mineral Oil (MLO 7625)

Test Fluid	Load, kg.	Test Atmosphere	Average Wear Scar Diameter, mm.	Pyridine Soluble Metal, mg.	Pyridine Insoluble Metal, mg.	Total Metal Loss, mg. (B)	Total Debris, mg. (A)	Organic Debris, mg. (A-B)
MLO 7710	10	Dry Air at 0.7 l./hour	0.59	0.021	0.092	0.113	0.15	0.037
	40	Dry Air at 0.7 l./hour	0.74	0.072	0.134	0.206	1.50	1.394
	10	Nitrogen at 4.8 l./hour	0.43	0.013	0.062	0.075	0.90	0.825
	40	Nitrogen at 4.8 l./hour	0.71	0.070	0.101	0.171	2.20	2.029

(Concluded on next page)

Table 15 (Concluded)

Test Fluid	Load, kg.	Test Atmosphere	Average Wear Scar Diameter, mm.	Pyridine Soluble Metal, mg.	Pyridine Insoluble Metal, mg.	Total Metal Loss, mg. (B)	Total Debris, mg. (A)	Organic Debris, mg. (A-B)
MLO 7789	10	Dry Air at 0.7 l./hour	0.47	0.028	0.096	0.124	0.600	0.476
	40	Dry Air at 0.7 l./hour	0.69	0.072	0.410	0.482	0.960	0.478
	10	Nitrogen at 4.8 l./hour	0.37	0.020	0.050	0.070	0.390	0.320
	40	Nitrogen at 4.8 l./hour	0.61	0.048	0.120	0.168	0.680	0.512
MLO 7625	10	Dry Air at 0.7 l./hour	0.30	0.011	0.058	0.069	0.420	0.351
	40	Dry Air at 0.7 l./hour	0.59	0.044	0.086	0.130	0.500	0.370
	10	Nitrogen at 4.8 l./hour	0.27	0.008	0.049	0.057	0.430	0.373
	40	Nitrogen at 4.8 l./hour	0.48	0.036	0.070	0.106	0.370	0.264

Table 16

MATERIAL BALANCE OF THE LUBRICATION DEBRIS OBTAINED FROM THE FOUR-BALL WEAR TESTS USING ATOMIC ABSORPTION SPECTROSCOPY

Four-Ball Wear Test Conditions Include: Test Speed = 600 r.p.m.; Load = 40 kg.; Test Temp. = 167°F.; Fluid Charged = 20 ml.; Test Time = 1 hr.; and Bearings = 52-100 Steel, PRL Batch No. 14.

Test Fluids: Super-refined Paraffinic Mineral Oil (MLO 7789)
Super-refined Naphthenic Mineral Oil (MLO 7625)
Di-2-Ethylhexyl Sebacate (MLO 7710)

Test Fluid	Average Wear Scar Diameter, mm.	Test Atmosphere	Pyridine Soluble Metal, mg.	Oil Soluble Metal, mg.	Pyridine Insoluble Metal, mg.	Total Metal Loss, mg. by bearing weight difference (B)	Total Metal Loss, mg. by adding all soluble and insoluble metals	Total Debris, mg. (A)	Organic Debris, mg. (A-B)
MLO 7710	0.74	Dry Air at 0.7 l./hour	0.0782	BDL*	0.1114	0.16	0.1896	1.17	1.01
MLO 7789	0.79	Dry Air at 0.7 l./hour	0.0566	BDL*	0.1400	0.19	0.1966	0.10	Nil
MLO 7625	0.53	Dry Air at 0.7 l./hour	0.0658	BDL*	0.1075	0.22	0.1733	1.09	0.87
MLO 7710	0.70	Nitrogen at 4.8 l./hour	0.0740	BDL*	0.1166	0.21	0.1906	1.17	0.96
MLO 7789	0.61	Nitrogen at 4.8 l./hour	0.0300	BDL*	0.0998	0.15	0.1298	0.50	0.35
MLO 7625	0.47	Nitrogen at 4.8 l./hour	0.0633	BDL*	0.0921	0.17	0.1554	0.54	0.37

* Below limit of detection.

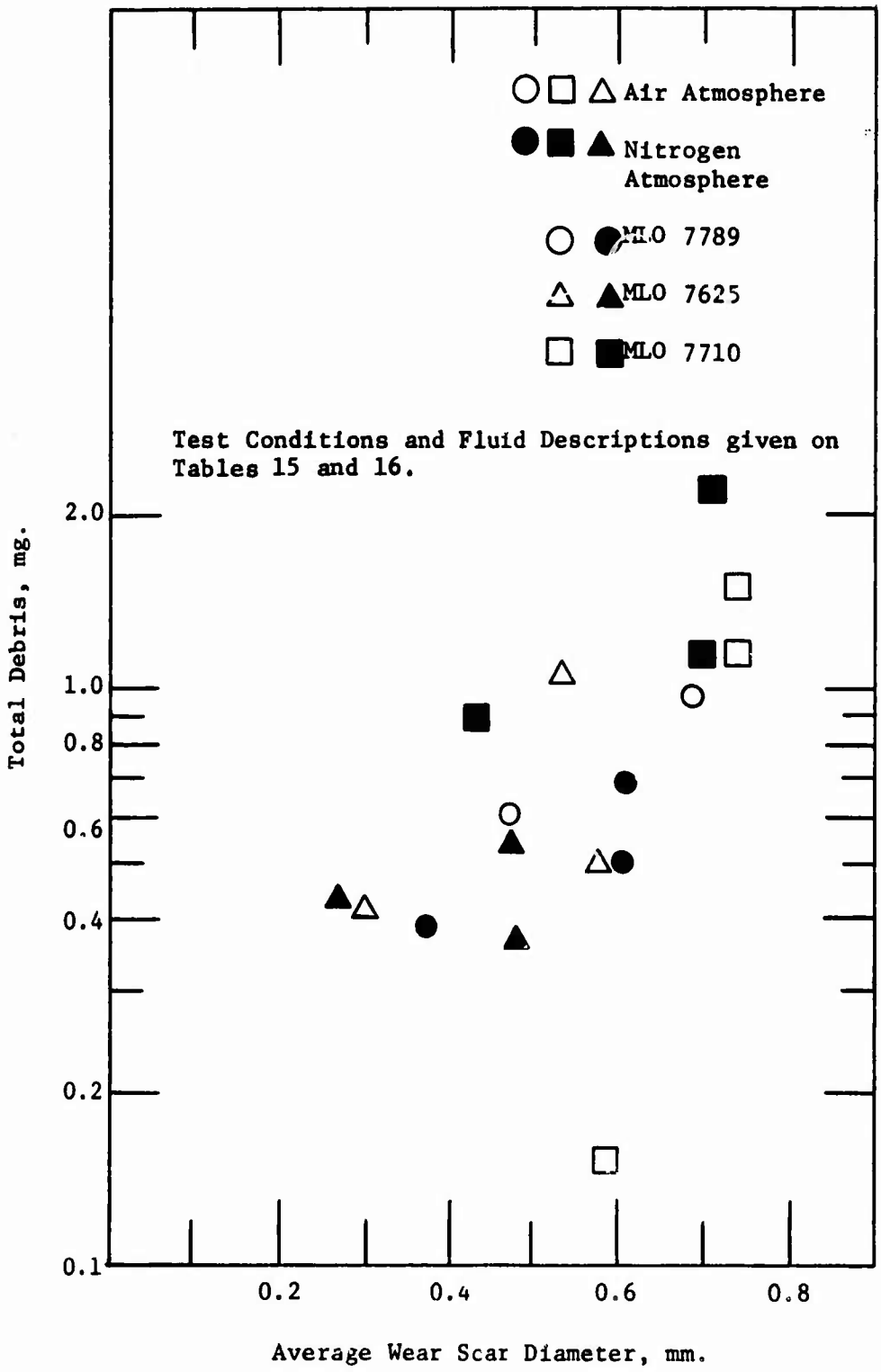

Figure 67. RELATIONSHIP OF TOTAL METALLIC DEBRIS TO AVERAGE WEAR SCAR DIAMETER

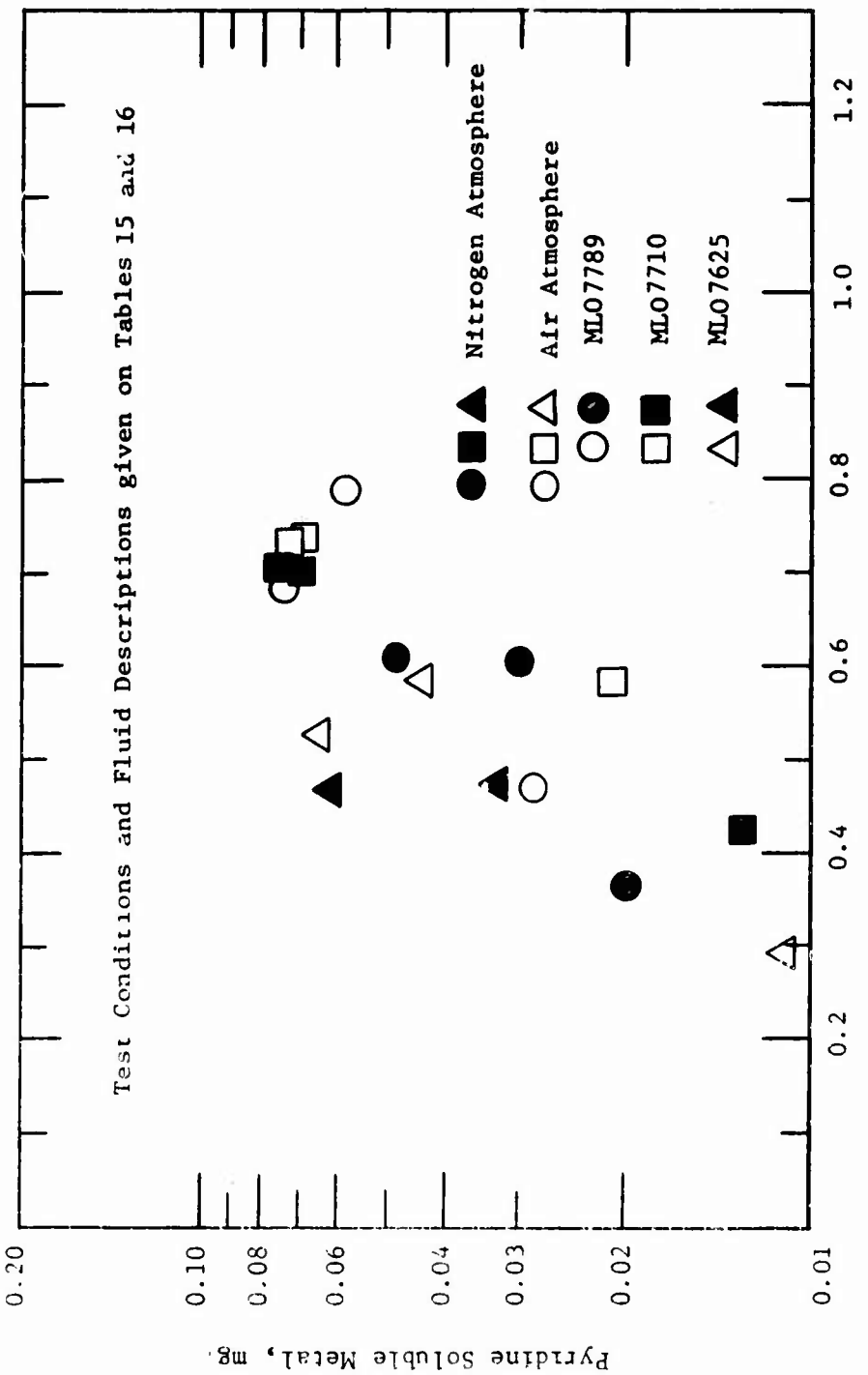

Figure 4 RELATIONSHIP OF PYRIDINE SOLUBLE METAL TO AVERAGE WEAR SCAR DIAMETER

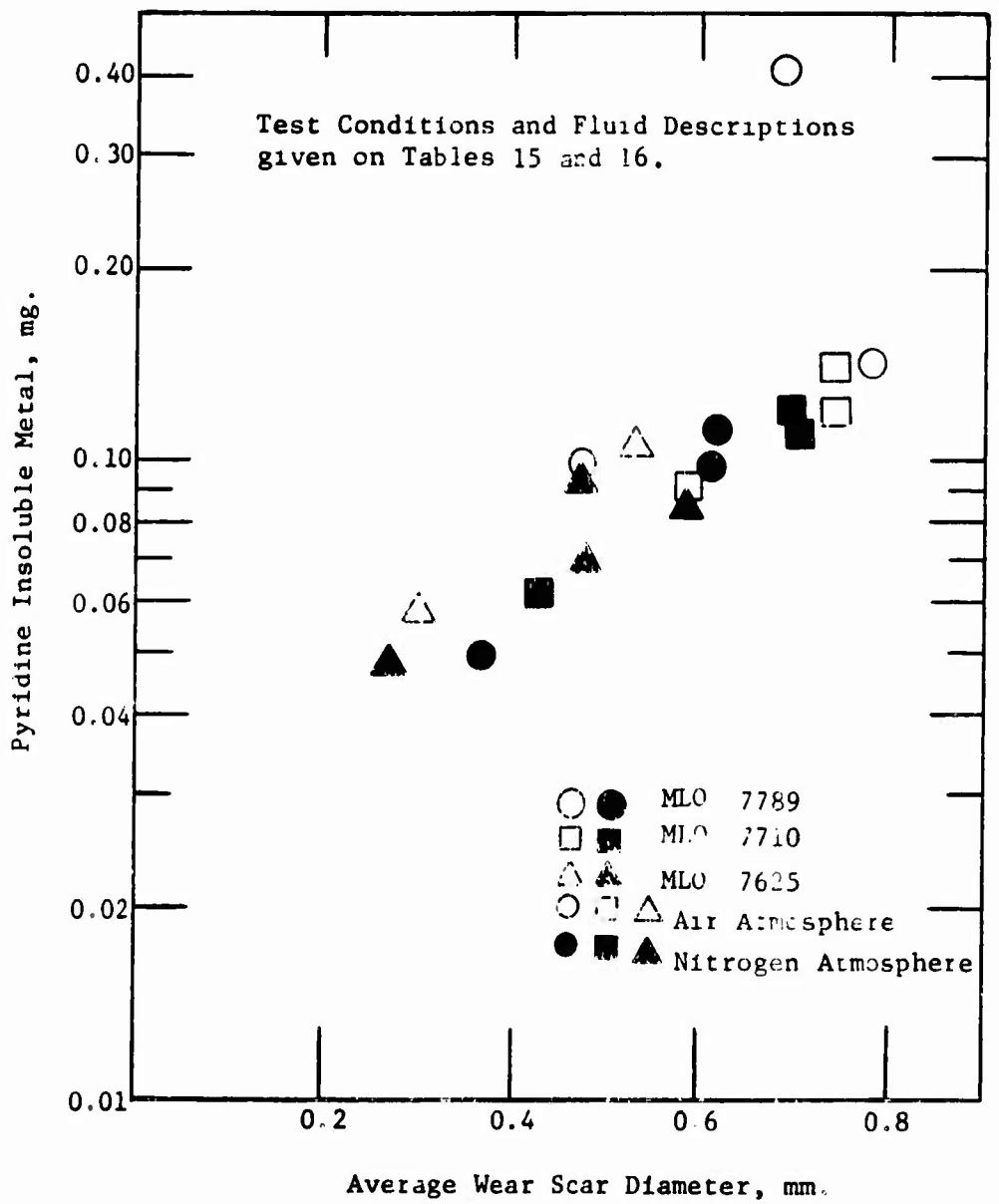

Figure 69. RELATIONSHIP OF PYRIDINE INSOLUBLE METAL TO AVERAGE WEAR SCAR DIAMETER

Table 17

WEAR DEBRIS FORMED BY SEVERAL INHIBITED FLUIDS

Four-Ball Wear Test Conditions Include: Test Speed = 600 r.p.m.; Load = 40 kg.; Test Temp. = 167°F.; Test Time = 1 hr.; Fluid Charged = 20 ml.; Test Atmosphere = Dry Air at 0.7 liter/hour and Bearings = 52-100 Steel, PRL Batch No. 15.

Test Fluids: Di-2-Ethylhexyl Sebacate (MLO 7710) + 0.5 Weight Percent Phenothiazine
Super-refined Paraffinic Mineral Oil (MLO 7789) + 1.0 Weight Percent Parabar 441
Super-refined Naphthenic Mineral Oil (MLO 7625) + 1.0 Weight Percent Ethyl 702.

Test Fluid	Average Wear Scar Diameter, mm.	Pyridine Soluble Metal, mg.	Oil Soluble Metal, mg.	Pyridine Insoluble Metal, mg.	Total Metal Loss, mg. by bearing weight difference (B)	Total Metal Loss, mg. by adding all soluble and insoluble metals	Total Debris, mg. (A)	Organic Debris, mg. (A-B)
MLO 7710 + 0.5 wt. % Phenothiazine	0.83	0.0073	0.0040	0.1493	0.18	0.1606	.253	0.093
MLO 7789 + 1.0 wt. % Parabar 441	0.70	0.0346	0.0031	0.1117	0.15	0.1494	1.20	1.051
MLO 7625 + 1.0 wt. % Ethyl 702	0.54	0.0066	BDL*	0.0765	0.09	0.0831	.65	0.567

* Below limit of detection.

Table 18

EFFECT OF DISSOLVED OXYGEN ON THE WEAR BEHAVIOR OF A SUPER-REFINED PARAFFINIC MINERAL OIL

Four-Ball Wear Test Conditions Include: Test Speed = 600 r.p.m.; Load = 10 kg.; Fluid Charged = 20 ml.; Test Time = 1 hr.; and Bearings = 52-100 Steel, PRL Batch No. 14.

Test Fluid: Super-refined Paraffinic Mineral Oil (MLO 7789)

Test Temperature, °F	Test Atmosphere	Average Wear Scar Diameter, mm.	Dissolved Oxygen Concentration ppm (by weight)
167°	Dry Air at 0.7 l./hour	0.48	41[a]
400°	Dry Air at 0.7 l./hour	0.40	1.3[a]
167°	*Nitrogen at 4.8 l./hour	0.32	0.43[a]
400°	*Nitrogen at 4.8 l./hour	0.43	0.2[a]

[a]Solubility values taken from previous reports

*Nitrogen tank contains 0.5 volume percent oxygen.

Table 19

EFFECT OF DISSOLVED OXYGEN ON THE WEAR BEHAVIOR OF A SUPER-REFINED MINERAL OIL AS FOUND BY DEBRIS ANALYSIS

Four-Ball Wear Test Conditions Include: Test Speed = 600 r.p.m.; Load = 10 kg. Fluid Charged = 20 ml.; Test Time = 1 hr.; and Bearings = 52-100 Steel, PRL Batch No. 14

Test Fluid: Super-refined Paraffinic Mineral Oil (MLO 7789)

Test Temperature, F	Test Atmosphere	Average Wear Scar Diameter, mm.	Pyridine Soluble Metal, mg.	Pyridine Insoluble Metal, mg.	Dissolved Oxygen Concentration ppm (by weight)
167°	Dry air at 0.7 l./hour	0 48	0.028	0.124	41[a]
400°	Dry air at 0.7 l./hour	0.40	0.021*	0.054*	1.3[a]
167°	Nitrogen at 4.8 l./hour	0.32	0.020	0.050	0.53[a]
400°	Nitrogen at 4.8 l./hour	0.43	0.021*	0.060*	0.20[a]

[a] Solubility values taken from previo

* Values extrapolated from the wear scar diameter versus pyridine soluble and insoluble metals relationship (Fig 68 and 69)

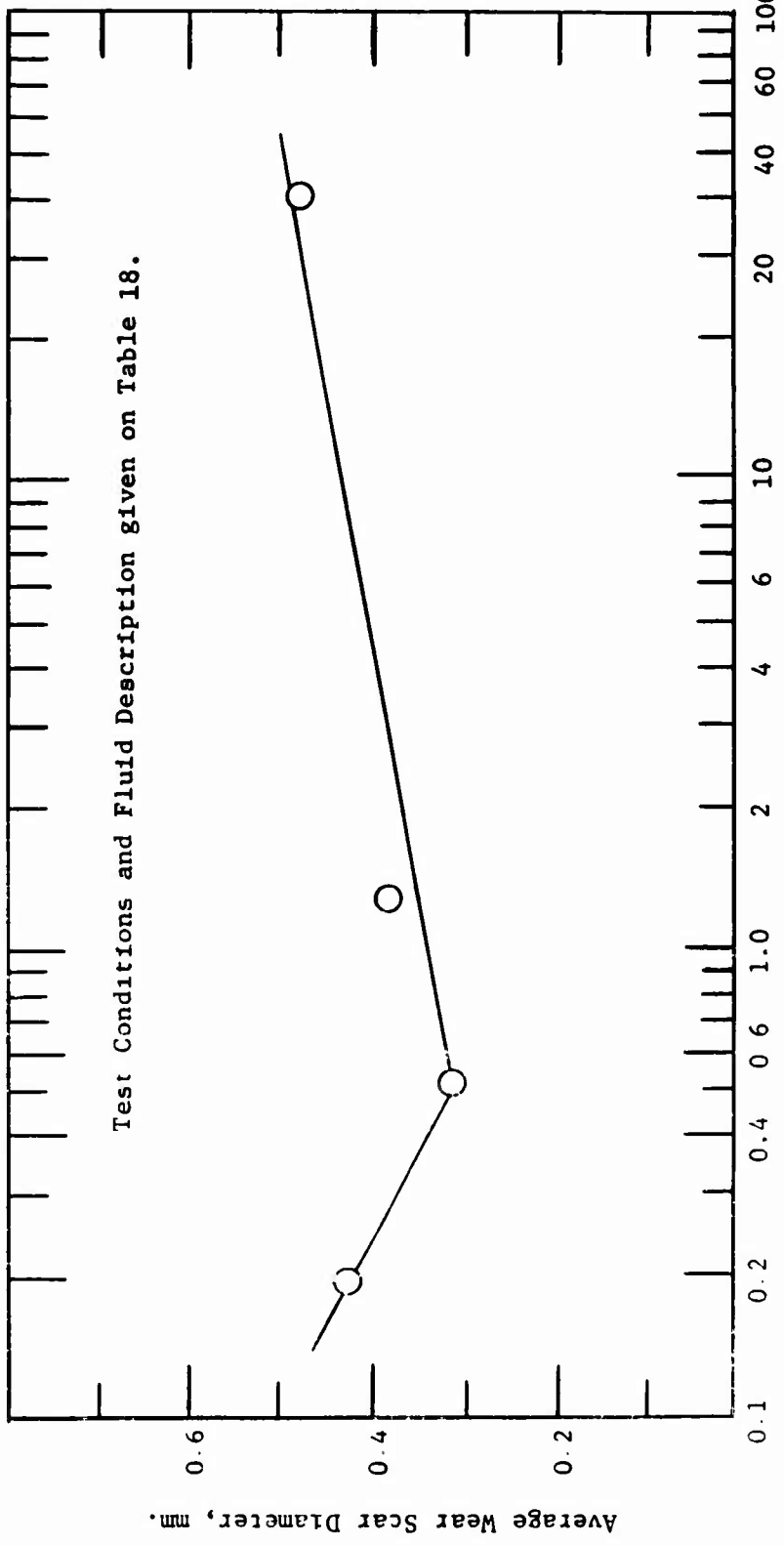

Figure 70. EFFECT OF DISSOLVED OXYGEN ON THE WEAR BEHAVIOR OF A SUPER-REFINED MINERAL OIL (MLO 7789)

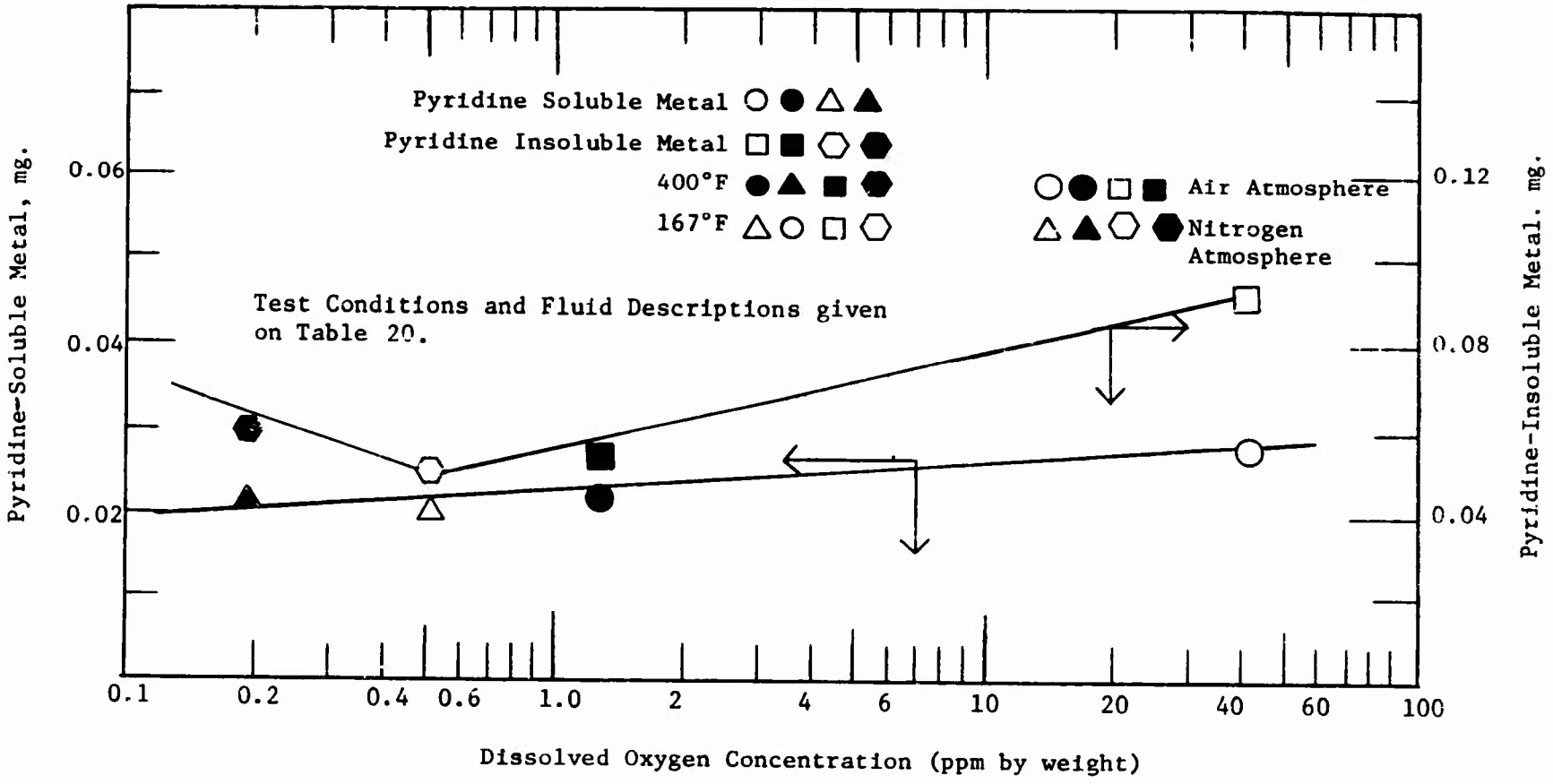

Figure 71. EFFECT OF DISSOLVED OXYGEN ON THE WEAR BEHAVIOR OF A SUPER-REFINED MINERAL OIL AS FOUND BY DEBRIS ANALYSIS

Table 20

EFFECT OF DISSOLVED OXYGEN ON THE
WEAR BEHAVIOR OF AN ESTER

Four-Ball Wear Test Conditions Include: Test Speed = 600 r.p.m.; Load = 10 kg.; Fluid Charged = 20 ml.; Test Time = 1 hr.; and Bearings = 52-100 Steel, PRL Batch No. 14

Test Fluid: Di-2-Ethylhexyl Sebacate (MLO 7710)

Test Temperature, °F	Test Atmosphere	Average Wear Scar Diameter, mm.	Dissolved Oxygen Concentration, µl/ml	Dissolved Oxygen Concentration, ppm (by weight)
167°	Dry Air at 0.7 l./hour	0.55	33[a]	53.0
400°	Dry Air at 0.7 l./hour	0.70	1.0[a]	1.80
167°	*Nitrogen at 4.8 l./hour	0.46	0.3[a]	0.48
400°	*Nitrogen at 4.8 l./hour	0.68	0.2[a]	0.36

[a]Solubility values taken from previous reports.

*Nitrogen tank contains 0.5 volume percent oxygen.

Table 21

EFFECT OF DISSOLVED OXYGEN ON THE WEAR BEHAVIOR OF AN ESTER AS FOUND BY DEBRIS ANALYSIS

Four-Ball Wear Test Conditions Include: Test Speed = 600 r.p.m., Load = 10 kg.; Fluid Charged = 20 ml; Test Time = 1 hr.; and Bearings = 52-100 Steel, PRL Batch No. 14

Test Fluid: Di-2- Ethylhexyl Sebacate (MLO 7710)

Test Temperature, °F	Test Atmosphere	Average Wear Scar Diameter, mm.	Pyridine Soluble Metal, mg.	Pyridine Insoluble Metal, mg.	Dissolved Oxygen Concentration, µl/ml	Dissolved Oxygen Concentration, ppm (by weight)
167°	Dry Air at 0.7 l./hour	0.55	0.021	0.092	33[a]	41[a]
400°	Dry Air at 0.7 l./hour	0.70	0.069*	0.125*	1.0[a]	1.8
167°	Nitrogen at 4.8 l./hour	0.46	0.013	0.063	0.3[a]	0.48
400°	Nitrogen at 4.8 l./hour	0.68	0.056*	0.110*	0.2[a]	0.36

[a]Solubility values taken from previous reports.

*Values extrapolated from the wear scar diameter versus pyridine-soluble and pyridine-insoluble metals relationship (Fig 68 and 69).

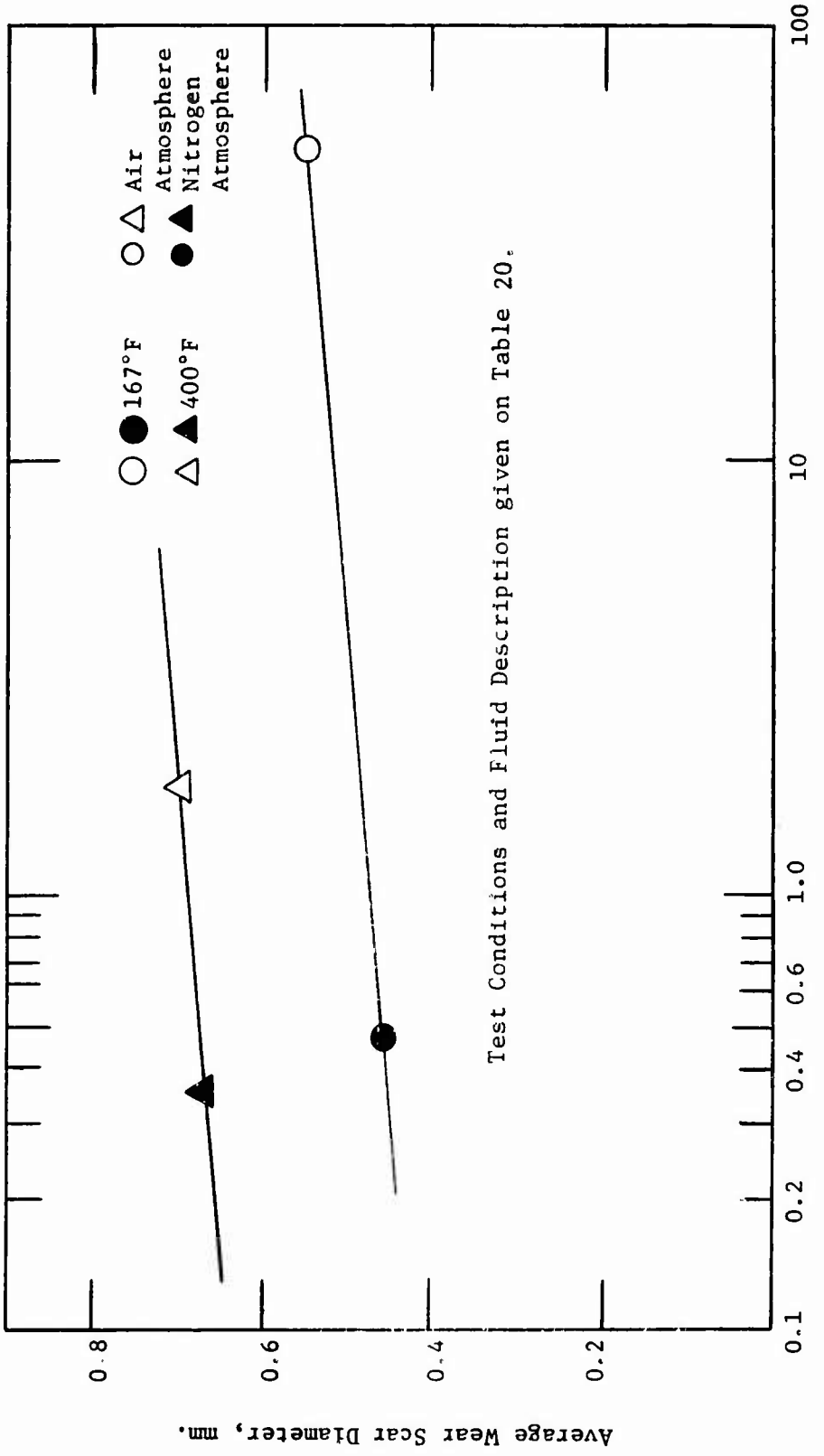

Figure 72 EFFECT OF DISSOLVED OXYGEN ON THE WEAR BEHAVIOR OF AN ESTER (MLO 7710)

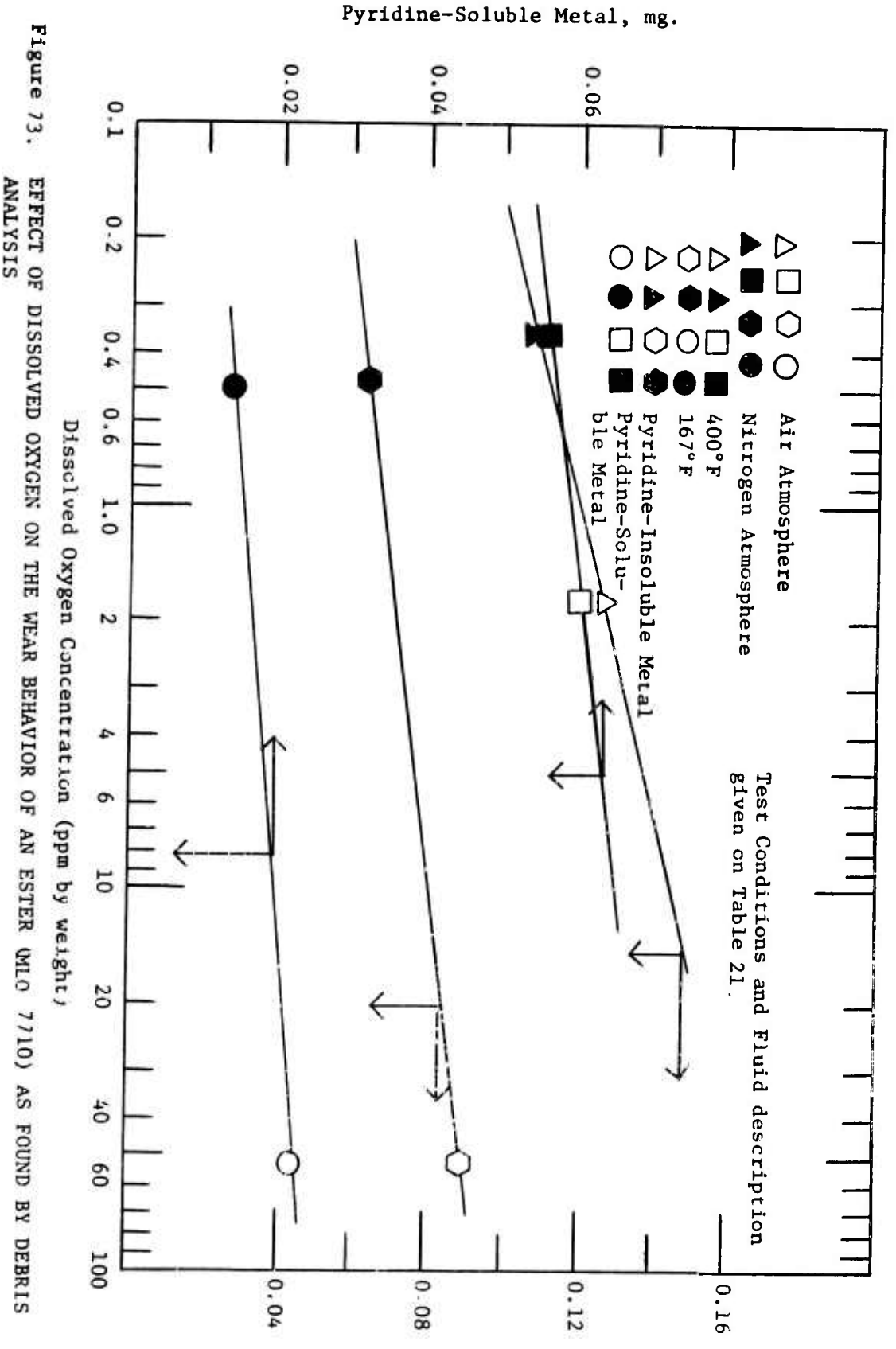

Figure 73. EFFECT OF DISSOLVED OXYGEN ON THE WEAR BEHAVIOR OF AN ESTER (MIL 7110) AS FOUND BY DEBRIS ANALYSIS

Table 22

WEAR PERFORMANCE OF THE ESTER INHIBITED WITH PHENOTHIAZINE AND A COMBINATION OF PHENOTHIAZINE AND TRICRESYL PHOSPHATE

Four-Ball Wear Test Conditions Include: Test Speed = 600 r.p.m.; Load: At Indicated; Test Temp. = 167°F.; Test Time = 1 hr.; Fluid Charged = 20 ml.; and Bearings = 52-100 Steel, PRL Batch No. 14

Test Fluids: Di-2-Ethylhexyl Sebacate (MLO 7710) + 0.5 Weight Percent Phenothiazine (PRL 3207)
PRL 3207 + 5.0 Weight Percent Tricresyl Phosphate (PRL 3462)

Test Fluid	Load, kg.	Average Wear Scar Diameter, min.
MLO 7710	1	--
	10	0.59
	20	--
	40	0.74
PRL 3207	1	0.25
	10	0.47
	20	0.60
	40	0.83
PRL 3462	1	0.13
	10	0.26
	20	0.28
	40	0.38

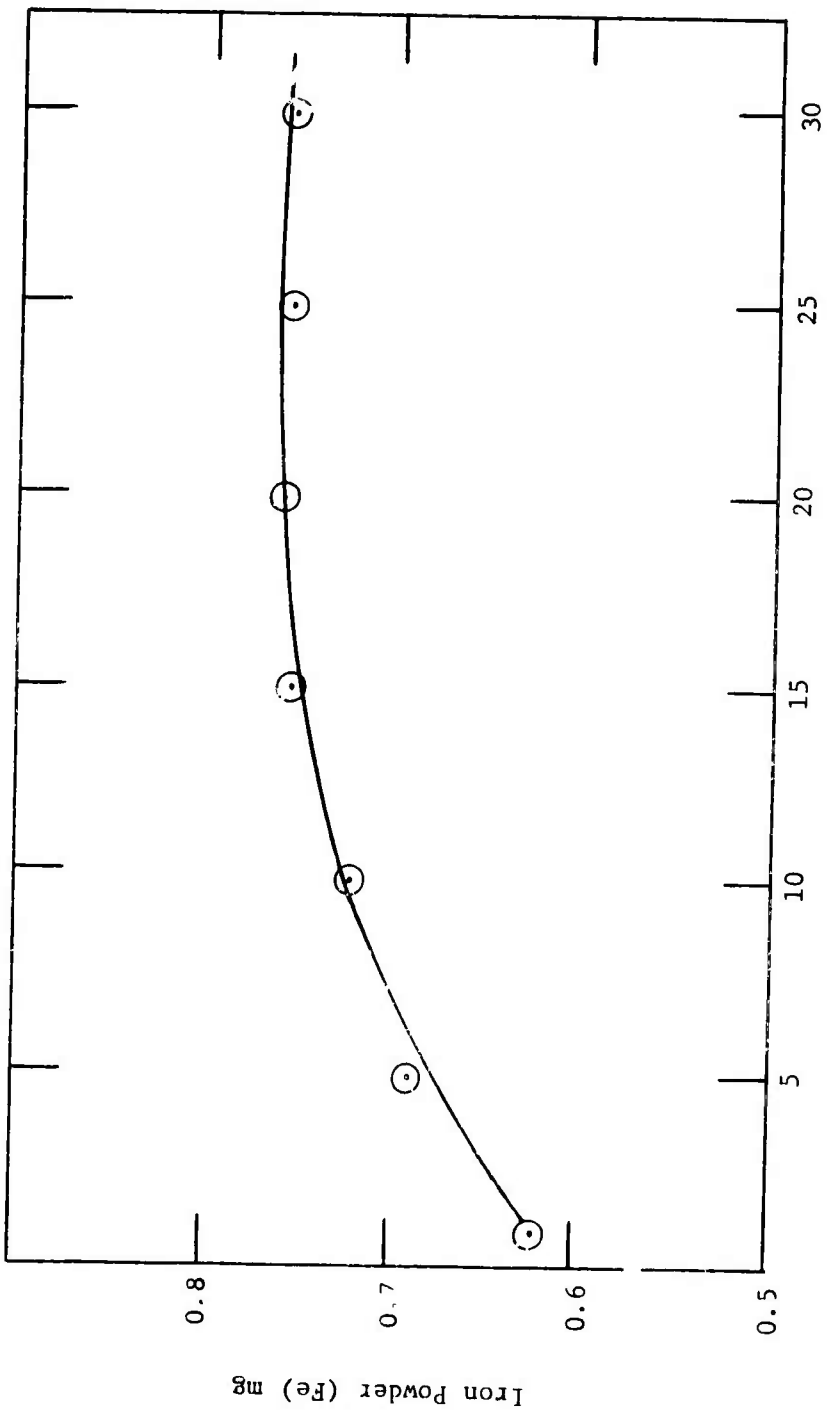

Figure 74 - RATE OF DISSOLUTION OF IRON POWDER (Fe) IN ACRIDINE-INHIBITED HYDROCHLORIC ACID SOLUTION

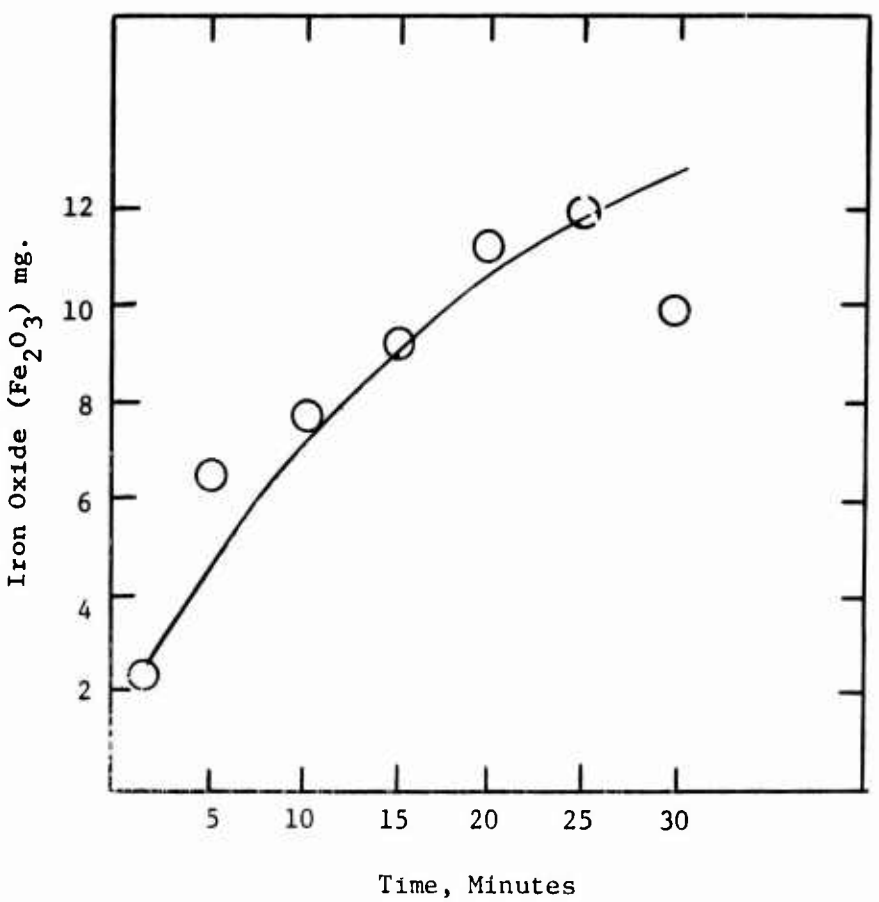

Figure 75. RATE OF DISSOLUTION OF IRON OXIDE (Fe_2O_3) IN ACRIDINE-INHIBITED HYDROCHLORIC ACID SOLUTION

Table 23

EXTRACTION OF THE METAL OXIDES FROM WEAR DEBRIS BY AN ACRIDINE-INHIBITED HYDROCHLORIC ACID SOLUTION

Four-Ball Wear Test Conditions Include: Test Speed = 600 r.p.m.; Load = 40 kg.; Test Temp. = 167°F; Fluid Charged = 20 ml.; Test Time = 1 hr.; and Bearings = 52-100 Steel, PRL Batch No. 15.

Test Fluid: Super-refined Paraffinic Mineral Oil (MLO 7789)

Average Wear Scar Diameter, mm.	Test Atmosphere	Pyridine Soluble Metal, mg.	Oil Soluble Metal, mg.	Pyridine Insoluble Metal, mg.		Total Metal Loss, mg.		Total Debris, mg. (A)	Organic Debris, mg. (A-B)
				Fe-Oxide	Fe-Metal	by bearing weight difference (B)	by adding all soluble and insoluble metals		
0.78	Dry Air at 0.7 l./hour	0.0752	BDL*	0.1287	0.0167	0.22	0.2206	1.50	1.28
0.71	Nitrogen at 4.8 l./hour	0.0427	BDL*	0.948	0.0292	0.18	0.1667	1.05	0.87
0.73	Argon at 4.8 l./hour	0.0198	BDL*	0.0806	0.0450	0.15	0.1454	0.64	0.49

*Below limit of detection.

Table 24

WEAR DEBRIS FORMED BY UNINHIBITED FLUIDS IN SEQUENTIAL TESTS

Four-Ball Wear Test Conditions Include: Test Speed = 600 r.p.m.; Load = 40 kg.; Test Temp. = 167°F.; Fluid Charged = 20 ml.; Test Time = 1 hr.; and Bearings = 52-100 Steel, PRL Batch No. 15.

Test Fluids: Di-2-Ethylhexyl Sebacate (MLO 7710)
Super-refined Paraffinic Mineral Oil (MLO 7789)
Super-refined Naphthenic Mineral Oil (MLO 7625)

Test Fluid	Average Wear Scar Diameter, mm.	Test Atmosphere	Pyridine Soluble Metal, mg.	Oil Soluble Metal, mg.	Pyridine Insoluble Metal, mg.	Total Metal Loss, Mg. (B)	Total Debris, mg. (A)	Organic Debris, mg. (A-B)
MLO 7710	0.99	Dry Air at 0.7 l./hour	0.0029	0.0023	0.1585	0.1637	3.24	3.08
MLO 7789	0.84	Dry Air at 0.7 l./hour	0.0130	0.0022	0.1655	0.1807	1.17	0.99
MLO 7625	0.58	Dry Air at 0.7 l./hour	0.0168	0.0029	0.0350	0.0539	3.40	3.35
MLO 7710	0.93	Nitrogen at 4.8 l./hour	0.0030	0.0089	0.1448	0.1567	3.33	3.17
MLO 7789	0.84	Nitrogen at 4.8 l./hour	0.0119	0.0011	0.0885	0.1015	1.41	1.31
MLO 7625	0.53	Nitrogen at 4.8 l./hour	0.0051	0.0005	0.0295	0.0351	2.94	2.90

Table 25

COMPARISON OF DEBRIS ANALYSIS FOR THE UNINHIBITED FLUIDS
IN THE ORIGINAL AND SEQUENTIAL TESTS

Four-Ball Wear Test Conditions Include: Test Speed = 600 r.p.m.; Load = 40 kg.; Test Temp. = 167°F.; Fluid Charged = 20 ml.; and Bearings = 52-100 Steel, PRL Batch No. 15.

Test Fluids: Super-refined Paraffinic Mineral Oil (MLO 7789)
Super-refined Naphthenic Mineral Oil (MLO 7625)
Di-2-Ethylhexyl Sebacate (MLO 7710)

Test Fluid	Test Atmosphere	Average Wear Scar Diameter, mm.		Pyridine Soluble Metal, mg.		Pyridine Insoluble Metal, mg.		Oil Soluble Metal, mg.	
		First Hour Original	Second Hour in Sequence	First Hour Original	Second Hour in Sequence	First Hour Original	Second Hour in Sequence	First Hour Original	Second Hour in Sequence
MLO 7710	Dry Air at 0.7 l./hour	0.74	0.99	0.0782	0.0029	0.1114	0.1585	BDL*	0.0023
MLO 7789	Dry Air at 0.7 l./hour	0.79	0.84	0.0566	0.0130	0.1400	0.1655	BDL*	0.0022
MLO 7625	Dry Air at 0.7 l./hour	0.53	0.58	0.0658	0.0168	0.1075	0.0350	BDL*	0.0029
MLO 7710	Nitrogen at 4.8 l./hour	0.70	0.93	0.0740	0.0030	0.1166	0.1448	BDL*	0.0089
MLO 7789	Nitrogen at 4.8 l./hour	0.61	0.84	0.0300	0.0119	0.0998	0.0885	BDL*	0.0011
MLO 7625	Nitrogen at 4.8 l./hour	0.47	0.53	0.0633	0.0051	0.0921	0.0295	BDL*	0.0005

*Below limit of detection.

Table 26

WEAR DEBRIS FORMED BY INHIBITED FLUIDS IN THE SEQUENTIAL TESTS

Four-Ball Wear Test Conditions Include: Test Speed = 600 r.p.m.; Load = 40 kg.; Test Temp. = 167°F.; Test Time = 1 hr.; Fluid Charged = 20 ml.; Test Atmosphere = Dry Air at 0.7 liter/hour; and Bearings = 52-100 Steel, PRL Batch No. 15.

Test Fluids: Di-2-Ethylhexyl Sebacate (MLO 7710) + 0.5 Weight Percent Phenothiazine
Super-refined Paraffinic Mineral Oil (MLO 7789) + 1.0 Weight Percent Parabar 441
Super-refined Naphthenic Mineral Oil (MLO 7625) + 1.0 Weight Percent Ethyl 702

Test Fluid	Average Wear Scar Diameter, mm.	Pyridine Soluble Metal, mg.	Oil Soluble Metal, mg.	Pyridine Insoluble Metal, mg.	Total Metal Loss, mg. (B)	Total Debris, mg. (A)	Organic Debris, mg. (A-B)
MLO 7710 + 0.5 wt. % Phenothiazine	1.09	0.0049	0.0054	0.1674	0.1777	1.31	1.13
MLO 7789 + 1.0 wt. % Parabar 441	0.76	0.0209	0.0052	0.1063	0.1324	1.12	0.99
MLO 7625 + 1.0 wt. % Ethyl 702	0.57	0.0049	BDL*	0.0580	0.0629	1.21	1.13

*Below limit of detection.

Table 27

COMPARISON OF DEBRIS ANALYSIS FOR THE INHIBITED FLUIDS
IN THE ORIGINAL AND SEQUENTIAL TESTS

Four-Ball Wear Test Conditions Include: Test Speed = 600 r.p.m.; Load = 40 kg.; Test Temp. = 167°F.; Fluid Charged = 20 ml.; Test Atmosphere = Dry Air at 0.7 liter/hour and Bearings = 52-100 Steel, PRL Batch No. 15.

Test Fluids: Di-2-Ethylhexyl Sebacate (MLO 7710) + 0.5 Weight Percent Phenothiazine
Super-refined Paraffinic Mineral Oil (MLO 7789) + 1.0 Weight Percent Parabar 441
Super-refined Naphthenic Mineral Oil (MLO 7625) + 1.0 Weight Percent Ethyl 702

Test Fluid	Average Wear Scar Diameter, mm.		Pyridine Soluble Metal, mg.		Pyridine Insoluble Metal, mg.		Oil Soluble Metal, mg.	
	First Hour Original	Second Hour in Sequence	First Hour Original	Second Hour in Sequence	First Hour Original	Second Hour in Sequence	First Hour Original	Second Hour in Sequence
MLO 7710 + 0.5 wt. % Phenothiazine	0.83	1.09	0.0073	0.0049	0.1493	0.1674	0.0040	0.0054
MLO 7789 + 1.0 wt. % Parabar 441	0.70	0.76	0.0346	0.0209	0.1117	0.1063	0.0031	0.0052
MLO 7625 + 1.0 wt. % Ethyl 702	0.54	0.57	0.0066	0.0049	0.0765	0.0580	BDL*	BDL*

*Below limit of detection.

Table 28

DETERMINATION OF THE OIL-SOLUBLE METAL FORMED BY THE UNINHIBITED FLUIDS IN THE ORIGINAL AND SEQUENTIAL TESTS

Four-Ball Wear Test Conditions Include: Test Speed = 600 r.p.m.; Load = 40 kg.; Test Temp. = 167°F.; Fluid Charged = 20 ml ; Test Time: Original = 1 hr.; Sequential = 1 hr.; and Bearings = 52-100 Batch No. 15

Test Fluids: Di-2-Ethylhexyl Sebacate (MLO 7710)
Super-refined Paraffinic Mineral Oil (MLO 7789)
Super-refined Naphthenic Mineral Oil (MLO 7625)

Test Fluid	Test Atmosphere	Average Wear Scar Diameter, mm.		Oil Soluble Metal, mg.	
		First Hour Original	Second Hour in Sequence	First Hour Original	Second Hour in Sequence
MLO 7710	Dry Air at 0.7 l./hour	0.69	0.87	BDL*	0.0023
MLO 7789	Dry Air at 0.7 l./hour	0.61	0.78	BDL*	0.0029
MLO 7625	Dry Air at 0.7 l./hour	0.49	0.52	BDL*	0.0028
MLO 7710	Nitrogen at 4.8 l./hour	0.64	0.89	BDL*	0.0029
MLO 7789	Nitrogen at 4.8 l./hour	0.71	0.81	BDL*	0.0028
MLO 7625	Nitrogen at 4.8 l./hour	0.48	0.58	BDL*	0.0020

*Below limit of detection.

Table 29

ABLATION OF THE OIL-SOLUBLE METALS FORMED BY THE INHIBITED FLUIDS IN THE ORIGINAL AND SEQUENTIAL TESTS

Four-Ball Wear Test Conditions Include: Test Speed = 600 r.p.m.; Load = 40 kg., Test Temp. = 167°F.; Fluid Charged = 20 ml.; Test Time: Original = 1 hr.; Sequential = 1 hr.; and Bearings = 52-100 Steel, [illegible] Batch No. 15

Test Fluids: Di-2-Ethylhexyl Sebacate (MLO 7710) + 0.5 Weight Percent Phenothiazine
Super-refined Paraffinic Mineral Oil (MLO 7789) + 1.0 Weight Percent Parabar 441
Super-refined Naphthenic Mineral Oil (MLO 7625) + 1.0 Weight Percent Ethyl 702

Test Fluid	Test Atmosphere	Average Wear Scar Diameter, mm.		Oil Soluble Metal, mg.	
		First Hour Original	Second Hour in Sequence	First Hour Original	Second Hour in Sequence
MLO 7710 + 0.5 wt % Phenothiazine	Dry Air at 0.7 l./hour	0.83	1.09	0.0040	0.0054
MLO 7789 + 1.0 wt. % Parabar 441	Dry Air at 0.7 l./hour	0.70	0.76	0.0031	0.0052
MLO 7625 + 1.0 wt. % Ethyl 702	Dry Air at 0.7 l./hour	0.55	0.57	BDL*	BDL*

*Below limit of detection.

Table 30

WEAR DEBRIS FORMED BY UNINHIBITED FLUIDS IN CYCLED TESTS

Procedure: Four-Ball Wear Tester turned on for 15 sec. and off for 15 sec. for a Total of 2 Hours

Four Ball Wear Test Conditions Include. Test Speed = 600 r.p.m.; Load = 40 kg.; Test Time = 2 hr.; Test Atmosphere = Dry Air at 0.7 liter/hour; Fluid Charged = 20 ml.; and Bearings = 52-100 Steel, PRL Batch No. 15

Test Fluids: Di-2-Ethylhexyl Sebacate (MLO 7710)
Super-refined Paraffinic Mineral Oil (MLO 7789)
Super-refined Naphthenic Mineral Oil (MLO 7625)

Test Fluid	Average Wear Scar Diameter mm.	Pyridine Soluble Metal, mg.	Oil Soluble Metal, mg.	Pyridine Insoluble Metal, mg.	Total Metal Loss, mg. by bearing weight difference (B)	Total Metal Loss, mg. by adding all soluble and insoluble metals	Total Debris, mg. (A)	Organic Debris, mg. (A-B)
MLO 7710	0.73	0.0117	BDL*	0.1868	0.21	0.1985	1.09	0.88
MLO 7789	0.73	0.0146	BDL*	0.1687	0.22	0.1833	1.26	1.04
MLO 7625	0.46	0.0133	BDL*	0.0980	0.11	0.1113	0.52	0.41

*Below limit of detection.

Table 31

PARTICLE SIZE OF THE WEAR DEBRIS

Particle Size Determined by Microscopic Examination of Product from Four-Ball Wear Tests

Four-Ball Wear Test Conditions Include: Test Speed = 600 r.p.m.; Load = 40 kg ; Test Temp. = 167°F.; Fluid Charged = 20 ml.; Test Atmosphere = Dry Air at 0.7 liter/hour; and Bearings = 52-100 Steel, PRL Batch No. 15

Test Fluids: Di-2-Ethylhexyl Sebacate (MLO 7710)
Super-refined Paraffinic Mineral Oil (MLO 7789)
Super-refined Naphthenic Mineral Oil (MLO 7625)

Test Fluid	First Hour Original Test		Second Hour in Sequence Test	
	Mean Length of Particle, micron	Mean Width of Particle, micron	Mean Length of Particle, micron	Mean Width of Particle, micron
MLO 7710	22.4	16.8	22.0	14.4
MLO 7789	25.9	16.2	20.0	11.5
MLO 7625	22.6	10.5	18.2	10.6

Table 32

SURFACE AREA OF THE WEAR DEBRIS

Surface Area Determined by Microscopic Examination of Product from Four-Ball Wear Tests

Four-Ball Wear Test Conditions Include: Test Speed = 600 r.p.m.; Load = 40 kg.; Test Temp. = 167°F.; Fluid Charged = 20 ml.; Test Atmosphere = Dry Air at 0.7 liter/hour and Bearings = 52-100 Steel, PRL Batch No. 15

Test Fluids: Di-2-Ethylhexyl Sebacate (MLO 7710)
Super-refined Paraffinic Mineral Oil (MLO 7789)
Super-refined Naphthenic Mineral Oil (MLO 7625)

Test Fluid	First Hour Original Test				Second Hour in Sequence Test			
	Average Wear Scar Diameter, mm.	Mean Length of Particle, micron	Mean Width of Particle, micron	Area of Particle $(micron)^2$	Average Wear Scar Diameter, mm.	Mean Length of Particle, micron	Mean Width of Particle, micron	Area of Particle $(micron)^2$
MLO 7710	0.79	24.4	16.8	409.9	0.96	22.0	14.4	316.8
MLO 7789	0.79	25.9	16.2	419.5	0.81	20.0	11.5	230.0
MLO 7625	0.55	22.6	10.5	238.0	0.61	18.2	10.6	192.9

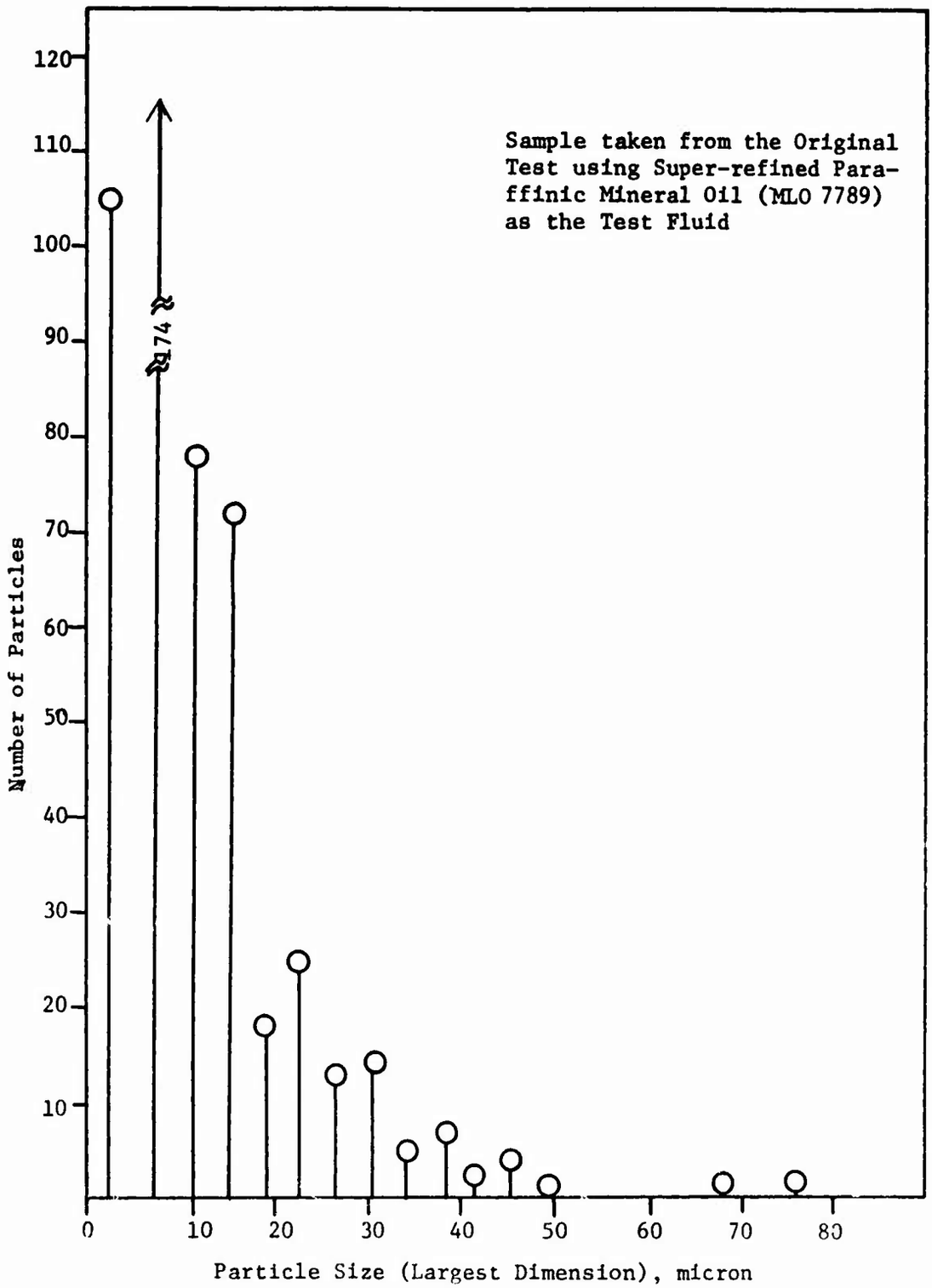

Figure 76. PARTICLE SIZE DISTRIBUTION OF THE WEAR DEBRIS

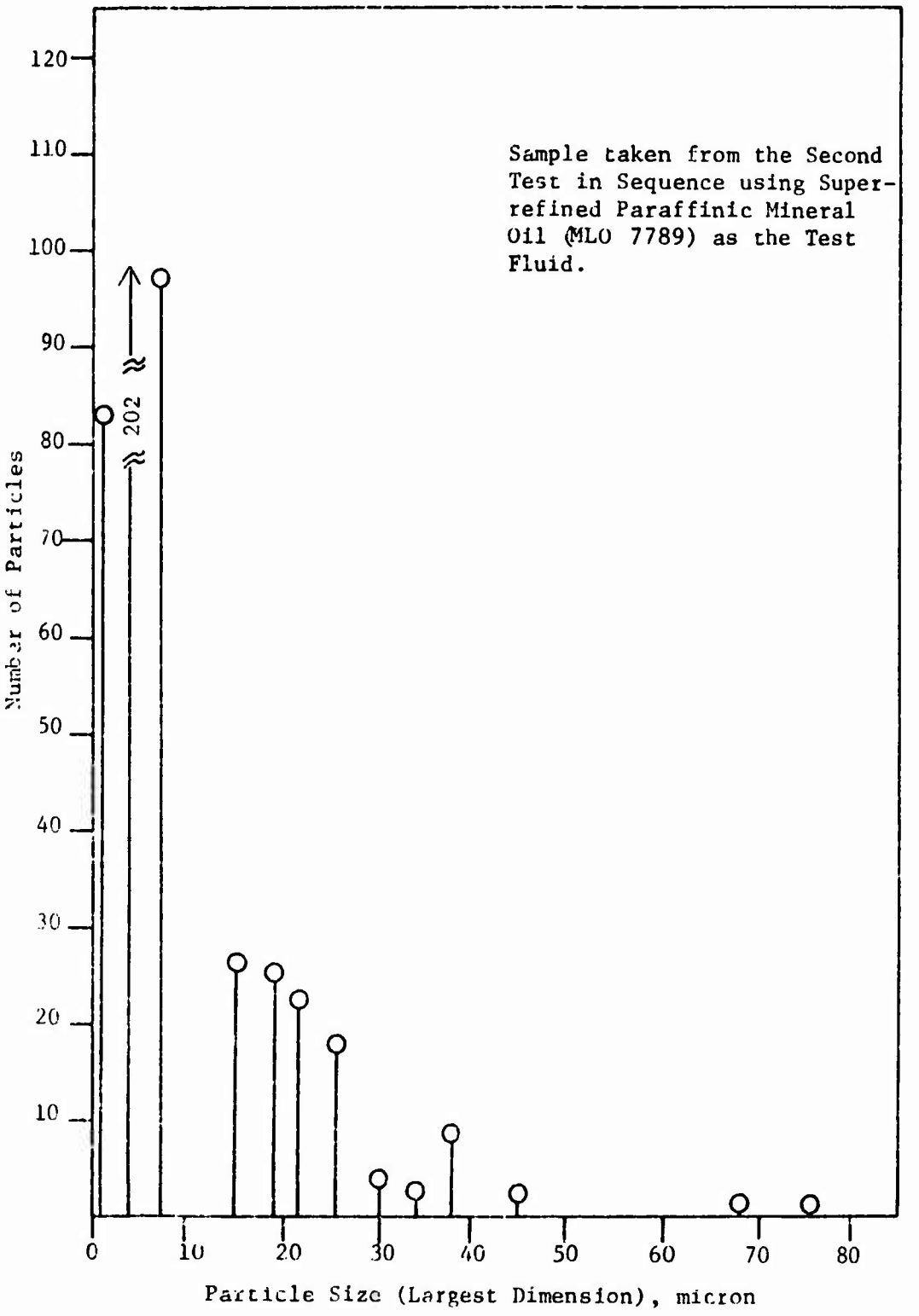

Figure 77. PARTICLE SIZE DISTRIBUTION OF THE WEAR DEBIS

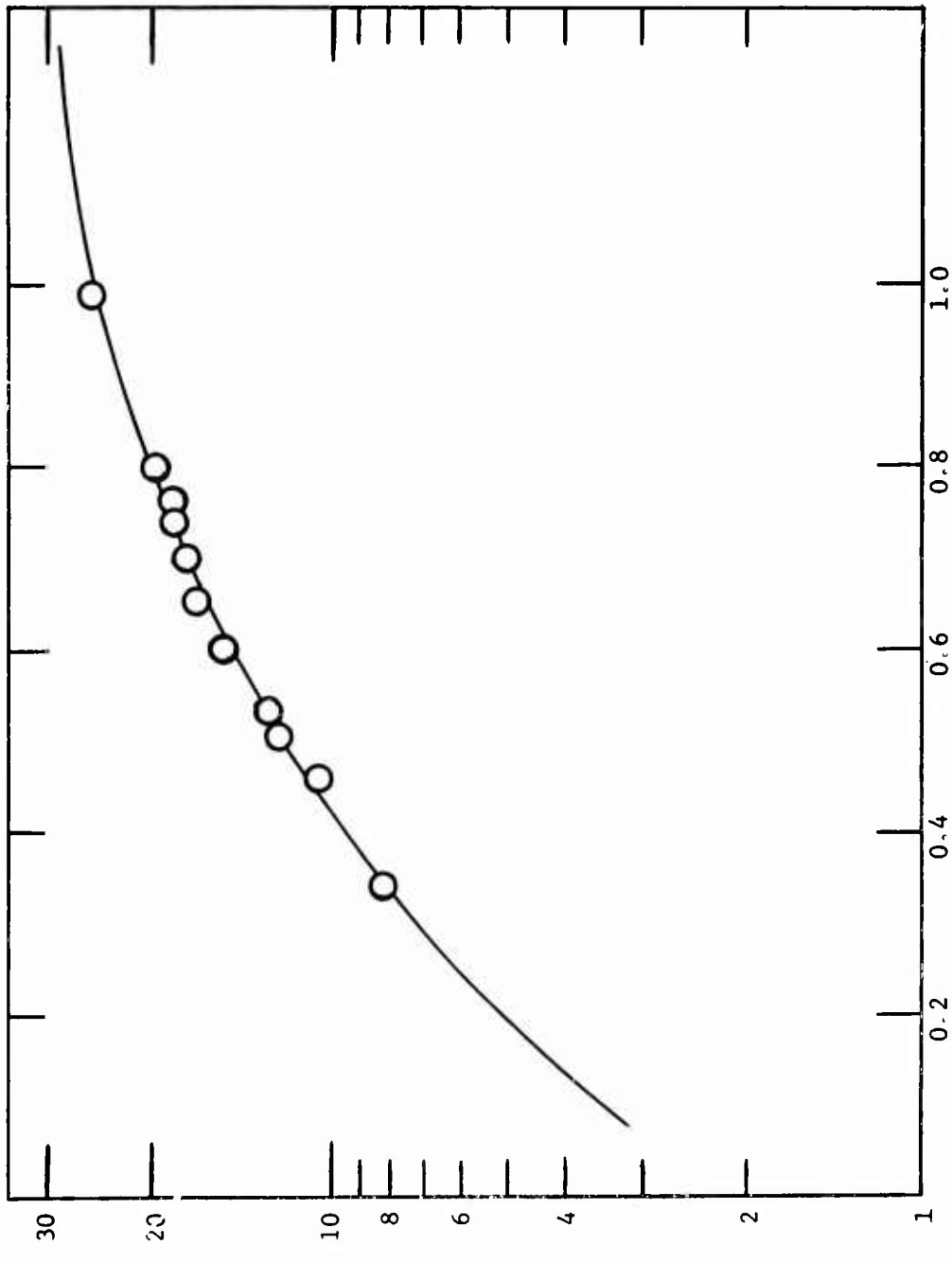

Figure 78. RELATIONSHIP OF THE BALL CONTACT AREA TO AVERAGE WEAR SCAR DIAMETER

Table 33

WEAR RATE STUDY WITH THE SHELL FOUR-BALL WEAR TESTER WITH AN ESTER

Four-Ball Wear Test Conditions Include: Test Speed = 600 r.p.m.; Load = 40 kg.; Test Temp. = 167°F.; Test Atmosphere = Dry Air at 0.7 liter/hour; Fluid Charged = 20 ml.; and Bearings = 52-100 Steel, PRL Batch No. 15

Test Fluid: Di-2-Ethylhexyl Sebacate (MLO 7710)

Test Time, Minutes	Average Wear Scar Diameter, mm.	Pyridine Soluble Metal, mg.	Oil Soluble Metal, mg.	Pyridine Insoluble Metal, mg.	Total Metal Loss, mg. by bearing weight difference (B)	Total Metal Loss, mg. by adding all soluble and insoluble metals	Total Debris, mg. (A)	Organic Debris mg. (A-B)
10	0.50	0.0070	0.0008	0.0117	0.06	0.0195	1.28	1.22
30	0.65	0.0317	0.0003	0.0901	0.12	0.1221	1.39	1.27
60	0.75	0.0708	BDL*	0.1240	0.24	0.1848	2.29	2.05
90	0.79	0.0720	BDL*	0.1740	0.21	0.2360	2.43	2.22
120	0.99	0.0748	BDL*	0.2441	0.35	0.3089	3.21	2.86
150	0.99	0.0759	BDL*	0.2385	0.34	0.3044	3.37	3.03

*Below limit of detection.

Table 34

WEAR RATE STUDY WITH THE SHELL FOUR-BALL WEAR TESTER WITH SUPER-REFINED MINERAL OILS

Four-Ball Wear Test Conditions Include: Test Speed = 600 r.p.m.; Load = 40 kg.; Test Temp. = 167°F.; Test Atmosphere = Dry Air at 0.7 liter/hour; Fluid Charged = 20 ml.; and Bearings = 52-100 Steel, PRL Batch No. 15

Test Fluids: Super-refined Paraffinic Mineral Oil (MLO 7789)
Super-refined Naphthenic Mineral Oil (MLO 7625)

Test Fluid	Test Time, Minutes	Average Wear Scar Diameter, mm.	Pyridine Soluble Metal, mg.	Pyridine Insoluble Metal, mg.	Oil Soluble Metal, mg.
MLO 7789	10	0.44	0.0241	0.0603	0.0007
	30	0.58	0.0485	0.0956	BDL*
	60	0.79	0.0566	0.1400	BDL*
	120	0.84	0.0660	0.2136	BDL*
MLO 7625	10	0.28	0.0232	0.0442	BDL*
	30	0.44	0.0465	0.0781	BDL*
	60	0.53	0.0658	0.1075	BDL*
	120	0.60	0.0664	0.1759	BDL*

*Below limit of detection.

Table 35

EFFECT OF LOAD ON THE WEAR BEHAVIOR OF A SUPER-REFINED MINERAL OIL AS FOUND BY DEBRIS ANALYSIS

Four-Ball Wear Test Conditions Include: Test Speed = 600 r.p.m.; Test Temp. = 167°F.; Test Atmosphere = Dry Air at 0.7 liter/hour.; Test Time = 1 hr.; Fluid Charged = 20 ml ; and Bearings = 52-100 Steel, PRL Batch No. 15

Test Fluid: Super-refined Paraffinic Mineral Oil (MIO 7789)

Test Load, kg.	Average Wear Scar Diameter, mm.	Pyridine Soluble Metal, mg.	Pyridine Insoluble Metal, mg.
4	0.30	0.0034	0.0498
10	0.47	0.0280	0.0960
20	0.60	0.048*	0.098*
40	0.79	0.0566	0.1400

*This is an estimated value from the wear scar diameter versus pyridine soluble and insoluble metal relationships (Figures 68 and 69).

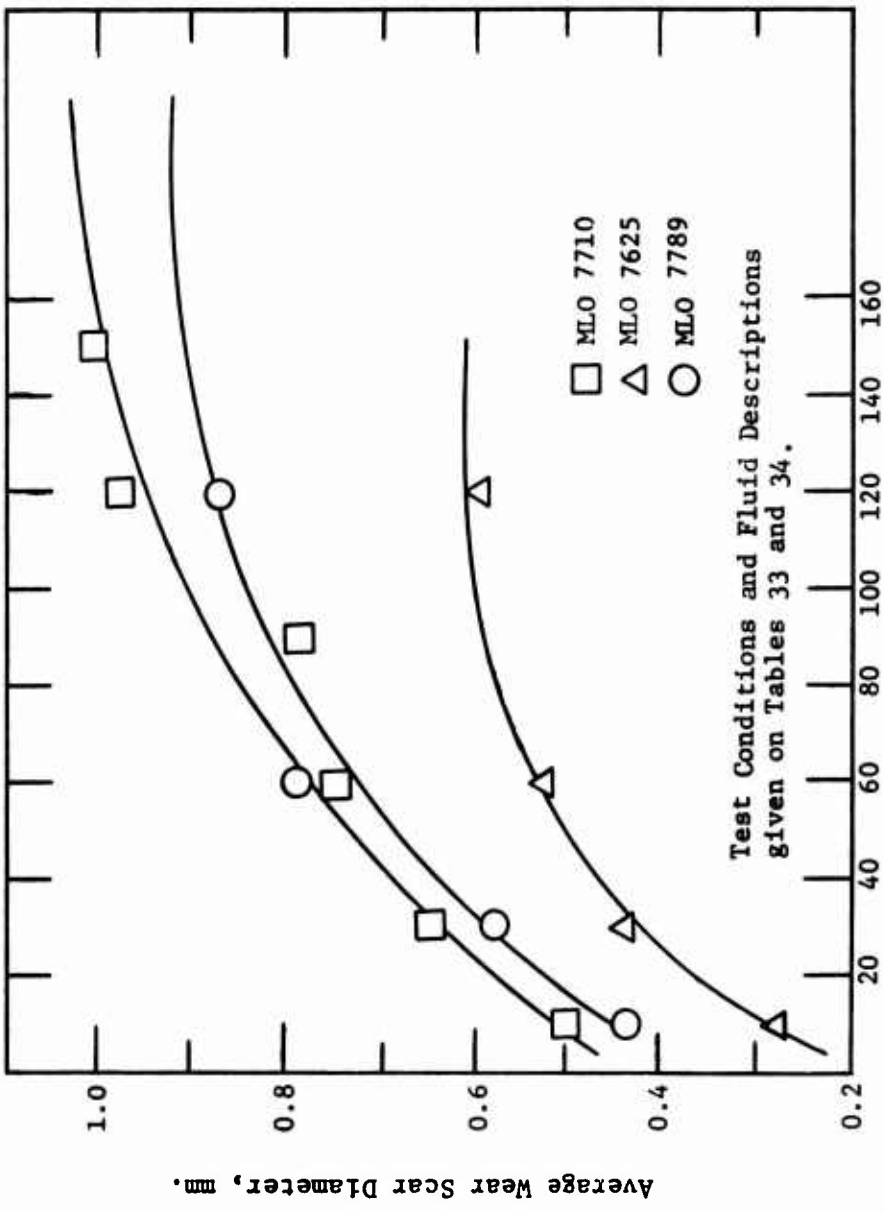

Figure 79. AVERAGE WEAR SCAR DIAMETER AS A FUNCTION OF TIME

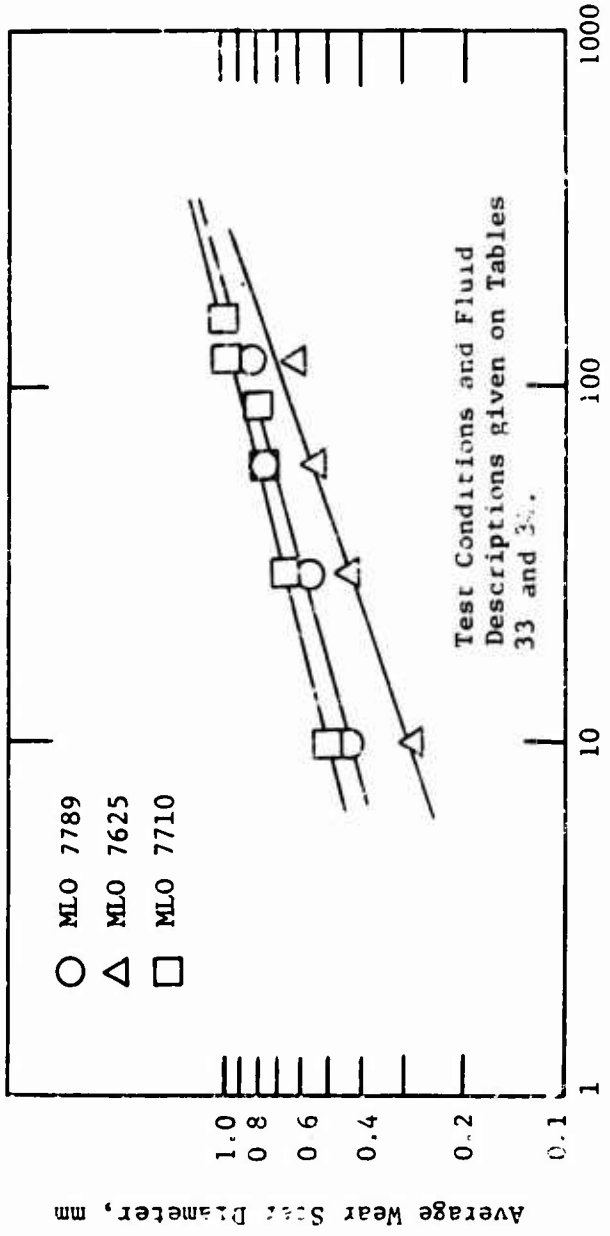

Figure 80. AVERAGE WEAR SCAR DIAMETER AS A FUNCTION OF TIME

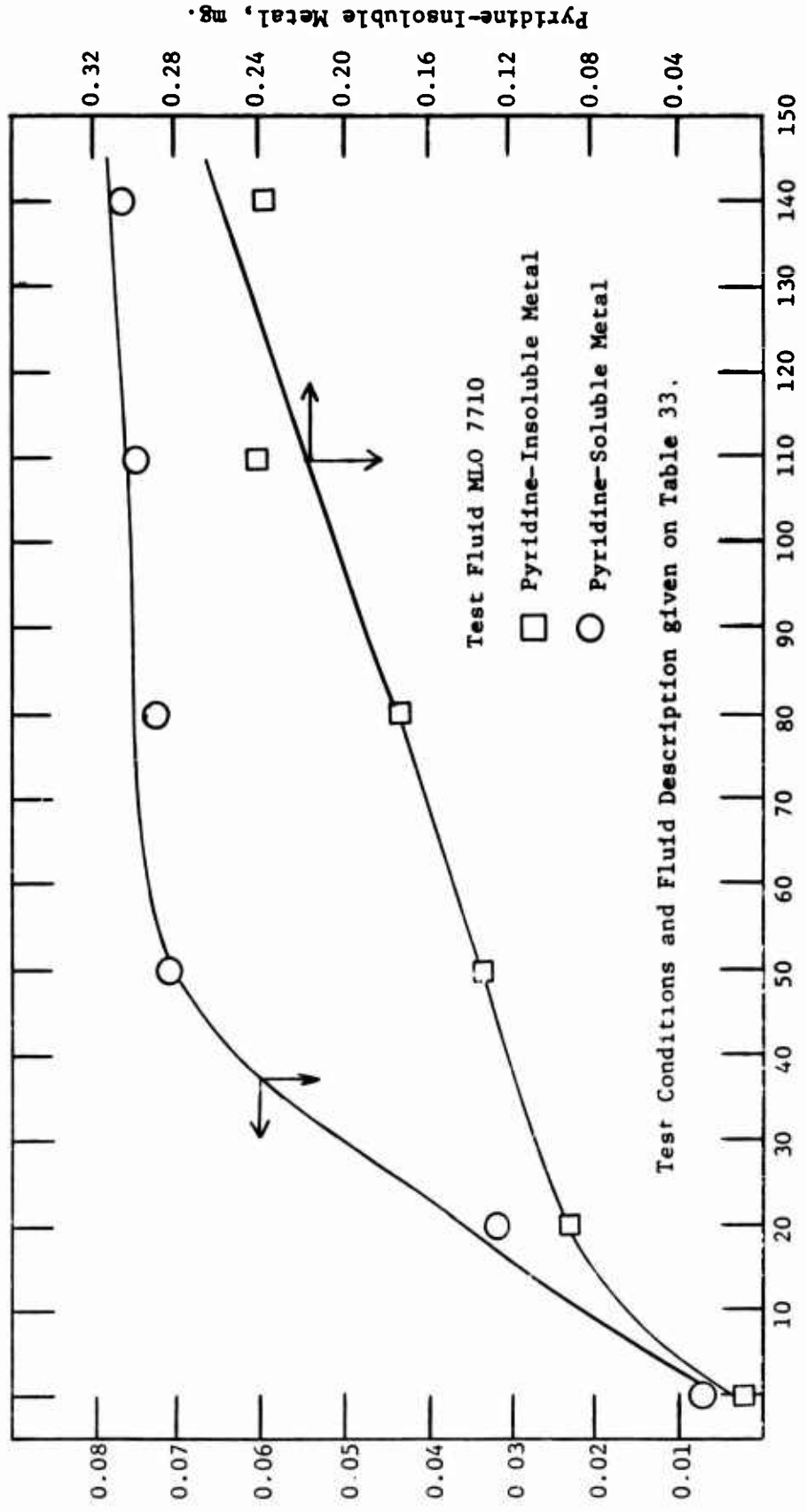

Figure 81. RATE OF FORMATION OF PYRIDINE-SOLUBLE AND INSOLUBLE METAL WITH AN ESTER

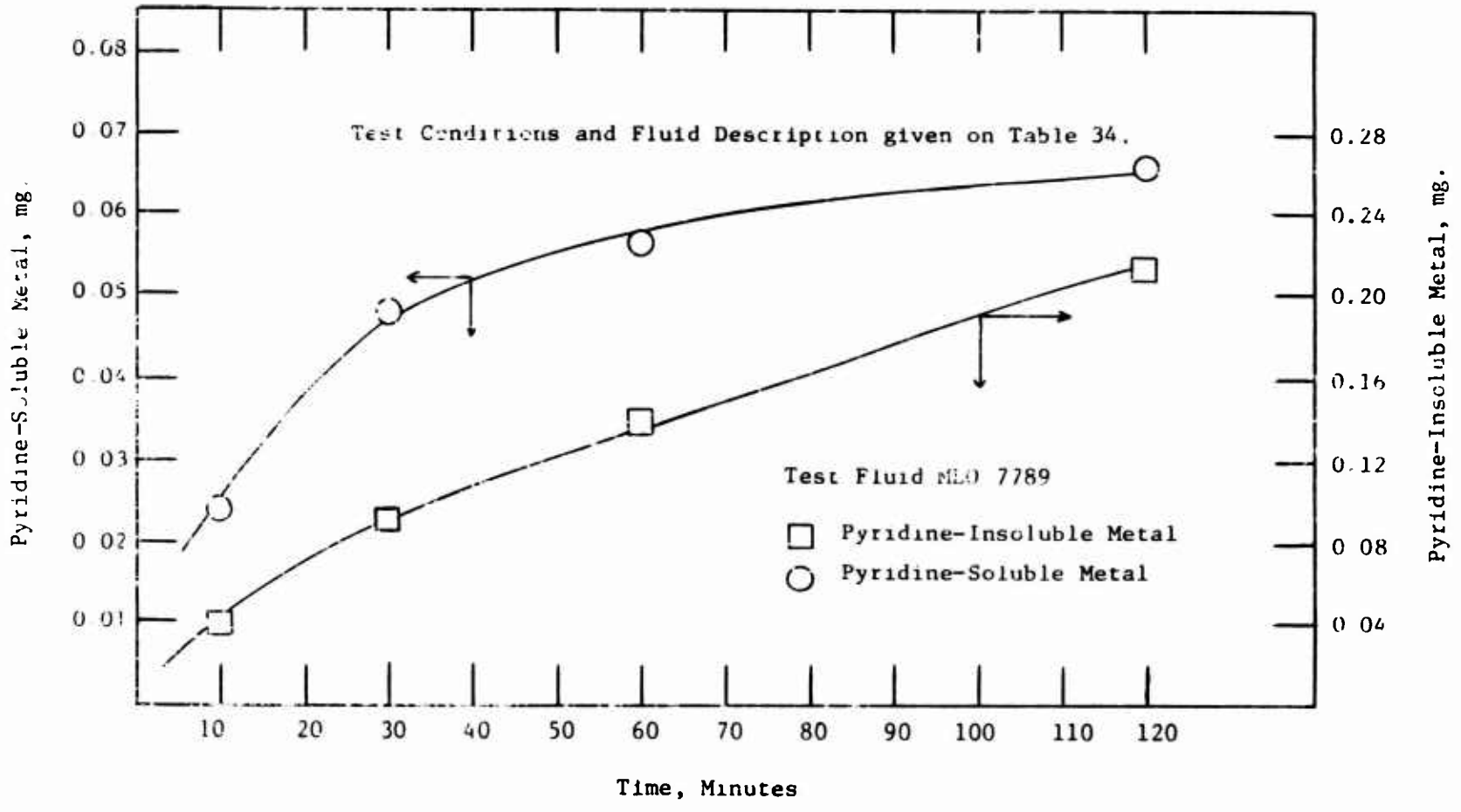

Figure 82 RATE OF FORMATION OF PYRIDINE-SOLUBLE AND INSOLUBLE METAL WITH A SUPER-REFINED MINERAL OIL

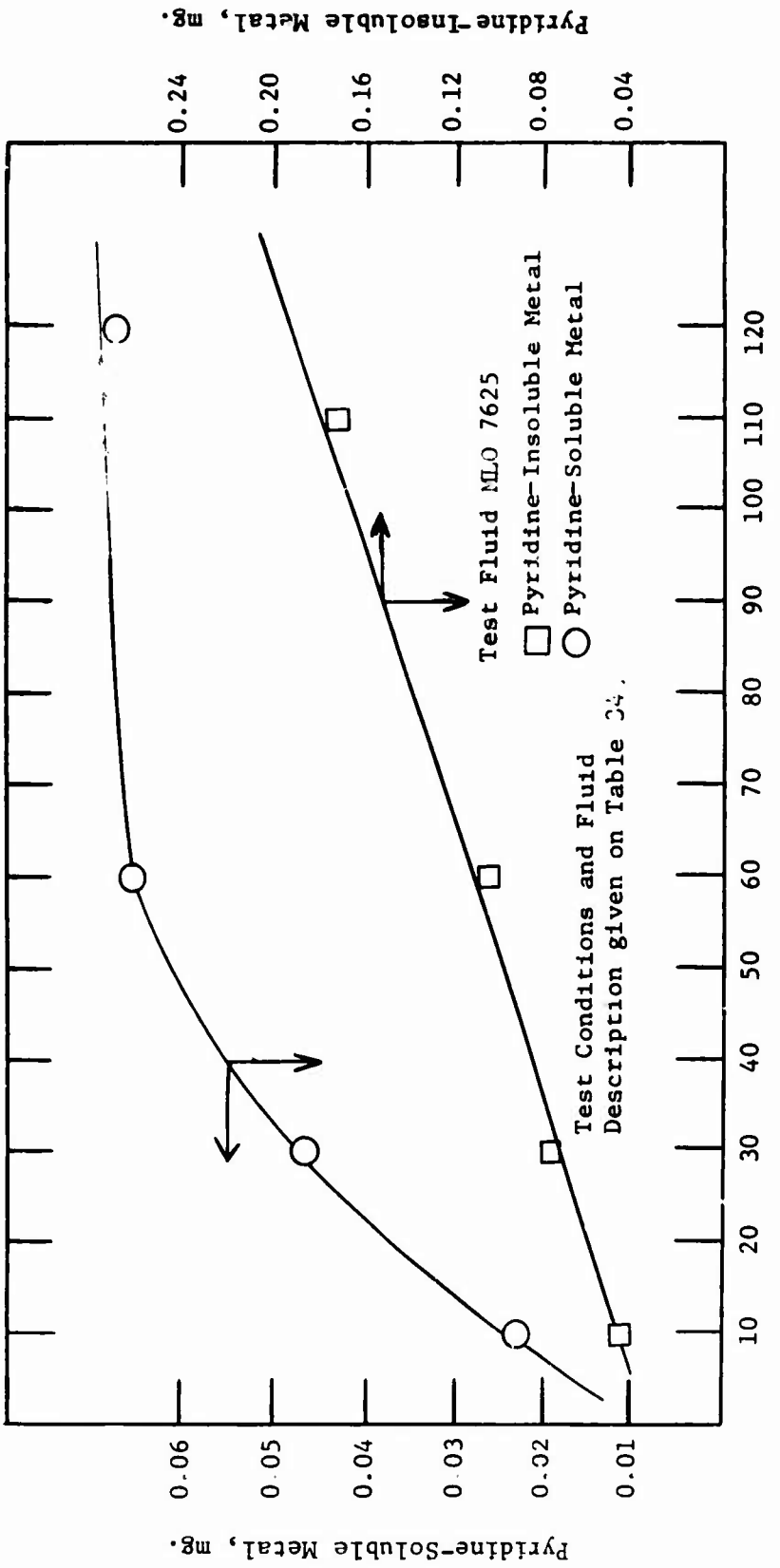

Figure 83. RATE OF FORMATION OF PYRIDINE-SOLUBLE AND INSOLUBLE METAL WITH A SUPER-REFINED MINERAL OIL

MLO 7710 - Di-2-Ethylhexyl Sebacate

MLO 7789 - Super-refined Paraffinic Mineral Oil

MLO 7625 - Super-refined Naphthenic Mineral Oil

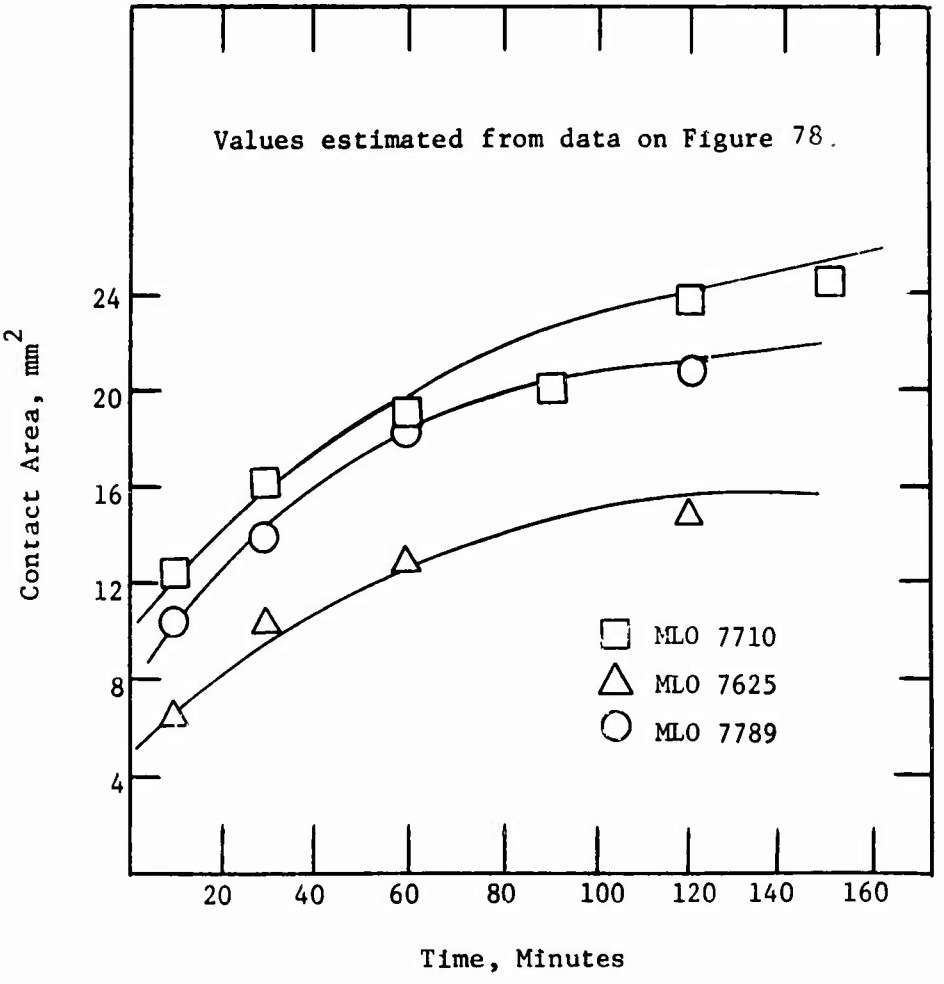

Figure 84. CONTACT AREA AS A FUNCTION OF TIME

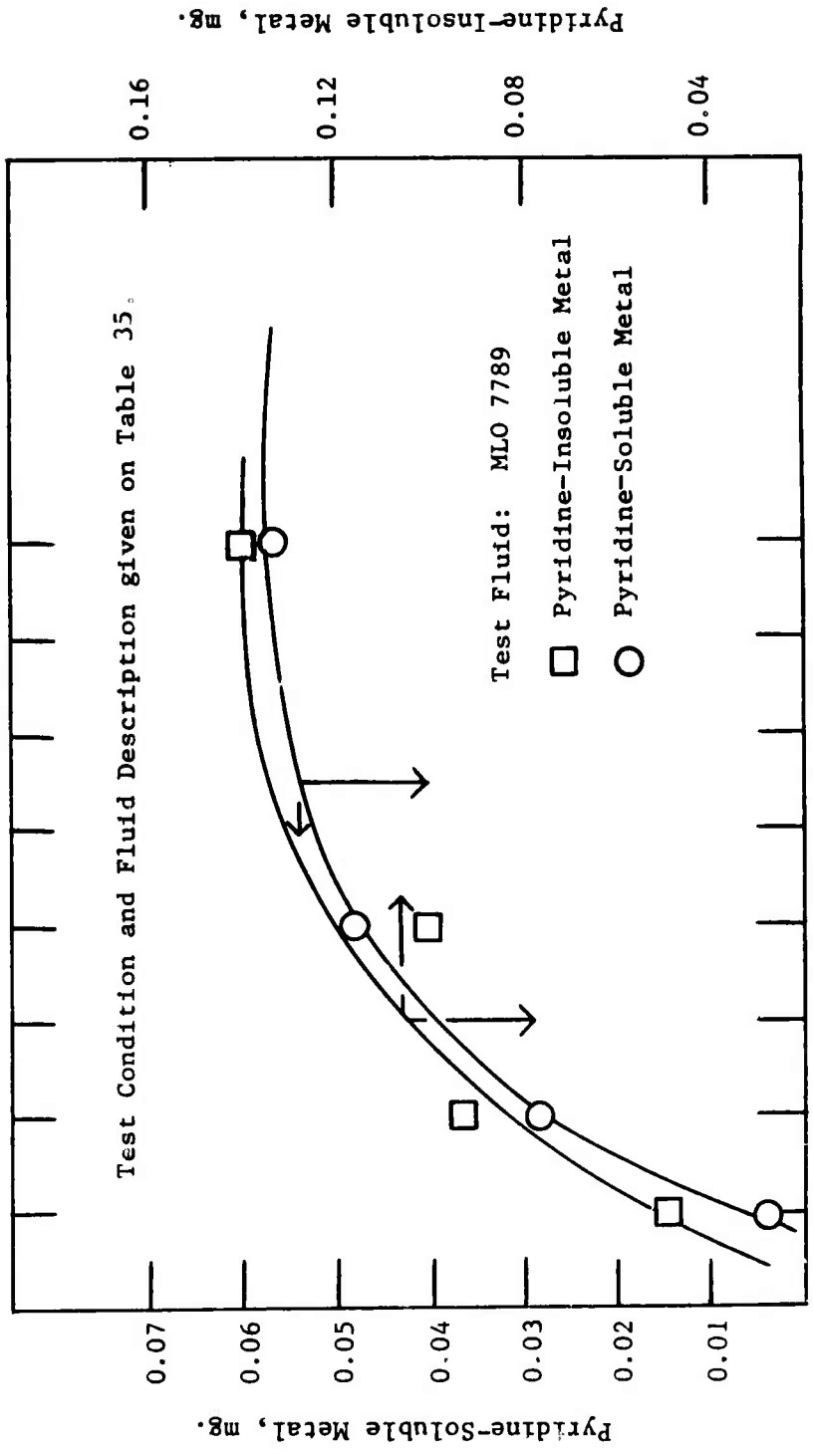

Figure 85. LOAD AS A FUNCTION OF PYRIDINE-SOLUBLE AND INSOLUBLE METAL GEN XATION

D. OTHER STUDIES IN PROGRESS. Progress is being made on a number of studies in addition to those emphasized in this report. Studies in which appreciable progress has been made during this period include the following.

1. Preliminary Studies in Titanium Lubrication. A number of 0.5-inch diameter titanium ball bearings were obtained from the Air Force Materials Laboratory. Some preliminary studies to determine the lubricity characteristics of titanium-on-titanium and titanium-on-other metal surfaces (primarily steel) have been carried out.

A new Shell four-ball wear tester obtained by the Department from the Roxanna Machine Works will be used in this work. This machine is a Brown-G E. Modification and is equipped for use at higher temperatures as well as operation under a controlled atmosphere.

The machine incorporates an air thrust bearing for support of the ball pot. A pneumatic-hydraulic loading piston provides continuouly variable loading at the wear surfaces. Two loading pistons having different diameters provide two ranges of loading. The load imposed on the bearing surfaces is indicated by a pressure gauge. Loading may be varied during a run while the spindle ball is turning. The wearing surface geometry is the same as that in the machines used previously.

A speed control allows a continuous range of shaft speeds. The duration of a run is controlled by a preset timing device. A friction transducer is attached to the arm of the ball pot and friction values are recorded on a chart recorder. The test temperature is also continuously indicated on the chart recorder.

Several calibration runs have been made to compare values obtained with the machine used previously and those obtained using the new tester The wear tester standards PRL 3207 (0 5 Wt.% phenothiazine in di-2-ethylhexyl sebacate) and PRL 3462 (5.0 Wt.% tricresyl phosphate in PRL 3207) have been used as test fluids The values obtained are shown on Table 36.

A paraffinic white oil having about 13 centistokes viscosity at 100°F has been used as the base fluid for experimental blends. Both titanium-on-titanium and steel-on-titanium wear surfaces have been evaluated. Two types of tests are used In one case, the test is started at a given load and run in the conventional manner. A second procedure involves starting the test at a very low load and increasing the load incrementally with time.

In order that surfaces in boundary lubrication can be lubricated, it is necessary to provide an easily sheared film on the surface. Reaction at the surface is difficult to achieve with titanium. Using steel-on-titanium, it may be possible to provide the reaction and resultant film at the steel surface. Additive types evaluated in the mineral oil base stock include acid phosphites and phosphates alone and in combination with materials containing zinc or sulfur. Several halogenated oils have been used both as test fluids and as additives in the mineral oil base stock Preliminary results indicate some effectiveness at relatively low loads for a halocarbon oil with both bearing surface

combinations and for the acid phosphite-zinc combination as well as a dithiophosphate for the steel-on-titanium system.

There have been many evaluations of the wear properties of titanium in bearings. In all cases titanium-on-titanium (Ti-on-Ti) bearings show extremely poor load carrying ability. Very reactive (corrosive) halogen-containing materials provide the best apparent lubrication properties for Ti-on-Ti. It is evident that a lubricant that will work on lightly loaded titanium bearings is much too reactive and unstable to be used advantageously in typical lubrication systems. Much of the so-called Ti lubrication studies were conducted with Ti members containing metal coatings on the Ti surface. In fact these are merely wear studies that could be conducted on other metal substrates. Some meaningful tests with steel-on-Ti have been conducted to demonstrate the problem of Ti lubrication. It is evident from these tests that any metal transfer from the Ti surface to the surface of the steel provides a Ti-on-Ti wear system and results in failure. The successful lubrication of steel-on-Ti appears to require a relatively thick coating (probably organometallic) on the steel bearing surface. Preliminary indications are that such films prevent the adhesive transfer of Ti to the steel surface by providing a sacrificial, easily sheared film.

These studies show some interesting features of lubrication additives. The successful tests in the four-ball wear tester were run-in by starting with a load of less than one kilogram and increasing to the desired load of 4 to 15 kilograms over several minutes run-in. Those tests started at the final load value gave erratic results indicating the problems of initial load and wear. The overall results show that an effective film formed on steel surfaces under boundary lubrication conditions such as zinc dialkyldithiophosphate can provide satisfactory lubrication for steel-on-Ti at moderate bearing loads.

An interesting additive effect was demonstrated by the steel-on-Ti studies. Zinc naphthenate, sulfurized terpene, and alkyl acid phosphates provide Zn, S, and P in polar form for comparison with the effect of the zinc dialkyldithiophosphate. Recent studies show that this latter material almost inevitably contains polar impurities rich in Zn and P. A comparison of the zinc dialkyldithiophosphate with combinations of the two polar compounds containing only P, Zn, or S has been made. These data (Table 37) show that the use of polar zinc compounds in combination with effective additives containing active sulfur or phosphorus approach the effectiveness of the zinc dialkyldithiophosphate.

1. Oxidation Studies of Several Fluids. A series of fluids has been received from the Air Force Materials Laboratory for evaluation of oxidation characteristics. These fluids include several commercial turbine engine lubricants, some compounded silicone formulations, and two dimerate esters. Some preliminary work has been done with these fluids. Stable life tests at 400° and/or 425°F have been conducted for each of the fluids and oxygen assimilation studies have been made with

several of the samples.

The data for the stable life evaluations are shown on Tables 38 through 41. The stable life values are determined by a sharp increase in neutralization number with test time. Stable life values for the gas turbine type lubricants at both 400° and 425°F are shown on Table 38. In general, the lubricants exhibit similar values at these temperatures. When looking at final properties of the test fluids, it should be remembered that these tests have been continued well beyond the stable life of the fluids.

Stable life evaluations for several silicone formulations are shown on Table 39. MLO 7813 is a fluorinated silicone containing three weight percent tricresyl phosphate. At about 50 hours test time at 400°F, a sludge or insoluble resin-like material is formed. This material is insoluble in naphtha but is readily soluble in such solvents as pyridine, acetone, and benzene. Several additional tests were carried out with this fluid. These tests and the results obtained are described on Table 40. The role of the oxygen and metal catalysts in the formation of this resin-like material is evident. To accomplish the filtrations shown, the fluid from run number one was decanted after the insoluble material has settled to the bottom of the tube. The other two silicone fluids, MLO 7814 and MLO 7815, did not increase in neutralization number during the test time although excessive metal corrosion is shown after the relatively long test time.

Data on Table 41 show stable life type tests for di-2-ethylhexyl dimerate and tri-2-ethylhexyl trimerate. An oxidation inhibitor, phenothiazine, has been added to each of these fluids. Both fluids, MLO 7817 and MLO 7818, show a steadily increasing neutralization number with time indicating no stable life or induction period. The di-2-ethylhexyl dimerate (MLO 7817) was hydrogenated over a nickel catalyst and the product (MLO 7817H) was again oxidized at 400°F. The neutralization number relationship with time for the hydrogenated fluid indicates a stable life of approximately 25 hours followed by oxidation. The effect of hydrogenation on oxidative stability is indicated by these preliminary data. Additional data at 347°F are desirable to provide more conclusive results.

Oxygen assimilation tests have been conducted on the gas turbine oils. Data from these tests are shown on Table 42. Both fluids (MLO 7798 and MLO 7799) have been oxidized at 425°F for periods in excess of their respective stable lives. Relatively small amounts of insolubles are formed in these tests. More work needs to be done before relative oxygen assimilation values can be determined for this series of fluids.

3. Pressure-Viscosity Studies. Film thickness of the lubricant in the bearing is an important consideration in aircraft applications where minimum high temperature viscosity levels are used to achieve low temperature operability. Film thickness is determined generally by the use of appropriate elastohydrodynamic (EHD) equations which require a value for the viscosity-pressure coefficient α. The PRL pressure viscometer can be used to determine α in the range (0 to 10,000 psig) which

appears to be pertinent to use in EHD equations.

Previous studies relative to the development and use of the PRL pressure viscometer are discussed in Annual Reports WADD-TR-60-898, Part III; AFML-TR-67-107, Part I; and AFML-TR-70-304, Part II. The latter two reports present the development of correlations for the prediction of α for fluids of various chemical types and for polymer-containing fluids, respectively.

Current work involves the determination of additional data on blends of varying molecular weight. Additional work on the time-pressure relationship on the viscosity of certain chemical types of hydrocarbons will be carried out. These are fluids which in previous studies have indicated a tendency for the pressure coefficient α to decrease as the pressure increases.

Pressure coefficients are being measured for a series of Pennsylvania mineral oils, some paraffinic resins, and various blends of these materials. Viscosity levels involved range from 10 to 8400 centistokes at 100°F. Preliminary studies indicate that the use of regression analysis and a correlation of the type discussed in Annual Report AFML-TR-67-107, Part I can predict the pressure coefficient of these mixtures covering a wide molecular weight range.

4. Bulk Modulus Determination. Bulk modulus values have been determined for a series of Spec. MIL-H-83282-type fluids received from the Air Force Materials Laboratory and Frankford Arsenal. Some of these fluids have been modified as indicated on Table 43. The determinations were made at 100°F in accordance with the procedure in Spec. MIL-H-27601. The isothermal secant bulk modulus values at 2000 psig intervals are shown on Table 43. Graphs indicating values over the range of 0 to 10,000 psig are included as Figures 86 through 91.

Table 36

CALIBRATION OF NEW FOUR-BALL WEAR TESTER

Test Conditions: Test Time = 1 hr.; Test Temperature = 75°C; and Test Speed = 600 ± 10 r.p.m.

Steel Balls: SKF Industries Grade No. 1 (0.5-inch Diameter) 52-100 Steel Ball Bearings, PRL Batch No. 14.

Test Fluids: PRL 3207 = 0.5 wt. % Phenothiazine in Di-2-Ethylhexyl Sebacate

PRL 3462 = 5.0 wt. % Tricresyl Phosphate in PRL 3207

Test Fluids	Average Wear Scar Diameter, mm. Steel-on-Steel Bearing Surfaces		
	1 Kg.	10 Kg.	40 Kg.
	Standard Values (Old Machine)		
PRL 3207	0.36	0.50	0.79
PRL 3462	0.16	0.23	0.38
	Values with New Machine		
PRL 3207	0.37	0.47	0.75
	0.38	0.47	
	0.39	0.55	
PRL 3462	0.18	0.25	0.36

Table 37

WEAR STUDIES WITH TITANIUM

Test Temperature = 165 ± 3°F.; Test Speed = 600 ± 10 rpm

Test Fluid	Bearing Surface	Wear Scar Diameter, mm. at Kg. load indicated	
Halocarbon Oil	Ti-on-Ti	0.80	4
		0.57	4*
	Steel-on-Ti	0.29	4
		0.50	10*
		1.38	15*
Mineral Oil (13 cs. @ 100°F.)	Steel-on-Ti	3.22	4
Zinc Dialkyldithiophosphate in Mineral Oil	Steel-on-Ti	0.29	4*
		0.33	10*
		0.39	15*
	Ti-on-Ti	3.81	4*
Zinc in Mineral Oil	Steel-on-Ti	4.16	4
Sulfur in Mineral Oil	Steel-on-Ti	3.11	4
Phosphorus in Mineral Oil	Steel-on-Ti	4.03	4
Sulfur and Zinc in Mineral Oil	Steel-on-Ti	0.40	4
Phosphorus and Zinc in Mineral Oil	Steel-on-Ti	0.23	4
Sulfur and Phosphorus in Mineral Oil	Steel-on-Ti	4.09	4

* Load increased from < 1 Kg. to value shown during first few minutes of run.

Table 38

OXIDATION CHARACTERISTICS OF SEVERAL GAS TURBINE LUBRICANTS

Test Conditions: Test Temperature and Time as Indicated; Catalysts = a 1-inch square each of copper, steel, and aluminum; Air Rate = 5 ± 0.5 l./hr.; Fluid Charge = 100 ml.

Test Fluid: MLO 7798 = Spec. MIL-L-23699, Type GTO (MLO-71-1)
MLO 7799 = Spec. MIL-L-7808G, Type GTO (MLO-71-2)
MLO 7812 = High Quality Ester Base Formulation (MLO-71-18)

Test Fluid	- - MLO 7798 - -		- - MLO 7799 - -		- - MLO 7812*- -	
Test Temp., °F.	400	425	400	425	400	425
Test Time, hrs.	168	72	168	42.5	168	42.5
Stable Life, hrs.	87	17	53	22	82	24
Centistoke Viscosity at 100°F.						
Original	27.4	27.4	13.4	13.4	27.0	27.0
Final	41.5	40.3	20.3	18.9	45.3	32.2
% Change	+51	+47	+51	+41	+68	+19
Neutralization No. (mg. KOH/g. Oil)						
Original	0.35	0.35	0.79	0.79	0.88	0.88
Final	4.85	4.8	5.5	6.6	2.8	3.6
Catalyst Wt. Change (mg./sq. cm.)						
Copper	-0.26	-0.83	-5.60	-0.73	-0.27	-0.32
Steel	+0.01	+0.00	+0.02	+0.03	-0.03	+0.12
Aluminum	0.00	-0.02	0.00	+0.02	-0.09	+0.10

* Small Volume Test: Fluid Charge = 25 ml.; Air Rate = 1.25 l./hr.; Catalysts were 1-cm square each of metals noted.

Table 39

OXIDATION CHARACTERISTICS OF SOME SILICONE TYPE FLUIDS

Test Conditions: Test Temperature = 400°F.; Test Time as Indicated; Catalysts = a 1-centimeter square each of copper, steel, and aluminum; Air Rate = 1.25 l./hr.; Charge = 25 ml.

Test Fluid:
MLO 7811 = Alkyl Methyl Silicone + 3% TCP (MLO-21-16)
MLO 7813 = Fluorinated Silicone + 3% TCP (MLO 71-26)
MLO 7814 = Dimethyl Silicone + 0.2% S-containing additive + 5.0% antiwear additive + 0.1% metal deactivator (MLO-71-101)
MLO 7815 = Dimethyl Silicone + 5% Antiwear Additive (MLO-21-101)

Test Fluid	7811	7813*		7814	7815
Test Time, hrs.	96.5	92	50	480	383
Stable Life, hrs.	41	10	--	--	--
Centistoke Viscosity at 100°F.					
Original	30.4	28.4	28.4	39.2	39.4
Final	56.3	72.4	69.7	53.3	45.6
% Change	+85	+155	+145	+36	+16
Neutralization No. (mg. KOH/g. Oil)					
Original	0.0	0.0	0.0	0.20	0.20
Final	12.0	11.5	--	0.20	0.20
Catalyst Wt. Change (mg./sq.cm.)					
Copper	-0.69	-1.04	-0.08	-34.8	-12.9
Steel	-0.02	-10.8	-0.38	+0.22	+0.14
Aluminum	+0.04	-0.02	-0.02	+0.05	+0.04

* A sludge or insoluble resin-type material forms at approximately 50 hours test time.

Table 40

ADDITIONAL TEST TO DETERMINE NATURE OF RESIN-LIKE SOLIDS FORMED

Test Fluid: MLO 7813 = Fluorinated Silicone + 3% TCP (MLO 71-26)

Run #	atm.	L/hr atm. rate	°F, temp.	ml size	mg./sq cm. wt. loss Fe.	Cu	Al	hrs. test time	wt. % fluid loss	wt.% insol. sludge[a]
1[b]	Air	5.0	400	100	-4.44	-1.92	0.00	96	4.95	6.3
2	Air	1.25	400	25	no catalysts present			96	9.82	1.68
3	N_2	1.25	400	25	-0.02	-0.05	-0.04	96	0.365	none

Notes: a. Melting point of solids approximately 210°F

b. Oxidized fluid from run 1 after the insoluble sludge had settled with the following results:

Pore Size	Solids Wt.	Filtrate Wt.	% Solids	Filtrate Condition
1	50.29 mg.	4.67 gm	1.08	clear*
5	60.63 mg.	5.14 mg	1.18	clear*
10	63.46 mg.	10.67 gm	0.59	cloudy

* turns cloudy in 1-2 hours

Table 41

OXIDATION CHARACTERISTICS OF TWO DIMERATE FLUIDS

Test Conditions: Test Temperature and Time as Indicated; Catalysts = a 1-centimeter square each of copper, steel, and aluminum; Air Rate = 1.25 l./hr.; Charge = 25 ml.

Test Fluid: MLO 7817 = Di-2-Ethylhexyl Dimerate (MLO-72-9)
MLO 7817H = MLO 7817 hydrogenated over a nickel catalyst
MLO 7817 = Tri-2-Ethylhexyl Trimerate (MLO-72-12)

Test Fluid*	MLO 7817	MLO 7817H	MLO 7817
Test Temp., °F.	425	400	400
Test Time, hrs.	42.5	96.5	51.5
Stable Life, hrs.	--	25	--
Centistoke Viscosity at 100°F.			
Original	91.5	91.8	273
Final	159	--	676
% Change	+74	--	+148
Neutralization No. (mg. KOH/g. Oil)			
Original	1.2	--	2.2
Final	6.6	8.5	9.3
Catalyst Wt. Change (mg./sq.cm.)			
Copper	-0.53	-3.65	-1.26
Steel	+0.05	-0.08	-0.37
Aluminum	+0.06	-0.08	-0.07

* 0.5 wt. phenothiazine was added to each of the test fluids.

Table 42

OXYGEN ASSIMILATION VALUES FOR SEVERAL FLUIDS

Test Conditions: For MLO 7798 and MLO 7999 - Test Temperature = 425°F., Air Rate = 5.0 ± 0.5 l./hr.; Test Time as Indicated; Catalysts = a 1-inch square each of copper, steel, and aluminum.

For MLO 7811 - Test Temperature = 400°F.; Air Rate = 1.25 l./hr.; Catalysts = 1 cm squares.

Test Fluids: MLO 7798 = Spec. MIL-L-23699, Type GTO (MLO-71-1)
MLO 7799 = Spec. MIL-L-7808G, Type GTO (MLO-71-2)
MLO 7811 = Alkyl Methyl Silicone + 3% TCP (MLO-71-16)

Test Fluid	MLO 7798	MLO 7799	MLO 7811
Test Time, hrs.	110	63	24
Liquid Charge, gm.	97.7	92.3	24.1
Liquid Less, Wt.%	9.3	5.2	6.6
Amt. O_2 Supplied, gm.	153	87.2	24.9
Amt. O_2 Used, gm.	5.39	6.00	2.23
Mols. O_2 Used/426 gm. Oil	0.803	0.866	1.23
Centistoke Viscosity at 100°F.			
Original	27.4	13.4	30.4
Final	49.1	18.8	62.3
% Change			
Wt.% Oil Insolubles	0.07	0.06	--
Catalyst Wt. Change (mg./sq.cm.)			
Copper	-0.67	-0.76	-0.07
Steel	+0.02	+0.03	-0.03
Aluminum	0.0	+0.01	-0.01

Table 43

ISOTHERMAL SECANT BULK MODULUS OF SEVERAL FLUIDS AT 100°F.

All are Spec. MIL-H-83282 Type Fluids

Fluid	Isothermal Secant Bulk Modulus, psi at 2000 psig	4000 psig	6000 psig	8000 psig	10,000 psig
MLO 73-76	204,200	217,700	231,300	245,000	258,700
MLO 7823	202,000	212,500	224,700	237,000	249,000
MLO 7824 (Contains 2.5 wt.% NA-SUL)	205,000	220,000	235,000	250,000	265,000
MLO 7825	201,000	215,500	230,000	244,500	259,000
MLO 7826 (Contains 2.5 wt.% NA-SUL)	206,000	219,300	232,700	246,300	259,700
MLO 7827 (Contains 2.5 wt.% NA-SUL)	206,000	219,700	234,000	248,000	262,000

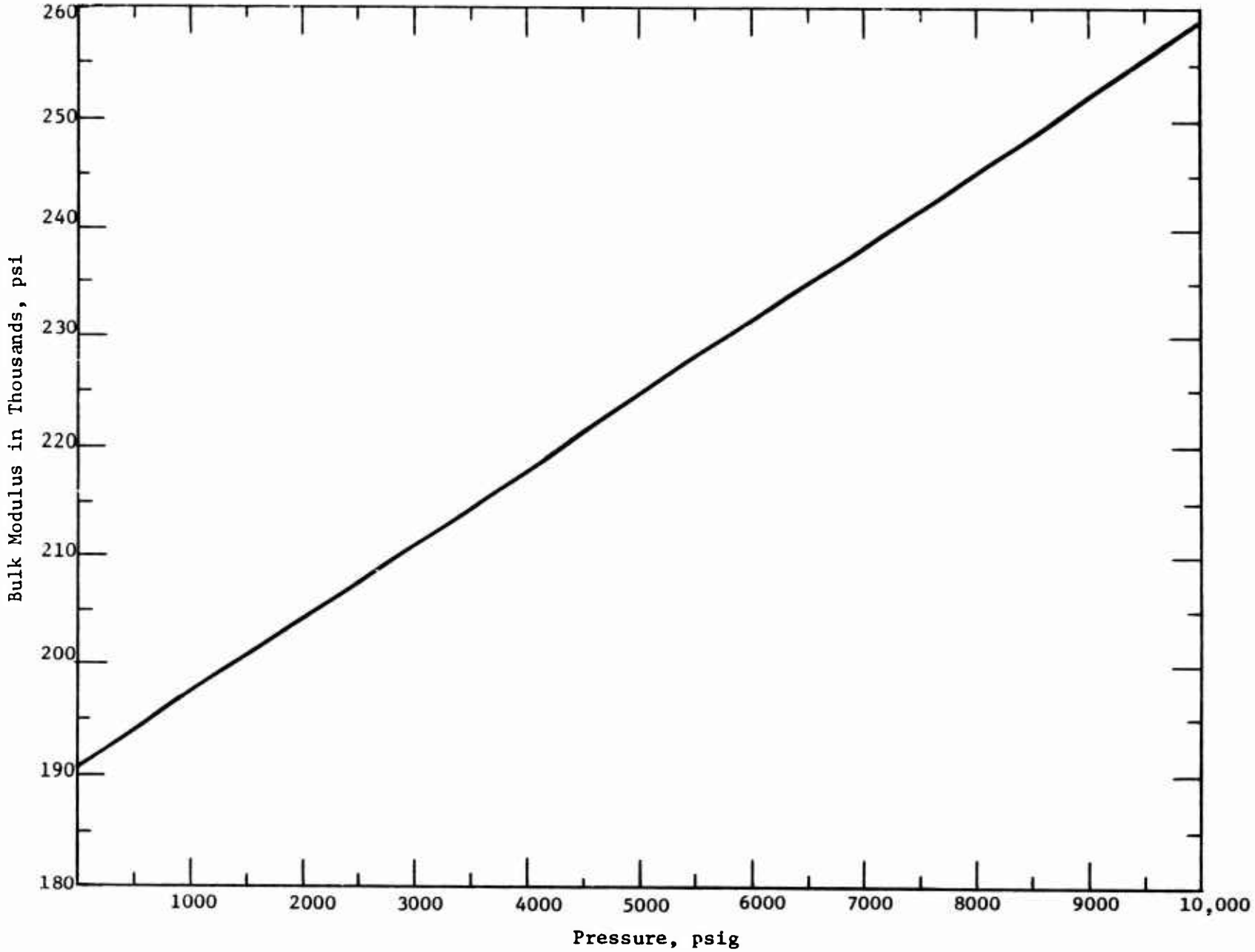

ISOTHERMAL SECANT BULK MODULUS OF MLO 73-76 at 100°F.

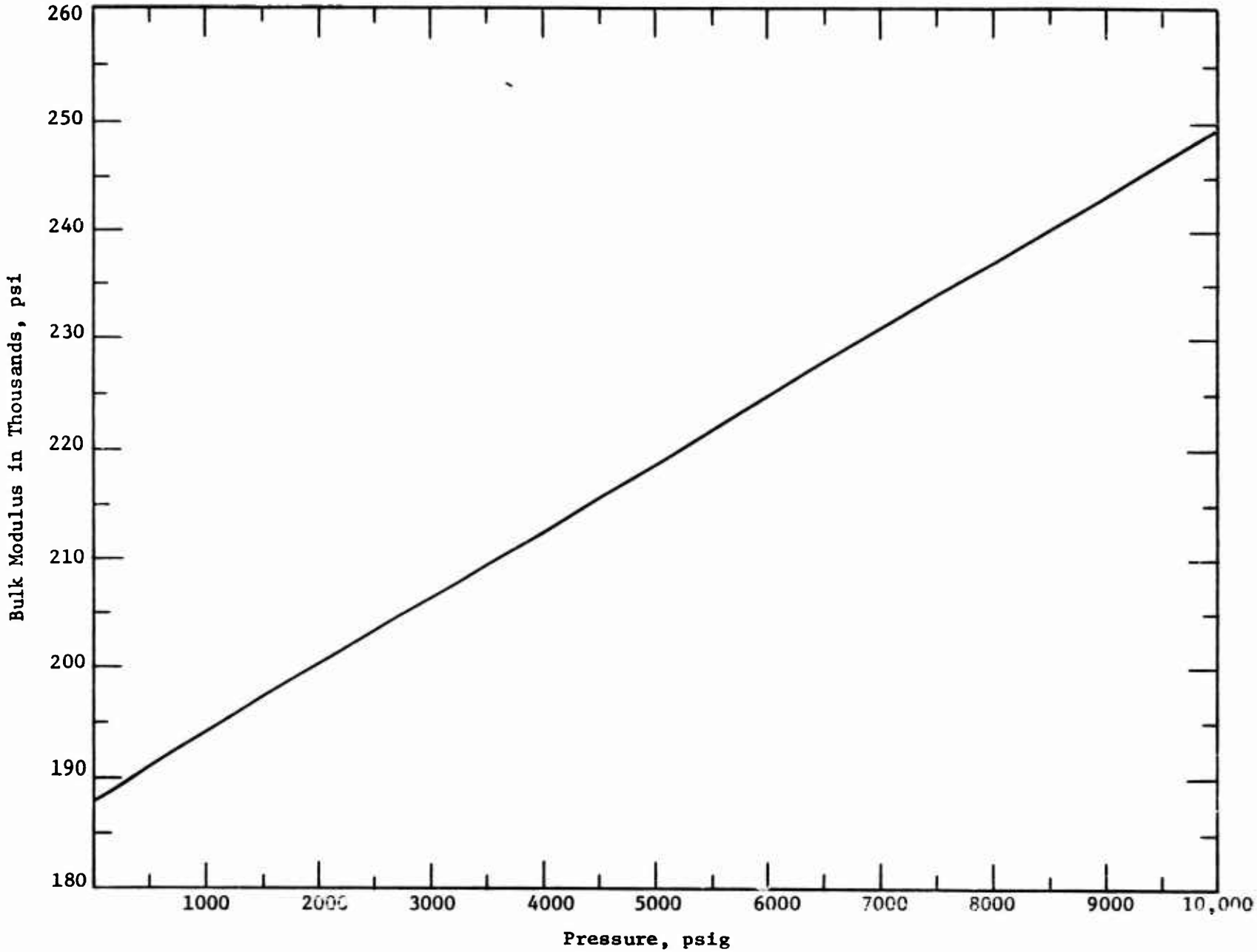

ISOTHERMAL SECANT BULK MODULUS OF MLO 7823 AT 100°F

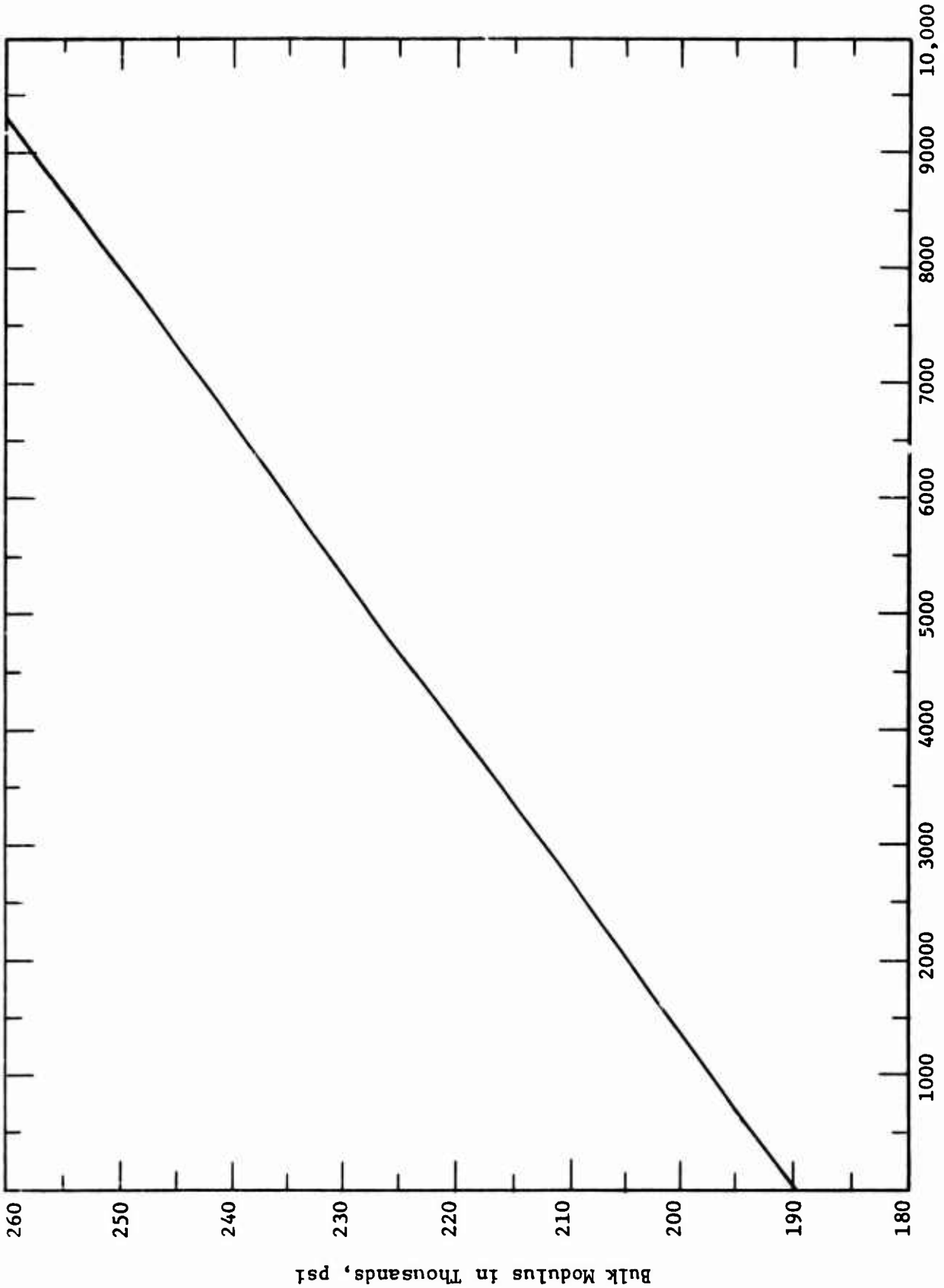

ISOTHERMAL SECANT BULK MODULUS OF MLO 7824 (CONTAINS NA-SUL) AT 100°F.

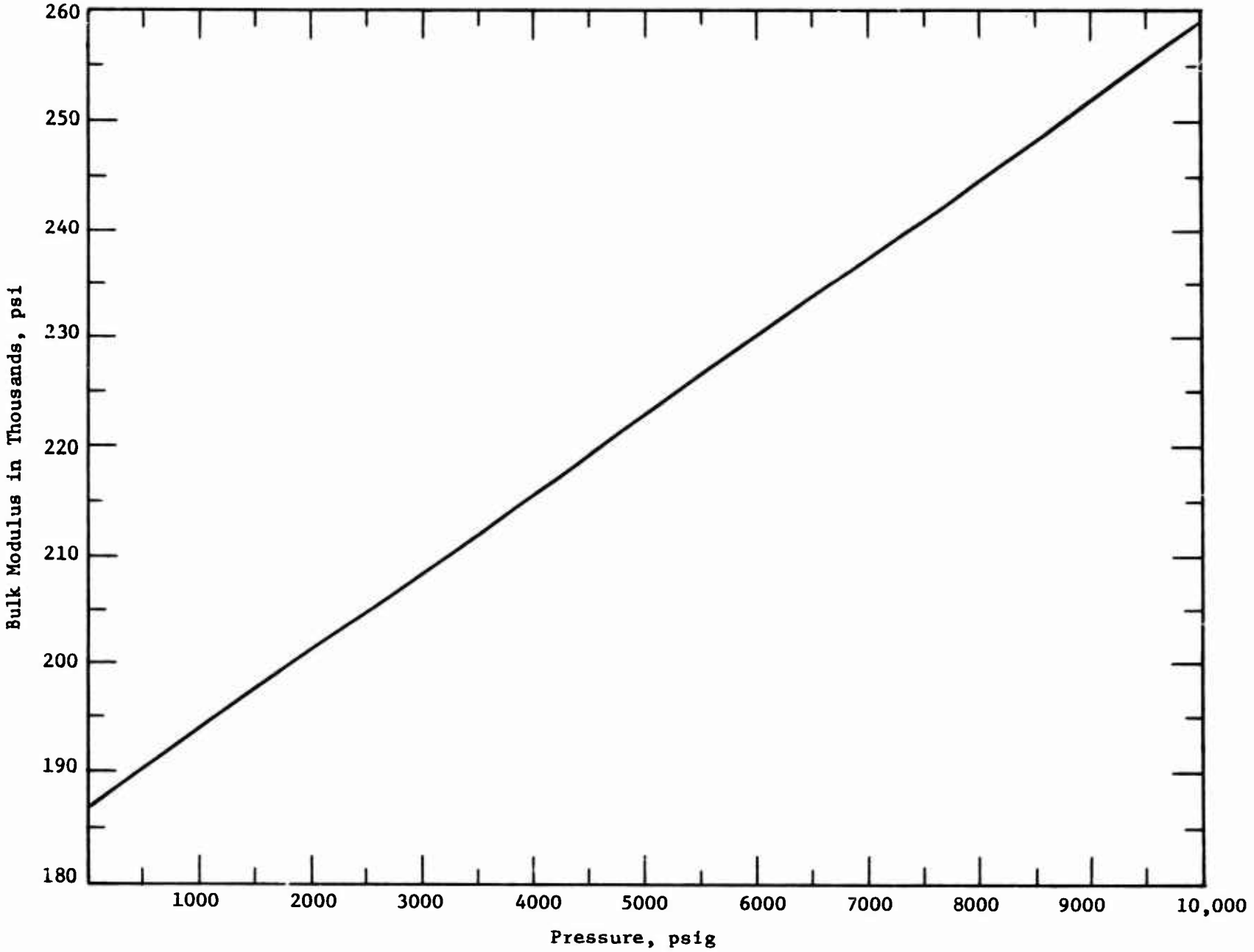

ISOTHERMAL BULK MODULUS OF MLO 7825 AT 100°F.

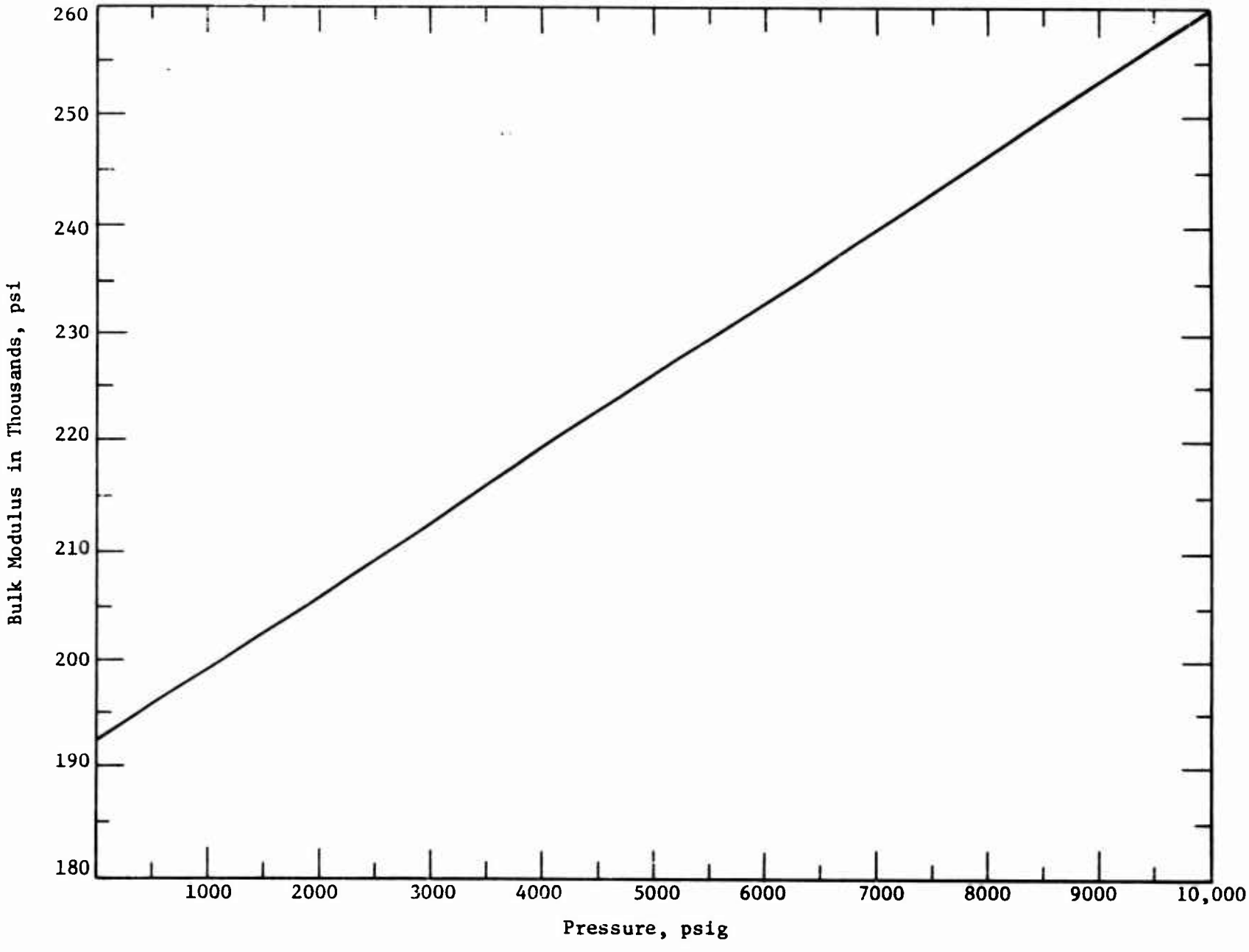

ISOTHERMAL SECANT BULK MODULUS OF MLO 7826 (CONTAINS NA-SUL) AT 100°F.

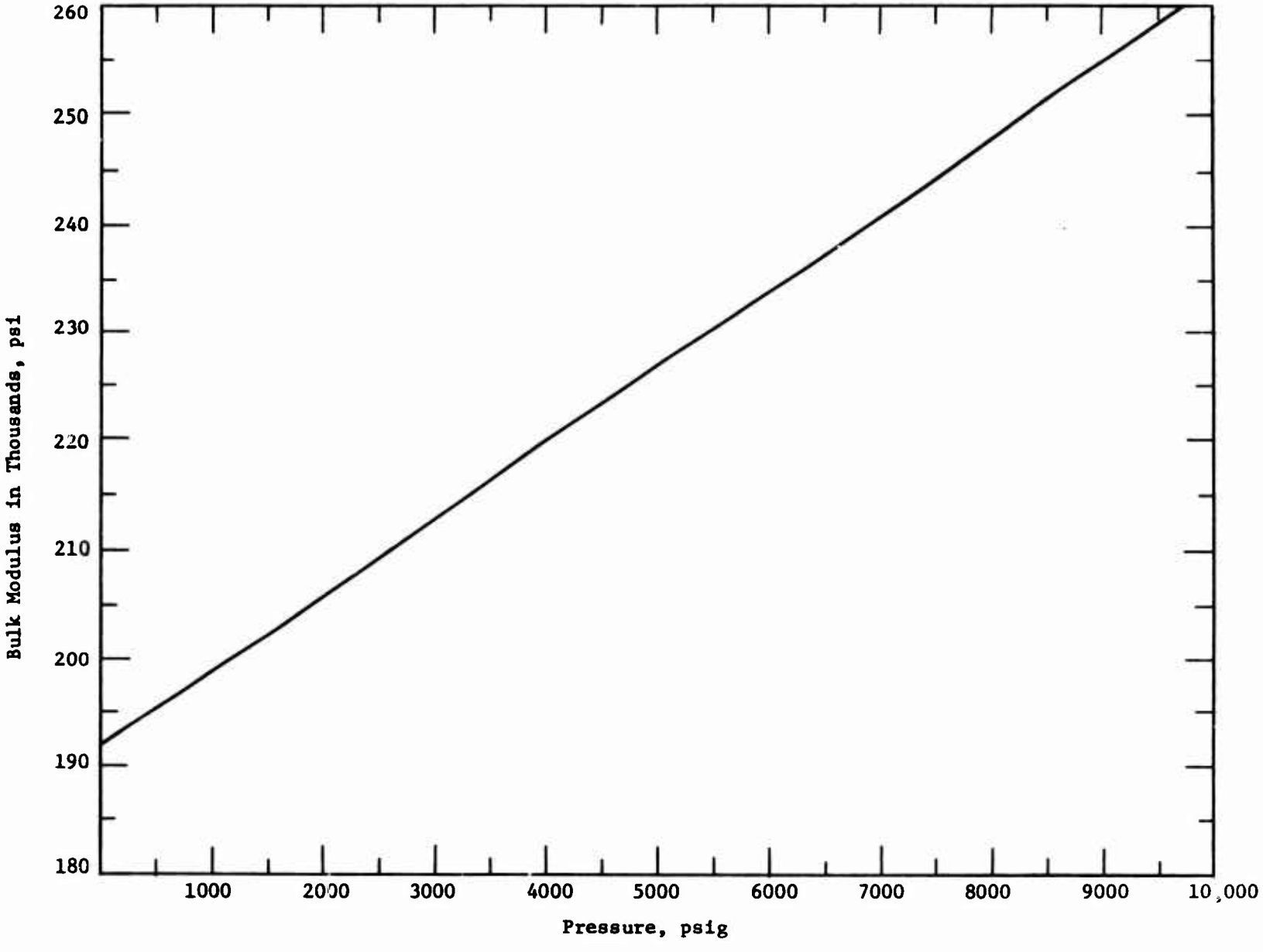

ISOTHERMAL BULK MODULUS OF MLO 7827 (CONTAINS NA-SUL) AT 100°F.

E. CONCLUSIONS. The characteristics of oxidation of liquid lubricants with air at 500°F using typical liquid phase oxidation test procedures have been evaluated critically. The rate of oxidation is increased by increasing the area of the oil-air interface; increasing the volume rate of flow of air through the fluid; increasing the partial pressure of oxygen in the gas; increasing the residence time of the gas bubble in the fluid; and increasing the amount of fluid vapor (including entrainment) in the heated gas space. The tests are very responsive to vapor phase oxidation and as a result can produce misleading results in comparing fluids of different volatility level or tests from equipment differing substantially in geometry related to volatility loss.

Test repeatability is adversely affected by the condensation and return of volatile oxidation products to the heated liquid phase. This results in bumping and a reduced liquid temperature during the oxidation. The use of an adequately heated vapor space provides the best temperature control and oxidation rate in liquid phase. The measurement of oxidation by total oxygen assimilated in tests involving a heated gas space tends to give misleading results because of the variation of vapor phase oxidation which is dependent on fluid entrainment by the gas, fluid volatility, and/or primary oxidation products. A combination of a test with the heated gas space but with test severity based on degree of oxidation in the liquid phase appears to be the optimum oxidation test based on repeatability.

Typical liquid phase tests tend to exhibit the highest rate of reaction in the early phases of oxidation. This behavior is observed in spite of the demonstrated trend of primary oxidation products to be more susceptible to oxidation than virgin fluid molecules. The reduction of oxidation rate of the liquid with test time appears to be a strong function of the build up of volatile liquid and gaseous oxidation products which reduce the amount of oxygen soluble in the system as well as the diffusion rate of the oxygen into the liquid system.

These studies suggest that the optimum conditions for comparative evaluation of oxidation of liquid lubricants include a test temperature where 10 to 50 percent of the available oxygen is reacted in the liquid phase. This requires a combination of temperature control and air bubble size.

Super-refined mineral oils and a good grade of di-2-ethylhexyl sebacate show a distinct trend toward decreasing wear with decreasing dissolved oxygen concentration in the fluid until a minimum wear value is obtained at some optimum dissolved oxygen concentration. Optimum oxygen concentration appears to be sensitive to load and fluid composition or polar impurities in the fluid. In the case of the super-refined mineral oils the wear-oxygen concentration curve is independent of temperature over the range of room temperature to 400°F. The ester appears to be temperature sensitive by defining two parallel wear-oxygen concentration curves. The 400°F tests define a line indicating higher wear than the test at 167°F. The obvious difference between the mineral oils and ester in these studies is the relatively low threshold of the ester to thermal degradation. The ester thermal degradation produces organic

acids which appear to be effective in producing corrosive wear in boundary lubrication. At 10 and 40 kilogram loads with the super-refined mineral oils, it is possible to show increased wear at oxygen concentrations below the optimum. The wear mechanism below the optimum wear appears to be different from the corrosive wear suggested for wear levels at oxygen concentrations above the optimum. The test procedures used to reduce oxygen concentration were not good enough to achieve the optimum wear level at one kilogram loads with the mineral oils or at any loads up to 40 kilograms with the ester. The inability to obtain the experimental conditions for optimum wear does not preclude the existance of this condition at lower oxygen concentrations.

There appears to be a distinct difference between the two super-refined mineral oils in their response to oxygen concentration. The lower level of oxygen sensitivity in the case of the viscous naphthenic mineral oil may be attributed to the presence of small quantities of polar impurities. The presence of oxygen in the basic ester molecule places the ester in a polar category which appears to modify the effect of dissolved oxygen.

Debris analysis provides a method of determining a material balance on fluid insoluble material as well as metal in the fluid and fluid insoluble material. The difference between metal particles and particles of metal oxide can be determined using an acridine-inhibited hydrochloric acid solution. The proper use of debris analysis with other chemical information on boundary lubrication provides a significant step in the evaluation of the lubrication mechanism.

Debris analysis in this study has been applied to the determination of relative polarity of lubricant constituents including oxygen; the effect of unit loading on reaction rate; and the effect of temperature and/or catalysis on triboreactions.

The unit loading in the four-ball wear tester is highest at the start of the test. The wear rate is highest at the start of the test with a large decrease in wear rate after the initial "wear-in" process. The decrease in wear rate with time is attributed to a decrease in unit loading, a decrease in surface temperature, a buildup in the formation of an elastohydrodynamic film, and an increase in the bearing surface area. This basic model applies to all of the tests run in this study including the sequential tests and those run as a function of time. In all of the tests there is evidence of organometallic wear products along with a metal-metal oxide fraction. In the first time increment of all sequence tests, where the most severe load and temperature conditions existed, the highest rate of formation of oil soluble organometallic products and total organometallic products were noted. Since the potential catalytic metal surface increases with time, it appears that temperature rather than the catalytic nature of the surface dominates the organometallic reaction. The formation of metal-metal oxide particles appears to be less temperature dependent. This fraction shows a smaller reduction in rate of formation with test time than does the organometallic fraction.

In general it appears that the total debris formation is

directly proportional to the amount of wear produced or inversely proportional to the lubricity. A general measure of debris tends to show a larger value for the contribution of the organic lubricant than from the metal bearing. The definite decrease in the rate of formation of organometallic product with time appears to be related to the method of removal of the reacted film on the metal surface rather than the formation of the film. As the bearing area increases and the bearing pressures decrease and a fluid film develops, the shear forces and/or cavitation effects on the bearing surface should decrease. This model is proposed as the reason for the decrease in rate of wear rather than a decrease in reaction rate on the surface.

Very reactive (corrosive) halogen-containing materials provide the best apparent lubrication properties for titanium-on-titanium wear surfaces. These lubricants are too reactive or unstable for use in a typical system. Steel-on-titanium wear surfaces can be lubricated so long as the lubricant and its componenets form a relatively thick coating (sacrificial, easily sheared film) on the surface of the steel. If this condition is not met, adhesive transfer of titanium to the steel occurs and lubrication fails. Additives containing a polar form of zinc, sulfur, and/or phosphorus provide effective coatings to reduce wear in steel-on-titanium wear surfaces.

APPENDIX I

PREFERENTIAL ADSORPTION IN THE LUBRICATION PROCESS OF ZINC DIALKLDITHIOPHOSPHATE

by

D. B. Barton
J. R. Strang
E. E. Klaus
E. J. Tewksbury

Prepared for Presentation at the ASLE-ASME
International Lubrication Conference,
New York, N.Y., October 9-12, 1972

Appendix I of Annual Report
AFML-TR-74-201, Part I Prepared by
Petroleum Refining Laboratory Division,
Chemical Engineering Department
The Pennsylvania State University

Preferential Adsorption in the Lubrication Process of Zinc Dialkyldithiophosphate

D. B. Barton[1], E. E. Klaus (ASLE)[2],
J. R. Strang (ASLE)[3], and E. J. Tewksbury (ASLE)[2]

Abstract

Paper chromatography has been used in combination with neutron activation analysis to analyze the polar lubricity additive zinc dihexyldithiophosphate. This additive is shown to contain small but significant quantities of both phosphorous- and zinc-containing polar impurities. Results of lubricity tests suggest that these polar impurities are adsorbed preferentially on a metal surface and therefore are available for the lubrication reaction in preference to the zinc dihexyldithiophosphate molecule itself. An acid phosphate-type compound is believed to be the active polar impurity controlling the wear behavior of zinc dihexyldithiophosphate.

A chemical lubrication mechanism for zinc dialkyldithiophosphate is proposed. This lubrication mechanism involves the formation of a metal phosphate surface film. The agreement between this mechanism and lubrication data presented by previous investigators is discussed.

I. Introduction

The effectiveness of a lubricity additive is dependent upon its polarity (affinity for the metal surface), with the more polar components controlling the wear reaction. It is known, for example, that polar phosphorous-containing impurities in tricresyl phosphate are adsorbed preferentially on metal surfaces (1). Very low concentrations (< 0.01 mole percent) of these polar impurities result in significant adsorption - the adsorption being controlled by impurity concentration. This low concentration of polar phosphorous-containing impurities dominates the wear reaction and causes wear reduction.

Zinc dialkyldithiophosphate (ZDP) is an excellent lubricity additive which also exhibits antioxidant, extreme pressure, detergent, and

[1]Senior Research Engineer, Mobil Research and Development Corporation, Paulsboro, New Jersey 08066.

[2]Professor and Associate Professor of Chemical Engineering, respectively, in the Department of Chemical Engineering, College of Engineering, The Pennsylvania State University, University Park, Pennsylvania 16802.

[3]Materials Engineer, Air Force Materials Laboratory, AFML/LNL, W-PAFB, Ohio 45433.

corrosion inhibition activity. Although this compound has been the subject of much study, the detailed mechanism by which this additive functions has not been completely understood.

Several investigators agree that the lubrication mechanism of ZDP involves a chemical reaction between the additive and the bearing metal (2-4). Both phosphorus and zinc have been identified in the reacted surface films. Other authors advance the theory that thermal decomposition of the ZDP additive molecule occurs prior to chemical reaction (4-7). The results of a study evaluating the antiscuff performance of ZDP used as a motor oil additive show that the atomic ratio of Zn: S:P changed upon decomposition of the zinc additive (8). This finding supports the theory (4) that the P to Zn linkage is broken when ZDP additives decompose.

Another investigation shows that the antiwear effectiveness of a number of common additives, including ZDP, is closely related to their adsorption kinetics - the more rapidly adsorbed additives being more effective (9). ZDP was found both to adsorb rapidly and to be a very effective antiwear additive when used in a corrosion preventive oil.

The thermal stability of zinc dialkyldithiophosphates has been proposed by several researchers as a parameter for determining the relative antiwear activities of these additives (8, 10-12). An examination of these references yields several serious differences. One paper (11) indicates that the more thermally stable structures are the more effective in reducing wear, while another (12) states that the thermally unstable compounds show better antiwear activity. Two others conclude that there appears to be no correlation between thermal stability and antiscuff performances (8,10). All authors do agree, however, that experimental conditions along with chemical structure are the critical factors in determining the thermal stability. The reason for the apparent inconsistencies of the results is that the experimental conditions and the chemical structures are not standardized in the investigations. One author (10) also claims that the zinc atom in the additive molecule directly affects the thermal stability of the molecule. Another (11) concludes that neither the alkyl group nor the zinc cation play a direct role in the effectiveness of the antiwear film, but only an indirect one by controlling thermal stability. A third (13) indicates that the antiwear effectiveness of ZDP depends directly upon the alkyl group. Two of these authors (10, 11) state that the thermal decomposition mechanism, the active antiwear species, and the surface reaction product leading to chemical wear are unknown.

This paper presents a study of the lubrication mechanism of the polar lubricity additive zinc dihexyldithiophosphate. Paper chromatography has been used to separate the zinc additive into its various constituents. Neutron activation analysis has been applied as the quantitative technique for analyzing the chromatographic separation (14). Comparative tests have been conducted on the four-ball machine to investigate the lubrication behavior of the ZDP additive on a metal substrate (15). Specifically, this study attempts to determine the presence of, identify, and define the role of polar impurities in the zinc dihexydithiophosphate additive, thus leading to a better understanding of the lubrication

mechanism of zinc dialkyldithiophosphates.

II. Analytical Techniques

Paper chromatography is a very sensitive quantitative separation technique based on relative polarity. This microanalytical technique generally is more effective in separating polar substances than the complementary and alternative method of thin layer chromatography (16). In this study, a commercial zinc dihexyldithiophosphate (PRL 3043) was separated into its constitutive components on high purity chromatography paper. This high purity paper contains only sodium as a major impurity. A single drop of the zinc additive (equivalent to 0.421 milligram phosphorus) was applied near one end of a strip of this paper. The strip then was held in a vertical position with the sample end immersed in a 70:30 (by volume) n-propanol:2N ammonia (aqueous) developing solvent. Separation of the ZDP components according to polarity occurred as the solvent migrated by capillary action up the chromatostrip - the least polar component traveling the farthest. After air drying to evaporate the solvent, the chromatostrip was sealed in polyethylene tubing for subsequent neutron activation.

All chromatographic samples were activated in the Pennsylvania State University nuclear reactor. The samples were positioned at the front face of the reactor core and irradiated for two hours at a power level of 500 kilowatts and a neutron flux of 9.1×10^{12} neutrons per square centimeter per second. After irradiation, the samples were left in the reactor pool for eight to twelve half-life periods of sodium-24 ($t_{1/2}$ = 15 hours) to allow this isotope to decay to an insignificant activity level. The samples then were analyzed quantitatively for their phosphorus-32 ($t_{1/2}$ = 14.3 days) and zinc-65 ($t_{1/2}$ = 245 days) distributions. Phosphorus-32 was measured by scanning the chromatographic strip with a sensitive end-window Geiger tube connected to a ratemeter-strip chart recorder system. Zinc-65 was measured by gamma-ray spectrometry.

Obtaining the sulfur distribution along a paper chromatogram is a more difficult task since both the phosphorus and the sulfur in ZDP activate to phosphorus-32 upon irradiation in a nuclear reactor. The problem thus becomes one of discriminating between the phosphorus-32 formed from the thermal (n,γ) reaction of phosphorus-31 and that formed from the threshold (n,p) reaction of sulfur-32. The phosphorus can be measured by waiting for the short-lived sulfur-37 to decay to an insignificant activity level and then using a calibrated aluminum absorber to screen out the weak beta particles emitted by sulfur-35. However, in order to measure sulfur directly, it is necessary to suppress the interfering (n,γ) reaction of phosphorus caused by both thermal and resonance neutrons.

It is known that cadmium is an extremely effective thermal neutron shielding material. Also, boron-10 in natural boron has a very large 1/v neutron capture cross-section which extends well into the resonance region (17) and thus is effective in reducing the resonance flux reaching a sample. Therefore, tests of the feasibility of utilizing boron in combination with cadmium to suppress (n,γ) phosphorus activation were conducted. Equal amounts of phosphorus and sulfur in the form of

$NH_4H_2PO_4$ and $(NH_4)_2SO_4$ were irradiated under three experimental conditions using a polyethylene-boron rabbit in conjunction with a cadmium liner as neutron shielding materials. The conditions and results are shown in Table 44. The relative amount of phosphorus-32 produced in each case has been normalized to the activity of sulfur irradiated in the unshielded condition. In the unshielded case, the activity of the phosphorus-32 from the phosphorus is about 16 times more than that from the sulfur. Using only the cadmium liner, the activity from the phosphorus is about 77 percent of that from the sulfur. Using the 30 percent boron rabbit plus a cadmium liner, the activity from the phosphorus is only 20 percent of that produced from the sulfur, a net improvement of about a factor of 80 over the unshielded condition in the ability to measure sulfur in the presence of phosphorus. Also, there is a relatively small loss of fast neutrons in passing through the boron-cadmium shielding materials and thus only a slight reduction in the threshold activation of sulfur. Therefore, after activation using boron-cadmium shielding, the sulfur distribution along the chromatostrip can be obtained in the same manner as previously described for phosphorus.

III. Activation Analysis of Zinc Dihexyldithiophosphate

A paper chromatographic separation of zinc dihexyldithiophosphate (ZDP) was made on high purity chromatography paper. After irradiation, the paper chromatogram was scanned for phosphorus-32 activity by the ratemeter-recorder system. A 137-milligrams per square centimeter aluminum absorber was used to screen out all beta activity due to sulfur-35 and zinc-65. Therefore, only the beta particles of phosphorus-32 were detected during the scan. The resultant phosphorus distribution of the zinc additive is shown in Figure 92. Two polar impurity peaks are evident - one near the starting point of the chromatographic separation and a less polar one next to the bulk ZDP additive peak. Each polar impurity peak represents about one percent of the phosphorus present in all three peaks.

After scanning the above paper chromatogram for its phosphorus distribution, it was cut into one-half-inch segments for a gamma zonal analysis in order to obtain the zinc distribution along this chromatogram. Each segment was subjected to an instrumental gamma spectrum analysis for the 1.12 MeV gamma photopeak of zinc-65. The gamma zonal analysis and resultant zinc distribution is shown in Figure 93. A very large polar impurity peak is evident near the starting point of the chromatographic separation. This polar component represents about 25 percent of the zinc present in the bulk additive and the polar impurity peaks.

In order to obtain the chromatographic sulfur distribution of ZDP, a boron-carbide polyethylene brick sample holder was designed and fabricated. This sample-containing brick then was wrapped in a cadmium liner prior to irradiation. However, no sulfur distribution was obtained since the irradiation dose necessary to see any polar impurity peaks exceeded the limiting irradiaiton dose of the polyethylene in the brick composite, thereby causing both cylindrical expansion and thermal welding of the brick container which destroyed the chromatographic sample. It is felt that in the future a "Bor-Al" material consisting of 35 percent boron carbide powder in an aluminum matrix might be used in place of the

boron-carbide polyethylene brick in order to obtain a definitive sulfur distribution of ZDP.

Figures 92 and 93 illustrate that the commercial lubricity additive zinc dihexyldithiophosphate (PRL 3043) is not homogeneous, but rather contains small but significant amounts of polar impurities. These figures show that the very polar material near the starting point of the chromatographic separations contains both phosphorus and zinc. The zinc-to-phosphorus ratio is much greater than the ratio of zinc-to-phosphorus in the ZDP molecule. Therefore, these polar impurities appear to be multicomponent.

In ZDP the molar ratio of zinc-to-phosphorus is 1:2 while in the polar impurities the molar ratio is 25:1. It is clear, therefore, that not all of the impurities contain phosphorus. On the other hand, these data do not indicate whether or not the phosphorous-containing impurity contains zinc. The polar phosphorous-containing compound has been observed to behave chromatographically in the same manner as an acid phosphate. This polar material may be a mono- or di-acid phosphate or a zinc salt of the mono- or di-acid phosphate. Other polar zinc-containing impurities present may be zinc oxide and/or the zinc salt of an organic C_6 acid.

The possibility of sulfur being associate with these polar impurities must be considered. Thioacids are excluded as polar impurities since the excess zinc present should neutralize any thioacids, thereby forming molecules of ZDP. However, an acid grouping could replace an alkyl group of ZDP and any two oxygens could lose their respective alkyl groups and be linked by zinc, thus producing a polar acid dithiophosphate molecule which could be of any chain length. This would build up the zinc-to-phosphorus ratio in these polar impurities.

IV. Comparison of ZDP and TCP

Bieber (18) used a thin-layer chromatography/activation analysis technique to determine the presence of polar phosphorous-containing impurities in tricresyl phosphate (TCP). It was shown that these polar impurities enter into the lubrication reaction in preference to the TCP molecule itself and are responsible for the antiwear effectiveness of TCP. Analyses of dialkyl acid phosphate and dialkyl acid phosphite lubricity additives indicated that both these compounds and the polar impurities in TCP are in the same class. It was concluded that the active wear-reducing species in TCP is a mono- or diaryl phosphate.

The present study examines the effect on wear of the polar impurities in zinc dihexyldithiophosphate (PRL 3043). The PRL 3043 was blended with a super-refined paraffinic mineral oil (MLO 7755) and tested at various concentrations in the four-ball tester. It was found that the minimum effective additive concentration for a ten kilogram load is about 0.01 weight percent. It is known that acid phosphates also show effective antiwear activity in this concentration range. The 0.01 weight percent PRL 3043-MLO 7755 blend then was subjected to iron powder percolation to remove the polar impurities. The percolation reduced the beneficial

effects of the additive. A further investigation of the effect of percolating the fluid was made by using the transition region of the wear-versus-load relationship. At any concentration of additive, there is a specific load above which the wear increases sharply. As shown in Figure 94, the effect of percolating the ZDP additive blend was to decrease the transition load. This suggests that the polar impurities in ZDP play a significant role in the lubrication process.

The effect of a barium sulfonate rust inhibitor on TCP susceptibility has been shown to be dependent on the concentration of the polar impurities in TCP (18). This active sulfonate will negate the antiwear effect of TCP if the concentration of the polar impurities in the TCP is relatively low. Barium and calcium sulfonates (PRL 3493 and PRL 2870) were added to blends of PRL 3043 in MLO 7755 and to MLO 7755 in concentrations of one weight percent. The sulfonates dominate the wear reaction but produce about the same overall wear values as the mineral oil MLO 7755 when used as the only additive. The sulfonates had little or no effect on the activity of ZDP in MLO 7755 as shown in Table 45. These results indicate that ZDP (PRL 3043) exhibits similar antiwear behavior to the arylacid phosphate impurities found in some grades of TCP.

Controlled atmosphere wear tests have been conducted on blends of ZDP and a sulfurized terpene containing equal weight percentages of sulfur (Table 46). Use of a nitrogen atmosphere did not affect the antiwear activity of ZDP but resulted in a large increase in wear for the sulfurized terpene. For a MLO 7755 blend containing both sulfurized terpene and TCP, the wear behavior of the TCP is shown to be the controlling factor. Likewise, for a blend containing both ZDP and the sulfurized terpene, the wear behavior of the phosphorous-containing ZDP additive is shown to be the controlling factor. The results of these comparisons indicate that phosphorus, rather than sulfur, is the principle wear-reducing element in zinc dihexyldithiophosphate. This indication is supported by the work of other investigators (3,4).

Extreme-pressure data for ZDP, dilauryl acid phosphate, and a sulfurized terpene in a super-refined naphthenic mineral oil base stock are shown in Table 47. These data indicate that the ZDP (PRL 3043) exhibits about the same incipient seizure and permanent welding loads as the acid phosphate and a markedly different permanent welding load than the sulfur additive. This similarity of E.P. characteristics for ZDP and an acid phosphate again suggest that phosphorus rather than sulfur is the principle active element in zinc dihexyldithiophosphate.

All of the species represented by the very polar impurity peaks in Figure 92 and 93 have the same polarity relative to bulk ZDP and, therefore, all should be adsorbed on a metallic surface preferentially. On the basis of the foregoing comparative lubricity tests, it is postulated that the multicomponent polar impurities in PRL 3043 contain predominantly phosphorus and zinc and that the active wear-reducing species in zinc dihexyldithiophosphate are acid phosphates and/or thioacid phosphates. A concentration of 0.1 to 0.3 percent of polar impurities was found in TCP (18) while at least one percent of polar impurities (based on P) was found in the ZDP. Assuming that the effective ingredients are the same (acid phosphates), the difference in quantity of polar impurities

(based on P) was found in the ZDP. Assuming that the effective ingredients are the same (acid phosphates), the difference in quantity of polar impurities could explain the difference in apparent lubricity level between the TCP and the ZDP when used as boundary lubricants.

V. The Chemical Lubrication Mechanism of Zinc Dialkyldithiophosphate

The results of this study suggest the following specific chemical lubrication mechanism for zinc dialkyldithiophosphate: (a) preferential adsorption of polar zinc- and phosphorous-containing impurities on the surface of the metal, (b) asperity contact producing relatively high local temperatures, and (c) chemical reaction of the polar phosphorous-containing impurities, which are believed to be a partial acid ester and/or a thioacid ester of phosphorus (both of which may contain zinc), with the bearing metal to produce a metal phosphate which functions as a protective surface film of lower shear strength than the base metal.

VI. Conclusion

Zinc dihexyldithiophosphate has been found by a chromatographic separation/activation analysis technique to contain both zinc- and phosphorous-containing impurities of the same relative polarity. These polar impurities appear to adsorb preferentially on the surface of a metal and enter into the lubrication reaction in preference to the zinc dihexyldithiophosphate molecule itself. The molar ratio of zinc-to-phosphorus in zinc dihexyldithiophosphate is 1:2, while the molar ratio of zinc-to-phosphorus in the polar impurities has been found to be about 25:1. Therefore, there appears to be more than one polar impurity. The active phosphorous-containing impurities in both TCP and ZDP show the same behavior in four-ball wear tests and in chromatographic separations. These data suggest that the effective impurity in ZDP is an acid phosphate. The zinc impurities may be zinc oxide, the zinc salt of an organic C_6 acid, or zinc phosphates. Analytical techniques were not available to determine whether or not sulfur is associated with these polar impurities. However, results of this and previous studies (3, 4) have shown that phosphorus, rather than sulfur, is the dominant wear-reducing element in zinc dialkyldithiophosphate. It is postulated that the multicomponent polar impurities in zinc dihexyldithiophosphate (PRL 3043) contain predominantly phosphorus and zinc and that the active wear-reducing species are acid phosphates and/or thioacid phosphates.

The following chemical lubrication mechanism for zinc dihexyldithiophosphate is proposed: (a) preferential adsorption of polar zinc- and phosphorous-containing impurities on the surface of the bearing metal, (b) asperity contact producing relatively high local temperatures, and (c) chemical reaction of the polar phosphorous-containing impurities, which are believed to be a partial acid ester and/or a thioacid ester of phosphorus, with the bearing metal to produce a metal phosphate surface film.

ACKNOWLEDGEMENT

This research was supported in part by the United States Air Force under Contracts AF33(615)-3379 and F33615-69-C-1183 monitored by

the Nonmetallic Materials Division (LNL), Air Force Materials Laboratory, Wright-Patterson AFB, Ohio.

REFERENCES

1. Bieber, H.E., Klaus, E.E., and Tewksbury, E.J., "A Study of Tricresyl Phosphate as an Additive for Boundary Lubrication," ASLE Trans., 11, 155-161 (1968).

2. Furey, M.J. and Kunc, J.F., Jr., "A Radiotracer Approach to the Study of Engine Valve Train Lubrication," Lubrication Eng., 14, 302-309 (1958).

3. Loeser, E.H., Wiquist, R.C., and Twiss, S.B., "Cam and Tappet Lubrication.III - Radioactive Study of Phosphorus in the EP Film," ASLE Trans., 1, 329-335 (1958).

4. Loeser, E.H., Wiquist, R.C., and Twiss, S.B., "Cam and Tappet Lubrication.IV - Radioactive Study of Sulfur in the EP Film, ASLE Trans., 2, 199-207 (1959).

5. Furey, M.J., "Film Formation by an Antiwear Additive in an Automotive Engine," ASLE Trans., 2, 91-100 (1959).

6. Bennett, P.A., "A Surface Effect Associated With the Use of Oils Containing Zinc Dialkyl Dithiophosphate," ASLE Trans., 2, 78-90 (1959).

7. Rowe, C.N., "Role of Additive Adsorption in the Mitigation of Wear," ASLE Trans., 13, 179-188 (1970).

8. Bennett, P.A. and Kabel, R.H., "The Anti-Scuff Performance of Metal Organodithiophosphate Additives," Lubrication Eng., 19(9), 365-370 (1963).

9. Quilty, C.J. and Martin, P., Jr., "The Effect of Anti-Wear Additives on tne Lubrication Properties of Corrosion Preventive Oils," Lubrication Eng., 25 (6), 240-245 (1969).

10. Gallopoulos, N.E., "Thermal Decomposition of Metal Dialkyldithiophosphate Oil Blends," ASLE Trans., 7, 55-63 (1964).

11 Rowe, C.N. and Dickert, J.J., Jr., "The Relation of Antiwear Function to Thermal Stability and Structure for Metal O,O-Dialkylphosphorodithioates," ASLE Trans., 10, 85-90 (1967).

12. Bennett, P.A., "A Look at the Effects of Lubricant Additives on Surfaces," SAE National Fuels and Lubricants Meeting, Tulsa, Oklahoma, November, 1958, Preprint No. 107B.

13. Zamberlin, I., Mikac-Cergolj, I., and Bencetic, M., "Effect of the Chemical Structure of Zinc Dithiophosphate Additives on the Antiwear and E.P. Properties of Lubricating Oils," Nafta (Zagreb), 20 (7), 351-358 (1969).

14. Strang, J.R., "The Role of Selective Adsorption in Boundary Lubrication," M.S. Thesis, The Pennsylvania State University (1970).

15. Barton, D.B., "A Study of Boundary Lubrication Mechanisms Using Atomic Absorption Spectroscopy," M.S. Thesis, The Pennsylvania State University (1968).

16. Browning, D.R., "Chromatography," McGraw-Hill, Berkshire, England, 1969.

17. DeSoete, D., Gijbels, R., and Hoste, J., "Modern Trends in Activation Analysis," National Bureau of Standards (U.S.) Spec. Publ., 312 (2), 1969, pp. 699-750.

18. Bieber, H.E., "Phosphate Esters and Their Function in Boundary Lubrication," Ph.D. Thesis, The Pennsylvania State University (1965).

Table 44

Relative Induced Phosphorus-32 Activities
For Equal Weights of Phosphorus and Sulfur
Under Three Different Shielding Conditions

Reaction	Unshielded	Cd Liner	30% B + Cd Liner
$^{31}P_{(n,\gamma)}{}^{32}P$	16	0.71	0.17
$^{32}S_{(n,p)}{}^{32}P$	1 (Basis)	0.93	0.88

Table 45

Effect of Barium and Calcium Sulfonates on the Antiwear Activity of Zinc Dihexyldithiophosphate in a Super-Refined Paraffinic Mineral Oil

Four-Ball Wear Test Conditions Include: Speed = 600 rpm.; Load = 10 kg.; Test Temp. = 167°F,; and Bearings = 52-100 Steel.
Test Fluid: Super-refined paraffinic mineral oil (MLO 7755).

Additive	Wear Scar Diameter, mm.
None	0.69
1.0 wt. % barium sulfonate (PRL 3494)	0.73
0.5 wt. % zinc dihexyldithiophosphate (PRL 3043)	0.33
0.5 wt. % PRL 3043 + 1.0 wt. % PRL 3494	0.25
1.0 wt. % calcium sulfonate (PRL 2870)	0.68
0.01 wt. % PRL 3043	0.34
0.01 wt. % PRL 3043 + 1.0 wt. % PRL 2870	0.30

Table 46

Effects of a Nitrogen Atmosphere and a Sulfurized Terpene on the Antiwear Activity of Tricresyl Phosphate and Zinc Dihexyldithiophosphate

Four-Ball Wear Test Conditions Include: Speed = 600 rpm,; Load = 10 kg.; Test Temp. = 167°F,; and Bearings = 52-100 Steel.
Test Fluid: Super-refined paraffinic mineral oil (MLO 7755).

Additive	Wear Scar Diameter, mm. Air	Nitrogen
None	0.52	--
0.84 wt.% zinc dihexyldithiophosphate (PRL 3043) (0.16 wt. % sulfur)	0.26	0.26
0.50 wt. % sulfurized terpene (PRL 3044) (0.16 wt. % sulfur)	0.42	0.89
0.50 wt. % tricresyl phosphate + 0.50 wt. % PRL 3044	--	0.25
0.50 wt. % PRL 3043 + 0.50 wt. % PRL 3044	0.26	0.26

Table 47

Comparison of Extreme-Pressure Characteristics of
Zinc Dihexyldithiophosphate to Dilauryl Acid Phosphate
and a Sulfurized Terpene

Four-Ball E.P. Test Conditions Include: Speed = 1750 rpm.; and Bearings = 52-100 Steel.

Test Fluid	Approx. Incipient Seizure Load, kg.	Approx. Welding Load, kg.
Super-refined naphthenic mineral oil having 77 cs. @ 100°F. (MLO 7516)	40	90
MLO 7516 + 2.0 wt. % zinc dihexyldithiophosphate (PRL 3043)	60-100	180
Super-refined naphthenic mineral oil having 21 cs. @ 100°F. (PRL 3184)	<40	80-120
PRL 3184 + 5.0 wt. % dilauryl acid phosphate	80	120-160
PRL 3184 + 5.0 wt. % sulfurized terpene	70	240-280

Test Conditions: Developer: 70:30 (by volume) n-propanol:2 N ammonia (aqueous); Nuclear Activation: Two Hours at 500 Kilowatts; Decay Time: 14 Days; Detector System: Ratemeter - Recorder; Absorber: 137 mg./cm.^{2} Al

* Values are Mole Percent of Phosphorus in the Impurity and Bulk Additive Peaks

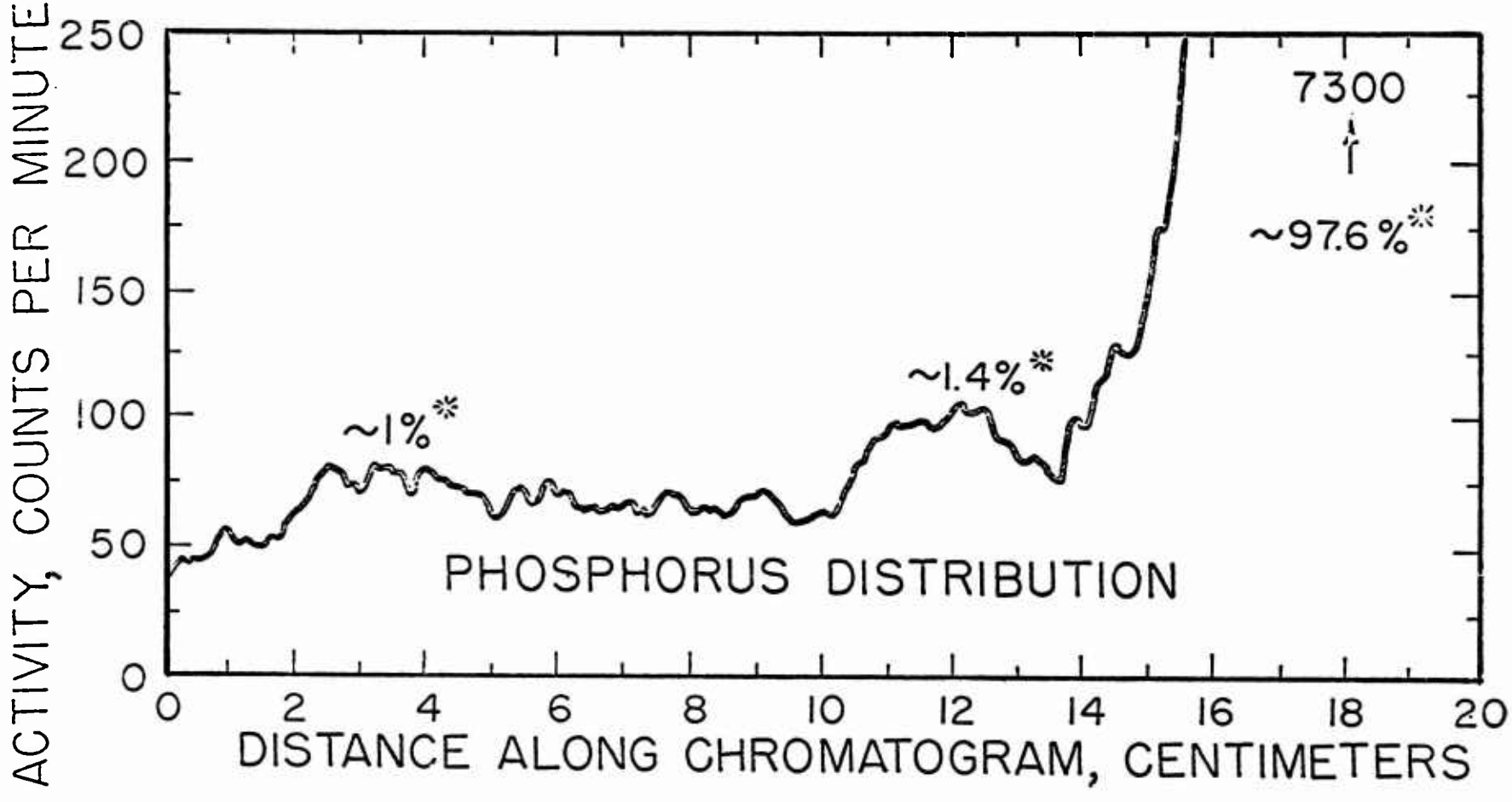

Figure 92 PAPER CHROMATOGRAPHIC SEPARATION AND ACTIVATION ANALYSIS OF ZINC DIHEXYLDITHIOPHOSPHATE - PHOSPHORUS DISTRIBUTION

Test Conditions: Developer: 70:30 (by volume) n-propanol:2 N ammonia (aqueous); Nuclear Activation: Two Hours at 500 Kilowatts; Decay Time: 15 Days; Detector System: Gamma-Ray Spectrometer

* Values are Mole Percent of Zinc in the Impurity and Bulk Additive Peaks

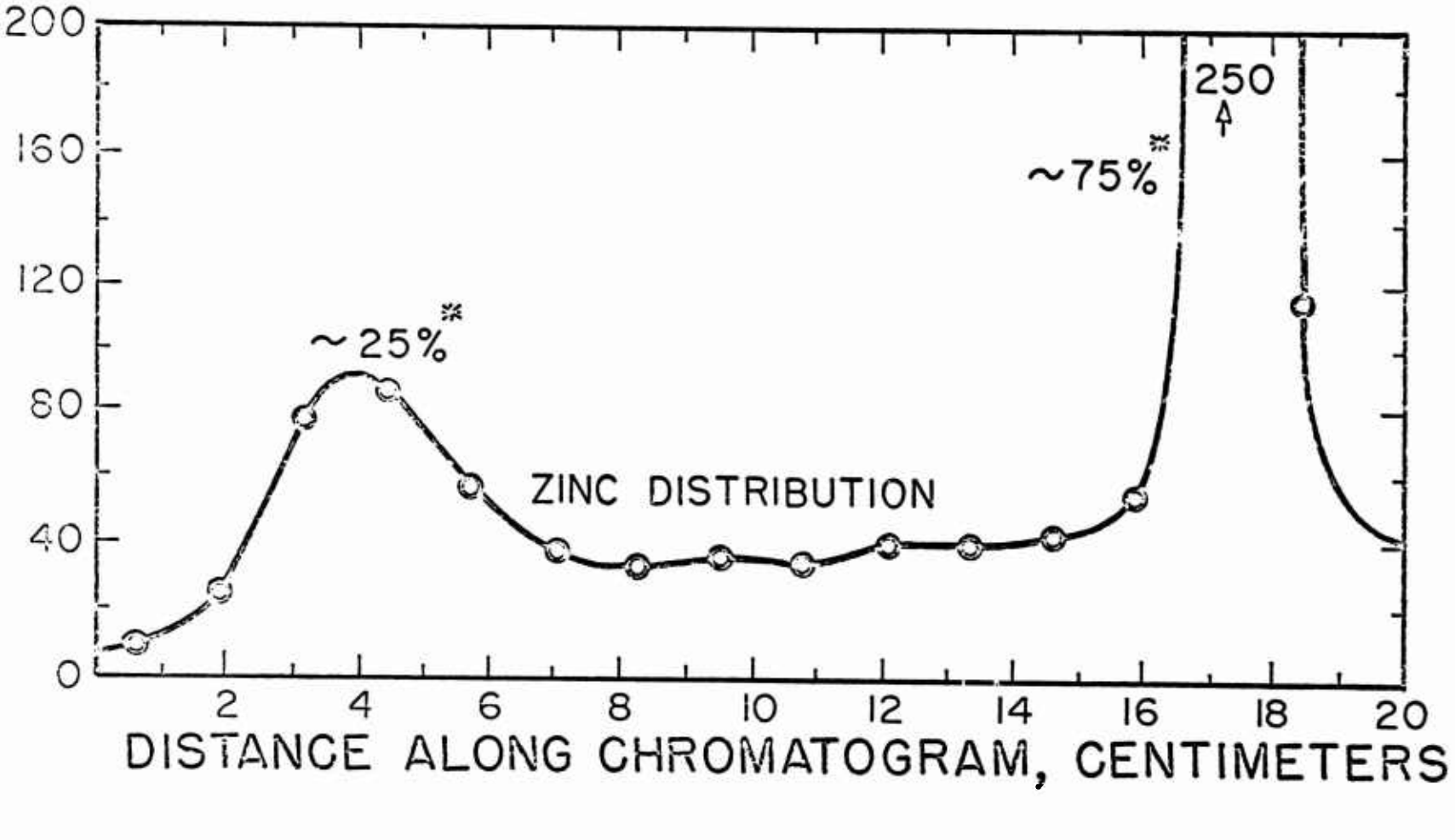

Figure 93 PAPER CHROMATOGRAPHIC SEPARATION AND ACTIVATION ANALYSIS OF ZINC DIHEXYLDITHIOPHOSPHATE - ZINC DISTRIBUTION

Figure 94

Four-Ball Wear Test Conditions: Speed: 600 rpm.; Temperature: 167°F; Bearings: 52-100 Steel

Test Fluid: Super-refined paraffinic mineral oil (MLO 7755) + 0.01 wt. % zinc dihexyldithiophosphate (PRL 3043)

○ Before Percolation

● After Percolation

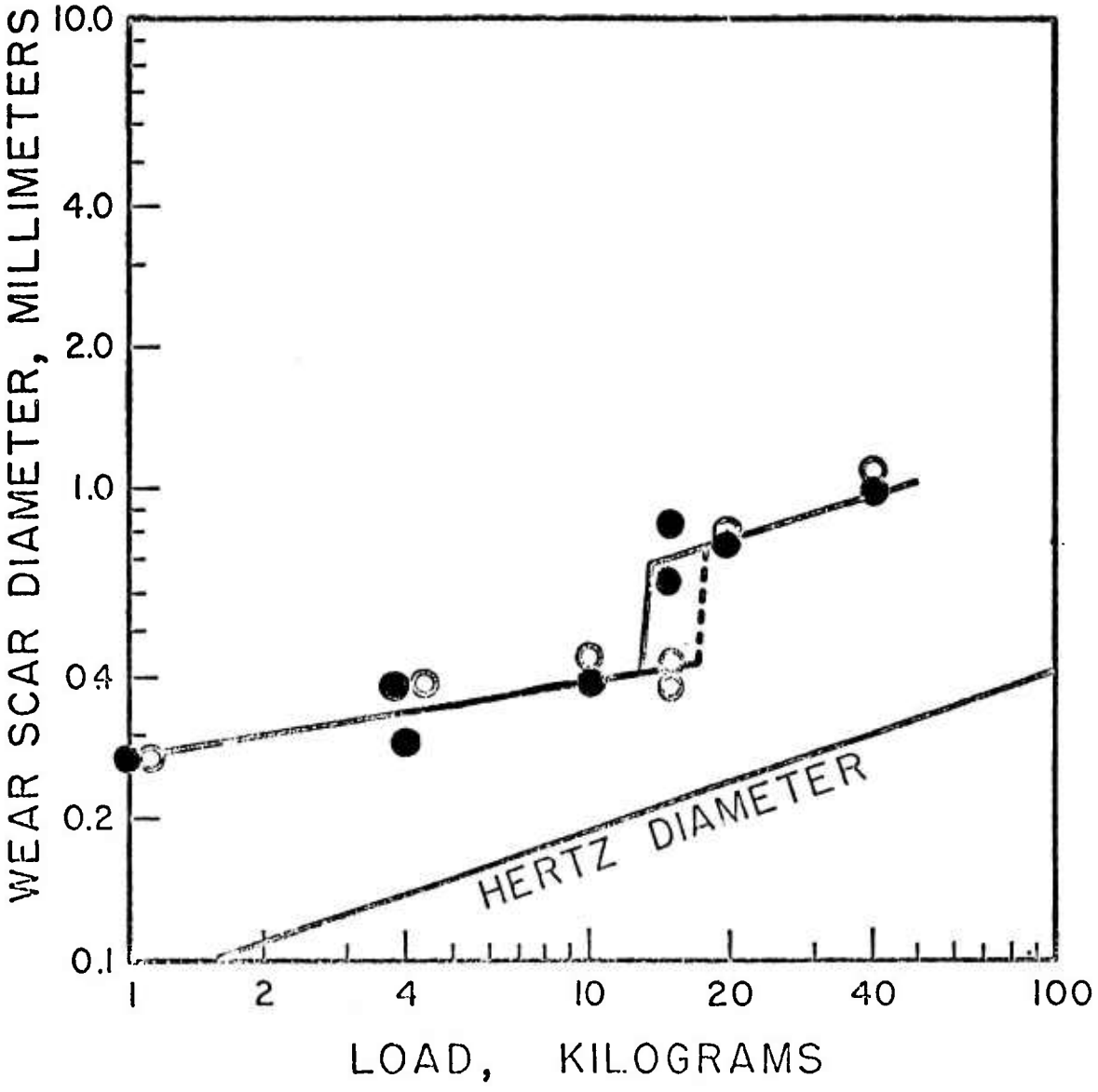

EFFECT OF IRON POWDER PERCOLATION ON TRANSITION REGION OF A ZINC DIHEXYLDITHIOPHOSPHATE - MINERAL OIL BLEND

APPENDIX II

CHEMICAL PROPERTIES OF LUBRICANTS

by

E. E. Klaus

Appendix II of Annual Report
AFML-TR-74-201, Part I Prepared by
Petroleum Refining Laboratory Division,
Chemical Engineering Department
The Pennsylvania State University

CHEMICAL PROPERTIES OF LUBRICANTS

BY

E. E. Klaus*

Introduction. The life of a lubricant in most cases and the basic function of the lubricant in many cases are dependent on the chemical reactions of the lubricant components with each other or environmental constituents in the lubrication system. Continuing trends in the design of the lubrication system as well as the bearing components in the system place increased emphasis on the chemical properties of the lubricant to provide a minimum level of life and performance. The goal of improved lubricant life is optimum chemical stability or minimum chemical reactivity under the most severe conditions encountered. On the other hand, optimum performance is based on sufficient chemical activity to provide an easily sheared film based on chemical reactions at the bearing surfaces. Since lubricant life and performance are closely related to controlled chemical reactivity, the chemical characteristics of the lubricant need improved definitions.

Bulk Fluid Properties. The life of a lubricant is generally determined by the thermal, oxidative, and corrosion reactions that take place in the lubrication system. These three basic chemical reactions involving the lubricant appear to be interrelated (1, 2). In conventional low temperature applications, the principal cause of fluid degradation is the reaction of the lubricant with oxygen (oxidation). Essentially all of the specification tests currently used to study the effects of an oxidizing environment on lubricants are based on test conditions designed to determine the level of effectiveness of oxidation inhibitors in the lubricant (3, 4). That is, the tests tend to be long-time, low-temperature tests during which little or no oxidation reaction takes place. As the temperatures in lubrication systems increase and oxidation inhibitors are no longer adequate to protect the lubricant from reaction with oxygen, present test methods are not appropriate for the study of the oxidation reaction (5, 6). Studies of the initial kinetics of this reaction at higher temperatures are available, but data combining time and temperature are not available. As a result of the paucity of information in these areas of oxidation reactions, prediction of lubricant stability in actual application based on laboratory information has been relatively poor. Studies of the variables affecting oxidation reaction on a time-temperature basis are needed

Some initial studies relating thermal degradation, oxidation and metal corrosion have been conducted (7). The products of thermal degradation and those of oxidation from the same hydrocarbon or ester appear to have essentially the same carbon skeleton. Oxidation in such cases may be considered a low-energy path for the basic thermal degradation reaction. The threshold of thermal degradation, as shown in Table 48, ranges from 400°F for some esters, 400° to 500°F for some polymeric hydrocarbons,

700°F for saturated hydrocarbons, to 850°F for aromatic ethers without alkyl side chains. Oxidation on the other hand may proceed at an appreciable rate at temperatures of 200° to 400°F. Metal corrosion products that are produced at these temperatures in the oxidation process may act as catalysts to accelerate the oxidation reaction. The metal corrosion products also appear to promote the formation of oil insoluble sludge and varnish. It has been demonstrated that by the proper use of additives, the initial corrosion products may in fact function as an effective metal deactivator. In this case the material causing the initial corrosion may act as an oxidation inhibitor or synergist for oxidation inhibitors.

In order to apply basic studies in thermal stability, oxidation, and corrosion of liquid hydrocarbons and esters to lubricant life in actual systems, additional studies relating time and temperature for these reactions are needed. It is clear from preliminary results that initial rates for these reactions cannot be used for extrapolation to determine lubricant life.

Analytical Considerations in Boundary Lubrication. The same chemical reactions discussed for the bulk fluid stability also appear to be involved in the lubricant chemistry under boundary conditions (8, 9,10,11,12,13,14,15,16). Boundary lubrication is the term used to describe the region where the behavior of the bearing system is dependent on the chemical properties rather than the viscosity properties of the lubricant. Boundary lubrication exists where the fluid film approaches molecular dimensions in thickness. The chemical area of lubrication appears to involve a three-step process of (a) adsorption on the bearing surface, (b) chemical reaction involving the adsorbed layer, and (c) removal of the reaction product from the bearing surface. The adsorbed material and the solid surface on which it is adsorbed may include the following components of the lubricant and/or bearing system.

1. Lubricant base stock
2. Lubricant additives
3. Impurities in the base stock or additives
4. Dissolved gases from the atmosphere in contact with the lubricant system (principally oxygen and water)
5. Bearing metal
6. Metal oxide
7. Impurities in the bearing

Since bearing surfaces are relatively small compared with lubricant volume, quantities of lubricant involved in the lubrication chemistry (boundary lubrication) are in the parts per million range. Effects of concentration changes of the order of five parts per million in the case of acid phosphate impurities have been shown to affect wear properties in mineral oil-tricresyl phosphate lubricant formulations (17, 18). Lubrication chemistry requires the use of sensitive microchemical measurements to demonstrate significant changes in lubricant behavior as a function of specific chemical reaction. Proof of the presence of specific reactants or reaction products at these concentration levels requires the development of new analytical procedures and/or the appropriate combination of existing microtechniques from other

areas of chemical technology. Among the techniques that have been applied successfully in studying the chemistry of lubrication are the following operations used singly or in combinaiton (1,8,9,18).

1. Neutron activation analysis
2. Atomic absorption spectroscopy
3. Gas chromatography (isothermal and temperature-programmed)
4. Thin layer chromatography
5. Paper chromatography
6. Micro and electro balances
7. Radiotracer techniques
8. Scanning electron microscope with microprobe
9. Millipore filtration
10. Gel permeation chromatography
11. Solvent extraction
12. Laboratory wear testers

In general, microtechniques are required to associate the specific reaction that plays the dominant role with lubrication chemistry. The change in concentration of an effective reactant or the rate of formation of the reaction product must be determined to establish the specific reaction and reactants involved.

Reaction Conditions. The reaction conditions in boundary lubrication also need further definition. The general range of these conditions has been determined from observations with bearing systems exhibiting wear. Measured metal surface temperatures in elastohydrodynamic lubrication have been reported to be as high as 600° to 650°F (19). Metal surface damage observed in incipient failure of bearing in boundary lubrication indicates actual surface melting. Pressures of successful bearing systems exhibiting boundary lubrication are generally 5×10^5 psig or less. Catalysts present which may influence the course of the lubrication reaction include the possibility of relatively clean metal surfaces and metal oxides generated from the bearing metals (20).

Specifically, the reactions postulated include those listed in Table 49. Based on the reactions and analytical techniques discussed, there are several major problems in the study of the chemical reactions involved in wear from boundary lubrication. The microchemical magnitude of the lubrication reaction has already been discussed. The number of potential reactants has also been pointed out. A typical system contains several potential reactants all exhibiting some degree of polarity. Early studies of lubrication chemistry suggested more than 20 possible chemical reactions from a simple wear system, including steel bearings and a conventional mineral oil in an air atmosphere (21). Recent studies suggest a much more limited possibility of competing reactions based on improved analytical capability. Under the best conditions principal reactions can be demonstrated but minor reactions involving other polar materials will probably always provide confusing evidence for analysis. The feasibility of identifying the principal reaction in the presence of the competing reactants is hard to demonstrate by simple static conditions (22,23,24,25). The environmental conditions in boundary lubrication are far more severe than those encountered in bulk lubrication systems or

stability tests.

Physical Properties Affecting Boundary Lubrication. Much has been written about the definition of EHD and boundary lubrication and the transition zone between them (26). Generally, EHD is defined as that condition in bearings where the viscosity properties of the lubricant exert a strong effect on bearing behavior. It has been suggested that physical properties only and viscosity properties particularly control EHD, but that physical properties do not play an important role in boundary lubrication (27). There is evidence that for a given bearing design and loading, physical properties of the lubricant do influence the transition zone between EHD and boundary lubrication. Viscosity properties as a function of temperature, pressure, and shear are the principal determining factors of the transition zone. In general, thermal conductivity and specific heat values for the range of liquid lubricants do not show more than 20 to 40 percent variation. The high levels of surface temperature measured in EHD lubrication are an indication of the frictional energy focused on a small volume of material. Under these conditions relatively small differences in thermal conductivity and specific heat may translate into more significant temperature and viscosity differences than predictions based on bulk properties would indicate.

Volatility and solvency of the liquid lubricants have been shown to be factors in boundary lubrication (28,29). In both cases there is some evidence that the effect is related to the removal of chemical reaction products produced at the bearing surface. In the case of volatility effects on the boundary lubrication characteristics of a lubricant, the mechanism of removal of adsorbed or chemically reacted films from the bearing surface may be primarily a cavitational phenomenon. In other cases where complex reaction products are formed at the bearing surface, the solubility of these materials in the bulk lubricant appears to be related to lubrication effectiveness. Reduced solubility of chemical reaction products in the bulk lubricant may result from increasing the molecular weight, polarity or both for the reaction product compared with the bulk lubricant. The effect of physical properties on lubrication chemistry is still a controversial area of lubrication research that requires careful fundamental investigation.

Metal Corrosion at the Bearing Surface. The role of oxidation and corrosion as a mechanism for bulk lubricant degradation is well established, but the role of these reactions in boundary lubrication is not well understood. Conventional oxidation behavior of the fluid at moderate temperatures is described on Figure 95 based on a conventional stable life concept. During the long induction period, the rate of oxidation is very low and property changes also tend to be low. A time-temperature relationship for these stable life curves is shown in Figure 96. This relationship stresses the lack of stability at temperatures predicted for boundary lubrication. Again little work has been done under the short-time, high-temperature conditions typical of boundary lubrication.

Some recent work in the area of corrosion shows that low-temperature, long-time tests may also need more careful treatment (30,31, 7,8,9). Metal corrosion measured on a macro scale shows no particularly

significant reaction between the fluid and the metal surface in bulk fluid oxidation tests. A specific measure of copper corrosion under the oxidative test conditions used in Figure 95 is shown in Figure 97. In this latter case careful measurements were made to determine not only the primary corrosion but the disposition of the corrosion products. The results show that metal corrosion occurs at a maximum rate in the initial phase of the moderate temperature oxidation test. This significant corrosion rate has been demonstrated for steel as well as copper. The phenomenon has been overlooked until recently because of the short life of corrosion at this high rate as indicated in Figure 97. The most interesting result of these corrosion studies is the conversion of soluble corrosion products by further reaction to insoluble materials, including varnish-like deposits that coat the metal surface effectively preventing further corrosion. These results predict sufficiently high reaction rates with conventional metal-metal oxide surfaces and lubricant components to indicate the possibility of chemical reactivity in boundary lubrication without the necessity of catalysis.

Thermal Versus Oxidation Reactions. In the discussion of fluid stability in bulk systems, it was indicated that thermal stability of the fluids exceeded bulk conditions found in lubricant and hydraulic systems (32, 33). The typical thermal stability limits of mineral oil and synthetic fluids shown in Table 48 may be exceeded in normal boundary lubrication. This information indicates that reactive fragments of lubricants can be generated at the bearing surface by temperature alone without the necessity of reaction with oxygen, metal, or metal oxide. In fact there is some preliminary evidence of such thermally induced reaction from four-ball wear tester experiments. A series of heavily loaded (40 kg) wear tester results are shown in Table 50. In these tests the lubricant insoluble material formed in the wear tests was measured and the metal content determined. The difference between the total insolubles and the metal is organic material insoluble in the lubricant. Further analysis indicates that there is some organometallic product and in most cases some purely organic insoluble product.

The formation of organic debris as shown in Table 50 can be related to the type of thermal degradation products rather than oxidation or corrosion products. The comparison of the super-refined mineral oil and the ester shows that for compounds having a low tendency to form insoluble thermal degradation products, the relative amount of corrosion may be observed. These preliminary results indicate important trends that need further investigation to confirm the mechanisms involved in boundary lubrication. It may be possible to measure the specific reaction conditions in boundary lubrication by considering chemical reactivity of various lubricants in static oxidation, corrosion, and thermal tests and comparing these results with reaction products found in boundary lubrication.

Preferential Adsorption. In order to design boundary lubrication experiments to compare with static experiments, it is necessary to obtain similar reactants in both systems. The first step in boundary lubrication is adsorption on the metal surface. This also appears to be the first step in a static corrosion test. Definitive tests for the study

of these chemical reactions should be conducted with one predominant polar type of additive in a nonpolar base stock. Simple adsorption studies on steel surfaces have shown the preferential adsorption of a specific polar material from a mixture of polar additives. Data shown in Figure 98 indicates that adsorption on the steel surface from a solution containing both tricresyl phosphate (TCP) and a more polar phosphate ester (probably dicresyl acid phosphate) is a function only of the polar phosphate ester concentration. Boundary lubrication experiments with these same mixtures of TCP and more polar phosphate esters show that it is the polar material that is preferentially adsorbed that reacts chemically with the bearing surface.

These findings provide a method of designing experiments capable of showing the similarity of moderate bulk condition reactions and boundary lubrication reactions. It is well established that aging or oxidative degradation changes the lubricity characteristics of the fluid in boundary lubrication. This change is presumed to be related to the formation of additional polar compounds in the fluid with use. It is important that careful studies be conducted to determine the static and dynamic behavior of polar lubricants before substantial oxidation takes place. On the other hand, little is known about the boundary lubrication reaction or the static thermal, oxidative, and corrosion properties of badly deteriorated or aged fluids. The study of used fluids is required to obtain a better understanding of the practical life of a lubricant in a system.

It is important to understand the effect of oxygen on boundary lubrication (34,34,28). Simply stated, dissolved oxygen in a liquid lubricant is a polar lubricity additive. In super-refined mineral oils where the dissolved oxygen is the most effective lubricity additive for boundary lubrication, an oxygen concentration-wear relationship such as that shown in Figure 99 can be established. There is an optimum concentration of oxygen for minimum wear. Above this concentration corrosive wear results in a higher wear level and below the optimum scuffing appears to cause high wear. The wear-oxygen concentration curve appears to be independent of temperature but does show a load dependence. These data show that the optimum wear for oxygen is about the same level as optimum wear for tricresyl phosphate. The data also show that TCP in the presence of dissolved oxygen dominates the boundary lubrication chemistry. These data suggest that for so-called nonreactive lubricants, oxygen is the most polar additive in solution and dominates the wear reaction.

The classification of lubricity additives as antiwear, antifriction, antisieze or antiweld is dependent on all three steps: adsorption, reactions, and removal. It appears that the rate of removal of the reacted product on the bearing surface differentiates between the antiwear additives and the others. The antiwear materials appear to provide a thick and tenancious reaction product on the bearing surface. The other type of lubricants appear to form a more easily removed film from the bearing surface.

A qualitative picture of boundary lubrication is beginning to take form from convincing circumstantial evidence. This evidence needs further confirmation and qualification. The payout from developments in this area appear to be substantial. Most of the current lubrication

problems are now in boundary lubrication. It should be emphasized that every gas, hydrodynamic, and elastohydrodynamic bearing goes through a boundary region during startup and shutdown. Further, more bearings are being forced into the boundary region by design parameters moving in the direction of smaller bearings, higher loads, and higher temperatures. The chemical aspects of boundary lubrication will require an effort of the same order of magnitude as that currently being focused on EHD to provide an adequate data base for establishing an acceptable mechanism.

Bibliography

1. Czarnecki, J. R., "High Temperature Degradation of Some Organic Esters," M.S. Thesis, The Pennsylvania State University (1971).

2. Charles, M. J., "High Temperature Oxidation of Some Organic Liquids," M.S. Thesis, The Pennsylvania State University (1974).

3. Anonymous, Federal Specification VV-L-791d, "Lubricants, Liquid Fuels, and Related Products: Methods of Sampling and Testing," U.S. Government Printing Office (1949).

4. Anonymous, Annual Book of ASTM Standards Part 17, "Petroleum Products," American Society of Testing Materials, Philadelphia, Pa. (1973).

5. Klaus, E. E. and Tewksbury, E. J., "New Processing Technology in the Preparation of Improved Mineral Oil and Synthetic Hydrocarbon Lubricants," pp. 121-126, Assessment of Lubrication Technology, American Society of Mechanical Engineers, New York, N.Y. (1972).

6. Klaus, E. E., Tewksbury, E. J., and Fenske, M. R., "Progress Report on Hydrocarbons and Mineral Oils as High Temperature Fluids and Lubricants," pp. 535-567, Proceedings of the Air Force-Navy-Industry Lubricants Conference, WADC Tech. Report 59-244, October 1959.

7. Klaus, E. E. and Tewksbury, E. J., "Microcorrosion Studies with Functional Fluids," Lubrication Engineering, vol. 29, 5, pp. 205-211 (1973).

8. Bose, A. C., "The Study of Chemical Reactions in Boundary Lubrication," M.S. Thesis, The Pennsylvania State University (1973).

9. Barton, D. B., "A Study of Boundary Lubrication Mechanisms Using Atomic Adsorption Spectroscopy," M.S. Thesis, The Pennsylvania State University (1968).

10. Fein, R. S., "Boundary Lubrication," Lubrication, vol. 57, no. 1, Texaco, Inc., New York (1971).

11. Fein, R. S., and Kreuz, K. L., "Chemistry of Boundary Lubrication of Steel by Hydrocarbons," ASLE Transactions, 8, pp. 29-38 (1965).

12. Quinn, T. F. J., "Oxidational Wear," Wear, 18, pp. 413-419 (1971).

13. Tao, F. F., "A Study of Oxidation Phenomena in Corrosive Wear," ASLE Transaction, 12, pp. 97-105 (1969).

14. Tao, F. F., "The Role of Diffusion in Corrosive Wear," ASLE Transactions, 11, pp. 121-130 (1968).

15. Sakurai, T., Ikeda, S., and Okabe, H., "A Kinetic Study on The Reaction of Labeled Sulfur Compounds with Steel Surfaces During Boundary Lubrication," ASLE Transactions, 8, pp. 39-47 (1965).

16. Sakurai, T., Okebe, H., and Takahashi, Y., "A Kinetic Study of the Reaction of Labeled Sulfur Compounds in Binary Additive Systems During Boundary Lubrication," ASLE Transactions, 10, pp 91-101 (1967).

17. Bieber, H. E., Klaus, E. E., and Tewksbury, E. J., "A Study of Tricresyl Phosphate as an Additive for Boundary Lubrication," ASLE Transactions, 11, pp. 155-61 (1968).

18. Bieber, H. E., "Phosphate Esters and Their Function in Boundary Lubrication," Ph.D. Thesis, The Pennsylvania State University (1965).

19. Winer, W. O., "Elastohydrodynamic Lubrication," Proceedings of the Tribology Workshop, Atlanta, Georgia, October 1973.

20. Eischens, R. P., "Catalysis Studies Related to Boundary Lubrication," Boundary Lubrication-An Appraisal of World Literature, pp. 61-85, ASME, New York, N.Y. (1969).

21. Larson, R. G., and Perry, G. L., "Chemical Aspects of Wear and Friction," in J. T. Burwell (ed.) Mechanical Wear, American Society of Metals, pp. 73-94 (1950).

22. Klaus, E. E., and Fenske, M. R., "Chemical Structure and Lubrication," Preprints Symp. Additives in Lubricants, Div. of Petl. Chem., ACS, Vol. 1, No. 4, pp. 58-69 (1956).

23. Barcroft, F. T., and Daniel, S. G., "The Action of Neutral Organic Phosphate Esters as E. P. Additives," Trans. ASME, Ser. D, Vol. 87, No. 3, pp. 761-67 (1965).

24. Godfrey, D., "The Lubrication Mechanism of Tricresyl Phosphate on Steel," ASLE Trans., Vol. 8, No. 1, pp. 1-10 (1965).

25. Klaus, E. E., and Bieber, H. E., "Effects of P^{32} Impurities on the Behavior of Tricresyl Phosphate-32 as an Antiwear Additive," ASLE Trans., Vol. 8, No. 1, pp. 12-20 (1965).

26. Dawson, D., "Transition to Boundary Lubrication from Elastohydrodynamic Lubrication," Boundary Lubrication-An Appraisal of World Literature, pp. 229-39, ASME, New York, N. Y. (1969).

27. Appeldoorn, J. K., "Physical Properties of Lubricants," Boundary Lubrication-An Appraisal of World Literature, pp. 133-40, ASME, New York, N. Y. (1969).

28. Klaus, E. E. and Bieber, H. E., "Effect of Some Physical and Chemical Properties of Lubricants on Boundary Lubrication," ASLE Transactions, Vol. 7, No. 1, pp. 1-10 (1964).

29. Kruez, K. L., Fein, R. S., and S. J. Rand, "Solubilization Effects in Boundary Lubrication," ACS Div. of Petrol Chem. Preprints, Vol. 14, No. 4, pp. A126-38 (1969).

30. Kelly, R. N., "Metal Corrosion Studies Using Activation Analysis," M.S. Thesis, The Pennsylvania State University (1965).

31. Ladov, E. N., "A Study of Boundary Lubrication Using Activation Analysis, M.S. Thesis, The Pennsylvania State University (1967).

32. Karali, M., "Thermal Stability and Corrosion Studies with Mineral Oils," M.S. Thesis, The Pennsylvania State University (1969).

33. Klaus, E. E., and Perez, J. M., "Thermal Stability Characteristics of Some Mineral Oil and Hydrocarbon Hydraulic Fluids and Lubricants," ASLE Trans. Vol. 10, No. 1, pp. 38-47 (1967).

34. Vinogradov, G., Korepova, I. V., Rodolskii, Y. Y., and Pavlovskaia, N.T., "Effect of Oxidation on Boundary Friction of Steel in Hydrocarbon Media and Critical Friction Duties Under Which Cold and Hot Seizure (or Welding) Develop," ASME Trans., Vol. 86, Ser. D, No. 3, pp. 741-45 (1965).

35. Fein, R. S., "Chemistry of Boundary Lubrication of Steel by Hydrocarbons," ASLE Trans., Vol. 8, No. 1, pp. 29-37 (1965).

Table 48

THERMAL STABILITY THRESHOLD FOR SEVERAL FLUIDS

Fluid	Thermal Stability, °F.
Super-Refined Mineral Oil	650 - 700
Di-2-Ethylhexyl Sebacate	450 - 550
Phosphate Ester-Base Formulation	400 - 500
Polyglycol Ether	500 - 550
Silicone	600 - 700
Phenyl Ether	800 - 900
Fluorinated Oil	650 - 700

Table 49

CHEMICAL REACTIONS WHICH MAY BE INVOLVED IN THE LUBRICATION SYSTEM

Oxidation
Lubricant plus Oxygen
Additive plus Oxygen
Thermal Degradation
Metal Corrosion
Metal plus Oxygen
Metal plus Additive
Metal plus Oxidation Product
Polymerization
Condensation

Table 50

WEAR DEBRIS FORMED BY SEVERAL FLUIDS

Four-Ball Wear Conditions Include: Test Speed = 600 r.p.m.;
Load = 40 kg.;
Test Temp. = 167°F.;
Test Time = 1 hr.;
and Bearings = 52-100 Steel,
Batch No. 13

Analysis by Neutron Activation Analysis

Test Fluid	Wear Scar Dia., mm	Metallic Debris, mg	Total Debris, mg	Organic Debris, mg
Super-Refined Mineral Oil	0.59	0.11	0.34	0.23
Di-2-Ethylhexyl Sebacate	0.76	0.15	1.61	1.46
Improved Lubricity Silicone	0.91	0.42	124	124
Polyphenyl Ether	1.39	5.0	33.4	28.0
Fluorinated Oil	0.70	0.12	0.61	0.49

Figure 95

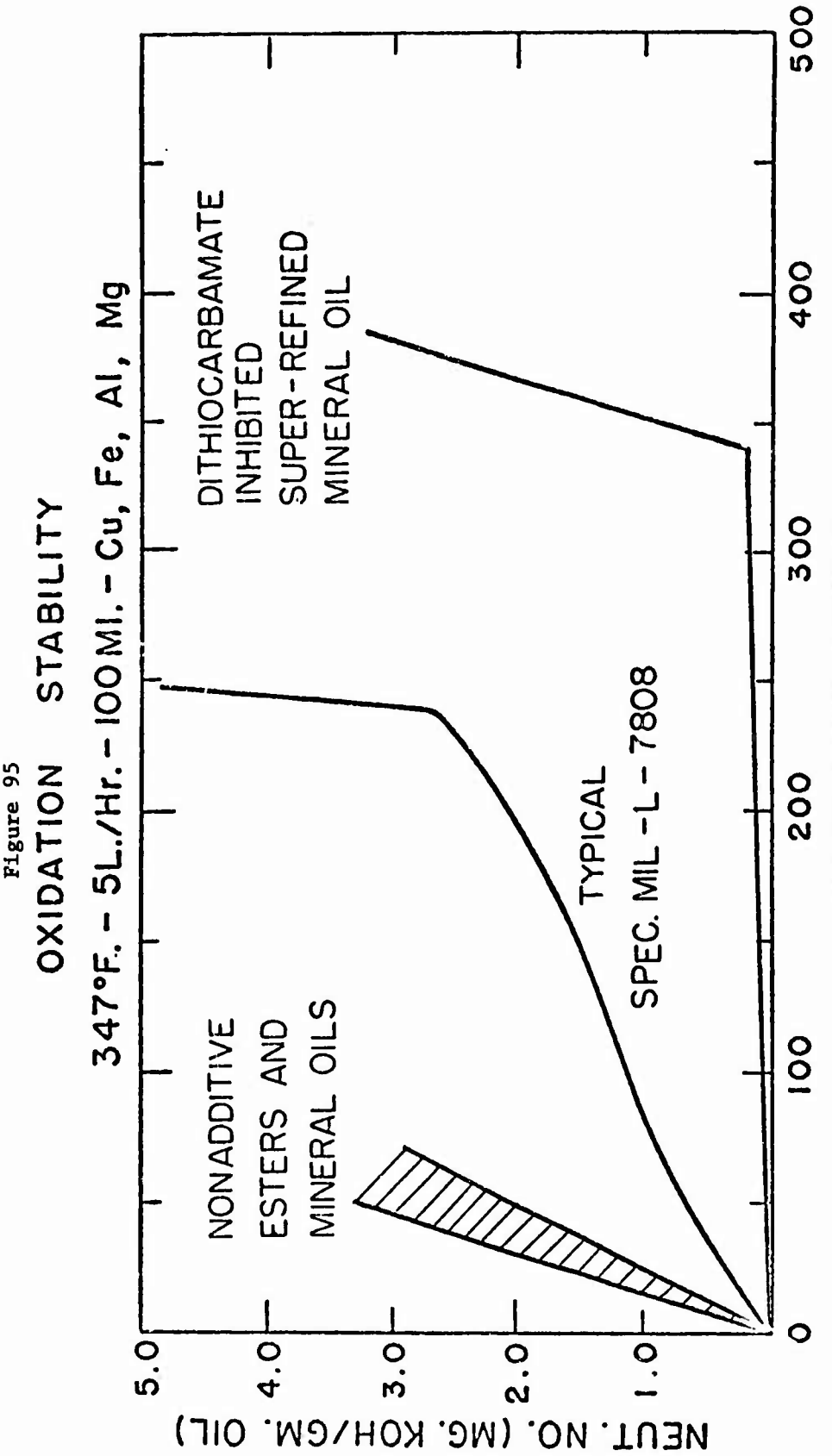

Figure 96

EFFECT OF TEMPERATURE ON OXIDATION STABILITY

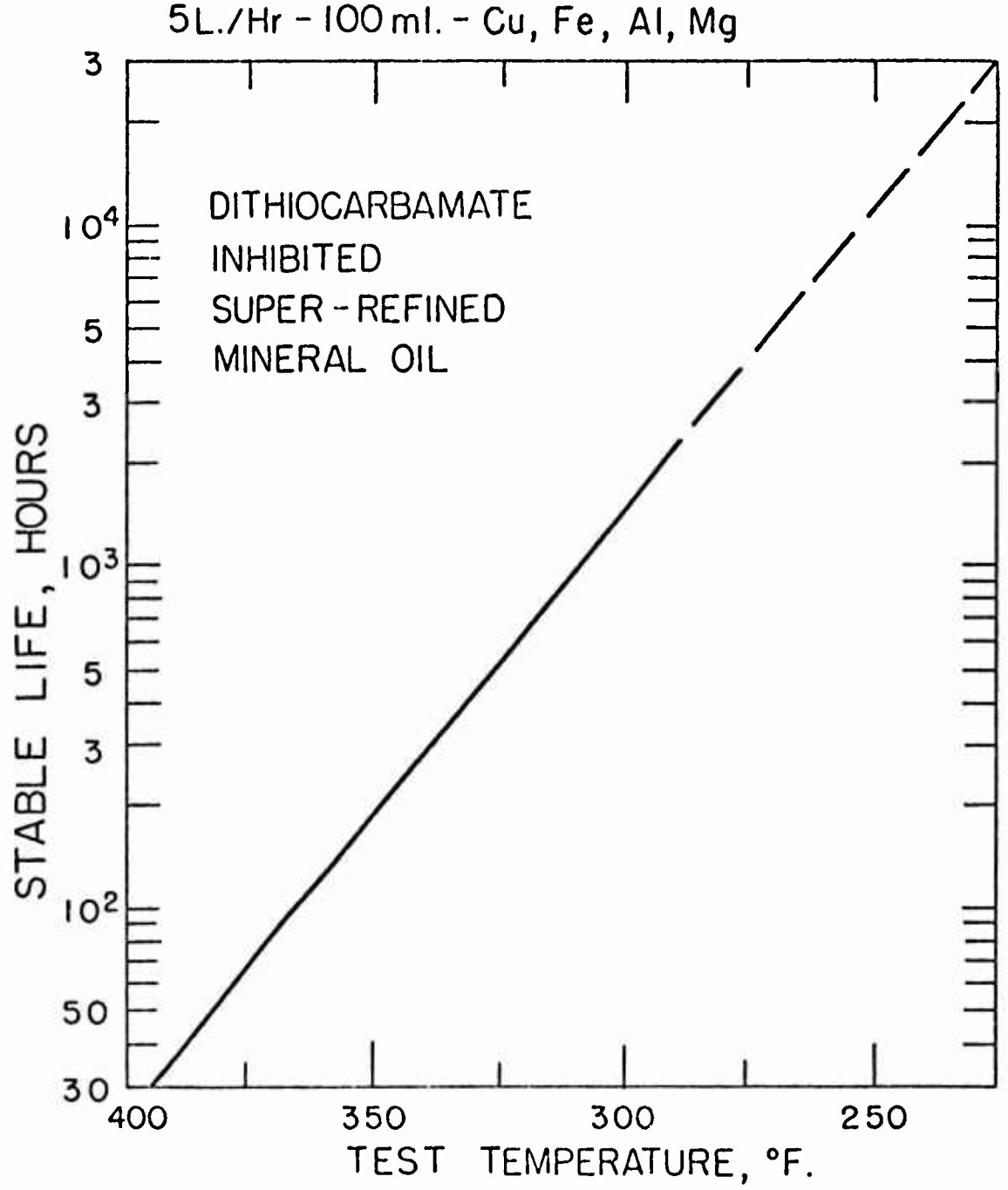

Figure 97

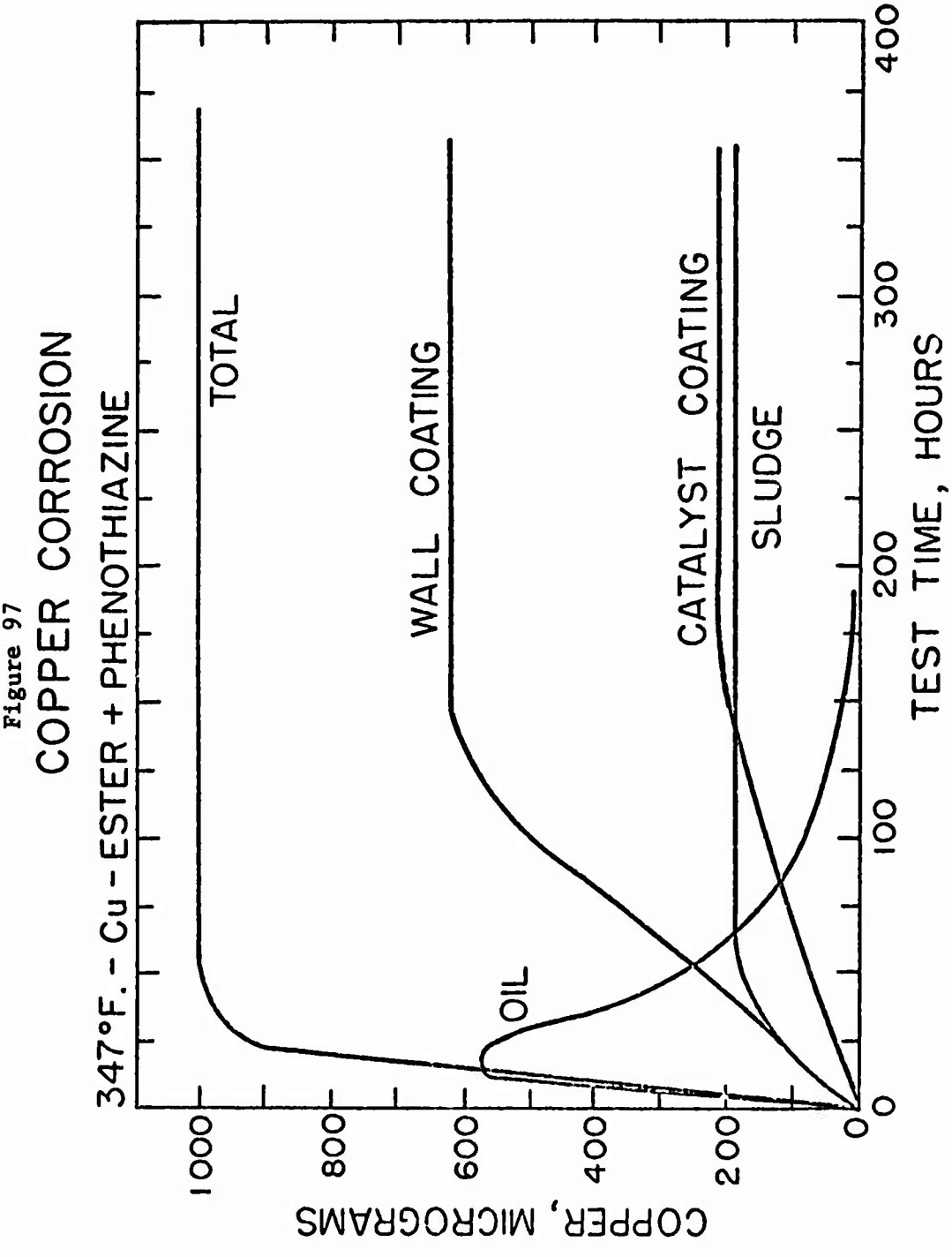

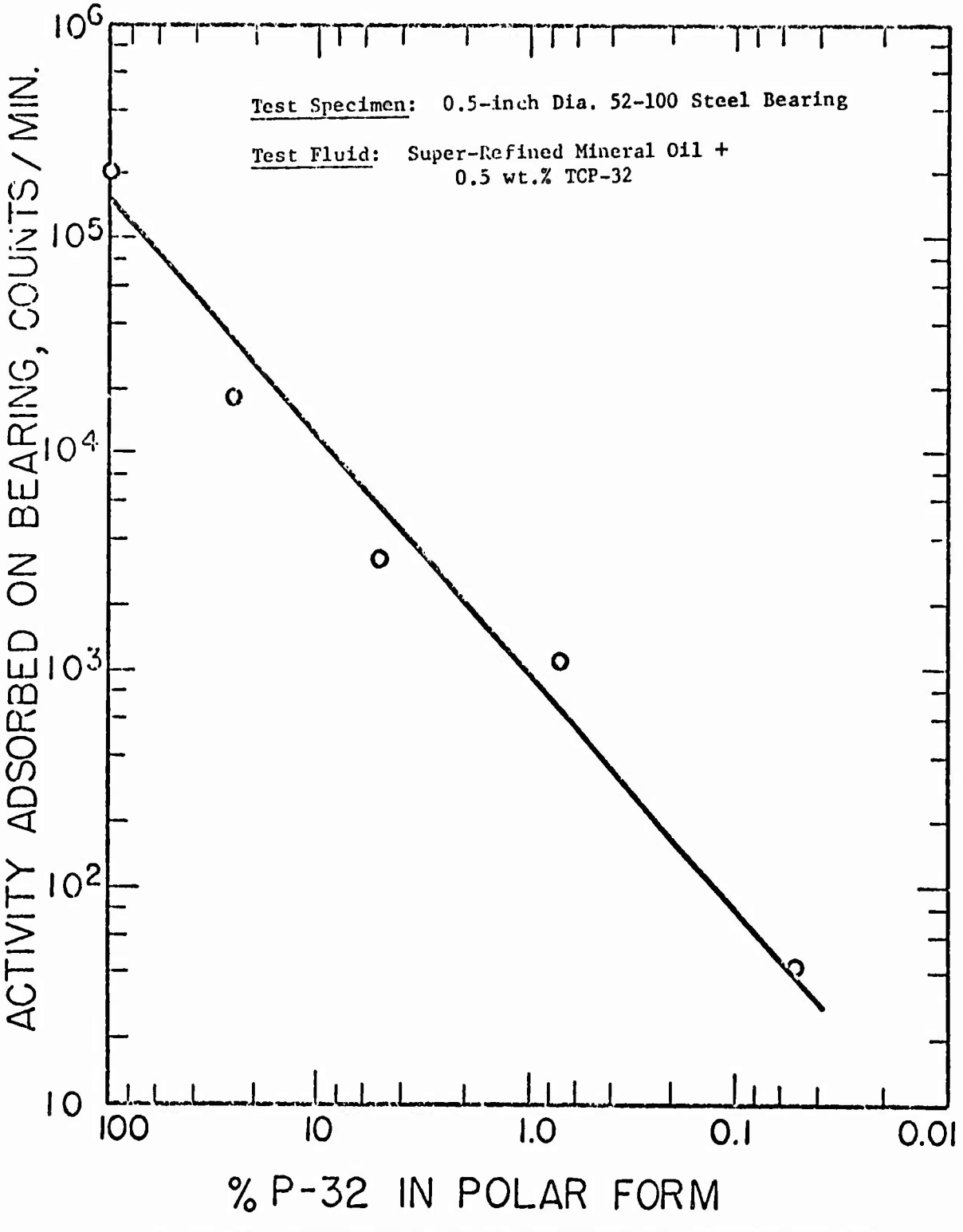

Figure 98. INFLUENCE OF POLAR PHOSPHORUS-32 CONCENTRATION ON PHOSPHORUS-32 ADSORPTION

Tests Conducted in Shell Four-Ball Wear Tester in which Atmosphere above Test Fluid can be controlled at Test Temperature indicated. All Tests conducted at 10 kg. Load. Open Symbols = 167°F.; Solid Symbols = 390°F.

Test Fluids: MLO 7470 is a Super-Refined Paraffinic Neutral
MLO 7516 is a Super-Refined Naphthenic Neutral

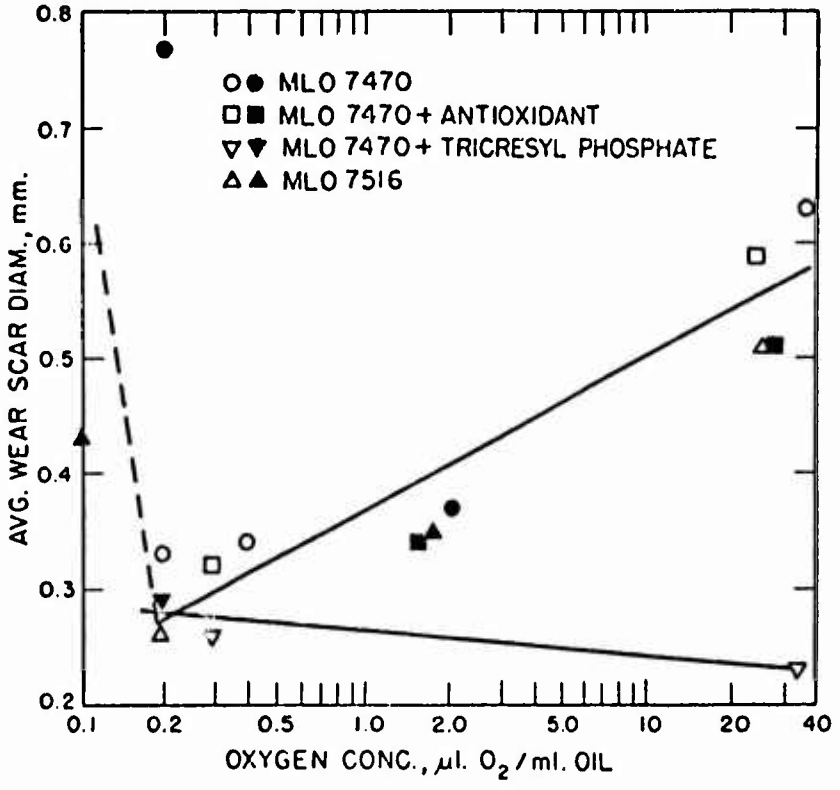

Figure 99. EFFECT OF DISSOLVED OXYGEN ON WEAR BEHAVIOR

☆U.S.Government Printing Office: 1975 — 657-020/538